ESCOLA POLITÉCNICA
PROGRAMA DE PÓS-GRADUAÇÃO EM ENGENHARIA E TECNOLOGIA DE MATERIAIS
MESTRADO EM ENGENHARIA E TECNOLOGIA DE MATERIAIS

VICTOR HUGO JACKS MENDES DOS SANTOS

UMA PERSPECTIVA DA MODELAGEM QSPR PARA TRIAGEM/DESENHO DE CATALISADORES PARA A SÍNTESE DE CARBONATOS OLEOQUÍMICOS

Porto Alegre
2018

Pontifícia Universidade Católica do Rio Grande do Sul
Programa de Pós-Graduação em Engenharia e Tecnologia de Materiais

UMA PERSPECTIVA DA MODELAGEM QSPR PARA TRIAGEM/DESENHO DE CATALISADORES PARA A SÍNTESE DE CARBONATOS OLEOQUÍMICOS

VICTOR HUGO JACKS MENDES DOS SANTOS
BACHAREL EM QUÍMICA INDUSTRIAL

DISSERTAÇÃO PARA A OBTENÇÃO DO TÍTULO DE MESTRE EM ENGENHARIA E TECNOLOGIA DE MATERIAIS

Porto Alegre
Maio, 2018

Pontifícia Universidade Católica do Rio Grande do Sul
ESCOLA POLITÉCNICA
PROGRAMA DE PÓS-GRADUAÇÃO EM ENGENHARIA E TECNOLOGIA DE MATERIAIS

UMA PERSPECTIVA DA MODELAGEM QSPR PARA TRIAGEM/DESENHO DE CATALISADORES PARA A SÍNTESE DE CARBONATOS OLEOQUÍMICOS

VICTOR HUGO JACKS MENDES DOS SANTOS
BACHAREL EM QUÍMICA INDUSTRIAL

ORIENTADOR: PROF. Dr. Marcus Seferin

Dissertação de Mestrado realizada no Programa de Pós-Graduação em Engenharia e Tecnologia de Materiais (PGETEMA) da Pontifícia Universidade Católica do Rio Grande do Sul, como parte dos requisitos para a obtenção do título de Mestre em Engenharia e Tecnologia de Materiais.

Porto Alegre

Maio, 2018

Ficha Catalográfica

S237p Santos, Victor Hugo Jacks Mendes dos

Uma perspectiva da modelagem QSPR para triagem/desenho de catalisadores para a síntese de carbonatos oleoquímicos / Victor Hugo Jacks Mendes dos Santos . – 2018.

185 p.

Dissertação (Mestrado) – Programa de Pós-Graduação em Engenharia e Tecnologia de Materiais, PUCRS.

Orientador: Prof. Dr. Marcus Seferin.

1. QSPR. 2. Relação quantitativa estrutura-propriedade. 3. Óleos vegetais. 4. CO2. 5. Carbonatos oleoquímicos. I. Seferin, Marcus.

Elaborada pelo Sistema de Geração Automática de Ficha Catalográfica da PUCRS
com os dados fornecidos pelo(a) autor(a).
Bibliotecária responsável: Salete Maria Sartori CRB-10/1363

Pontifícia Universidade Católica do Rio Grande do Sul
ESCOLA POLITÉCNICA
PROGRAMA DE PÓS-GRADUAÇÃO EM ENGENHARIA E TECNOLOGIA DE MATERIAIS

UMA PERSPECTIVA DA MODELAGEM QSPR PARA TRIAGEM/DESENHO DE CATALISADORES PARA A SÍNTESE DE CARBONATOS OLEOQUÍMICOS

CANDIDATO: VICTOR HUGO JACKS MENDES DOS SANTOS

Esta Dissertação de Mestrado foi julgada para obtenção do título de MESTRE EM ENGENHARIA E TECNOLOGIA DE MATERIAIS e aprovada em sua forma final pelo Programa de Pós-Graduação em Engenharia e Tecnologia de Materiais da Pontifícia Universidade Católica do Rio Grande do Sul.

DR. MARCUS SEFERIN - ORIENTADOR

BANCA EXAMINADORA

DR. ADILSON BEN DA COSTA - PROGRAMA DE PÓS-GRADUAÇÃO EM TÉCNOLOGIA AMBIENTAL - UNIVERSIDADE DE SANTA CRUZ DO SUL

DR. ADRIANO LISBOA MONTEIRO - PROGRAMA DE PÓS-GRADUAÇÃO EM QUÍMICA - PPGQ - UFRGS

DRA. ROSANE ANGÉLICA LIGABUE - DO PGETEMA - PUCRS

PUCRS
Campus Central
Av. Ipiranga, 6681 - Prédio 32 - Sala 505 - CEP: 90619-900
Telefone: (51) 3353.4059 - Fax: (51) 3320.3625
E-mail: engenharia.pg.materiais@pucrs.br
www.pucrs.br/politecnica

“A alegria pode prescindir da razão, mas reflexão sem compreensão é vazia”.
(Peter William Atkins)

DEDICATÓRIA

Dedico este trabalho aos meus pais, por todo incentivo e confiança depositados em mim, e a todos aqueles que em gestos, pensamentos ou orações mantiveram-se presentes.

AGRADECIMENTOS

Aos meus pais, Luiz Alfredo e Fátima Regina, por todo incentivo, conselhos e amor.

À Alessandra Côrte Real Lança, por todo amor, carinho e compreensão com meus momentos de ausência.

Ao meu orientador Marcus Seferin por todas as oportunidades, ensinamentos, conselhos, dedicação, confiança depositada, anos de amizades e empenho no desenvolvimento deste trabalho.

À Faculdade de Química (FAQUI) da PUCRS pelo acolhimento, auxílio financeiro e pelo espaço cedido para realização dos experimentos.

Aos meus colegas e amigos do Laboratório de Química Industrial de hoje e de outrora, em especial Pedro Rocha, Wagner Menezes, Igor Barden e Vinícius Maciel, por todo o apoio, anos de amizade, pelas conversas edificantes e cafés compartilhados.

Aos Bolsistas Darlan Pontin e Gabriele Sória, sem os quais o desenvolvimento deste trabalho seria muito dificultado.

Aos colegas e amigos do IPR, em especial o Corpo Técnico, que acompanharam o desenvolvimento desse trabalho e sempre me incentivaram, mesmo em momentos de desânimo.

Aos amigos, Dr. Raoní Scheibler Rambo e Dr. Tiago de Abreu Siqueira pelo auxílio prestado durante a etapa de execução do presente trabalho.

Ao Laboratório de Catálise Molecular da UFRGS, pelo auxílio com as análises de ^{1}H-RMN.

Ao IPR (Instituto de Petróleo e Recursos Naturais), por todas as oportunidades, aprendizados e sensibilidade ao me liberar para o desenvolvimento deste trabalho.

Ao Dr. Luiz Frederico e ao Prof. Dr. Rogério Lourega, por seus incentivos, conselhos e compreensão com minhas ausências.

À HP, pela bolsa de mestrado que oportunizou a continuidade de meus estudos.

E a todos que direta ou indiretamente fizeram parte do desenvolvimento deste trabalho.

SUMÁRIO

LISTA DE FIGURAS

LISTA DE TABELAS

LISTA DE SÍMBOLOS

CTAB – Brometo de cetiltrimetilamônio (do inglês *cetyltrimethylammonium bromide*)

FTIR – Espectroscopia de infravermelho com transformada de Fourier (do inglês *fourier-transform infrared spectroscopy*)

^{1}H-NMR – Ressonância magnética nuclear de hidrogênio (do inglês *Hydrogen nuclear magnetic resonance*)

LMO – Deixe-vários-de-fora (do inglês *leave-many-out*)

LOO – Deixe-um-de-fora (do inglês *leave-one-out*)

PCA – Análise de componentes principais (do inglês *principal component analysis*)

PLS – Regressão por mínimos quadrados parciais (do inglês *partial least square regression*)

Q^2 - Coeficiente de correlação da validação cruzada

QSAR – Relação quantitativa estrutura-atividade (do inglês *quantitative structure-activity relationship*)

QSPR – Relação quantitativa estrutura-propriedade (do inglês *quantitative structure-property relationship*)

R^2 - Coeficiente de determinação

RMSEC – Erro médio quadrático de calibração (do inglês *root mean square error of calibration*)

RMSECV – Erro médio quadrático de validação cruzada (do inglês *root mean squared error of cross-validation*)

RMSEP – Erro médio quadrático de previsão (do inglês *root mean square error of prediction*)

SVM – Regressão por vetores de suporte (do inglês *support vector regression*)

TBAB – Brometo de tetrabutilamônio (do inglês *tetrabutylammonium bromide*)

Descritores Moleculares

ALogP – Coeficiente de partição octanol-água (Ghose-Crippen-Viswanadhan)

apol – Soma das polarizabilidades atômicas (incluindo hidrogênios implícitos)

ATS2e – Autocorrelação de Broto-Moreau - lag 2 / sobre as eletronegatividades de Sanderson

bpol – Soma dos valores absolutos da diferença entre polarizabilidades atômicas de todos os átomos ligados na molécula (incluindo hidrogênios implícitos)

C2SP3 – Carbono ligado por ligação simples a dois outros carbonos

ETA Shape Y – Índex Y de forma de átomo topoquímico estendido

GATS6i – Autocorrelação de Geary - lag 6 / sobre o primeiro potencial de ionização

Lipoaffinity Index – Índice de lipoafinidade do estado eletrotopológico

MATS4m – Autocorrelação de Moran - lag 4 / sobre a massa

nAtom – Número de átomos

nAtomLAC – Número de átomos na cadeia alifática mais longa

nBr^- – Número de átomos de bromo

nBonds2 – Número totais de ligações (incluindo ligações a hidrogênios)

nCl^- – Número de átomos de cloro

nI^- – Número de átomos de iodo

nRotBt – Número de ligações rotativas, incluindo ligações terminais

$SssCH_2$ – Soma do *E-State* do tipo de átomo: $-CH_2-$

VABC – Volume de Van der Waals

RESUMO

SANTOS, Victor Hugo Jacks Mendes dos. **Uma perspectiva da modelagem QSPR para triagem/desenho de catalisadores para a síntese de carbonatos oleoquímicos**. Porto Alegre. 2018. Dissertação. Programa de Pós-Graduação em Engenharia e Tecnologia de Materiais, PONTIFÍCIA UNIVERSIDADE CATÓLICA DO RIO GRANDE DO SUL.

Até o momento, apenas um pequeno número de organocatalisadores foram aplicados para produção de carbonatos oleoquímicos, enquanto a descrição de novos sistemas de catalisadores ainda é limitada. O presente trabalho apresenta uma perspectiva preliminar da modelagem por Relação Quantitativa Estrutura-Propriedade (QSPR) para auxiliar na escolha/desenho de novos organocatalisadores para produção de carbonatos cíclicos. O QSPR foi desenvolvido aplicando os descritores moleculares (2D) para modelar a relação estrutura-propriedade entre as características dos organocatalisadores e sua atividade para produção de carbonatos oleoquímicos. A partir da triagem virtual, um total de 122 catalisadores tiveram sua atividade prevista e os melhores alvos moleculares são propostos. As principais características moleculares (estrutura orgânica, arranjo molecular, tamanho da cadeia de carbono e tipo de substituinte) foram identificadas através da mineração de dados, enquanto a análise de componentes principais (PCA) mostrou-se adequada para realizar a análise exploratória do conjunto de moléculas. Além disso, é apresentado o primeiro relato da aplicação do brometo de cetiltrimetilamônio (CTAB) como um catalisador para a produção de carbonato oleoquímico derivados dos óleos de soja, canola e arroz. As reações foram realizadas em uma autoclave de aço inoxidável de 50 cm^3 a 120 ° C, durante 48 horas, sem agitação, 5 MPa (*p*, CO_2), 2 g de óleo epoxidado, 4 mL de butanol e 5% molar de CTAB. A partir do método proposto, todas as reações apresentaram mais de 98% de conversão de epóxido em carbonato cíclico para todos os óleos vegetais. Desta forma, a modelagem QSPR pode ser aplicada para reduzir os custos e tempo na seleção/desenho de organocatalisadores para a síntese de carbonatos cíclicos a partir de CO_2 e epóxidos.

Palavras-Chaves: QSPR, relação quantitativa estrutura-propriedade, óleos vegetais, CO_2, carbonatos oleoquímicos

ABSTRACT

SANTOS, Victor Hugo Jacks Mendes dos. **A perspective of QSPR modeling to screen/design organocatalysts for oleochemical carbonates synthesis**. Porto Alegre. 2018. Master Thesis. Graduation Program in Materials Engineering and Technology, PONTIFICAL CATHOLIC UNIVERSITY OF RIO GRANDE DO SUL.

To date, only a small number of organocatalysts have been applied to produce oleochemical carbonates, while the description of new catalysts system still limited. This work presents a preliminary perspective of Quantitative Structure-Property Relationship (QSPR) modeling to assist in the targeted choice/design of active organocatalysts to produce cyclic carbonates. The QSPR was developed by applying the molecular descriptors (2D) to model the structure-property relationship between the organocatalysts features and its activity to produce oleochemical carbonates. From the virtual screening, a total of 122 catalysts have their activity predicted and the best molecular targets are proposed. The principal molecular features (organic structure, molecular arrangement, carbon chain size and substituent type) were identified through data mining, while the principal component analysis (PCA) proved to be suitable to perform the exploratory analysis of the molecules set. In addition, is presented the first report of the application of cetyltrimethylammonium bromide (CTAB) as a new catalyst to produce oleochemical carbonate derived from soy, canola and rice oils. The reactions were performed in a 50 cm^3 stainless steel autoclave at 120°C, for 48 hours, without stirring, 5 MPa (*p*, CO_2), 2 g of epoxidized oil, 4 mL of butanol and 5 mol% of CTAB. From the proposed method, all reactions showed more than 98% of epoxide conversion to cyclic carbonate for all the vegetable oil. In this way, the QSPR modelling can be applied to reduce the costs and time in the organocatalysts screening/design for the cyclic carbonates synthesis from CO_2 and epoxides.

Keywords: QSPR, quantitative structure-property relationship, vegetable oils, CO_2, oleochemical carbonate

1. INTRODUÇÃO

Existe uma crescente preocupação com a perenidade das reservas fósseis e acerca da extensão da influência do ser humano sobre o meio ambiente. A humanidade depende dos recursos fósseis como principal fonte de energia e de matérias-primas, porém, o CO_2 residual é um importante passivo ambiental atuando nas mudanças climáticas globais (NORTH; PASQUALE; YOUNG, 2010).

Hoje em dia, o conceito de sustentabilidade é indissociável dos processos químicos, e ferramentas como a Avaliação do Ciclo de Vida são cada vez mais robustas e capazes de auxiliar na identificação de pontos críticos ambientais, econômicos e sociais ao longo da cadeia de produção (KRALISCH et al., 2012).

Mesmo valendo-se de conceitos como a intensificação do processo (PI-*Process Intensification*) e novas janelas de processo (NPWs - *Novel Process Windows*), a mera melhoria dos processos convencionais, muitas vezes, não é suficiente para melhorar significativamente a sustentabilidade ambiental e econômica da produção química (KRALISCH et al., 2012).

Dessa forma, uma vez que as reservas fósseis conhecidas não serão suficientes para suprir todas as crescentes demandas da sociedade e, observada a preocupação com prevenir acréscimos substanciais na concentração de CO_2 na atmosfera, existe uma apelo por buscar alternativas tecnológicas que promovam mudanças de paradigmas na concepção de desenho e desempenho dos processos químicos (KRALISCH et al., 2012; NORTH; PASQUALE; YOUNG, 2010; PANCHAL et al., 2017).

Recentemente, a utilização de fontes renováveis na preparação de diversos materiais foi revitalizada devido às preocupações ambientais (SENIHA GÜNER; YAĞCI; TUNCER ERCIYES, 2006). Entre as principais oportunidades, está o estabelecimento e consolidação de uma cadeia perene de matérias-primas capazes

de substituir as fontes atuais e reduzir a pegada ecológica do ser humano (CAI et al., 2008; MEIER; METZGER; SCHUBERT, 2007) .

Por outro lado, o desafio de substituir progressivamente as matérias-primas fósseis por materiais provenientes de fontes renováveis, implica no desenvolvimento de novos catalisadores, rotas sintéticas e materiais que sejam competitivos em propriedades e custos (LATHI; MATTIASSON, 2007; RONDA et al., 2011). Dentro desse contexto, os óleos vegetais tornaram-se objetos de interesse para a pesquisa acadêmica e industrial como uma possível plataforma de produtos químicos devido à sua disponibilidade universal, biodegradabilidade inerente e baixo custo de aquisição (CAI et al., 2008; MIAO et al., 2014).

Os óleos vegetais estão entre as classes mais importantes de biorrecursos disponíveis e, no que se refere às questões ambientais e energéticas, os triglicerídeos deverão desempenhar um papel fundamental durante o século XXI como base de combustíveis sintéticos e de materiais poliméricos (ADHVARYU; ERHAN, 2002; PANCHAL et al., 2017; SARPAL et al., 2015).

As insaturações, presentes em todos os óleos vegetais, são ao mesmo tempo pontos de fragilidade e potenciais sítios ativos para modificações químicas controladas. A epoxidação, processo crucial pelo qual as insaturações são convertidas em grupos epóxidos ou grupos oxiranos, apresenta papel fundamental na obtenção de derivados poliméricos de triglicerídeos (Panchal et al., 2017).

Entre as possíveis modificações sequenciais a partir do grupo oxirano têm-se a carbonatação, processo em que o grupo epóxido reage com CO_2, com 100% de eficiência atômica, a fim de obter um carbonato cíclico em um anel de 5 membros (NORTH; PASQUALE; YOUNG, 2010).

Uma rica literatura já encontra-se disponível acerca da cicloadição de CO_2 em epóxidos pequenos, tais como óxido de propileno e óxido de etileno (LI et al., 2008), porém a disponibilidade comercial de óleos vegetais epoxidados estimulou a pesquisa acerca da produção de carbonatos cíclicos de cadeia longa (HOLSER, 2007).

A vasta variedade de fontes de triglicerídeos, e a atenção que tem sido dado à incorporação de CO_2 em moléculas orgânicas (LI et al., 2008; LIU; WANG, 2017; TAMAMI; SOHN; WILKES, 2004; YANG; GAO; LIU, 2016), são motivadores do presente trabalho, que propõe-se a utilizar a modelagem por relação quantitativa

estrutura-propriedade (QSPR) para auxiliar na escolha/desenho de novos organocatalisadores para produção de carbonatos cíclicos.

Desta forma, a ferramenta QSPR pode ser aplicada para reduzir custo e tempo envolvido no desenvolvimento de novos organocatalisadores para a síntese de carbonatos cíclicos a partir de epóxidos e CO_2.

2. OBJETIVOS

O presente trabalho propôs-se aplicar a modelagem por QSPR para selecionar/desenhar novos catalisadores para a síntese de carbonatos oleoquímicos.

2.1. Objetivos Específicos

- Desenvolver e validar um método QSPR que descreva a relação estrutura-propriedade de catalisadores para a produção de carbonatos oleoquímicos.

- Utilizar as ferramentas de análise multivariada para a análise exploratória de dados, seleção de dados e desenvolvimento de modelos preditivos da atividade catalítica dos catalisadores;

- Aplicar a modelagem QSPR para seleção de um potencial novo catalisador para a produção de carbonatos oleoquímicos;

- Sintetizar e caracterizar os carbonatos oleoquímicos derivados de óleos vegetais, utilizando um catalisador convencional e um novo catalisador selecionado pela abordagem QSPR.

3. REVISÃO BIBLIOGRÁFICA

A limitada extensão das reservas mundiais de petróleo, o aumento dos preços do óleo bruto e as questões relacionadas com o meio ambiente são problemas a serem herdados pelas gerações futuras (PANCHAL et al., 2017). A partir desse cenário, é provável que apareçam inúmeras oportunidades no setor da bioindústria devido a existência de uma quantidade relativamente grande de produtos e resíduos gerados no dia-a-dia pelos setores industriais e agropecuários (TAN; CHOW, 2010).

As matérias-primas renováveis desempenham um papel muito importante no desenvolvimento da química verde e sustentável (LATHI; MATTIASSON, 2007; MIAO et al., 2014). Algumas das matérias-primas renováveis, para aplicações não-combustíveis, mais amplamente aplicadas na indústria química incluem os polissacarídeos, açúcares, madeira e os óleos vegetais (MEIER; METZGER; SCHUBERT, 2007).

Em especial, os óleos derivados de plantas têm um grande potencial para inserção na cadeia petroquímica atual na confecção de produtos químicos finos e materiais poliméricos (MEIER; METZGER; SCHUBERT, 2007).

3.1. **Triglicerídeos**

Um triacilglicerol ou triglicerídeo pode ser definido como um éster obtido a partir de uma molécula de glicerol e três moléculas de ácidos graxos de cadeia longa (ISSARIYAKUL; DALAI, 2014; SENIHA GÜNER; YAĞCI; TUNCER ERCIYES, 2006). Os ácidos graxos normalmente apresentam cadeias carbônicas variando entre 14 e 22 carbonos e dividem-se principalmente entre saturados, sem presença de ligações duplas carbono-carbono e insaturados variando majoritariamente de 1 a 3 ligações duplas por ácido graxo (MCNUTT; HE, 2016; RONDA et al., 2011; SENIHA GÜNER; YAĞCI; TUNCER ERCIYES, 2006).

Dentro da estrutura dos ácidos graxos insaturados, existem algumas posições possíveis para a disposição das ligações duplas C=C, que normalmente situam-se nas posições 6, 9, 12 e/ou 15. Para cadeias poli-insaturadas, têm-se que se as ligações duplas podem ser isoladas, se estiverem separadas por pelo menos 2 átomos de carbono (RONDA et al., 2011), ou conjugadas, se as ligações simples e duplas se alternam entre os átomos de carbono da cadeia (RONDA et al., 2011; SENIHA GÜNER; YAĞCI; TUNCER ERCIYES, 2006).

Considerando a atividade das moléculas de triglicerídeos, em especial os poli-insaturados, são vários os sítios reativos que estão sujeitos a modificações controladas, fazendo destes compostos plataformas químicas de grande potencial. Tendo por objetivo a obtenção de monômeros para a produção de materiais poliméricos, os grupos ésteres, as ligações duplas e as posições alílicas são os pontos reativos mais importantes (KHOT et al., 2001; MIAO et al., 2014). Na Figura 3.1, podem ser observados alguns pontos ativos das moléculas de triacilglicerol.

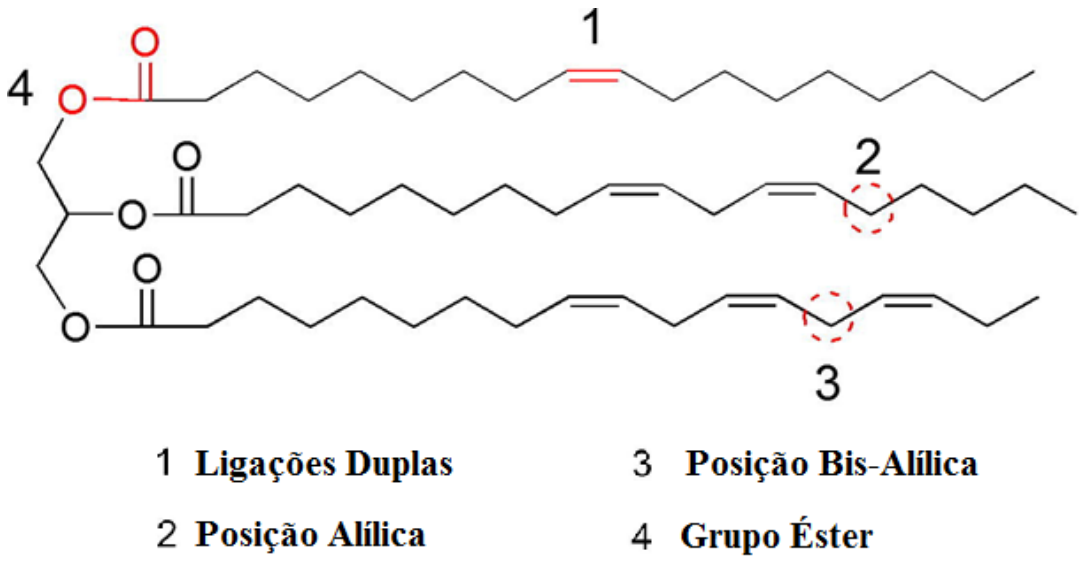

Figura 3.1. Pontos ativos das moléculas de triglicerídeos insaturados.
Fonte: (MIAO et al., 2014)**.**

Adicionalmente, alguns ácidos graxos naturais têm estruturas diferenciada com a cadeia de carbono apresentando grupos como hidroxila, epóxi ou oxo (MIAO et al., 2014). Na Figura 3.2 é apresentado a estrutura dos principais ácidos graxos encontrados em fontes naturais.

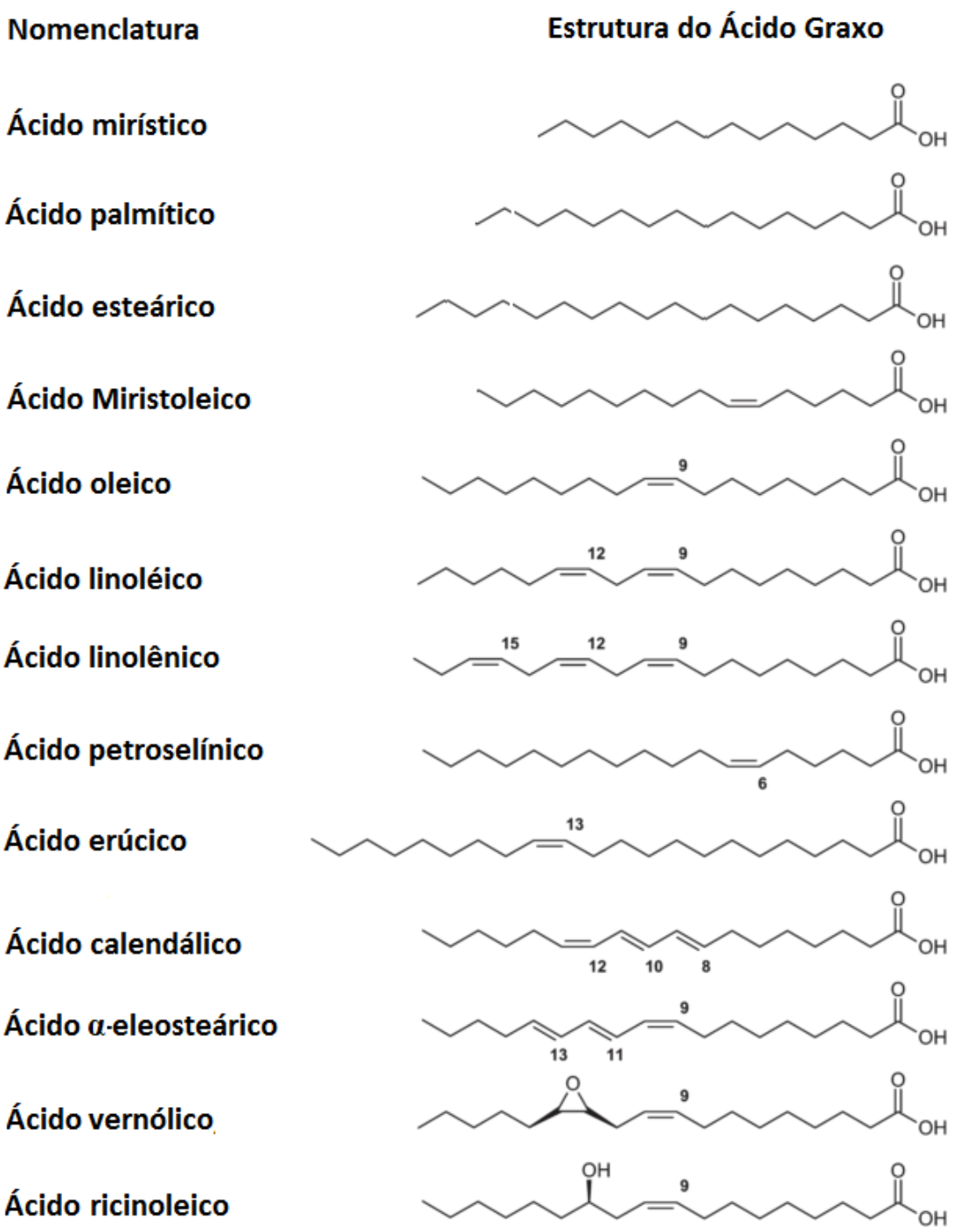

Figura 3.2. Nomenclatura e estrutura dos principais ácidos graxos naturais.
Fonte: (CHUA; XU; GUO, 2012; MEIER; METZGER; SCHUBERT, 2007)**.**

As fontes graxas naturais podem ser de origem animal ou vegetal, são constituídas majoritariamente por triglicerídeos, são recursos renováveis e são

encontrados em abundância em todas as partes do mundo, tornando esses produtos químicos matérias-primas alternativas ideais (MIAO et al., 2014)**.**

O termo “óleos vegetais” se aplica às misturas de triglicerídeos que mantém-se no estado líquidos a temperaturas ambiente, sendo normalmente derivados de fontes vegetais como girassol, algodão, linhaça, soja, etc. (SENIHA GÜNER; YAĞCI; TUNCER ERCIYES, 2006).

A escolha da fonte dos triglicerídeos desempenha um papel importante nas propriedades dos materiais derivados dos mesmos, uma vez que as suas propriedades físicas e químicas são fortemente influenciadas pela estrutura dos seus ácidos graxos constituintes (SENIHA GÜNER; YAĞCI; TUNCER ERCIYES, 2006).

Apesar de existir vários ácidos graxos que podem constituir um triglicerídeo, os óleos vegetais são, com raras exceções, majoritariamente constituídos pelos ácidos graxos insaturados oleico (C18:1), linoleico (C18:2) e linolênico (C18:3), que contêm 1 a 3 ligações duplas por ácido graxo (HUANG et al., 2015).

Baseado nesse princípio, diversos estudos tem sido conduzidos com o objetivo de realizar a identificação e classificação desses óléos vegetais com base no percentual de cada ácido graxo presente, na configuração dos triglicerídeos ou na assinatura espectral do óleo (JAVIDNIA et al., 2013; LI et al., 2016; ZHANG et al., 2014b). Os óleos vegetais possuem propriedades excelentes como boa lubricidade, baixa volatilidade, alto índice de viscosidade, solvência para aditivos lubrificantes e fácil miscibilidade com outros fluidos (BOYDE, 2002).

Muitos pesquisadores se valeram das características estruturais dos triglicerídeos de diversas fontes para propor modelos preditivos de suas propriedades baseados nas suas constituições químicas e espectrais. Variáveis como o índice de insaturação (BARTHUS; POPPI; ANDRADE, 2001), nível de oxidação do óleo (BARTHUS; POPPI, 2002), estabilidade oxidativa do óleo (DE LIRA et al., 2010), ponto de fulgor (DUAN et al., 2011), índice de umidade (MIRGHANI et al., 2011), densidade (FERRÃO et al., 2011) e viscosidade cinemática (BALABIN; LOMAKINA; SAFIEVA, 2011) já foram estimadas com razoável eficácia a partir dessa estratégia.

Na Tabela 3.1 são apresentados os valores de ácidos graxos reportados para algumas das principais plantas oleoaginosas produzidas no mundo.

Tabela 3.1. Principais plantas oleaginosas e sua composição de ácidos graxos

Ácido graxo	C:LD	Canola	Milho	Algodão	Linhaça	Oliva	Palma	Soja	Mamona	Arroz	Girassol
Mirístico	14:0	0,1	0,1	0,7	0,0	0,0	1,0	0,1	0,0	0,4	0,0
Miristoleico	14:1	0,0	0,0	0,0	0,0	0,0	0,0	0,0	0,0	0,0	0,0
Palmítico	16:0	4,1	10,9	21,6	5,5	13,7	44,4	11,0	1,4	18,2	9,2
Palmitoleico	16:1	0,4	0,3	0,8	0,0	1,2	0,3	0,1	0,0	0,2	0,0
Esteárico	18:0	1,8	2,0	2,6	3,5	2,5	4,1	4,0	0,9	1,9	3,5
Oleico	18:1	60,9	25,4	18,6	19,1	71,1	39,3	23,4	3,5	41,7	20,4
Linoleico	18:2	21,0	59,6	54,4	15,3	10,0	10	53,2	4,9	34,6	68,1
Linolênico	18:3	8,8	1,2	0,7	56,6	0,6	0,4	7,8	0,3	1,2	0,4
Ricinoleico	18:1	0,0	0,0	0,0	0,0	0,0	0,0	0,0	88,9	0,0	0,0
Araquídico	20:0	0,7	0,4	0,5	0,0	0,9	0,4	0,4	0,0	0,7	0,0
Gadoleico	20:1	1,0	0,1	0,0	0,0	0,0	0,0	0,0	0,0	0,5	0,0
Erúcico	22:0	1,2	0,0	0,0	0,0	0,0	0,0	0,0	0,0	0,2	0,0
Média de LD no óleo		3.9	4.5	3.9	6.6	2.8	1.8	4.6	3,1	3,4	4,7

C – Número de carbonos; LD – Número de ligações duplas

Fonte: (DUBOIS et al., 2007; KHOT et al., 2001)

Mesmo com propriedades interessantes, a existência de ligações insaturadas (C=C) é responsável pela baixa estabilidade oxidativa dos triglicerídeos, especialmente para os óleos vegetais poli-insaturados, que são constituidos predominantemente de ácidos linoleico e linolênico (WU et al., 2000).

Uma vez que as propriedades físicas e químicas dos óleos são fortemente influenciadas pela estrutura e configuração dos ácidos graxos (SENIHA GÜNER; YAĞCI; TUNCER ERCIYES, 2006), a modificação química dos óleos vegetais busca reduzir seus pontos de fragilidades e obter estruturas químicas que possibilitem futuras modificações controladas (HWANG; ERHAN, 2001).

Ao olhar a natureza, verifica-se que o óleo natural de vernonia (*Vernonia galamensis)* apresenta estrutura parcialmente oxidada, rico em ácido vernólico (Fig 3.2), que apresenta um grupo epóxidos que o estabiliza oxidativamente. Essa característica permite que o mesmo possa ser aplicado em situações em que o estresse térmico é inerente. (CHUA; XU; GUO, 2012; MEIER; METZGER; SCHUBERT, 2007)**.**

Sendo assim, a modificação artificial das ligações C=C, a fim de produzir derivados químicos epoxidados, vem atraindo a atenção de muitos grupos de pesquisa (HUANG et al., 2015). Essas alterações aumentam o leque de oportunidades

para utilização dos óleos vegetais como plataforma química para produção de materiais poliméricos (HUANG et al., 2015; OMONOV; KHARRAZ; CURTIS, 2016).

3.2. **Óleos Epoxidados**

O epóxido é utilizado para definir a formação de um éter cíclico em um anel com três elementos também conhecido como anel oxirano (PANCHAL et al., 2017). Os compostos químicos epoxidados devem apresentar em sua estrutura pelo menos um grupo epóxido, que normalmente costuma ser obtido a partir de uma reação entre um derivado insaturado e um composto que apresente oxigênio ativado (XIA; BUDGE; LUMSDEN, 2016).

O grupo epóxido, oxirano ou epóxi, é um dos grupamentos químicos mais interessantes devido a sua reatividade elevada e a quantidade de transformações a que podem ser sujeitos (SWERN, 1970). Na Figura 3.3, é apresentado a estrutura básica de um grupo epóxido.

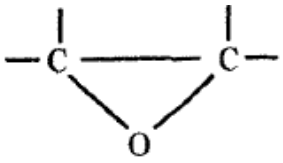

Figura 3.3. Estrutura básica do grupo epóxi.
Fonte: (SWERN, 1970)

Tal qual definido anteriormente, os óleos epoxidados devem apresentar em sua estrutura pelo menos um grupo epóxido, porém tanto os óleos naturais quanto os sintéticos costumam possuir mais de uma funcionalidade por molécula de triglicerídeo (XIA; BUDGE; LUMSDEN, 2016).

Conforme Muturi, Wang e Dirlikov (1994) o óleo de Vernonia (*Vernonia galamensis)* é o único óleo vegetal naturalmente epoxidado. O óleo de Vernonia contém 80-82% de ácido vernólico, que apresenta estrutura molecular com uma insaturação na posição 9 e o grupo epóxi formando o anel com os carbonos das posições 12 e 13. A estrutura dos triglicerídeos consiste predominantemente de trivernolina, que é um triglicerídeo esterificado com 3 ácidos vernólicos, cuja estrutura pode ser encontrada representada na Figura 3.2 da seção 3.1.

O óleo de Vernonia normalmente é utilizado como um diluente reativo para o preparo de formulações alquídicas e epoxídicas com baixo teor de compostos orgânicos voláteis (MUTURI; WANG; DIRLIKOV, 1994). Apesar de ser obtido naturalmente, as condições de cultivo e baixo rendimento extrativo do óleo de vernonia fazem com que a demanda por óleos epoxidados fique muito acima do que o potencial agrícola do cultivar.

Dessa forma, os óleos epoxidados devem ser obtidos sinteticamente de maneira a suprir a demanda de mercado existente de entorno de 240.000 toneladas/ano (KRALISCH et al., 2012). Essa obtenção se dá por meio da reação de epoxidação, Figura 3.4, na qual as duplas ligações carbono-carbono dos ácidos graxos reagem com um composto com oxigênio ativo, resultando na adição de um átomo de oxigênio na configuração do anel oxirano (GAMAGE; O'BRIEN; KARUNANAYAKE, 2009).

A epoxidação de alcenos constitui uma das reações mais úteis na síntese orgânica, uma vez que o grupo epóxido é um intermediário ativo facilmente transformado em outras funcionalidades (ERHAN et al., 2008; PANCHAL et al., 2017)

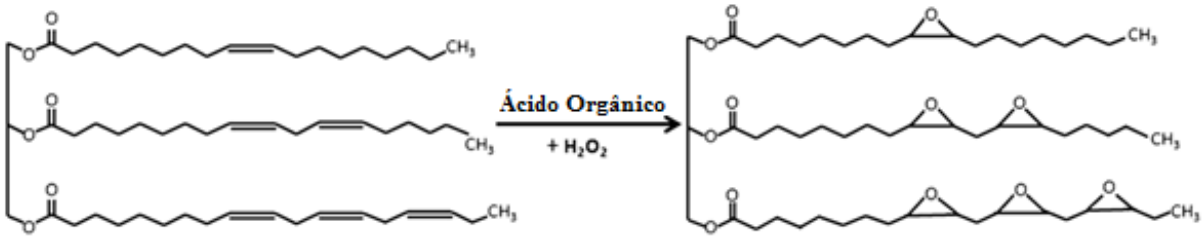

Figura 3.4. Reação genérica de epoxidação de triglicerídeos.

Fonte: (ANUAR et al., 2012)

A epoxidação de óleos vegetais é uma reação bem conhecida, com pedidos de patentes depositadas já em 1946 e com extensa literatura disponível ANUAR et al., 2012; BORUGADDA; GOUD, 2014, 2015; DE QUADROS; GIUDICI, 2016; PALUVAI; MOHANTY; NAYAK, 2015; SHARMA; DALAI, 2013; WU et al., 2000. O mercado mundial atual gira na faixa de 240.000 toneladas/ano, dos quais 90.000 toneladas/ano refere-se apenas ao mercado europeu (KRALISCH et al., 2012). Conforme a empresa *Markets and Markets* (2017), o mercado de óleo de soja epoxidado é projetado para

chegar a um volume financeiro movimentado de US$ 0,3 bilhões/ano em 2020, o que significa uma expectativa de crescimento de 10,3% ao ano entre 2015 e 2020. Esse aumento é justificado pelo aumento da demanda por plastificantes de base natural em substituição aos derivados de ftalatos, restringidos por lei nos mercados de países desenvolvidos e em nações emergentes como China, Índia e Brasil.

A epoxidação com oxigênio molecular, catalisada heterogeneamente pela prata, seria a rota mais barata e menos agressiva ao meio ambiente, porém trata-se de uma rota quase que restrita a olefinas com cadeia molecular curta, como o etileno e o butadieno (DINDA et al., 2008; GOUD; PRADHAN; PATWARDHAN, 2006). Quando esse processo é aplicado aos alquenos com cadeia carbônica mais longa, é normal a obtenção de uma quantidade substancial de derivados oxigenados como aldeídos e cetonas, resultantes da clivagem das insaturações presentes.

A alternativa encontrada para a epoxidação de triglicerídeos passa por processos nos quais estão envolvidos: uma molécula com oxigênio ativo, um catalisador, uma molécula que realizará o transporte do oxigênio e o substrato a ser epoxidado.

Genericamente, as demais maneiras de epoxidação podem ser encaixadas em: a) epoxidação com peróxidos orgânicos e inorgânicos, que inclui a epoxidação com peróxido de hidrogênio; b) epoxidação com haloidrinas, utilizando ácidos hipofosfatados (HOX) e seus sais como reagentes e c) epoxidação enzimática, com a utilização de lipases suportadas (GOUD; PATWARDHAN; PRADHAN, 2006).

Aplicados para triglicerídeos, encontra-se na literatura os seguintes métodos de reação: a) reação de Prilezhaev, catalisado por perácidos; b) epoxidação enzimática, catalisada por uma lipase e intermediado por um perácido de cadeia longa; c) epoxidação com metais, como molibdênio, ferro, tungstênio e titânio; d) epoxidação catalisada por líquidos iônicos e e) epoxidação com resina de troca iônica ácida (CHUA; XU; GUO, 2012; TAN; CHOW, 2010). Na Tabela 3.2 é apresentado um resumo de algumas publicações que se utilizam das reações descritas.

Entre os métodos mais comuns, a indústria comumente opta pela utilização da reação de Prilezhaev, catalisado por perácidos. Estes processos podem ser separados em duas categorias principais: a) na qual o perácido é pré-formado antes da reação de epoxidação e b) onde o perácido é gerado *in situ* no recipiente de reação (RANGARAJAN et al., 1995).

Tabela 3.2. Reação de epoxidação por diferentes métodos.

Epoxidação	Óleo vegetal	Condição do processo			Conversão (%)	Referência
		Temperatura (°C)	*Adição de H_2O_2 (h)	Tempo (h)		
Convencional	Soja	45; 55; 65; 75	0,5	12	nd	(CAI et al., 2008)
	Jatrofa	30; 50; 70; 85	0,5	3,4; 4,5; 10	35-88	(GOUD et al., 2010)
	Algodão	30; 45; 60; 75	0,5	4	80	(DINDA et al., 2008)
	Canola	40; 55; 65; 75	0,5	7	50-90,8	(MUNGROO et al., 2008)
RTI	Soja	30; 60; 75	0,5	8	73,1-97,7	(SANTACESARIA et al., 2011)
	Borracha	50-60	1; 2,5	5,5; 8	86-92	(PAN; SENGUPTA; WEBSTER, 2011)
Enzimática	Soja	50	0,083	24	50-98,9	(RÜSCH GEN. KLAAS; WARWEL, 1999)
COM	Soja	25	Nd	1-2	16-92	(GERBASE et al., 2002)

RTI – Resina de troca iônica; COM – Catálise organometálica; nd – não determinado; * peróxido adicionado à reação ao longo do tempo descrito

Uma vez que os peróxidos orgânicos são extremamente perigosos e apresentam riscos de detonação quando sujeitos a aquecimento e/ou outros estímulos físicos, levam a indústria a normalmente optar pela produção *in situ* do perácido orgânico derivado do ácido acético ou do ácido fórmico (ERHAN et al., 2008; PANCHAL et al., 2017; RANGARAJAN et al., 1995).

Na Figura 3.5 é apresentado um esquema simplificado da reação de epoxidação. A reação de epoxidação *in situ* ocorre em duas etapas: a) formação do perácido e b) reação do perácido com a ligação dupla (PANCHAL et al., 2017). A conversão das insaturações em epóxido depende de vários fatores tais como: a razão de peróxido por insaturação, razão de ácido carboxílico por insaturação, temperatura reacional, concentração de catalisador, velocidade da agitação e tempo de adição de H_2O_2 (SANTACESARIA et al., 2011).

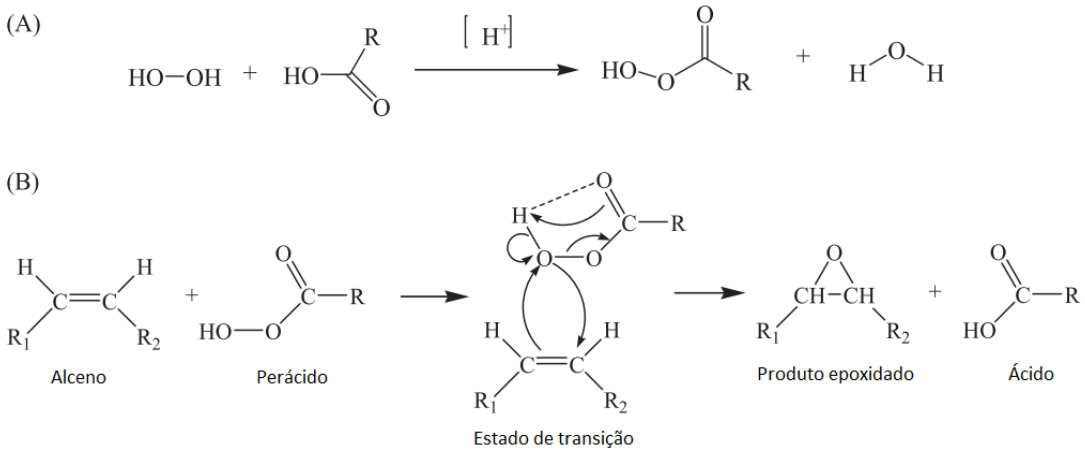

Figura 3.5. Esquema da reação de epoxidação.

Fonte: (CHUA; XU; GUO, 2012).

A reação de epoxidação de triglicerídeos, por meio de geração de perácidos *in situ*, trata-se de uma catálise bifásica que ocorre em emulsão de uma fase oleosa e uma fase aquosa (PANCHAL et al., 2017).

O mecanismo de epoxidação, representado na Figura 3.6, envolve os seguintes passos: a) formação do perácido (PAA) na fase aquosa - catalisada por um ácido

mineral e envolvendo a reação do H_2O_2 com o ácido carboxílico; b) transferência do perácido da fase aquosa para a fase oleosa; c) reação do perácido para formar o epóxido com consequente regeneração do ácido carboxílico e d) transferência do ácido carboxílico da fase oleosa para a fase aquosa (RANGARAJAN et al., 1995; SANTACESARIA et al., 2011).

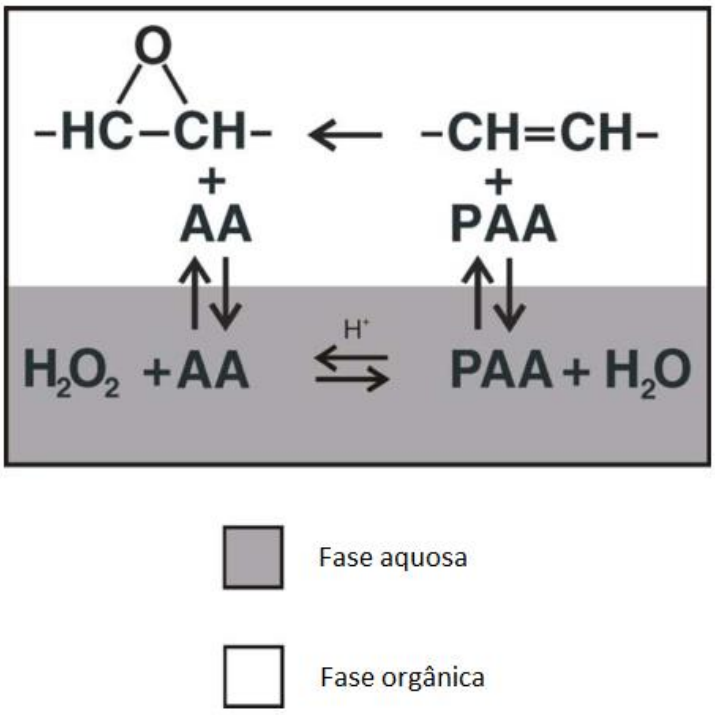

Figura 3.6. Dinâmica reacional da epoxidação em emulsão.

Fonte:(CAMPANELLA; BALTANÁS, 2006; CAMPANELLA; FONTANINI; BALTANÁS, 2008)

Nesse sistema de duas fases, que envolve reações em ambas, os fenômenos de transferência de massa interfacial e a termodinâmica do processo são fundamentais para a otimização do sistema produtivo (RANGARAJAN et al., 1995).

Outro fator que influencia as taxas de epoxidação é a composição de ácidos graxos do triglicerídeo. Na literatura, encontra-se descrito que a taxa de epoxidação aumenta com o aumento no número de insaturações do ácido oleico (18:1) para o linolênico (18:3) (COMERFORD et al., 2015). Enquanto a atividade de cada ligação dupla do ácido oleico e linoleico são equivalentes, as ligações duplas do ácido

linolênico são aproximadamente três vezes mais reativas do que as presentes nos demais ácidos graxos (COMERFORD et al., 2015; SCALA; WOOL, 2002).

Essa reatividade mais elevada pode resultar em produtos indesejados, uma vez que, da mesma forma que elas são mais sujeitas a sofrerem epoxidação, elas são igualmente propensas a sofrerem reações secundárias de maneira a diminuir a eficiência e seletividade do processo (COMERFORD et al., 2015).

Na indústria, os óleos epoxidados destinam-se, majoritariamente, à aplicação como estabilizantes e/ou plastificantes para o polímeros clorados como o PVC (BENANIBA; BELHANECHE-BENSEMRA; GELBARD, 2007; KRALISCH et al., 2012)

Em relação aos óleos vegetais de partida, os óleos epoxidados apresentam sua densidade, viscosidade e estabilidade oxidativa aumentados (HARO et al., 2016). Isto é resultado das alterações na massa molecular, redução no índice de insaturação e modificação dos tipos e intensidades das forças intermoleculares existentes (WU et al., 2000).

Até o momento, já foram relatados a epoxidação de vários óleos vegetais como: Mahua (GOUD; PATWARDHAN; PRADHAN, 2006), Canola (ANUAR et al., 2012; SHARMA; DALAI, 2013; WU et al., 2000), Mamona (BORUGADDA; GOUD, 2014, 2015; PALUVAI; MOHANTY; NAYAK, 2015), Soja (HWANG; ERHAN, 2001; KRALISCH et al., 2012), Algodão (DINDA et al., 2008), Karanja (GOUD et al., 2007; GOUD; PRADHAN; PATWARDHAN, 2006), Girassol (BENANIBA; BELHANECHE-BENSEMRA; GELBARD, 2007), Jatropha (GOUD et al., 2010), Linhaça (MUTURI; WANG; DIRLIKOV, 1994), Milho (PENG; LIN, 2014), Arroz (NIHUL; MHASKE; SHERTUKDE, 2014) e Uva (HARO et al., 2016). Na Tabela 3.3 podem ser encontradas as condições otimizadas de epoxidação de diversos óleos vegetais.

Tabela 3.3. Condições otimizadas de epoxidação de triglicerídeos

Óleo	Ácido	C=C/Ácido/H_2O_2 (mol/mol/mol)	Catalisador (w/w)	Condição da Reação	Rend	Referência
Algodão	Ácido acético glacial	2,5:0,75:1,1	H_2SO_4 2%	60°C, 8h, 2400 rpm	93,9%	(DINDA et al., 2008)
Algodão	Ácido fórmico	2,5:0,75:1,1	H_2SO_4 2%	60°C, 8h, 2400 rpm	94,6%	(DINDA et al., 2008)
Soja	Ácido acético	2,0:0,75:1,3	H_2SO_4 2%	60°C, 10h, 1800 rpm	83,3%	(MEYER et al., 2008)
Jatrofa	Ácido acético	2,0:0,75:1,3	H_2SO_4 2%	60°C, 10h, 1800 rpm	87,4%	(MEYER et al., 2008)
Mahua	Ácido acético glacial	2,00:0,75:0,8	H_2SO_4 2%	85°C, 3.5h, 1500 rpm	83%	(GOUD; PATWARDHAN; PRADHAN, 2006)
Canola	Ácido acético	1:0,5:1,5	Amberlite IR-120	65°C	90%	(MUNGROO et al., 2008)
Karanja	Ácido acético glacial	1:0,5:1,5	H_2SO_4 2%	70°C, 6h, 1500 rpm	80%	(GOUD; PRADHAN; PATWARDHAN, 2006)
Soja	Ácido fórmico	1:2:20	-	40°C, 20h	-	(CAMPANELLA; BALTANÁS, 2006)
Girassol	Ácido fórmico	1:2:20	-	40°C, 20h	-	(CAMPANELLA et al., 2010)
Soja	Ácido acético glacial	1:0:1	Novozyme 435	60°C, 24h, 350 rpm	96,3%	(VLČEK; PETROVIĆ, 2006)
Canola	Ácido acético	1:0,5:2	Amberlite IR-120	75°C, 5.5h	93%	(MONONO; HAAGENSON; WIESENBORN, 2015)
Arroz	Ácido fórmico	1:0,5:1,5	H_2SO_4 3%	60°C, 6h, 1600 rpm	92%	(NIHUL; MHASKE; SHERTUKDE, 2014)

Rend - Rendimento

Uma vez que o ambiente reacional da epoxidação contém água, ácido mineral (catalisador) e ácido orgânico, reações subsequentes podem resultar na decomposição dos grupos epóxi. Na Figura 3.7 são apresentadas algumas das reações de decomposição do anel oxirano como resultado da hidrólise, acilação, etc. (KÖCKRITZ; MARTIN, 2008).

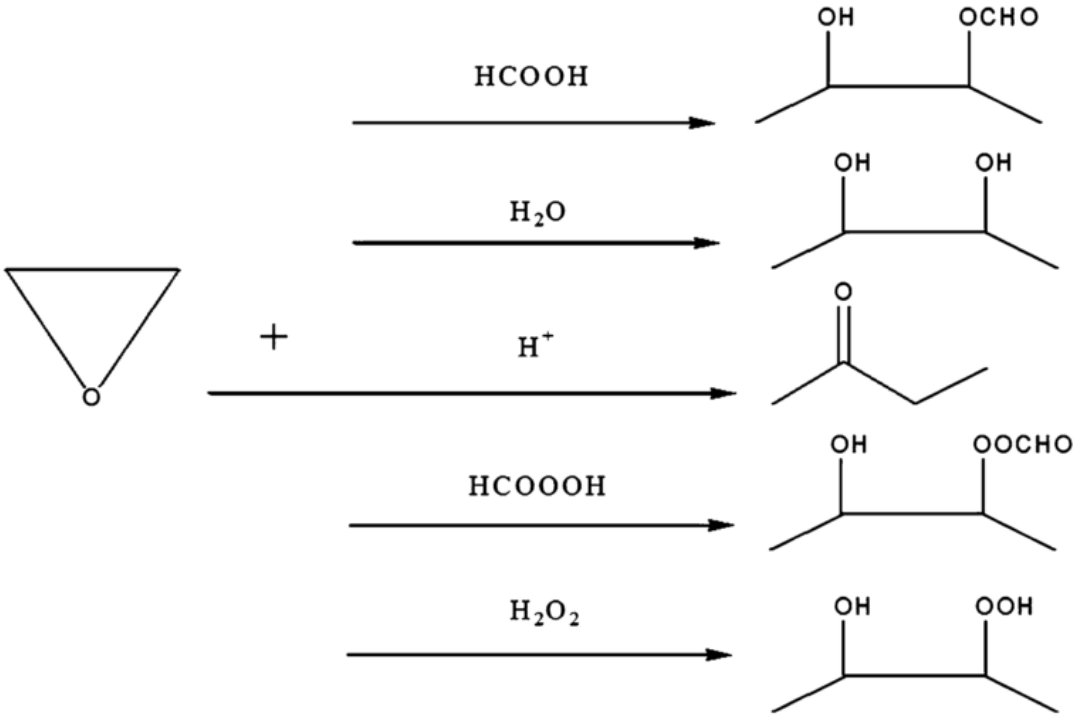

Figura 3.7. Reações laterais da reação de epoxidação.
Fonte: (NIHUL; MHASKE; SHERTUKDE, 2014)

Muito embora o anel oxirano esteja sujeito a muitos processos degradativos, a sua atividade química permite que o grupo epóxi possa ser utilizado como ponto de partida para obtenção de produtos com maior valor agregado. Classicamente, os grupos oxiranos são utilizados como intermediários para produção de compostos químicos tais como: álcoois, glicóis, alcanolaminas e materiais poliméricos como poliésteres e resinas epóxi (CAI et al., 2008; GOUD; PATWARDHAN; PRADHAN, 2006).

Mais recentemente, a pesquisa acadêmica e industrial tem se voltado para novas oportunidades. Grupos como os polióis, os acetais cíclicos e os carbonatos cíclicos, representados na Figura 3.8, estão entre as funcionalidades com potencial

para constituição de novas plataformas químicas derivados de triglicerídeos (RILEY; VERKADE; ANGELICI, 2015).

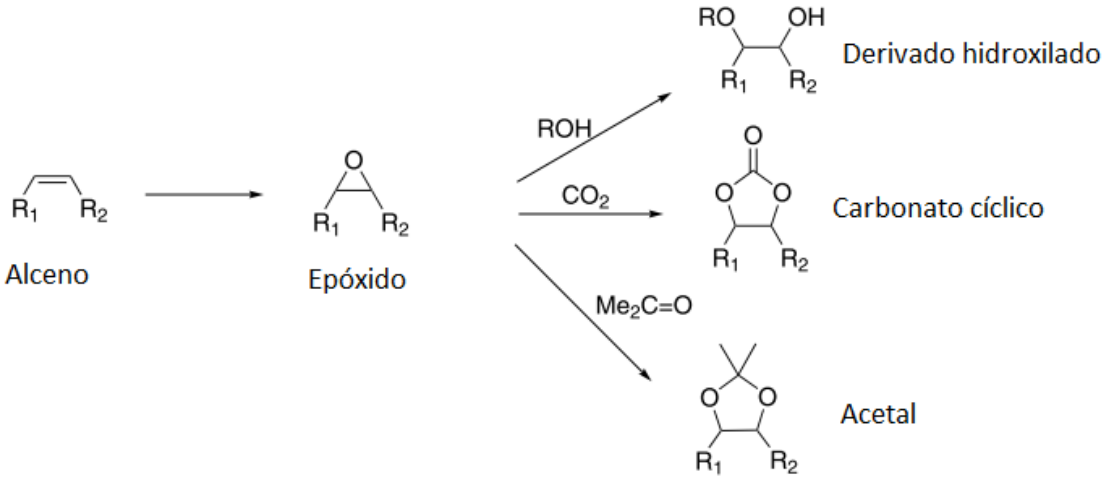

Figura 3.8. Possíveis derivados que podem ser obtidos a partir do grupo oxirano.
Fonte: (RILEY; VERKADE; ANGELICI, 2015).

3.3. **Óleos Carbonatados**

3.3.1. **Utilização de CO_2**

A humanidade depende dos recursos fósseis como principal fonte de energia e matérias-primas, porém o CO_2 residual é um importante passivo ambiental atuando nas mudanças climáticas globais (NORTH; PASQUALE; YOUNG, 2010). A preocupação com as emissões antropogênicas têm despertado recentemente interesse em promover estudos sobre fontes alternativas de energia e desenvolvimento de sistemas para a utilização química de CO_2 (APPEL et al., 2013; SAPTAL; BHANAGE, 2017; ZHENG et al., 2015).

Atualmente, a captura e o armazenamento de carbono, bem como a utilização do CO_2 excedente, são estratégias amplamente fomentadas e investigadas para reduzirem-se as emissões de carbono, porém trata-se de uma prática que demanda muita energia e com processos ainda pouco viáveis para aplicação em larga escala (NORTH; PASQUALE; YOUNG, 2010). Por outro lado, a existência de um excedente de CO_2 lançado na atmosfera, por vezes produzidos com elevada pureza, representa

uma oportunidade interessante de utilizá-lo como matéria-prima para síntese de derivados químicos de alto valor agregado e com propriedades que nenhuma outra classe de materiais possui.

O gás carbônico é atóxico, não combustível, pode servir como solvente “verde” e pode ter suas propriedades como densidade, polaridade, parâmetro de solubilidade otimizados para a aplicação destinada (MILOSLAVSKIY et al., 2014). Do ponto de vista químico, o dióxido de carbono é uma molécula linear com uma distância muito curta das ligações C-O, na ordem de 1,16 Å. Embora ela seja globalmente apolar, o CO_2 contém ligações polares devido à diferença na eletronegatividade entre os átomos de carbono e oxigênio (APPEL et al., 2013).

O CO_2 é cineticamente e termodinamicamente estável, com características eletrofílicas no átomo de carbono e nucleofílicas no átomo de oxigênio (SAPTAL; BHANAGE, 2017). Com LUMO localizado no carbono, a estrutura eletrônica do CO_2 é melhor representada como $O^{-\delta}–C^{+2\delta}–O^{-\delta}$, destacando sua suscetibilidade ao ataque nucleofílico no carbono e ataque eletrofílico no oxigênio (APPEL et al., 2013). Do ponto de vista sintético, o dióxido de carbono é considerado um bloco de construção C1, isto é, a partir do qual pode-se obter novos compostos por meio da incorporação de uma molécula com um único carbono (ZHENG et al., 2015). Porém, sua limitada reatividade constitui-se em uma barreira técnica ainda em processo de superação (LI et al., 2008).

3.3.2. **Óleos Carbonatados**

A fixação química de CO_2 é altamente atraente do ponto de vista da utilização de recursos de carbono (LIU; WANG, 2017). O carbonato orgânico se refere a um grupo funcional que contém um átomo de carbono ligado a três átomos de oxigênio, sendo constituído por uma carbonila (C=O) ligada a dois grupos alcoxi (O-R). Se esses átomos estão organizados em uma cadeia de carbono em formato de um anel, trata-se, então, de um caso especial chamado de "carbonato cíclico" (DOLL, 2015). A síntese de carbonatos acíclicos, cíclicos e policarbonatos vêm crescendo em importância, sendo o dimetil carbonato e o difenilcarbonato os principais derivados acíclicos comercializados (NORTH; PASQUALE; YOUNG, 2010). Já os carbonatos de etileno, propileno e glicerol estão entre os carbonatos orgânicos cíclicos mais comuns

(DOLL, 2015). Na Figura 3.9, são apresentados alguns dos principais carbonatos disponíveis comercialmente.

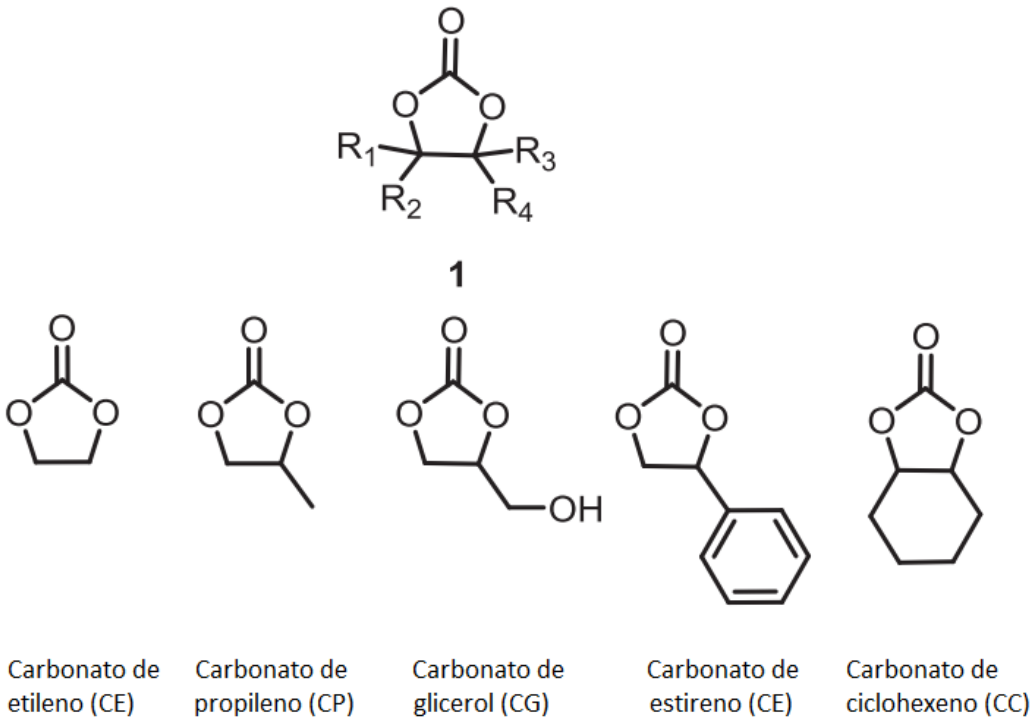

Figura 3.9. Principais carbonatos cíclicos comerciais.
Fonte: (BOBBINK; DYSON, 2016)

Ao passo em que os carbonatos de cadeia curta, tais como os apresentados anteriormente, são frequentemente derivados de matérias-primas fósseis, os carbonatos orgânicos de cadeia longa podem ser preparados a partir de substratos oleoquímicos e servir como importantes intermediários sintéticos (HOLSER, 2007; SUN et al., 2009).

O crescente interesse do meio acadêmico em carbonatos oleoquímicos é perceptível a partir do aumento no número de artigos indexados em revistas científicas internacionais. A análise bibliométrica descritiva foi conduzida com base nas referências obtidas durante a revisão bibliográfica utilizando o banco de dados de resumos e citações *Scopus* (Elsevier).

Definido o escopo da revisão bibliográfica, definiu-se as palavras-chave para estabelecer o primeiro filtro para a seleção dos artigos. Os termos que delimitam o

eixo temático principal do trabalho são: *“alkyl esters”*, “*fatty acid”*, *“fatty acid esters”*, *oleochemicals*, *“soybean oil”*, *triglyceride* e *“vegetable oil”*.

O primeiro filtro delimita as publicações encontradas ao eixo temático principal do trabalho e, a fim de tornar os resultados obtidos mais específicos, um segundo filtro foi aplicado de maneira a conjugar os resultados iniciais com a produção de carbonatos cíclicos, segundo eixo temático do trabalho. As palavras-chave que delimitam o segundo eixo temático do trabalho são: *“biobased carbonates”*, *biocarbonates*, *carbonated*, *carbonates*, *carbonation*, *“cyclic carbonates”*, NIPUs, “nonisocyanate *polyurethane” e “non-isocyanate polyurethane”*.

As publicações identificadas resultam de múltiplas combinações das palavras-chave do primeiro e do segundo filtro e, na Tabela 3.4, são discriminadas, por ano, todas as publicações identificadas que envolvem a produção e/ou aplicação de carbonatos oleoquímicos.

Tabela 3.4. Carbonatos oleoquímicos, referências discriminadas por ano.

Ano	Documentos	Referências
2004	1	(TAMAMI; SOHN; WILKES, 2004)
2005	2	(DOLL et al., 2005; DOLL; ERHAN, 2005)
2006	2	(NADUPPARAMBIL; STOFFER, 2006; PARZUCHOWSKI et al., 2006)
2007	1	(HOLSER, 2007)
2008	5	(JALILIAN; YEGANEH; HAGHIGHI, 2008; JAVNI; HONG; PETROVIĆ, 2008; LI et al., 2008; MANN et al., 2008; TÜRÜNÇ et al., 2008)
2009	0	-
2010	1	(JALILIAN; YEGANEH; HAGHIGHI, 2010)
2011	0	-
2012	4	(BÄHR; MÜLHAUPT, 2012; MAHENDRAN et al., 2012; MAZO; RIOS, 2012; WANG et al., 2012)
2013	6	(FIGOVSKY et al., 2013; HAMBALI et al., 2013; JAVNI; HONG; PETROVIČ, 2013; LANGANKE; GREINER; LEITNER, 2013; MAZO; RIOS, 2013; XU, WEN-JIE et al., 2013)
2014	5	(MAHENDRAN et al., 2014; MILOSLAVSKIY et al., 2014; SCHÄFFNER et al., 2014; WERNER; TENHUMBERG; BÜTTNER, 2014; ZHANG et al., 2014a)
2015	7	(ALVES et al., 2015; BÜTTNER et al., 2015; BÜTTNER; STEINBAUER; WERNER, 2015; JALILIAN; YEGANEH, 2015; LEE; DENG, 2015; LEVINA et al., 2015; ZHENG et al., 2015)
2016	8	(AIT AISSA et al., 2016; BÜTTNER et al., 2016; DOLL et al., 2016; GRIGNARD et al., 2016; NARRA et al., 2016; POUSSARD et al., 2016; SAMANTA et al., 2016; TENHUMBERG et al., 2016)
2017	11	(BÜTTNER et al., 2017a; CAI et al., 2017; DOLL et al., 2017; FARHADIAN et al., 2017; GUZMÁN; ECHEVERRI; RIOS, 2017; HANIFFA et al., 2017; LOULERGUE et al., 2017; MALIK; KAUR, 2017; PEÑA CARRODEGUAS et al., 2017; RUIZ et al., 2017; STEINBAUER et al., 2017)
2018	3	(DOLEY; DOLUI, 2018; LONGWITZ et al., 2018; ZHENG et al., 2018)
Total	56	

Na Figura 3.10 é apresentado o gráfico de publicações/ano, que abrange desde a primeira publicação, realizado por Tamami, Sohn e Wilkes (2004), até às mais recentes publicações de Zheng et al. (2018) e Longwitz et al. (2018).

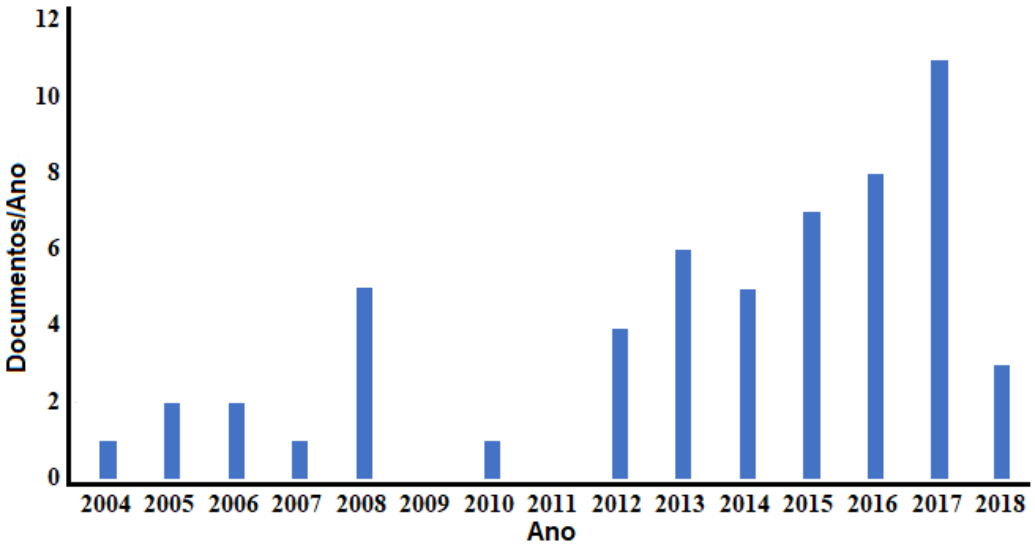

Figura 3.10. Gráfico de publicações/ano sobre carbonatos oleoquímicos.

Conforme apresentado na Figura 3.10, após a primeira publicação sobre a produção de carbonatos cíclicos derivados de triglicerídeos, há um pequeno número de publicações durante o período de 2005 - 2008, onde a investigação limitou-se aos tópicos: catálise com CO_2 supercrítico e produção de poliuretano sem isocianato. As primeiras publicações seguem um período (2009 - 2011) onde registra-se apenas uma publicação (JALILIAN; YEGANEH; HAGHIGHI, 2010), sem grande acréscimo à literatura prévia.

Um terceiro período, 2012 - presente, registra um aumento gradual de publicações sobre a produção de carbonatos oleoquímicos e representa uma retomada de interesse acadêmico no tópico, principalmente motivado pelo interesse no desenvolvimento das tecnologias de utilização de carbono e da “Química Verde”. Nos últimos anos, observa-se avanços significativos para a área, podendo ser destacado os estudos sobre a Avaliação do Ciclo de Vida, a produção de poliuretano sem isocianato e a triagem e descrição de diversos catalisadores.

A produção de carbonatos cíclicos encontram muitas aplicações industriais devido às suas propriedades químicas únicas como biodegradabilidade, baixa toxicidade e ponto de fulgor elevados (KENAR; TEVIS, 2005). Enquanto os

carbonatos de cadeia curta tem aplicações patenteadas como solventes “verdes”, eletrólitos para baterias de lítio e base de polímeros com massa molecular baixa/média, os carbonatos oleoquímicos apresentam patentes depositadas para aplicações como plastificantes, agentes terapêuticos e plataforma para produção de polímeros com elevada massa molecular (DOLL et al., 2005)

Existem vários métodos para preparar carbonatos, sendo uma das mais atraentes a reação entre o dióxido de carbono (CO_2) e um epóxido (ALVES et al., 2015). Esta rota de síntese apresenta 100% de eficiência atômica, ou seja, o CO_2 é incorporado completamente no substrato epoxidado sem liberação de subprodutos ou resíduos (ALVES et al., 2015).

A eficiência atômica é apenas um de um total de doze princípios da química verde, sendo estes: (1) prevenção de geração resíduos, (2) economia de átomos, (3) síntese menos perigosa, (4) design de produtos químicos menos agressivos, (5) uso de solventes menos agressivos e auxiliares, (6) eficiência energética, (7) uso de fontes renováveis, (8) redução de geração de subprodutos/derivados, (9) uso de catálise, (10) design de moléculas para degradação, (11) análise em tempo real para prevenção da poluição e (12) prevenção de acidentes (ANASTAS; EGHBALI, 2010; DEVIERNO KREUDER et al., 2017; GAŁUSZKA; MIGASZEWSKI; NAMIEŚNIK, 2013).

Dessa forma, no contexto atual de redução da pegada ecológica da humanidade, essa rota tecnológica apresenta-se como uma forma potencial de incorporar dióxido de carbono residual em matérias primas com valor agregado e propriedades diferenciadas (NORTH; PASQUALE; YOUNG, 2010). Na Figura 3.11 é apresentado um esquema simplificado da reação de formação de carbonatos cíclicos a partir do anel oxirano e do dióxido de carbono.

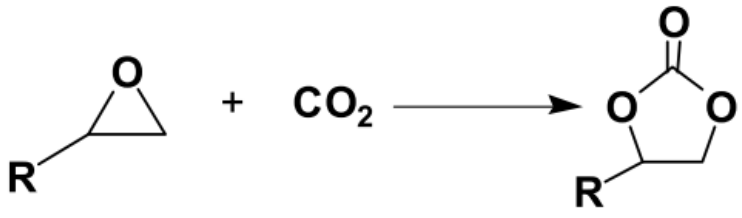

Figura 3.11. Reação de carbonatação simplificada.

Fonte: (SUN et al., 2009)

Já foram descritos na literatura a carbonatação a partir de diversas fontes oleaginosas. Da mesma forma como já descrito anteriormente, para a síntese de carbonatos oleoquímicos a rota mais interessante é pela incorporação de CO_2 diretamente nos óleos epoxidados (MANN et al., 2008). Na Figura 3.12 é apresentado a estrutura de um triglicerídeo carbonatado.

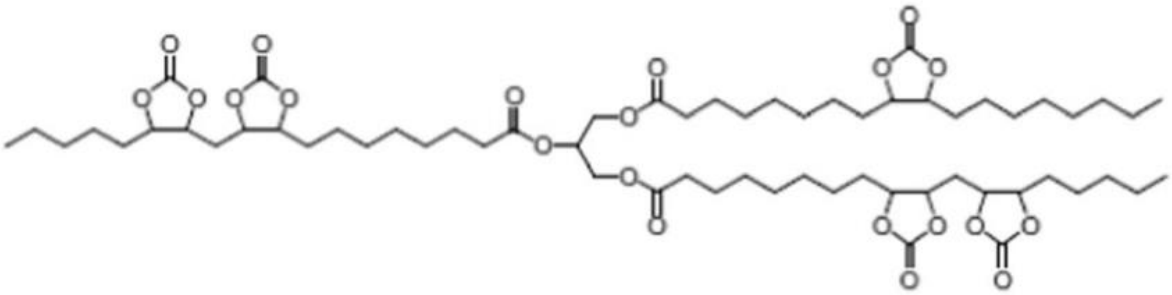

Figura 3.12. Estrutura de um triglicerídeo carbonatado.
Fonte: (KATHALEWAR et al., 2013)

Embora a cicloadição de CO_2 em pequenos epóxidos tenha atingido níveis adequados de eficiência, a carbonatação de derivados oleoquímicos apresenta o impedimento estérico dos grupos funcionais internos da molécula de triglicerídeo, sendo necessário elevadas temperaturas (>100°C) e pressões (>10 Bar) para alcançar níveis adequados de rendimento (LI et al., 2008).

A cicloadição de gás carbônico em epóxidos é aplicável, sem muitas diferenças, tanto para triglicerídeos quanto para os ésteres metílicos derivados dos óleos vegetais (DOLL et al., 2005; HOLSER, 2007; KENAR; TEVIS, 2005). Embora existam muitas matérias primas a serem exploradas, até o momento os óleos carbonatados descritos são: Soja (DOLL; ERHAN, 2005; LI et al., 2008; MAZO; RIOS, 2012; PARZUCHOWSKI et al., 2006; TAMAMI; SOHN; WILKES, 2004), Vernonia (MANN et al., 2008), Linhaça (ALVES et al., 2015; BÄHR; MÜLHAUPT, 2012), Algodão (ZHANG et al., 2014a), Alga (XU, WEN-JIE et al., 2013), Canola (MALIK; KAUR, 2017), Jatropha (HANIFFA et al., 2017), Brócolis (LOULERGUE et al., 2017) Girassol (BÜTTNER et al., 2017a) e Mamona (GUZMÁN; ECHEVERRI; RIOS, 2017).

Os trabalhos sobre a síntese de carbonato de óleos vegetais podem ser classificados em três grupos de processamento tecnológico, na qual a principal

diferença se encontra na pressão de CO_2 (MILOSLAVSKIY et al., 2014). Constituem-se nas rotas técnicas exploradas até o momento: a) as reações sob fluxo de CO_2 à pressão atmosférica (HOLSER, 2007; MAZO; RIOS, 2012; TAMAMI; SOHN; WILKES, 2004); b) síntese em reatores com pressões de CO_2, compreendendo reações conduzidas com pressões acima da pressão atmosférica e abaixo do ponto crítico do CO_2 (73,8 Bar e 31,04°C) (ALVES et al., 2015; ZHANG et al., 2014a) e c) reação com CO_2 supercrítico, com pressões e temperatura acima do ponto crítico do dióxido de carbono (DOLL; ERHAN, 2005; MANN et al., 2008).

Cada um dos processos descritos apresenta vantagens e desvantagens. A reação realizada sob fluxo de CO_2 se constitui na rota técnica de menor custo produtivo, porém os elevados tempos reacionais diminuem o potencial produtivo do processo. As reações conduzidas sob pressões elevadas apresentam tempos de reação menores e conversão superiores, porém o custo de produção eleva-se devido a necessidade de aquisição de reatores adequados ao fim. Por fim, as reações utilizando CO_2 supercrítico apresentam tempo de reação substancialmente menores, custos elevados e ainda necessitam de extenso estudo para otimização do processo. Uma vez que o CO_2 supercrítico na reação de carbonatação atua simultaneamente como solvente e reagente, o ajuste da densidade do fluído e sua polaridade é essencial para que o tempo reacional seja reduzido sem que a atividade catalítica seja prejudicada.

Uma vez observado os óleos que já foram utilizados na literatura, na Tabela 3.5 é apresentado uma breve descrição da condição otimizada de carbonatação encontrada por diversos autores.

Tabela 3.5. Condição de carbonatação descrito na literatura

Óleo	Temperatura	Agitação	Pressão	Solvente	Catalisador	Cat (mol%)	Conversão	Tempo	Referências
Soja	100°C	500 rpm	1 Bar	DMF	TBAB	3%	~45%	70h	(MAZO; RIOS, 2013)
Soja	120°C	500 rpm	1 Bar	DMF	TBAB	5%	~80%	70h	
Soja	140°C	500 rpm	1 Bar	DMF	TBAB	7%	~85%	70h	
Soja	100°C	500 rpm	1 Bar	DMF	TBAB/água	5%	50%	70h	
Soja	120°C	500 rpm	1 Bar	DMF	TBAB/água	5%	90%	70h	
Soja	140°C	500 rpm	1 Bar	DMF	TBAB/água	5%	90%	70h	
Soja	120°C	NE	10 Bar	DMF	TBAB	3%	71,30%	20h	(LI et al., 2008)
Soja	120°C	NE	10 Bar	DMF	$SnCl_4$. $5H_2O$	3%	64,40%	20h	
Soja	120°C	NE	10 Bar	DMF	TBAB/$SnCl_4$. $5H_2O$ (5/1)	3%	84,70%	20h	
Soja	120°C	NE	10 Bar	DMF	TBAB/$SnCl_4$. $5H_2O$ (4/1)	3%	87,40%	20h	
Soja	120°C	NE	10 Bar	DMF	TBAB/$SnCl_4$. $5H_2O$ (2/1)	3%	85,80%	20h	
Soja	120°C	NE	10 Bar	DMF	TBAB/$SnCl_4$. $5H_2O$ (1,5/1,5)	3%	81,10%	20h	
Soja	120°C	NE	10 Bar	DMF	TBAB/$SnCl_4$. $5H_2O$ (1/2)	3%	79,00%	20h	
Soja	120°C	NE	10 Bar	DMF	TBAB/$SnCl_4$. $5H_2O$ (3/1)	3%	89,20%	20h	
Soja	140°C	NE	10 Bar	DMF	TBAB/$SnCl_4$. $5H_2O$ (3 /1)	3%	95%	20h	
Soja	140°C	NE	6 Bar	DMF	TBAB/$SnCl_4$. $5H_2O$ (3 /1)	3%	92%	20h	
Soja	140°C	NE	15 Bar	DMF	TBAB/$SnCl_4$. $5H_2O$ (3 /1)	3%	95%	20h	
Soja	140°C	NE	15 Bar	DMF	TBAB/$SnCl_4$. $5H_2O$ (3 /1)	3%	86,90%	10h	
Soja	110°C	NE	10 Bar	SS	TBAB	5%	94,00%	70h	
Soja	100°C	NE	103 Bar (SC)	SS	TBAB	5%	100,00%	40	(DOLL; ERHAN, 2005)
Soja	100°C	NE	103 Bar (SC)	SS	TBAB	5%	94,00%	20	
Soja	100°C	NE	103 Bar (SC)	SS	TBAB	5%	82,00%	10	
Linhaça	140°C	NE	10 Bar	SS	TBAB	3%	NE	NE	(BÄHR; MÜLHAUPT, 2012)
Linhaça	140°C	NE	30 Bar	SS	TBAB	3%	NE	NE	
Soja	110°C	NE	1 Bar	SS	TBAB/$CaCl_2$	5% molar	98,00%	NE	(JALILIAN; YEGANEH; HAGHIGHI, 2008)

Tabela 3.5. (Continuação).

Óleo	Temperatura	Agitação	Pressão	Solvente	Catalisador	Cat (mol%)	Conversão	Tempo	Referências
Algodão	100°C	NE	30 Bar	SS	TBAB	5%	50,00%	24h	
Algodão	110°C	NE	30 Bar	SS	TBAB	5%	65,00%	24h	
Algodão	120°C	NE	30 Bar	SS	TBAB	5%	75,00%	24h	
Algodão	130°C	NE	30 Bar	SS	TBAB	5%	88,00%	24h	
Algodão	140°C	NE	30 Bar	SS	TBAB	5%	99,00%	24h	
Algodão	140°C	NE	25 Bar	SS	TBAB	5%	90,00%	24h	
Algodão	140°C	NE	20 Bar	SS	TBAB	5%	83,00%	24h	
Algodão	140°C	NE	15 Bar	SS	TBAB	5%	81,00%	24h	
Algodão	140°C	NE	10 Bar	SS	TBAB	5%	77,00%	24h	
Algodão	140°C	NE	30 Bar	SS	TBAB	5%	94,00%	6h	(ZHANG et al., 2014a)
Algodão	140°C	NE	30 Bar	SS	TBAB	5%	95,50%	9h	
Algodão	140°C	NE	30 Bar	SS	TBAB	5%	97,00%	12h	
Algodão	140°C	NE	30 Bar	SS	TBAB	5%	98,50%	15h	
Algodão	140°C	NE	30 Bar	SS	TBAB	5%	99,00%	18h	
Algodão	140°C	NE	30 Bar	SS	TBAB	5%	99,00%	21h	
Algodão	140°C	NE	30 Bar	SS	TBAB	1,50%	65,00%	24h	
Algodão	140°C	NE	30 Bar	SS	TBAB	3%	80,00%	24h	
Algodão	140°C	NE	30 Bar	SS	TBAB	5%	99,00%	24h	
Algodão	140°C	NE	30 Bar	SS	TBAB	7%	99,00%	24h	
Algodão	140°C	NE	30 Bar	SS	TBAB	10%	99,00%	24h	

SS – Sem solvente; DMF – Dimetilformamida; SC – Supercrítico; TBAB – Brometo de tetrabutilamônio; NE – Não especificado

Pelo que já está consagrado pelas pesquisas acadêmicas, a temperatura, a concentração de catalisador e quantidade de gás carbônico dissolvido na fase líquida são fatores que controlam a taxa reacional (ZHENG et al., 2015). Sendo assim, a taxa de carbonatação deve ser expressa em relação a concentração de TBAB, a concentração de grupo oxirano e quantidade de CO_2 dissolvido (CAI et al., 2017).

À medida em que a reação avança, e os grupos oxiranos são convertidos, a viscosidade do meio aumenta e influencia fortemente o fenômeno de transferência de massa gás-líquido (CAI et al., 2017). Já foi descrito que o coeficiente de transferência de massa de CO_2 diminui com a conversão de epóxido, como consequência da alteração da viscosidade do meio, porém a solubilidade de CO_2 mostra-se independente do avanço da reação e inversamente relacionado com o aumento da temperatura (ZHENG et al., 2015)

Sendo o CO_2 uma molécula muito estável, atribui-se o sucesso da reação à habilidade do catalisador em ativar o dióxido de carbono. O bom desempenho dos sais quaternários de amônio para carbonatação pode ser explicado pelo comportamento lábil do ânion. O volume e densidade eletrônica do cátion leva o ânion a se afastar e a reduzida interação eletrostática torna o ânion um nucleófilo mais efetivo (CALÓ et al., 2002). Ao final da reação, o brometo ainda mostra-se um bom grupo de saída e desloca-se de maneira a permitir a formação do carbonato e regeneração do catalisador (COMERFORD et al., 2015).

O mecanismo mais aceito para esta reação inicia pela abertura do anel oxirano por meio do ataque nucleofílico do brometo e segue os seguintes etapas: a) o ânion do catalisador realiza o ataque nucleofílico no anel epóxido; b) existe então a formação de um alcóxido e c) o alcóxido realiza um ataque ao dióxido de carbono para formar o carbonato e regenerar o catalisador (COMERFORD et al., 2015). Na Figura 3.13, é apresentado o mecanismo reacional proposto para reação de carbonatação por intermédio do TBAB.

Além da clássica reação de carbonatação com brometo de tetrabutilamônio e aquecimento convencional, outras alternativas de síntese foram reportadas como: a) intensificação por micro-ondas (MAZO; RIOS, 2012); b) adição de água junto com TBAB (MAZO; RIOS, 2013) e c) sistema de catálise com a utilização de TBAB mais algum co-catalisador (BÜTTNER et al., 2016; COMERFORD et al., 2015; LI et al., 2008; TENHUMBERG et al., 2016).

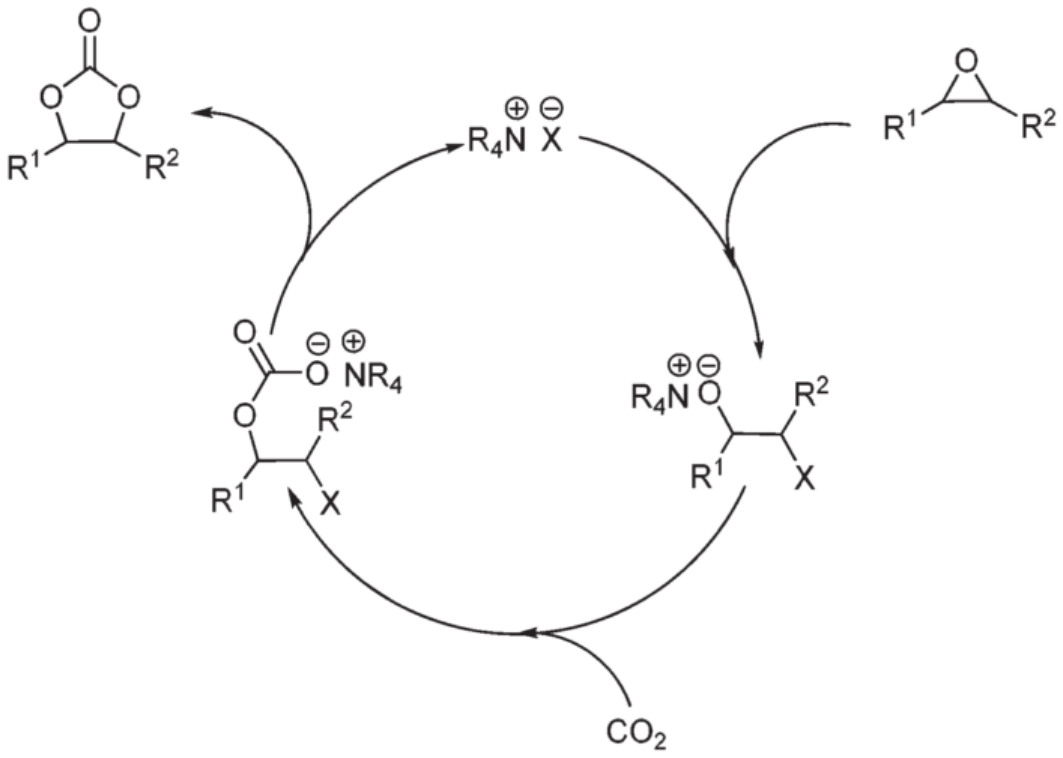

Figura 3.13. Mecanismo de reação de carbonatação.
Fonte: (LANGANKE; GREINER; LEITNER, 2013)

Uma vez que muito do esforço dedicado aos trabalhos de carbonatação estão voltados à produção de poliuretanos ou na apresentação de novos catalisadores, muito pouco têm-se atentado para promover estudos de otimização dos sistemas já descritos, o que configura a existência de oportunidades de estudos para essas rotas tecnológicas.

Nos Anexos B-E são apresentados os melhores resultados obtidos por diferentes catalisadores (Anexo B e D) e sistemas de catalisadores (Anexo C e E) aplicados para produção de carbonatos oleoquímicos derivados de óleos vegetais (Anexo B e C) e carbonatos oleoquímicos derivados de ésteres monoalquílicos (Anexo D e E).

Por fim, é observado que a produção de produtos químicos a partir do CO_2 não só tem apelo econômico, mas também ambiental. Têm-se que a cicloadição de CO_2 em epóxidos, a fim de obter carbonato cíclicos de cinco membros, poderá constituir-

se em uma plataforma química importante para subsequente produção de poliuretanos sem intermédio de isocianatos (LI et al., 2008).

3.4. **Relação quantitativa estrutura-propriedade (QSPR)**

O uso de CO_2 como bloco de construção C1 desempenhará um papel importante na indústria química de baixo carbono (BÜTTNER et al., 2017b; STERNBERG; JENS; BARDOW, 2017). No entanto, o dióxido de carbono é um agente químico termodinamicamente estável, cuja ativação apresenta significativas barreiras energéticas que devem ser superados por meio de processos físicos e químicos (CAI et al., 2017; POLIAKOFF; LEITNER; STRENG, 2015). Portanto, o uso de catalisadores é essencial para que os processos baseados em dióxido de carbono sejam economicamente viáveis e com uma razoável penalidade energética (ALVES et al., 2017; POLIAKOFF; LEITNER; STRENG, 2015).

A triagem/desenho de catalisadores para promover a cicloadição de dióxido de carbono a epóxidos é um desafio que deve ser ativamente abordado pela comunidade acadêmica. Sendo assim, a fim de reduzir o tempo e os custos envolvidos na pesquisa científica, as ferramentas de quimioinformática: Dinâmica Molecular (*Molecular Dynamics - MD*), Teoria do Funcional da Densidade (*Density Functional Theory - DFT*) e Relação Quantitativa Estrutura-Propriedade (*Quantitative Structure-Property Relationship* - QSPR) poderiam ser aplicadas para aumentar a compreensão química e mecanística da reação (BLAY et al., 2016).

A modelagem QSPR é baseada na suposição de que, a partir da estrutura molecular de um composto, é possível descrever suas características (KATRITZKY; LOBANOV, 1995; STEC et al., 2015). O principal papel da metodologia é, através de ferramentas matemáticas e estatísticas, estabelecer uma relação de causa-efeito entre as características moleculares (descritores moleculares) e a propriedade observada (BEGAM; KUMAR, 2016; ROY et al., 2012; ROY; AMBURE; AHER, 2017)**.**

Os descritores moleculares transcrevem as características químicas, físicas e biológicas da estrutura química em termos matemáticos, que são posteriormente tratados por ferramentas estatísticas (GOLBRAIKH; TROPSHA, 2002; KATRITZKY; KARELSON; LOBANOV, 1997). Na Figura 3.14, é resumido uma forma típica de como

a modelagem QSAR/QSPR transcreve, seleciona e aplica a informação molecular para construção de um modelo matemático.

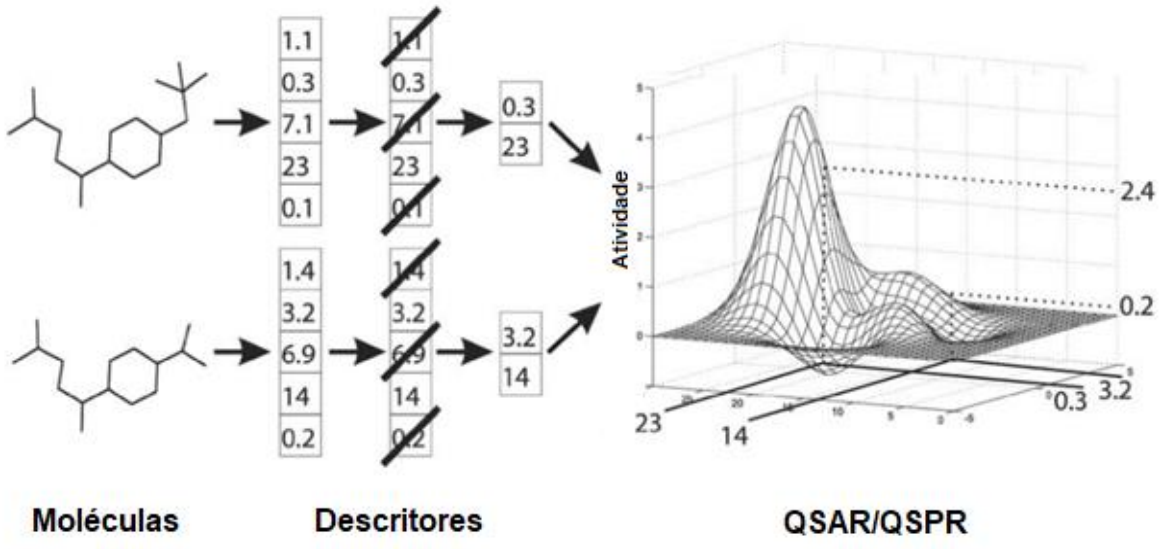

Figura 3.14. Transcrição da informação molecular em termos matemáticos

Fonte: Adaptado de (DUDEK; ARODZ; GÁLVEZ, 2006)

Um composto químico é caracterizado pelo arranjo de átomos dentro da sua estrutura molecular. No entanto, uma vez que a estrutura não pode ser usada diretamente para criar mapeamentos de estrutura-atividade, o conjunto de átomos e ligações que definem um composto são codificados e essa informação é aplicada para estudos de quimioinformática.

Inicialmente, as estruturas químicas geralmente não contêm, de forma explícita, as informações relacionadas à atividade. Esta informação tem que ser extraída a partir da representação matemática (descritores moleculares) de um composto e, posteriormente, ser relacionados com uma propriedade de interesse. Vários descritores moleculares, projetados racionalmente, projetam diferentes propriedades químicas implícitas da estrutura da molécula. Somente essas propriedades podem se correlacionar mais diretamente com a atividade.

Conforme representado na Figura 3.14, os métodos quimioinformáticos utilizados na construção de modelos QSAR/QSPR podem ser divididos em três grupos: i) gerar os descritores da estrutura molecular, ii) selecionar aqueles informativos no contexto da atividade analisada e iii) utilizar os valores dos descritores

como variáveis independentes (variáveis) para definir um mapeamento que os correlaciona com a atividade controlada.

No presente trabalho, os descritores moleculares 2D das estruturas otimizadas são gerados utilizando o software PaDEL-Descriptor, resultando em conjuntos de dados iniciais de 1444 descritores (YAP, 2011). O PaDEL, acrônimo para *Pharmaceutical Data Exploration Laboratory*, é um software de código aberto, baseado em Java script, que consta com mais de 400 citações de artigos publicados em periódicos internacionais indexados (YAP, 2011). Na Figura 3.15 é apresentado a interface de usuário do software, enquanto maiores informações podem ser obtidas na página oficial do programa (http://www.yapcwsoft.com/dd/padeldescriptor).

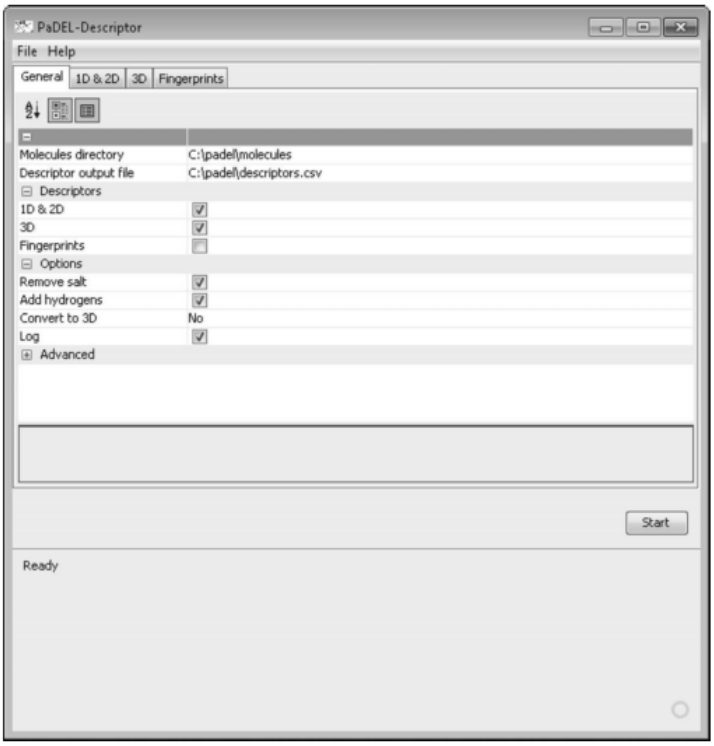

Figura 3.15. Interface de usuário do software PaDEL.

Fonte: Adaptado de (YAP, 2011)

Resumidamente, três etapas estão envolvidas na modelagem do QSPR: representação de estrutura, análise dos descritores moleculares e construção dos modelos estatísticos/matemáticos (BEGAM; KUMAR, 2016; ROY et al., 2012; ROY; AMBURE; AHER, 2017). A representação da estrutura molecular pode ser realizada da maneira mais simples (1D), que levam em consideração as características constitucionais (e.g. massa atômica, número de átomos) e a contagem de fragmentos

moleculares (e.g. número de ácidos, número de átomos doadores de ligação H), até as formas mais abrangentes de representação (2D e 3D) que, respectivamente, transcrevem as características moleculares topológicas e geométricas (TERFLOTH, 2003).

Para fins práticos, à medida que características moleculares mais complexas passam a ser incorporadas aos estudos de QSAR/QSPR, os modelos preditivos tendem a apresentar um melhor ajuste com a propriedade estimada (HECHINGER; LEONHARD; MARQUARDT, 2012). Essa tendência é representada na Figura 3.16.

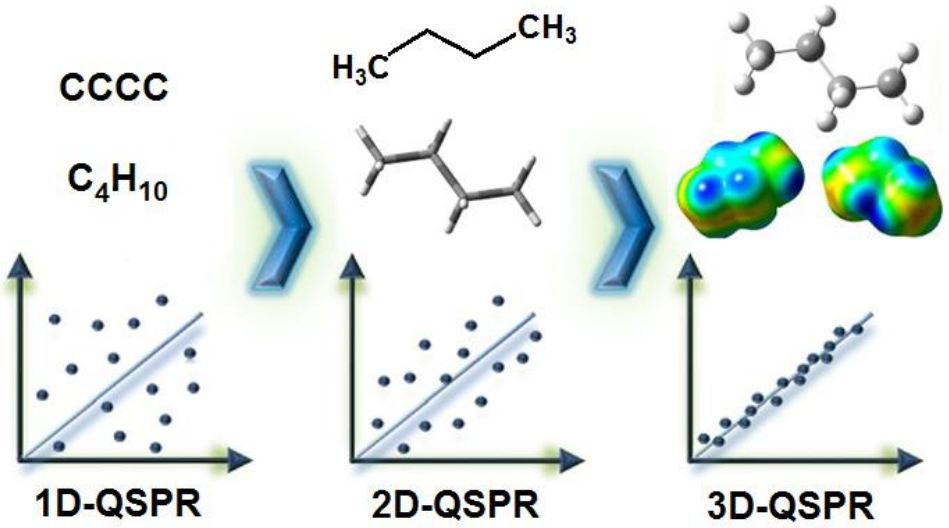

Figura 3.16. Melhora no ajuste do modelo para os diferentes tipos de descritores.
Fonte: Adaptado de (HECHINGER; LEONHARD; MARQUARDT, 2012)

A seguir, na etapa de análise dos descritores moleculares, diversos métodos de seleção de variáveis são aplicados para reduzir o conjunto inicial de dados para um seleto número de descritores que se relacionam com a propriedade medida. A terceira etapa passa pela construção dos modelos estatísticos/matemáticos, na qual utiliza-se dos métodos de análise multivariada (e.g. regressão por mínimos quadrados parciais - PLS e regressão por vetores de suporte - SVM) para estabelecer a relação entre os descritores e a propriedade/atividade controlada. Na Figura 3.17 é resumido o fluxograma de trabalho envolvido no tratamento de dados para o desenvolvimento de modelos QSAR/QSPR.

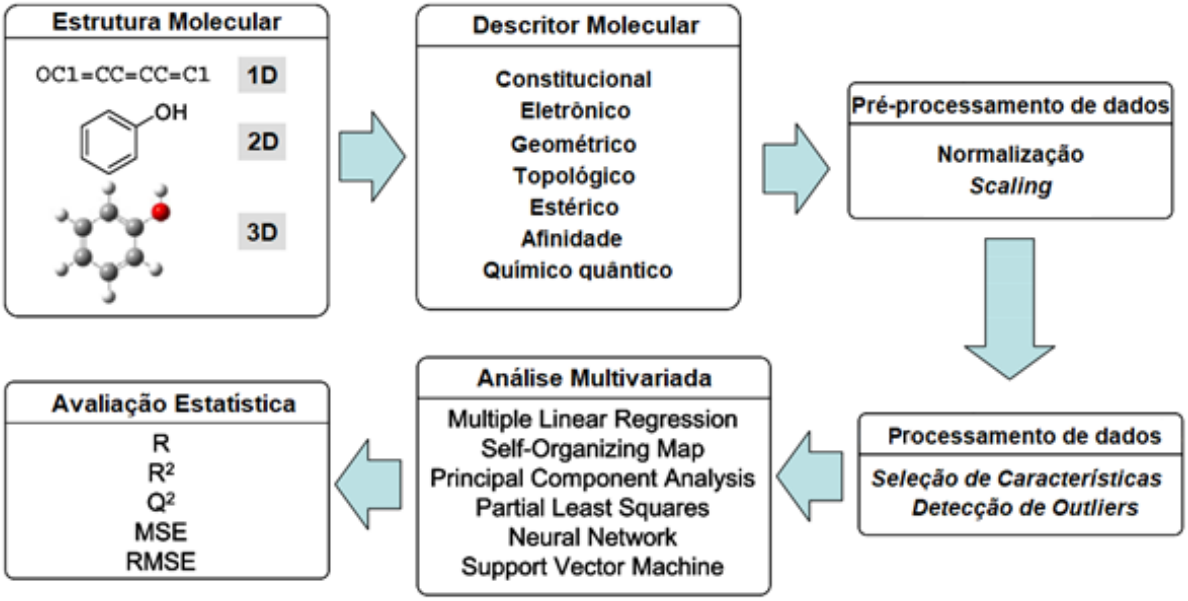

Figura 3.17. Framework para a modelagem QSPR

Fonte: Adaptado de (NANTASENAMAT et al., 2009)

O QSPR pode ser aplicado como ferramenta para a análise exploratória, mineração de dados e triagem de catalisadores e, posteriormente, orientar o processo de desenvolvimento de novos catalisadores (MALDONADO; ROTHENBERG, 2010; ROTHENBERG, 2008; ZEINI JAHROMI; GAILER, 2010). Na literatura, são encontrados exemplos de aplicações do método QSPR para estudos de catálise homogênea (MARTÍNEZ et al., 2012; YAO et al., 1999) e heterogênea (CRUZ et al., 2007; FAYET et al., 2009).

Mesmo que a aplicação dos métodos QSAR/QSPR para o estudo de catalisadores já tenha sido comprovada, ainda é limitado o número de sistemas estudados. Entre os sistemas estudados mais relevantes, encontram-se os trabalhos aplicados aos processos de polimerização de olefinas catalisados por metalocenos (YAO et al., 1999), zirconocenos (MARTÍNEZ et al., 2012) complexos ansa-zirconoceno,(CRUZ et al., 2007), complexos de ferro bis(arilimino)piridina (FAYET et al., 2009) e catalisadores tipo Ziegler−Natta (ACHARY et al., 2016; RATANASAK et al., 2015).

Do ponto de vista da catálise, do primeiro relatório sobre a produção de carbonatos oleoquímicos conduzido por Tamami, Sohn, and Wilkes (2004), ao mais recente estudo utilizando indução por micro-ondas (ZHENG et al., 2018), a maioria das publicações apresentam resultados redundantes ao aplicar os haletos de

tetrabutilamônio para o processo de carbonatação. Apenas recentemente foram observados estudos que realizam triagem de catalisadores para produção de carbonatos oleoquímicos (ALVES et al., 2015; BÜTTNER et al., 2016, 2017a; LONGWITZ et al., 2018; SCHÄFFNER et al., 2014; TENHUMBERG et al., 2016; WANG et al., 2012). No entanto, a descrição de novos catalisadores para obtenção de carbonatos cíclicos a partir de dióxido de carbono e derivados epoxidados ainda é limitada.

Dessa forma, a partir das informações obtidas a partir da modelo de quimioinformática, o QSPR pode ser usado para preencher as lacunas de dados, prever propriedades de materiais, estabelecer novos alvos moleculares e reduzir o tempo e os custos envolvidos no processo (KARELSON; LOBANOV; KATRITZKY, 1996; ROY et al., 2018). Sendo assim, o presente trabalho apresenta uma perspectiva preliminar da modelagem QSPR para auxiliar na escolha/desenho de novos organocatalisadores ativos para produção de carbonatos oleoquímicos a partir de CO_2 e epóxidos.

4. PROCEDIMENTO EXPERIMENTAL E RESULTADOS

A seção, “Procedimento Experimental e Resultados” divide-se em duas partes, na qual, os procedimentos experimentais/caracterizações e resultados da aplicação do catalisador convencional TBAB para a produção de carbonatos oleoquímicos são apresentados, respectivamente, nos Apêndices **A** e **B**, enquanto os resultados obtidos a partir da modelagem QSPR e da etapa sintética, utilizando um novo catalisador, são apresentados neste capítulo em forma de artigo. O manuscrito foi submetido na data 04/05/2018 à revista ***Journal of Catalysis*** (ISSN: 0021-9517) conforme Anexo **A.** O periódico foi qualificado pela Capes com o Qualis A1 (Engenharias II), apresenta o *Cite Score* de 6.99 e Fator de Impacto de 6,84.

4.1. Artigo 1

A Perspective of QSPR Modeling to Screen/Design Catalysts for Oleochemical Carbonates Synthesis

Victor H. J. M. dos Santos [†,‡], Darlan Pontin [†], Raoní S. Rambo [†], Marcus Seferin [*†,‡]

† Escola de Ciências – PUCRS – Pontifícia Universidade Católica do Rio Grande do Sul, Av. Ipiranga, 6681 – Prédio 12, 90619-900, Porto Alegre, Brasil.

‡ Escola Politécnica, Programa de Pós-Graduação em Engenharia e Tecnologia de Materiais – PUCRS – Pontifícia Universidade Católica do Rio Grande do Sul, Av. Ipiranga, 6681 – Prédio 32, 90619-900, Porto Alegre, Brasil.

[*] **Email of corresponding authors:** seferin@pucrs.br

ABSTRACT

This work presents a preliminary perspective of Quantitative Structure-Property Relationship (QSPR) modeling to assist in the targeted choice/design of new active organocatalysts to produce cyclic carbonates. The QSPR model was developed by applying the 2D molecular descriptors to establish a structure-property relationship between the organocatalysts features and its activity to produce oleochemical carbonates. From the virtual screening, a total of 122 catalysts have their activity predicted and the best molecular targets were proposed. The principal molecular features (i.e. organic structure, molecular arrangement, carbon chain size and substituent type) were identified through data mining, while the PCA proved to be suitable to perform the exploratory analysis of the molecules set. In addition, we provide the first report of application of cetyltrimethylammonium bromide (CTAB) as a new catalyst to produce oleochemical carbonates, with more than 98% of epoxide conversion to cyclic carbonate for all the vegetable oil. In this way, the QSPR can be useful to reduce costs and time in the catalysts screening/design for this reaction.

Keywords: Vegetable oil, Oleochemical carbonate, QSPR, Quantitative Structure-Property Relationship, Cyclic carbonate, Carbon dioxide, Multivariate Analysis, Organocatalyst, Metal-free catalyst, Green chemistry

Graphical Abstract

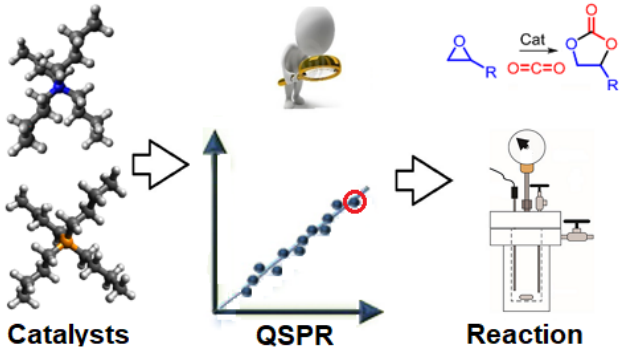

Graphical abstract. The QSPR can be applied to reduce costs and time in the catalysts screening/design for cyclic carbonates synthesis.

INTRODUCTION

The replacement of the petrochemical production base and the development of low carbon technologies have become one of the main concerns of humanity in the early century. Reduce the ecological footprint, increase the efficiency of production processes and the exploitation/mitigation of the CO_2 surplus are widely discussed by the Life Cycle Assessment and Carbon Capture Utilization and Storage topics [1,2].

The CO_2 is an important anthropogenic greenhouse gas, with increasing atmospheric concentration and a significant role in climatic changes on a global scale [3]. From an industrial waste to a renewable raw material readily accessible, the perception of the carbon dioxide role in a scenario of low carbon economy has been changing significantly.

In this way, the use of CO_2 as a C1 building block will play a major role in the low carbon based chemical industry [4,5]. However the CO_2 is notoriously unreactive chemical, whose activation presents significant energetic barriers and thermodynamic drawbacks, that must be surpassed by chemical and physical process [6,7]. Therefore, the use of catalysts is

essential for the carbon dioxide-based processes to be economically viable and with a reasonable energetic penalty [3,6].

One of the most prominent alternatives for the use of carbon dioxide in the chemicals production is through the cycloaddition of CO_2 to epoxides with the formation of cyclic carbonates [8–10]. The carbon dioxide coupling has 100% of atomic efficiency and presents great industrial potential, since there is a consolidated industry of epoxidized derivatives [3,11]. Once again, the activation of the CO_2 and epoxy group is carried out by means of catalysts, like transition metal catalysis, phase transfer catalysts in combination with alkali halides and organocatalysis [4,10,12,13].

In order to reduce the time and costs involved in scientific research, the chemoinformatics tools: Molecular Dynamics, Quantum Mechanics and Quantitative Structure−Property Relationships (QSPR) could be applied to increase the chemical and mechanistic understanding of the process [14].

The QSPR modelling is based on the assumption that, from the molecular structure of a compound, it is possible to describe its characteristics [15,16]. The major role of the methodology is, through mathematical and statistical tools, establish a cause/effect relationship between the molecular features and observed property [17–19]. Briefly, three steps are involved in the QSPR modelling: structure representation, descriptor analysis and model building [17–19].

Thus, by changing the purely intuitive decisions in the scientific process by the targeted choice, the QSPR can be used to complete data gaps, predict material properties, stablish new molecular targets and reduce time and costs involved in the process [20,21].

The catalyst is a fundamental component of the chemical process, which cost, and efficiency are fundamental for making decisions, process upscaling and economic viability. The

QSPR can be applied as an exploratory tool for data mining and catalyst screening, and, subsequently, guide the development of new catalysts [22–30].

The vegetable oils and their derivatives are abundant, low cost, biodegradable and non-toxic [31–33]. Recently, a growing interest has been observed in the production and application of cyclic carbonates derived from fatty acids, methyl esters and triglycerides. Among the fundamental characteristics to explain the great potential of oleochemical carbonates is the existence of a consolidated industry for the production of epoxidized oleochemical derivatives and the high availability of CO_2 [34,35].

From the first report on the production of oleochemical carbonates conducted by Tamami, Sohn and Wilkes [36], to the most recent publications using microwave induction [37], Al complex [38] and CaI_2/Crown Ethers [39], most publications are seemingly redundant by using the tetrabutylammonium halides for carbonation process. Only recently, studies that perform catalysts/co-catalyst screening to produce oleochemical carbonates have been reported [10,39–44], however the description of new catalysts to produce cyclic carbonates from carbon dioxide and epoxidized derivatives is still limited. In this way, the screening/design of new catalyst for the cycloaddition of carbon dioxide to epoxides is a challenge that should be actively addressed by research community

This work presents a preliminary perspective of QSPR modeling to assist in the targeted choice/design of new active organocatalysts to produce oleochemical carbonates from CO_2 and epoxide. To best of our knowledge this study is the first QSPR approach on catalysts to produce cyclic carbonates. In addition, the cetyltrimethylammonium bromide (CTAB) are presented as a new catalyst to produce oleochemical carbonates.

MATERIALS AND METHODS

To date, only a small number of organocatalysts have been applied to produce oleochemical carbonates from CO_2 and epoxides. Even fewer reactions were performed under fair conditions that allow data modeling by QSPR method. A third, and relevant, aspect is that many organocatalysts applied in the scientific reports do not present optimized or described chemical structures in public databases as PubChem.

In view of all these factors, the present work brought together the largest number as possible of organocatalysts applied in oleochemical carbonates studies and presents a preliminary study on the application of QSPR tool for screening/design of active organocatalysts for the carbonation reaction. The scope of the present work comprises the oleochemical carbonates, a class of natural-oil-based chemicals derived from the triglycerides, fatty acids and fatty acid alkyl esters, represented in the Figure 1.

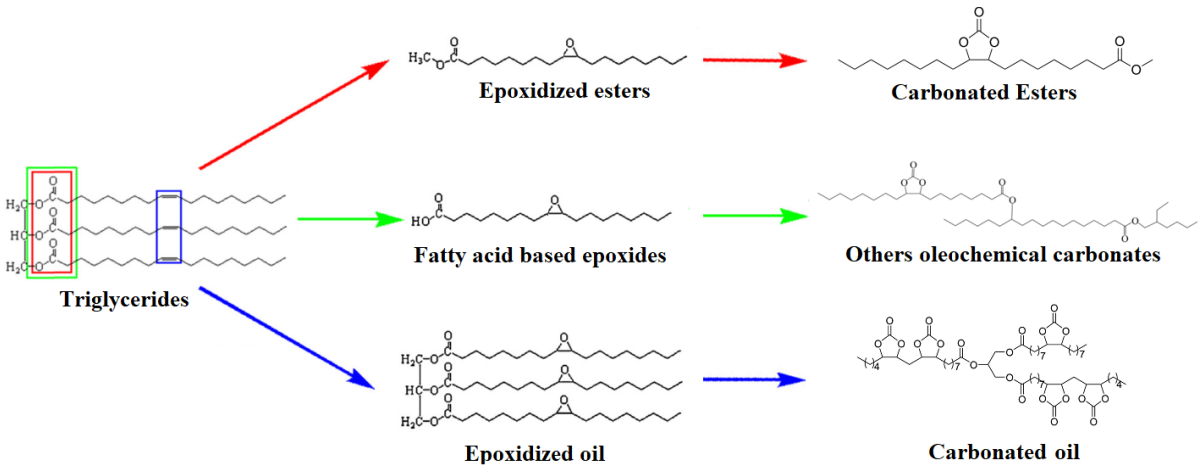

Figure 1. Oleochemical carbonates derived from triglycerides

Materials

Three vegetable oil (rice bran oil, canola oil and soybean) were obtained from local suppliers. The hydrogen peroxide (35% purity) were obtained from Synth. The glacial acetic

acid (>99%), the sulfuric acid (>95%) and the n-butanol (99% purity) were obtained from Fluka. The cetyltrimethylammonium bromide or hexadecyltrimethylammonium bromide (CTAB, 98% purity) were obtained from Sigma-Aldrich. The high purity carbon dioxide (CO_2, 99.995%) were obtained from Air Liquide. All reagents were used without further purification.

Data Sets.

The present paper presents a total of 03 data sets that were applied for exploratory and QSPR modelling based on the 2D-molecular descriptors. The Data Set 01 (Table 1) are retrieved from the Alves and coworkers paper [10], and comprises 12 catalyst with structure registered in public database. The application domain of this set comprises the synthesis of cyclic carbonate derived from epoxidized triglycerides and CO_2 under the reaction conditions: T = 100°C, P = 10 MPa, t = 5h and catalyst load = 1 mol%. This data set was applied for the variables selection procedure, QSPR model building and predict the activity of new organocatalysts.

Table 1. Catalyst Data Set 01 applied for the QSPR modelling.

Catalyst	PubChem CID	CAS	Conversion (%)
Tetrabutylammonium iodide	67553	311-28-4	26%
Tetrabutylammonium bromide	74236	1643-19-2	30%
Tetrabutylammonium chloride	70681	1112-67-0	17%
Tetrabutylphosphonium iodide	201022	3115-66-0	21%
Tetrabutylphosphonium bromide	76564	3115-68-2	28%
Tetrabutylphosphonium chloride	75311	2304-30-5	19%
1-Methyl-3-octylimidazolium iodide	71353115	188589-28-8	25%
1-Methyl-3-octylimidazolium bromide	10849985	61545-99-1	30%
1-Methyl-3-octylimidazolium chloride	2734223	64697-40-1	20%
Triethylsulfonium iodide	74589	1829-92-1	0%
1-Butyl-1-methylpyrrolidinium iodide	11076461	56511-17-2	19%
1-Butylpyridinium iodide	14007922	874-81-7	12%

Retrieved from the Alves and coworkers paper [10]

The Data Set 02 (Table S1) are retrieved from the Büttner and coworkers papers,[44] and comprises 09 catalyst with structure registered in public database. The application domain of this set comprises the synthesis of cyclic carbonate derived from epoxidized methyl oleate and CO_2 under the reaction conditions: T = 100°C, P = 5 MPa, t = 16h and catalyst load = 2 mol%. This data set was applied to evaluate the transferability of the QSPR model and are built based on the same descriptors selected for Data Set 01.

The Data Set 03 (Table 2) results from the literature search of all organocatalysts applied to produce oleochemical carbonates from epoxide and CO_2 and comprises 29 catalysts with structure registered in public database. The exploratory analysis was applied to this data set, based on unsupervised multivariate method and the 2D-molecular descriptors, with the objective of evaluating the data set profile based on the variables applied in the QSPR model.

Descriptor Calculation

The molecular descriptors transcribes the chemical, physical and biological features of the chemical structure in mathematical terms which are posteriorly treated by statistical tools [45,46]. The catalysts molecular structures were mostly obtained from the PubChem database and the molecular representation stored in SDF files (Structured Data Format)[47]. In the present work, the 2D molecular descriptors of the optimized structures are generated using the PaDEL-Descriptor (http://www.yapcwsoft.com/dd/padeldescriptor) software, resulting in an initial data sets of 1444 descriptors [48].

Variable Selection

The variable selection is an essential step in the QSAR/QSPR study to reduce the initial number of descriptors to a selected variable set which extract the data features to an interpretable model. For the predictive modelling of the present work, the molecular descriptors are applied as predictor variables (X) while the epoxide conversion to carbonates are applied as response variable (Y).

In a first moment, the variable correlation analysis was applied to the entire data set and the linear correlation of each of the 1444 molecular descriptors with the epoxide conversion to carbonates was evaluated. Only the variables which presents fair correlation with the response variable were kept in the data set for the subsequent variable selection steps. The value of > 0.3 or < -0.3 was taken as reference for this first selection [49].

Following the correlation analysis, the variable selection proceeds through the stepwise method, based on combination of forward selection and backward elimination procedure, applied within the PLS algorithm by using the leave-one-out (LOO) internal validation method. The stepwise variable selection is an exhaustive and time-consuming modelling which proceeds "step by step" with the predictor variables being interactively included/excluded, one by one, from the regression model until no further gain to be obtained [50–52]. Taking into account that the data set of this work is small, the variable selection procedure was repeated several times at each cycle of LOO cross validation until there is no more significant model gain from the variables removal of the dataset. This strategy was presented previously as an alternative to make QSAR/QSPR models based on small data set as robust as possible [51].

Table 2. Catalyst Data Set 03 applied for the exploratory analysis of organocatalyst.

Catalyst	PubChem CID	CAS	Ref.
(2-Hydroxyethyl)triphenylphosphonium bromide	2733550	7237-34-5	[44]
(2-Hydroxyethyl)triphenylphosphonium chloride	520034	23250-03-5	[44]
(2-Hydroxyethyl)triphenylphosphonium iodide	89439517	4336-77-0	[44]
(4-Hydroxyethyl)-methyl-diphenylphosphonium iodide	20267393	20650-57-1	[44]
1-Butyl-3-methylimidazolium Bromide	2734236	85100-77-2	[41]
1-Butyl-4-methylpyridinium iodide	329763177	32353-64-3	[41]
1-Tetradecyl-3-methylimidazolium bromide	77520435	471907-87-6	[53]
(2-Hydroxyphenyl)-methyl-diphenylphosphonium iodide	71400991	60254-13-9	[44]
Benzyltrimenthylammonium bromide	21449	5350-41-4	[36]
1-Butyl-3-methylimidazolium chloride	2734161	79917-90-1	[41]
Methyl-triphenylphosphonium iodide	638159	2065-66-9	[44]
Tetraheptylammonium Bromide	78073	4368-51-8	[53]
Tributyl(2-hydroxyethyl) chloride	CT1084236377	54580-84-6	[44]
Tributyl(2-hydroxyethyl) iodide	CT1081904619	54580-85-7	[44,54,55]
Tributyl(2-hydroxyethyl) bromide	CT1081904620	54580-43-7	[44]
Tetraoctylphosphonium bromide	3015167	23906-97-0	[42]
Cetyltrimethylammonium Bromide	5974	57-09-0	This work
1-Butyl-1-methylpyrrolidinium iodide	11076461	56511-17-2	[10]
1-Butylpyridinium iodide	14007922	874-81-7	[10]
1-Methyl-3-octylimidazolium bromide	10849985	61545-99-1	[10]
1-Methyl-3-octylimidazolium chloride	2734223	64697-40-1	[10]
1-Methyl-3-octylimidazolium iodide	71353115	188589-28-8	[10]
Tetrabutylammonium bromide	74236	1643-19-2	[10,41,53]
Tetrabutylammonium chloride	70681	1112-67-0	[10,53]
Tetrabutylammonium iodide	67553	311-28-4	[10,41,53]
Tetrabutylphosphonium bromide	76564	3115-68-2	[10,44]
Tetrabutylphosphonium chloride	75311	2304-30-5	[10,44]
Tetrabutylphosphonium iodide	201022	3115-66-0	[10,44]
Triethylsulfonium iodide	74589	1829-92-1	[10]

Molecular Descriptors

After the variable selection step, the 18 molecular descriptors that were important for the development of the QSPR model are: nCl^-, nBr^-, nI^-, ALogP, apol, ATS2e, bpol, C2SP3, ETA Shape Y, GATS6i, Lipoaffinity Index, MATS4m, nAtom, nAtomLAC, nBonds2, nRotBt, $SssCH_2$ and VABC. The detailing of the selected variables can be found in the Nomenclature section, and their definition can be found in the literature [56–61].

Data Analysis

The data analysis was carried out by using the Solo+MIA software (Eigenvector Research) and the statistical tools applied in the present work for the exploratory and predictive analysis are the Correlation Analysis (CA), Principal Competent Analysis (PCA), Partial Least Squares Regression (PLS) and Support Vector Machine Regression (SVM)**.**

QSPR Development

For the QSPR modelling of the present work, the molecular descriptors are applied as predictor variables (X) while the epoxide conversion to carbonates are applied as response variable (Y). After the exhaustive variable selection step, the 18 molecular descriptors are applied to perform the multivariate regression with the data autoscaled and mean centered [24]. The PLS was performed using the SIMPLS algorithm, while the SVM was developed using the Linear Kernel Function.

QSPR Validation

The model validation is a crucial step on the QSPR development and over the years several criteria / threshold values have been presented as minimum requirements, but not always sufficient, to ensure the robustness and transferability of QSAR/QSPR models [62–66]. The

present work applies the Golbraikh and Tropsha's criteria [46,66,67], in addition to the Roy and coworkers r^2_m metrics[51,62,68,69]. A summary of the validation parameters and the respective threshold values are presented in the Table 3.

Table 3. Parameters for the QSPR model validation

Parameter	Threshold value
R^2	>0.6
Q^2	>0.5
$\frac{(R^2 - R^2_o)}{R^2}$	<0.1
$\frac{(R^2 - R'^2_o)}{R^2}$	<0.1
k	$0.85 \leq k \leq 1.15$
k'	$0.85 \leq k \leq 1.15$
$\lvert R^2 - R^2_o \rvert$	<0.3
$\lvert R^2 - R'^2_o \rvert$	<0.3
R^2_m	>0.5
R'^2_m	>0.5
$\lvert R^2_m - R'^2_m \rvert$	<0.2
$\frac{\lvert R^2_m - R'^2_m \rvert}{2}$	>0.5

R^2 - Denotes the correlation coefficient between the predicted and observed activities for a test set

Considering the small size of the data set, the stability of the model was evaluated based on both leave one out (Q^2-LOO) and leave-many-out (Q^2-LMO) internal validation and the model predictivity was evaluated by using the $r^2_{m\ (LOO)}$ and $r^2_{m\ (LMO)}$ parameters by replacing the R^2 (test set) with the cross validation Q^2 [51,62,65,69].

In addition to the internal validation, the 12 catalysts data are splitted into independent the training (9 samples) and test sets (3 samples). To avoid any underestimation or overestimation of the model, a total of 220 PLS models, comprising all possible combinations of training/validation samples (9 samples/3 samples), was performed and the $R^2_{(Cal)}$, $Q^2_{(LOO)}$, $R^2_{(Ext)}$ and RMSEP parameters are presented in the form of distribution histograms.

Lastly, the transferability of the QSPR model is confirmed by the construction and validation of the QSPR model based on Data Set 02 by applying the same molecular descriptors. The development, validation, and discussion of the QSPR model based on Data Set 02 are presented separately in the Supporting Information throughout the Figures S1-S3 and Tables S1-S5.

Virtual screening

The virtual screening is a computational method that guides, based on structure or property, the search for new active compounds in large chemical libraries [70,71]. The PubChem search tools was applied to perform the virtual screening of potential molecular targets with similar chemical structures to those used for calibration models [47].

The descriptor calculation was performed as described previously and, after the variables removal, the data are evaluated for the existence of missing data and outliers (by mean of PCA) with subsequent removal of these samples from the data set. A total of 122 potential catalysts were retrieved and their identification can be found in the Supporting Information, presented in Table S6, while a summary of the data analysis procedures performed on the present work are represented in the Figure 2.

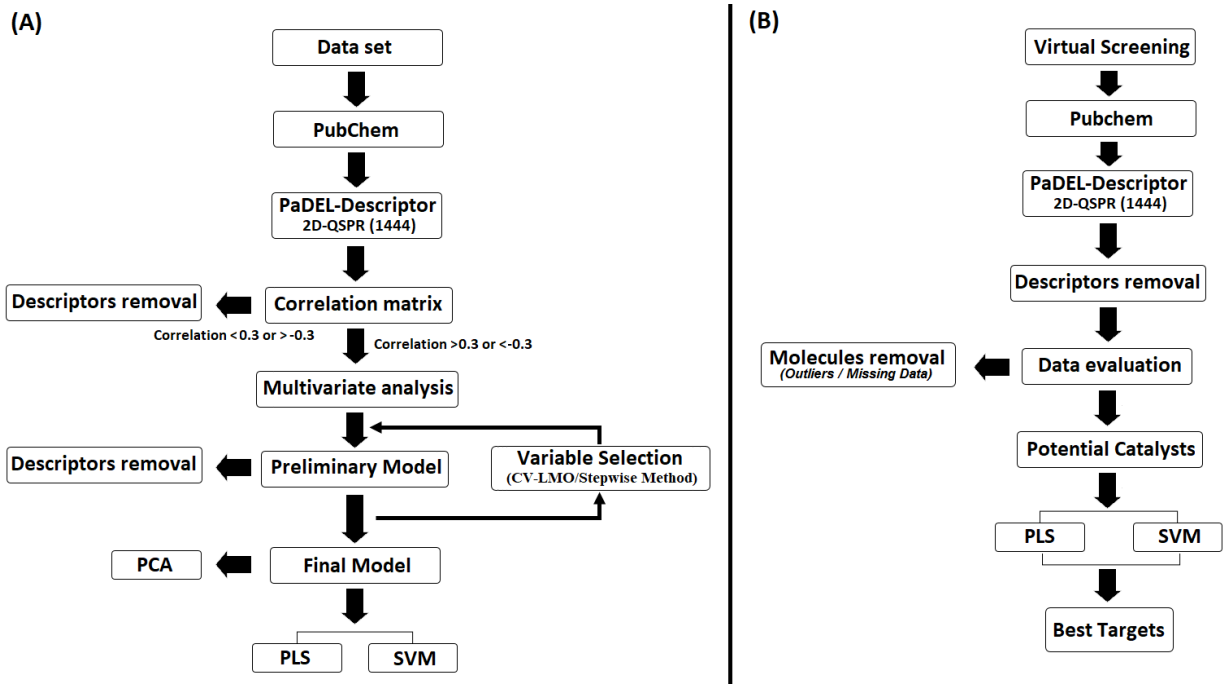

Figure 2. Summary of the procedures used to construct the QSPR models. A) QSPR Calibration/Validation and B) Virtual screening work flow.

Synthesis Procedures

The synthesis procedures of the present work are performed in two stages: the epoxidation reaction of the raw vegetable oil and the direct carbonation of the epoxidized product with CO_2.

Epoxidation. The vegetable oils in situ epoxidation reactions was conducted using glacial acetic acid, hydrogen peroxide 35% and sulfuric acid. The reaction was performed at 75°C, for 6 hours, with mechanical stirring and using the reactants molar ratio of 2:1 (H_2O_2:ethylenic unsaturation), 0.5:1 (CH_3COOH:ethylenic unsaturation) and 2% sulfuric acid (wt% of the aqueous fraction) [72,73]. After the reaction, the product was dissolved in ethyl ether and washed with water until neutral pH, followed by the solvent removal under vacuum.

Carbonation. The carbonation reaction of the epoxidized triglycerides was conducted using cetyltrimethylammonium bromide (CTAB) catalyst, high purity carbon dioxide and n-

butanol as solvent. The reaction was performed in a 50 cm^3 stainless steel autoclave at 120°C, for 48 hours, without stirring, 5 MPa (*p*, CO_2), 2 g of epoxidized oil, 4 mL of butanol and 5 mol% of CTAB. After the reaction, the butanol is removed under vacuum, which causes the catalyst to precipitate after some time. After the butanol removal, the product was dissolved in ethyl acetate and washed two times with water and once with brine. The oleochemical carbonate product are dried with anhydrous sodium sulfate and the solvent removed under vacuum.

Characterization Methods

All the vegetable oil, epoxidized oil and carbonated products are characterized by the Fourier-transform infrared spectroscopy (FTIR) and nuclear magnetic resonance spectroscopy detailed below.

Infrared analysis (FTIR). The infrared spectra are acquired using the Spectrum One spectrometer (PerkinElmer) with HATR accessory. The spectral ranges from 4000 to 650 cm^{-1} wavenumber, resolution of 4 cm^{-1}, 16 scans per spectrum.

^{1}H-NMR. All NMR spectra were recorded on a Bruker Avance 400 running at 400 MHz for ^{1}H. Chemical shifts (δ) are reported in parts per million (ppm) relative to TMS signal (0 ppm) for ^{1}H-NMR and using deuterated chloroform ($CDCl_3$) as solvent.

RESULTS AND DISCUSSION

The results and discussion are divided into five parts: Development of the QSPR model based on the 2D-molecular descriptors; The virtual screening to select new catalyst target for the synthesis process; Data mining description; The exploratory analysis of organocatalysts applied in the literature; Synthesis of oleochemical carbonate using CTAB as catalyst.

QSPR model

The QSPR model was developed based on the Alves and coworkers data [10], and comprises 12 catalyst with structure registered in public database (Table 1). After the variable selection step, the 18 molecular descriptors are applied to the PLS and SVM model and the respective variables values are available in the Table S7 in the Supporting Information.

The internal validations of the models are performed by mean of LOO and LMO cross-validation. Furthermore, to evaluate the model sensitivity to the sample removal from the training set, the LMO was performed by keeping out 16.7% and 25% of the data at each cycle of model training. The results of the QSPR model are presented in the Table 4.

Table 4. QSPR model for the synthesis of oleochemical carbonate through organocatalysis

Data set 1	LOO		[a]LMO		[b]LMO	
	PLS	SVM	PLS	SVM	PLS	SVM
R^2_{Cal}	0.9762	0.9747	0.9741	0.9715	0.9762	0.9769
Q^2_{CV}	0.9040	0.9142	0.9118	0.8373	0.8868	0.8896
RMSEC	1.25	1.30	1.31	1.58	1.26	1.26
RMSECV	2.56	2.44	2.44	3.30	3.57	2.94
F/SV	4	12	3	8	4	12

F - Factor, SV – Support vectors, [a] – 16.7% of the sample kept out in the Leave-Many-Out cross-validation,[b] - 25% of the sample kept out in the Leave-Many-Out cross-validation.

In a first assessment, the model presents considerable good outputs, with high calibration R^2 (>0.95) and good cross validation coefficient of determination (Q^2 >0.6) satisfying the minimum criteria for obtaining a reliable QSPR model. Also, acceptable values of Root-mean-square error of cross-validation (RMSECV) are obtained, with values around 10% of mean squared error.

The validation of the QSPR model was performed based on the Golbraikh and Tropsha's criteria [46,66,67], in addition to the Roy and coworkers r^2_m metrics [51,62,68,69]. The Table S8 presents the estimated conversion values for each of PLS and SVM models, while the Table 5 presents the respective values obtained for the QSPR validation.

Table 5. Validation of the PLS and SVM model performed based on the Data Set 01.

Data Set 01	PLS			SVM			Reference threshold value
	LOO	[a]LMO	[b]LMO	LOO	[a]LMO	[b]LMO	
R^2	0.98	0.97	0.98	0.97	0.97	0.98	>0.6
Q^2	0.90	0.91	0.89	0.91	0.84	0.89	>0.5
$\frac{(Q^2 - Q^2_o)}{Q^2}$	0.00	0.00	0.01	0.00	0.00	0.02	<0.1
$\frac{(Q^2 - Q'^2_o)}{Q^2}$	0.02	0.02	0.06	0.02	0.04	0.09	<0.1
k	0.00	0.00	0.01	0.00	0.00	0.02	<0.3
k′	0.02	0.01	0.05	0.02	0.03	0.08	<0.3
$\lvert Q^2 - Q^2_o \rvert$	0.99	0.99	0.99	0.99	0.99	0.99	$0.85 \leq k \leq 1.15$
$\lvert Q^2 - Q'^2_o \rvert$	0.99	1.00	0.99	1.00	0.99	0.99	$0.85 \leq k \leq 1.15$
Q^2_m	0.87	0.89	0.80	0.86	0.83	0.77	>0.5
Q'^2_m	0.78	0.80	0.68	0.78	0.69	0.63	>0.5
$\lvert Q^2_m - Q'^2_m \rvert$	0.09	0.08	0.12	0.09	0.14	0.13	<0.2
$\frac{\lvert Q^2_m - Q'^2_m \rvert}{2}$	0.82	0.85	0.74	0.82	0.76	0.70	>0.5
Validation	V	V	V	V	V	V	All criteria met

V – Validated, [a] – 16.7% of the sample kept out in the Leave-Many-Out cross-validation,[b] – 25% of the sample kept out in the Leave-Many-Out cross-validation.

From the Table 5, we found that all the developed QSPR models are validated based on the Table 3 criteria. In addition to the internal validation, further validation procedures are performed by splitting the catalyst data into training (9 samples) and test sets (3 samples). To avoid any underestimation or overestimation of the model, a total of 220 PLS models, comprising all possible combinations of training/validation samples (9 samples/ 3 samples), was performed and the $R^2_{(Cal)}$, $Q^2_{(LOO)}$, $R^2_{(Ext)}$ and Root-mean-square error of prediction (RMSEP) parameters are presented in the form of distribution histograms (Figure 3).

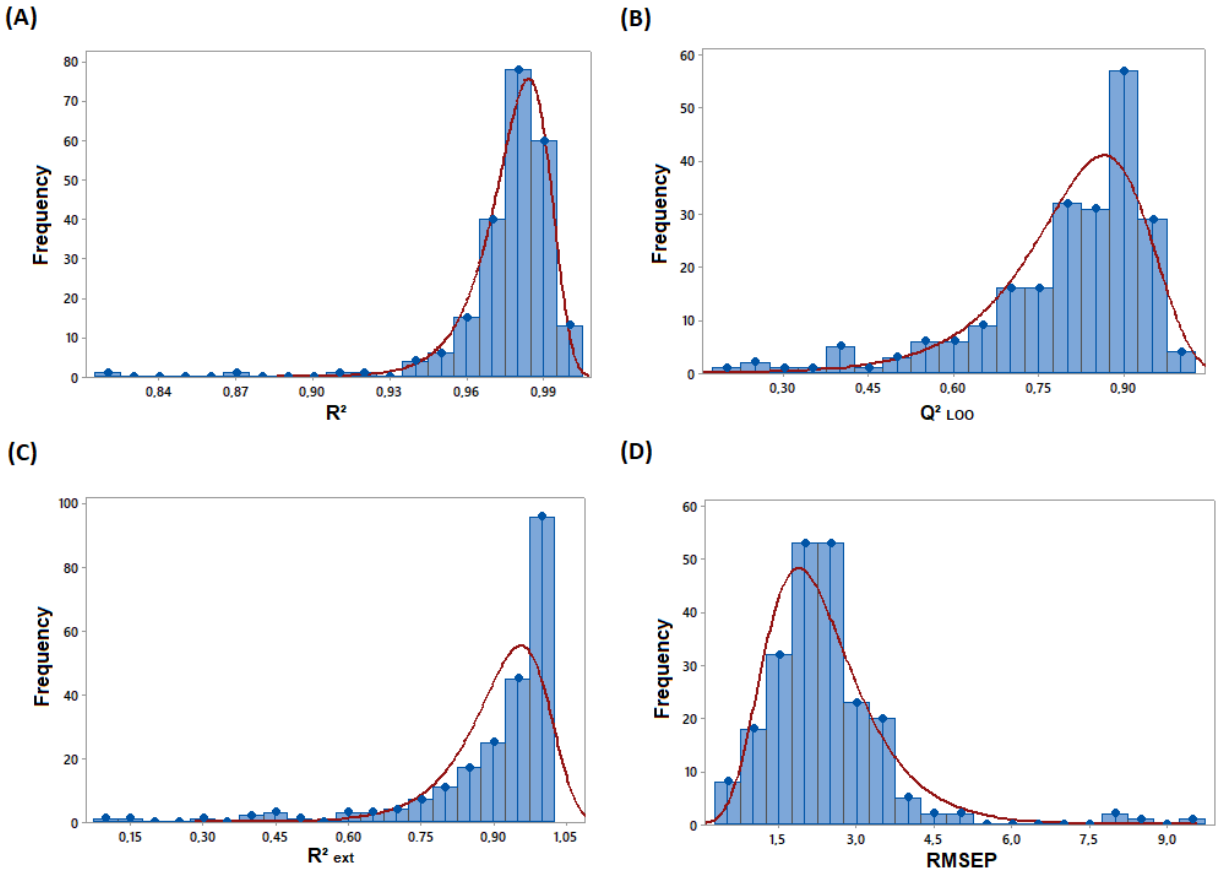

Figure 3. Distribution histograms: A) $R^2_{(Cal)}$, B) $Q^2_{(LOO)}$, C) $R^2_{(Ext)}$ and D) RMSEP.

From the Figure 3, is observed that most of the R^2(Cal), Q^2(LOO), R^2(Ext) histogram data are concentrated at higher values, while the prediction error (RMSEP) is concentrated at lower values. In the Table 6, a summary of the QSPR model histogram results are presented.

Table 6. Summary of the QSPR model histogram results

Parameter	**[a] R^2**	**[a] Q^2LOO**	**[a] R^2 etx**	**[a] RMSEP**
Mean	0.9776	0.8011	0.9036	2.360
Standard Deviation	0.0189	0.1532	0.1483	1.170
Minimum	0.8172	0.1800	0.0880	0.410
Maximum	0.9994	0.9916	0.9999	9.570
Cumulative Distribution (80%)	>0.9683	>0.7167	>0.8469	<3.14
Cumulative Distribution (95%)	>0.9526	>0.5718	>0.7396	<4.37

[a] – Results of the 220 PLS models performed with 75% of the data for calibration and 25% used as an independent test sets

From the Table 6, it is observed that $R^2_{(Cal)}$, $Q^2_{(LOO)}$, $R^2_{(Ext)}$ present mean values above the minimum requirement for the QSPR model validation and, from the cumulative distribution function, it is observed that 95% of the QSPR models present parameters values above the threshold $Q^2_{(LOO)}$ (>0.5) and $R^2_{(Ext)}$ (>0.6). With respect to the prediction error, within the 220 models evaluated there was found an acceptable value of mean RMSEP (2.36), with 80% of the models presenting mean square error below 10%, and 95% of them presenting mean square error below 15%.

These results can be considered as good ones, since each QSPR model has been developed with 25% of the original set kept outside the training set. Considering that, both internal and external validation had met the minimum requirements and it is considered that the developed QSPR models are suitable to be applied in the subsequent steps.

After the validation phase, we move to the interpretation of the data obtained by calibration models. In the Figure 4, are represented the predicted *versus* reference plot obtained from the LOO cross-validation of PLS and SVM models.

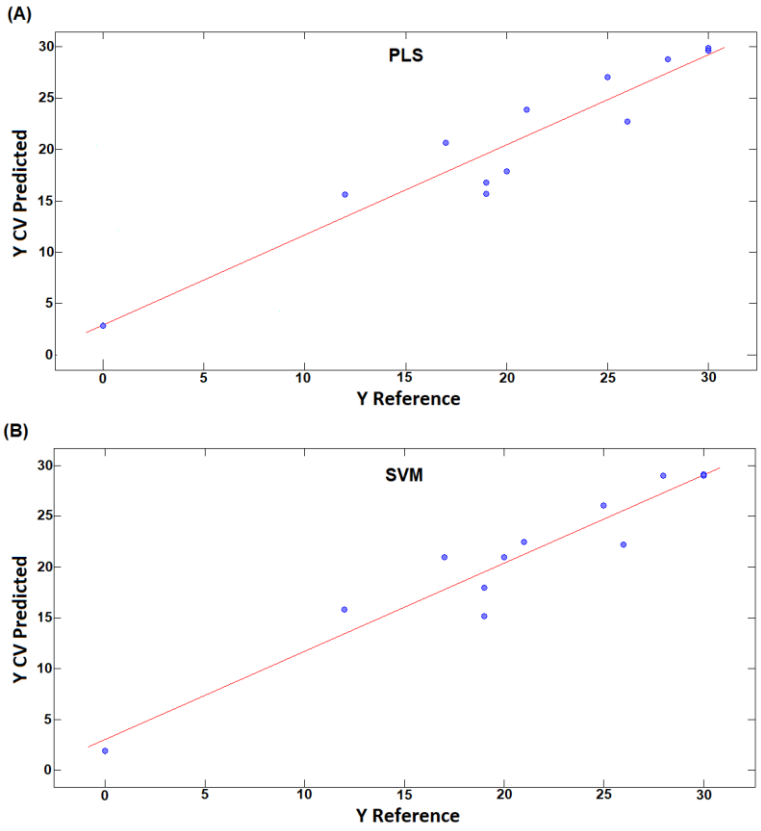

Figure 4. Predicted versus reference plot for the estimation of epoxide conversion to cyclic carbonate. A) PLS model and B) SVM model.

The interpretation of the principals relationship between the molecular descriptors (X) and the estimated conversion response (Y) is performed through the PLS Regression Coefficient, presented in the Figure 5 [74,75].

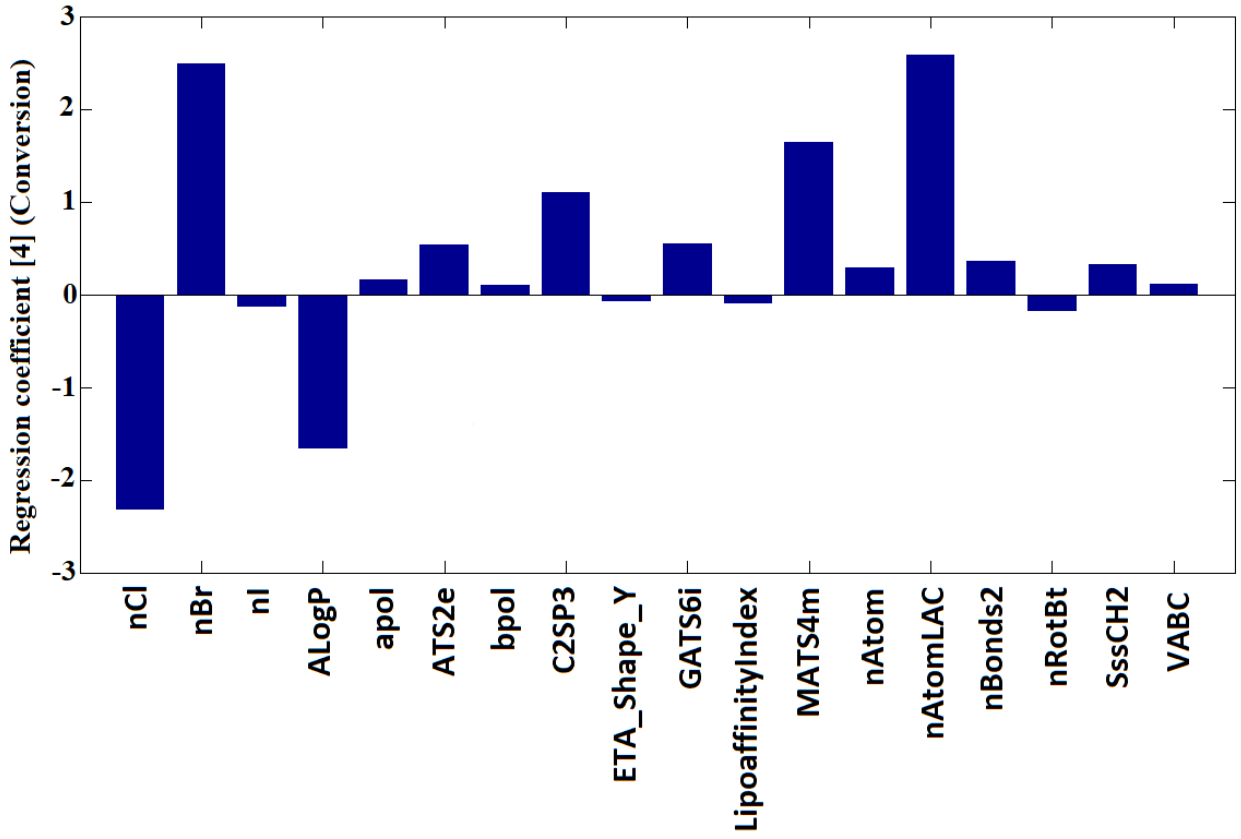

Figure 5. PLS regression coefficient for the estimation of epoxide conversion to cyclic carbonate.

From the regression coefficient obtained it is possible to observe the halide influence on the catalyst effectiveness, with the order of anion activity being identified as $Br^- > I^- > Cl^-$. This same pattern have already been described by Langanke and coworkers (2013), which attribute the higher bromide efficiency as a result of the balance between nucleophilicity and leaving group character of the chemical species [53]. Also, the influence of the solvent effect of the supercritical CO_2 and the changing in the mass transfer phenomena involved could play an important role in this order [7,76,77].

The autocorrelation descriptors (ATS2e, GATS6i and MATS4m) presents a positive regression coefficient and are related with a property distribution along the molecular structure. Due to the complexity of these indices, no clear interpretation is possible.

Another important feature of the catalyst is the size of the organic structure and the molecule polarizability. This behavior is translated by the model in function of the molecular descriptors apol, bpol, C2SP3, nAtom, nAtomLAC, nBonds2, $SssCH_2$ and VABC, all presenting the positive regression coefficient with respect to the conversion. This characteristic has already been described in the literature, which relate the increase in the bulkiness of the catalyst to the weakening of the electrostatic interactions between cation and anion, which lead to an increase in the nucleophilic character of the halide [78–82]. Also, from the C2SP3 regression coefficient, it is concluded that the lengthening of the carbon chain with saturated carbon is preferable.

The catalyst solubility play an important role in the reaction in homogeneous phase, however the catalysts solubility in epoxidized derivatives is limitedly addressed in the literature [3]. From the QSPR regression coefficient, we found that the lipophilicity descriptors (ALogP and Lipoaffinity Index) are important to justify the catalyst efficiency, since the effectiveness of the catalysts increases with their lipophilicity.

Since application domain of this model comprises the synthesis of cyclic carbonate derived from epoxidized triglycerides, the lipophilicity character is being related with the catalyst solubility in the medium. The solvent effects of the oily matrix and supercritical CO_2 over the bulky organic cation results in charge stabilization and increases the nucleophilicity of halide anion [81,83]. After observing the regression coefficients, the Variable Influence on Projection (VIP scores) was analyzed to rank the relative importance of the molecular descriptors for the model [74,75].

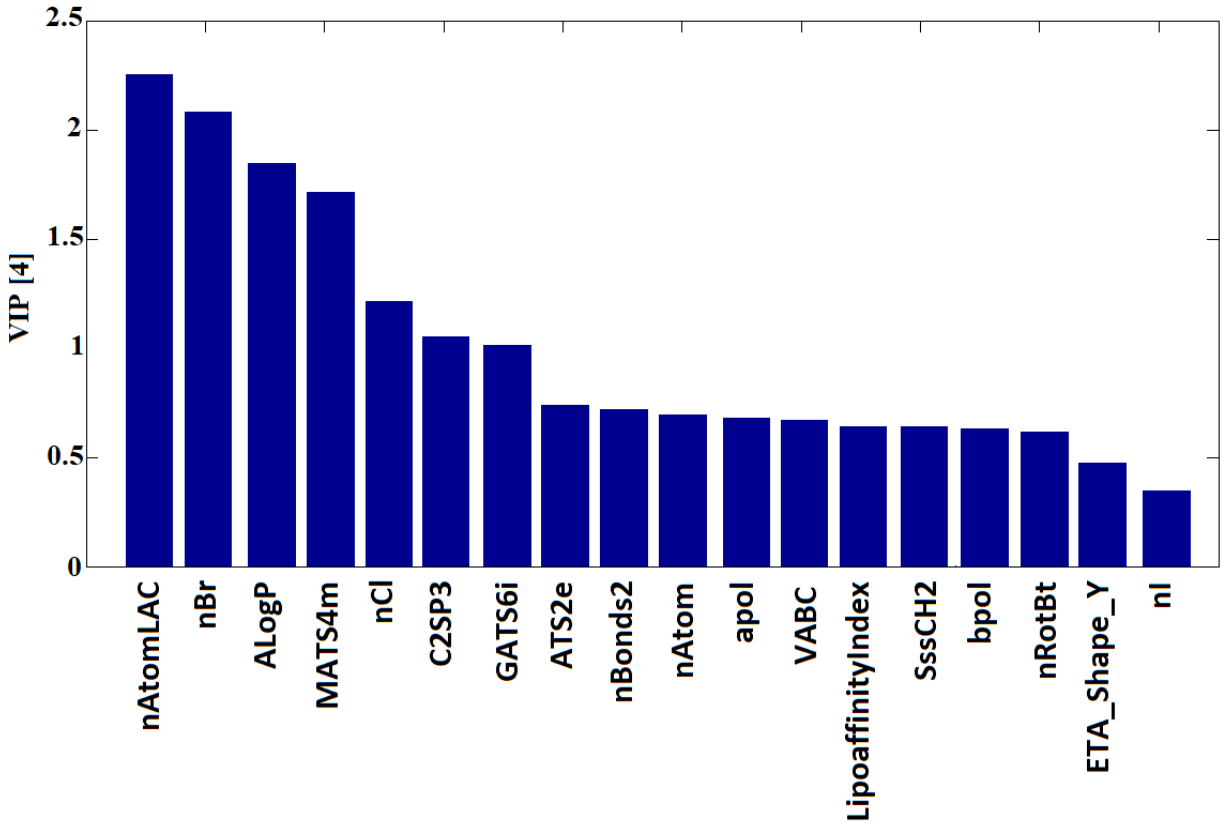

Figure 6. Variable influence plot of the PLS model

From Figure 6, it is possible to easily identify the relative importance of all the molecular descriptors applied for the regression. From the VIP plot, in addition to the regression coefficient, it's possible to conclude that: the halide species, the size of the carbon chain, the lipophilicity/solubility of the catalyst and the distribution of the properties along the molecular structure define the effectiveness of the catalyst to produce oleochemical carbonates.

Within the application domain of the QSPR model, it is concluded that it is possible to establish a structure-property relationship between the organocatalysts features and its activity to produce oleochemical carbonates from epoxides and CO_2. Thus, after the validation and interpretation of the QSPR model, the virtual screening was applied to identify potential actives compounds and suggest the best molecular targets among the catalyst set.

Virtual screening and new catalyst target

In the present work, a structure based virtual screening was performed by using the PubChem search tools, with the search being restricted to the actives compounds of the QSPR model application domain (i.e. organic halides derived from: ammonium, phosphonium, imidazolium, pyrrolidinium and pyridinium). From the virtual screening, a total of 122 potential catalysts were retrieved from a virtual library and their identification can be found in the Supporting Information (Table S6) while its respective calculated molecular descriptors are presented in the Table S9.

To estimate the activity of the potential catalysts, the Table S9 descriptors have been applied to both multivariate calibration models (PLS and SVM) and its average results predicted for the epoxide conversion to carbonate is considered as the catalyst output. In the Table 7, the best 20 molecular targets predicted by the QSPR model are presented, while in the Table S10 and Table S11, the conversion values estimated by each of the multivariate regression methods are specified.

Based on the Table 7 results, its observed that, among the catalysts best targets, only the tetraoctylphosphonium bromide [42] and the tetraheptylammonium bromide [53] have already been applied to produce oleochemicals both presenting high catalytic activity, as expected from our QSPR model.

Corroborating with our results, other high active catalysts with structures very similar to those listed in Table 7 have been reported for the conversion of styrene oxide into cyclic carbonate product (tetraoctylammonium chloride and tetradodecylammonium chloride) and to produce oleochemical carbonates (1-tetradecyl-3-methylimidazolium bromide and the trihexyltetradecylphosphonium bromide)[41,53,78].

Table 7. Best molecular targets predicted to produce oleochemical carbonates.

Catalyst	PubChem CID	CAS	[a]Conversion (%)
Hexacosyl(trimethyl)ammonium bromide	23196158	-	71.9%
Tetrakis(decyl)ammonium bromide	3014876	14937-42-9	63.0%
Docosyl(trimethyl)ammonium bromide	10216960	21396-56-5	63.0%
1-Docosyl-3-methylimidazolium bromide	86647477	943834-80-8	61.7%
Eicosyltrimethylammonium bromide	23767	7342-61-2	58.5%
Tributyl(hexadecyl)ammonium bromide	11420451	6439-67-4	56.4%
Tributyl(hexadecyl)phosphonium bromide	84716	14937-45-2	54.9%
Octadecyltrimethylammonium bromide	70708	1120-02-1	54.4%
Heptadecyl(trimethyl)ammonium bromide	10045219	21424-24-8	51.9%
Didodecyl(dimethyl)ammonium bromide	18669	3282-73-3	51.2%
1-Butyl-3-hexadecylimidazolium bromide	90220325	937716-18-2	50.6%
Hexadecyl-(2-hydroxyethyl)-dimethylammonium bromide	10960220	20317-32-2	50.1%
Cetyltrimethylammonium Bromide	5974	57-09-0	49.7%
Tetraoctylphosphonium bromide	3015167	23906-97-0	47.7%
Trimethyl(pentadecyl)ammonium bromide	14611710	21424-22-6	47.5%
1-Hexadecyl-3-methylimidazolium bromide	2846928	132361-22-9	47.4%
Ethyl-hexadecyl-dimethylammonium bromide	31280	124-03-8	47.2%
Trioctyl(propyl)ammonium bromide	90449	24298-17-7	46.1%
Tetraheptylammonium bromide	78073	4368-51-8	46.1%
1-Methyl-3-pentadecylimidazolium bromide	45045358	349148-74-9	45.3%

[a] Mean predicted results by the PLS and SVM models

Among the catalysts listed (Table 7) there are examples of compounds applied for carbonation of other epoxidized derivatives. The cetyltrimethylammonium bromide (CTAB) and hexadecyl-(2-hydroxyethyl)-dimethylammonium bromide (HEA16Br) were applied to produce cyclic carbonates derived from styrene oxide and present the same order of activity reported to the

found in our work, with the bifunctional one-component catalysts being more active [84]. Also, the predicted activity for HEA16Br was found as higher than for ethyl-hexadecyl-dimethylammonium bromide. These two compounds differ only in the presence of a hydroxyl substituent at the end of the ethyl chain and the advantages of a bifunctional catalyst was previously reported by several works [54,55,85,86].

In the literature, there is a low number of reports that apply the CTAB as a catalyst for the production of cyclic carbonates, most of them employing CTAB as a co-catalyst [80,81,84,87–93]. From Wei and collaborators [80], the conventional TBAB presents lower efficiency for cyclic carbonate production when compared to the catalyst with longer carbon chain length (employed as co-catalyst of zinc-cobalt double metal cyanide complex).

The order of activity found (TBAB < trimethyl(decyl)ammonium bromide < trimethyl(dodecyl)ammonium bromide < CTAB) is similar to those found by the QSPR model (for details see Supporting Information, Table S10). It is attributed to the increasing halide nucleophilicity, induced by the lengthening in the carbon chain, the enhance in the catalytic activity [78–82].

Data Mining

After the application of QSPR model over the virtual screening set, an additional data mining step was applied to evaluate the data features relating to catalyst structure. In this evaluation, the methyl group was established as the standard substituent and only one molecular feature is changed at a time (i.e. organic structure, molecular arrangement, carbon chain size and substituent type) and the results are presented in the Figure 7.

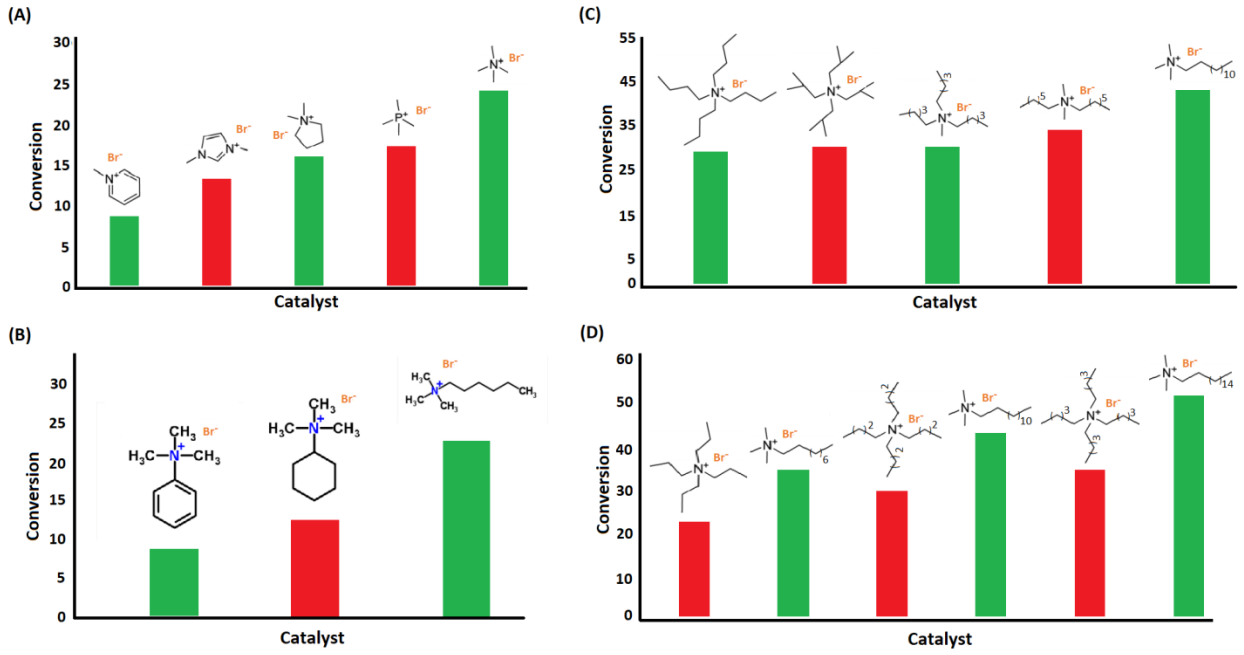

Figure 7. Structure–property relationships of organocatalyst to produce oleochemical carbonates. A) halide organic structure, B) carbons molecular arrangement, C) substituent type and D) lengthening of the carbon chain.

At first, the influence of the molecular structure is evaluated. From Figure 7a, it is possible to identify which of the organic structure included in the QSPR model application domain presents the higher estimated conversion and the following order of activity is found: pyridinium < imidazolium < pyrrolidinium < phosphonium < ammonium.

Identified the ammonium salts as the most actives, the number of carbons of the catalyst is kept constant while its distribution is altered. From Figure 7b two features are identified: i) the conversion increases with the lengthening of the carbon chain, and these results are related with the higher regression coefficient of the nAtomLAC descriptor; ii) the substituent branching results in a slight increase in conversion and this is explained through the modification of a set of descriptors (ALogP, C2SP3, GATS6i and $SssCH_2$).

In addition to the molecular arrangement in the catalyst structure, the influence of the substituent type on the estimated conversion was evaluated through the hexyl, cyclohexyl and aryl group, and the results are shown in Figure 7c. Maintaining the same carbon number (06), the catalyst activity increases in the following order: aromatic < cycloaliphatic < linear aliphatic chain.

This difference can be explained mainly by the modification in the molecular volume, linear carbon chain length, molecular polarizability and catalyst lipophilicity, indicated by the descriptors (ALogP, apol, bpol, C2SP3, nAtomLAC, $SssCH_2$ and VABC). In this way, it is concluded that both the solubility of the catalyst and the nucleophilic character of the halide are strongly influenced by the substituent structure.

Finally, from Figure 7d, it is observed that the lengthening of the carbon chain results in an increase in the estimated conversion value, regardless of the carbon arrangement profile in the catalyst. Therefore, the increase in the bulkiness of the catalyst results in the increase of the nucleophilic character of the halide [78–82].

Exploratory analysis

From the virtual screening data set, we selected the cetyltrimethylammonium bromide (CTAB) to be applied in the synthetic step of the present work. The CTAB combines the chemical characteristics (i.e. long carbon chain and large molecular volume) with practical issues (relatively low cost and readily available).

Before proceeding to the synthetic step, the exploratory analysis is applied to evaluate the similarity of CTAB compared to catalysts with known activity to produce oleochemical (Table 2). The PCA was applied to the molecular descriptor (Table S12) and its scores graph are presented

in Figure 8, while the PCA loading graph (Figure S4) and residual plot (Figure S5) are provided in the Supporting Information.

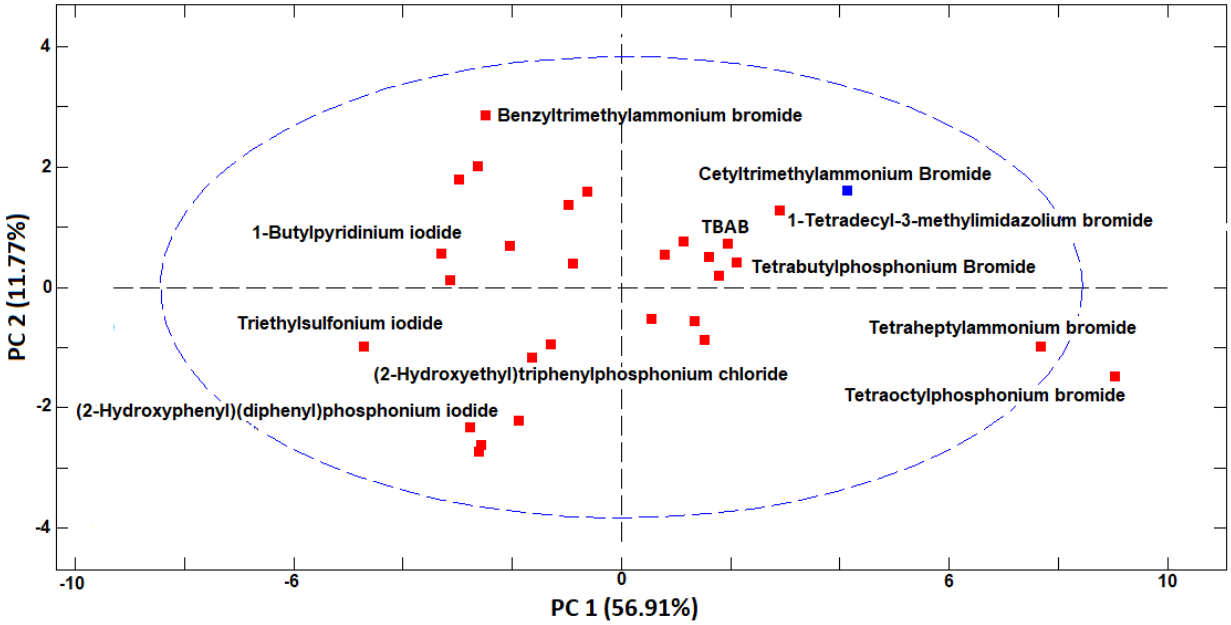

Figure 8. Exploratory analysis of the organocatalyst.

From the analysis of the PCA score and loading results, we found that the PC1 (56.91% of explained variance) and the PC2 (11.77% of explained variance) separates the catalysts with respect to their chemical structures. The compounds that presents higher molecular volume, linear carbon chain length, molecular polarizability and lipophilicity, indicated by the descriptors PC1 loadings (ALogP, apol, bpol, C2SP3, nAtomLAC, $SssCH_2$ and VABC), are displaced to PC1 positive scores values. Considering the regression coefficient of the QSPR model, it is concluded that the catalysts with higher activity, including the target catalyst (CTAB), are shifted to the right side of the PCA score plot, to positive values of PC1.

The PC2 separate the catalysts, particularly, with respect to the molecular arrangement carbons in the catalyst structure. Displaced to the PC2 positive scores are founded the catalysts with higher linear carbon chain length and lipophilicity, indicated by the descriptors PC2 loadings (ALogP and nAtomLAC), while to the negative PC2 scores are found the catalyst with higher molecular volume and molecular polarizability.

Another important finding is obtained from the PCA residue graph (Figure S5), which highlight three catalysts of the Data Set 03 as outliers: benzyltrimenthylammonium bromide, tetraoctylphosphonium bromide and triethylsulfonium iodide.

The benzyltrimenthylammonium bromide, with high Q-Residual, is described by the Tamami and coworkers as presenting a negligible activity to produce oleochemical carbonate.[36] To this result it should be noted that the chemical process was carried out at atmospheric pressure, with reduced amount of CO_2 dissolved in the oil phase, and the catalyst solubility was described as limited. The same catalyst applied to our QSPR model indicates a mean estimated conversion of 21.8% (PLS - 23.5%; SVM - 20.1%), which are lower than the standard catalyst TBAB (30%) but considerable higher than reported in the literature, if applied within the QSPR application domain (T = 100°C, P = 10 MPa, t = 5h and catalyst load = 1 mol%).

The triethylsulfonium iodide, outside the Hotelling T^2 limit (95%), composes the calibration set of the QSPR model and does not present any chemical activity for the production of oleochemical carbonates [10]. On the other hand, the tetraoctylphosphonium bromide, with high Q-Residual and outside the Hotelling T^2 limit, is a very active catalyst to produce oleochemical carbonate [42].

From a combined approach of QSPR modeling and exploratory analysis (PCA), based on a comprehensive set of data, it would be possible to quickly identify whether a molecular target is suitable to be tested in a synthetic procedure.

Synthesis of oleochemical carbonate

Identified the best molecular targets and interpreted the data features relating the catalyst structure with the conversion of epoxide to cyclic carbonates based on the QSPR and PCA methods, the CTAB is then applied as catalyst to produce cyclic carbonate from epoxidized oleochemical substrates and CO_2.

Three vegetable oil epoxides, derived from rice bran oil, canola oil and soybean oil have been employed to produce their respective oleochemical carbonates. The diversity of raw material is justified due to the influence of fatty acids composition on the conversion efficiency of epoxides to cyclic carbonates [38,39].

Initially, the solubility test indicated that CTAB it is very little soluble in epoxidized oil even at high temperature and, from the literature, similar results were found reported by Tamami for the benzyltrimenthylammonium bromide, a catalyst with a similar structure to the CTAB [36]. The effective interaction between the CTAB polar head and the bromide ion, together with the low polarity of the medium, difficult the solubilization and ions stabilization in the oily matrix. Unlike TBAB, which is readily solubilized in the oil due to the weaker ion pair between the bromide and a farthest nitrogen center[4,94], the application of CTAB must be assisted using polar solvent or phase transfer catalysts.

To overcome the solubility limitation, the n-butanol, a protic solvent with known miscibility with triglycerides and reported little influence on the conversion of epoxides to cyclic

carbonates, was employed [54,55]. Furthermore, considering the n-butanol structure, it can also act as a hydrogen bond donors activators (HBD) to facilitate the epoxy ring-opening and change the mass transfer phenomena involved by reducing the media viscosity and modifying the CO_2 solubility/diffusion rate [7,76,95,96].

In this way, the synthetic protocol was performed as described on the Materials and Methods Section and the products are then characterized by means of infrared spectroscopy (Figure 9a) and ^{1}H NMR (Figure 9b and 9c) and representatively illustrated in Figure 9. The FTIR spectra (Figure S6-S14) and the ^{1}H NMR with the detailed attribution Figure (S15-S23) are provided in the Supporting Information.

The first characterization by means of infrared (Figure 9a), is performed to identify the presence of the cyclic carbonate in the product. The disappearance of the oxirane band between 842cm^{-1} and 823 cm^{-1} indicates the epoxide consumption, while the new intensive carbonyl band (C=O) at 1795 cm^{-1} indicate the formation of the 5-member cyclic carbonate. The following ^{1}H NMR analysis (Figure 9b and Figure 9c) confirms the initial consumption of the vegetable oil unsaturation, multiplet between 5.40 ppm and 5.30 ppm (–C**H**=C**H**–), to produce the epoxy group (–C**H**OC**H**–), two multiplets at 2.9 ppm and 3.1 ppm [97,98]. In the second reaction step, the epoxide conversion to cyclic carbonate are accompanied by the disappearance of the epoxy group signals (2.9 ppm to 3.1 ppm) and the appearance of new signals related to the cyclic carbonate protons from 4.19 ppm to 4.24 ppm and 4.45 ppm to 5.12 ppm [43,99].

After characterization of the products, the epoxide conversion to cyclic carbonate is calculated based on the ^{1}H NMR spectra and the results are presented in the Table 8.

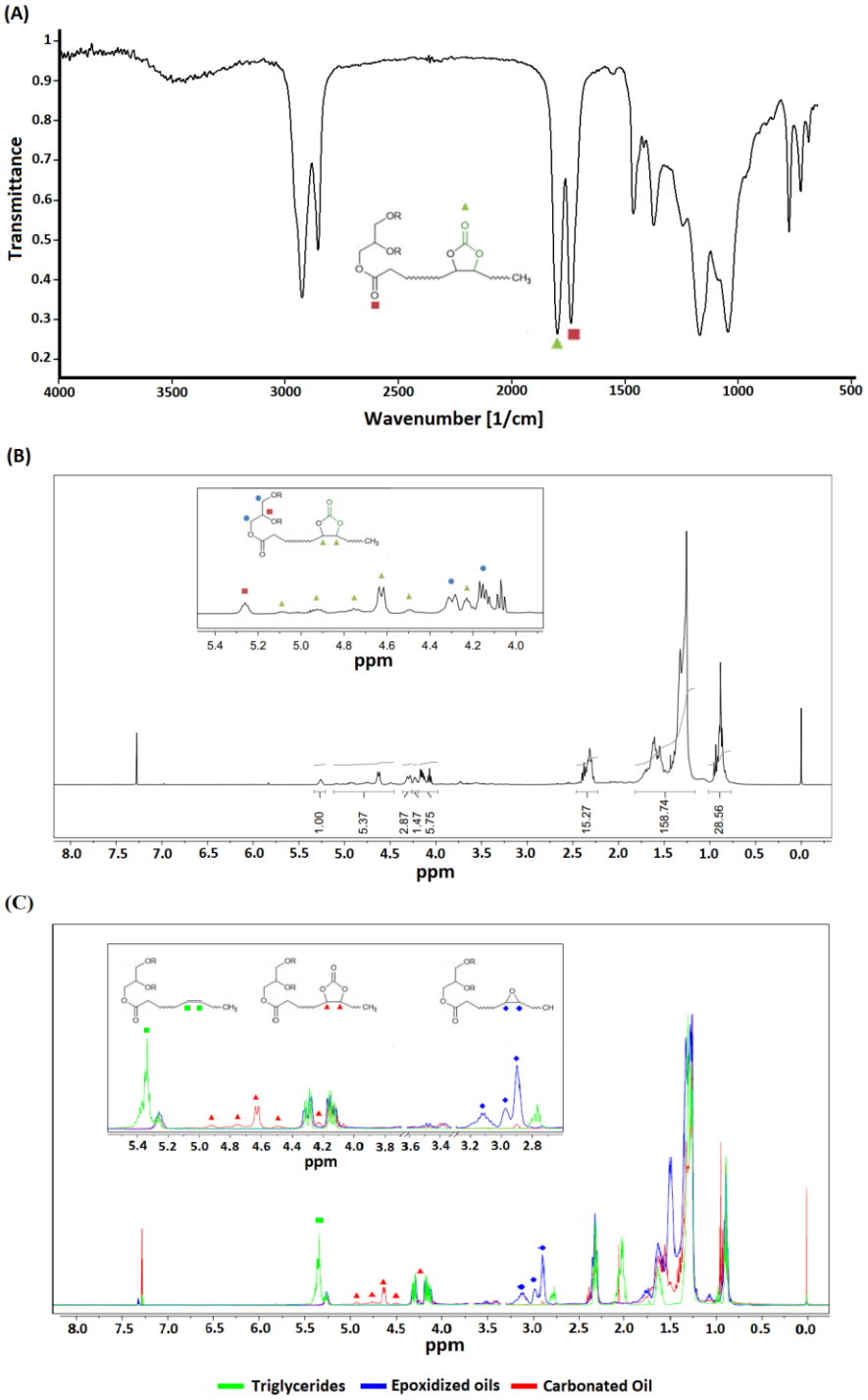

Figure 9. Infrared and ^{1}H NMR spectra of the oleochemical carbonated. A) FTIR spectra, B) Carbonate ^{1}H NMR spectra and C) ^{1}H NMR overlapping spectra of vegetable oil, epoxidized oil and carbonated oil.

Table 8. Epoxide conversion to cyclic carbonate.

Base Oil	[a]C=C	[b]Epoxy Group	[c]Conversion (%)
Rice Bran Oil	4.00	2.29	98.4%
Canola Oil	4.40	3.18	>99%
Soybean Oil	4.95	3.55	>99%

[a] - Mean carbon double bonds number per triglyceride unit, [b] - Mean epoxy group per triglyceride unit after epoxidation,[c] – Conversion to the cyclic carbonate group estimated based on the initial epoxy value

Based on Table 8, the CTAB showed high activity to produce oleochemical carbonates, regardless of the base raw material, with more than 98% of epoxide conversion to cyclic carbonate for all the vegetable oil. Respectively, a conversion of 98.4% was obtained for rice bran oil, (> 99%) for the soybean oil and (> 99%) for the canola oil. In Figure 10 are presented the proposed mechanism for the CTAB catalytic system.

The proposed catalytic system is composed by three steps and four transitions state, which are: Step 1) The epoxy ring, activated by hydrogen bonding, is opened by the bromide nucleophilic attack (Figure 10a), resulting in an oxyanion stabilized by both the CTAB polar head and the protic solvent hydrogen bonding (Figure 10b) [84]. Step 2) The insertion of CO_2 by oxyanion attack leads to formation of a carbonate ion (Figure 10c), also stabilized by hydrogen bonding and electrostatic interaction with the CTAB polar head. Step 3) The last step proceeds with the disruption of the C-Br chemical bond and the intramolecular formation of the 5-member cyclic carbonate (Figure 10d).

Differently from the TBAB catalytic system, in which the intermediate species stabilization is through a weak Van Der Waals interaction between the anions and the alkyl chain [95], the CTAB could promote a better stabilization of the intermediate species as results of a more intensive electrostatic interaction between the anions and the accessible nitrogen center of the

catalyst polar head [84]. We believe that the directional electrostatic interaction between the anions involved in the carbonation reaction and the CTAB polar head (with accessible nitrogen center) can account for the product stereoselectivity, however this statement should be further explored through computational simulations such as Density Functional Theory (DFT) methods and additional experimental procedures.

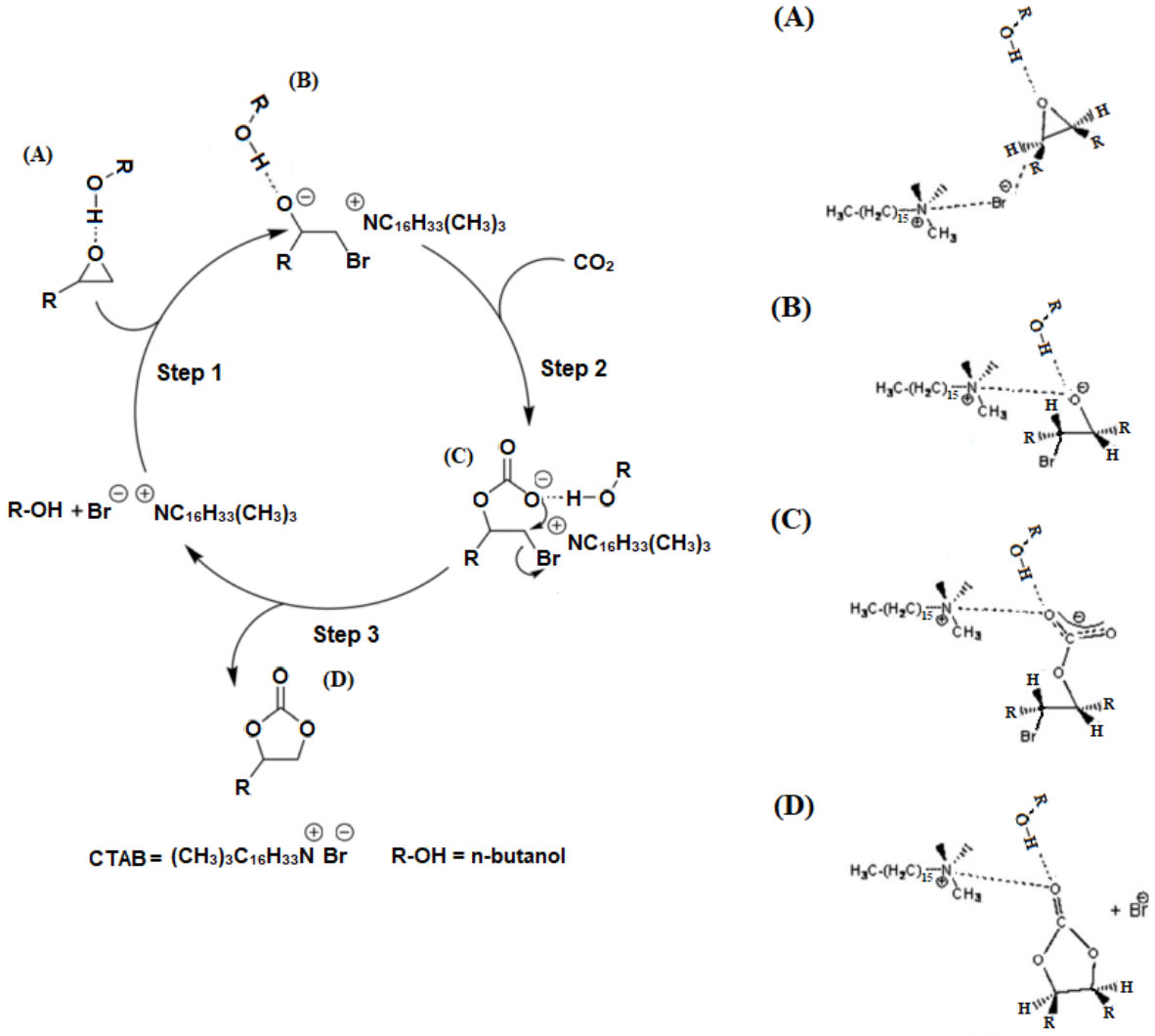

Figure 10. Proposed reaction mechanism for the CTAB-based catalytic system

CONCLUSIONS

To summarize, this work presents a preliminary perspective of QSPR modeling to assist in the targeted choice/design of new active organocatalysts to produce cyclic carbonates. The QSPR model was developed by applying the 2D molecular descriptors and validated based on criteria recognized by the academic community. From our results, it is concluded that it is possible to establish a structure-property relationship between the organocatalysts features and its activity to produce oleochemical carbonates from epoxides and CO_2.

From the virtual screening, a total of 122 catalysts have their activity predicted, the best molecular targets are proposed and the cetyltrimethylammonium bromide (CTAB) was selected for synthetic application. The principal molecular features (i.e. organic structure, molecular arrangement, carbon chain size and substituent type) were identified and described through data mining, while the PCA proved to be an adequate method to perform a rapid exploratory analysis of the molecules set.

Based on the synthetic outcomes, we provide the first report of the application of CTAB as a new active catalyst to produce oleochemical carbonate. In the present work, the experimental conditions were not fully optimized, the influence of the experimental parameters on the reaction system (i.e. pressure, time, temperature, stirring rate, catalyst load and solvent type) should be addressed in future work. Nevertheless, the high conversion, recommend further investigation of the CTAB-based catalytic system to achieve the optimization of procedures and experimental conditions.

In this way, the QSPR can be applied to reduce costs and time in the organocatalysts screening/design for the cyclic carbonates synthesis from CO_2. Since this work was developed

based in a small but representative number of catalysts, future work should increase the number and diversity of catalysts included in the QSPR model to increase its robustness. To best of our knowledge, this work presents the first QSPR approach on catalysts to cyclic carbonates.

ASSOCIATED CONTENT

The Supplementary material is available free of charge in the online version at DOI:

Data set 02: transferability evaluation of the QSPR model (Table S1), Molecular descriptors for the QSPR modeling of the data set 02 (Table S2), QSPR model for the synthesis of oleochemical carbonate: Data set 02 (Table S3), Predicted values of the conversion of epoxide to cyclic carbonate: Data set 02 (Table S4), Validation of the PLS and SVM model performed based on the Data Set 02 (Table S5), Potential catalyst set compiled based on virtual screening method (Table S6), Molecular descriptors for the QSPR modeling of the data set 01 (Table S7), Predicted values of the conversion of epoxide to cyclic carbonate: Data set 01 (Table S8), Molecular descriptors of the potential catalyst set (Table S9), Predicted activity for the potential catalyst set based on the PLS and SVM methods (Table S10), Predicted activity of the best organocatalyst targets based on the PLS and SVM models (Table S11), Molecular descriptors for the exploratory analysis of the data set 03 (Table S12). Predicted versus reference plot for the estimation of epoxide conversion to cyclic carbonate: Data set 02 (Figure S1), PLS regression coefficient for the estimation of epoxide conversion to cyclic carbonate: data set 02 (Figure S2), Variable influence plot of the PLS model:data set 02 (Figure S3), PCA loading of the exploratory analysis of the organocatalyst (Figure S4), PCA residuals of the exploratory analysis of the organocatalyst (Figure

S5), FTIR spectra of rice bran oil (Figure S6), FTIR spectra of rice canola oil (Figure S7), FTIR spectra of rice soybean oil (Figure S8), FTIR spectra of epoxidized rice bran oil (Figure S9), FTIR spectra of epoxidized canola oil (Figure S10), FTIR spectra of epoxidized soybean oil (Figure S11), FTIR spectra of carbonated rice bran oil (Figure S12), FTIR spectra of carbonated canola oil (Figure S13), FTIR spectra of carbonated soybean oil (Figure S14), ^{1}H NMR spectra of rice bran oil (Figure S15), ^{1}H NMR spectra of rice canola oil (Figure S16), ^{1}H NMR spectra of rice soybean oil (Figure S17), ^{1}H NMR spectra of epoxidized rice bran oil (Figure S18), ^{1}H NMR spectra of epoxidized canola oil (Figure S19), ^{1}H NMR spectra of epoxidized soybean oil (Figure S20), ^{1}H NMR spectra of carbonated rice bran oil (Figure S21), ^{1}H NMR spectra of carbonated canola oil (Figure S22) and ^{1}H NMR spectra of carbonated soybean oil (Figure S23).

AUTHOR INFORMATION

Corresponding Author

* Tel: +55 51 3320-4212.

E-mail: seferin@pucrs.br

ACKNOWLEDGMENTS

The authors would like to thank the Pontifical Catholic University of Rio Grande do Sul for the provided infrastructure, to the HP – Hewlett Packard-HP (PUCRS) for the research scholarships and to the Laboratory of Molecular Catalysis (UFRGS) for the assistance with the H-NMR analysis.

NOMENCLATURE

Molecular descriptors

nCl$^-$ - Number of chlorine atoms

nBr$^-$ - Number of bromine atoms

nI$^-$ - Number of iodine atoms

ALogP - Ghose-Crippen-Viswanadhan octanol-water partition coefficient

apol - Sum of the atomic polarizabilities (including implicit hydrogens)

ATS2e - Broto-Moreau autocorrelation - lag 2 / weighted by Sanderson electronegativities

bpol - Sum of the absolute value of the difference between atomic polarizabilities of all bonded atoms in the molecule (including implicit hydrogens)

C2SP3 - Singly bound carbon bound to two other carbons

ETA Shape Y – Extended topochemical atom shape index Y

GATS6i - Geary autocorrelation - lag 6 / weighted by first ionization potential

Lipoaffinity Index - Atom type electrotopological state lipoaffinity index

MATS4m - Moran autocorrelation - lag 4 / weighted by mass

nAtom - Number of atoms

nAtomLAC - Number of atoms in the longest aliphatic chain

nBonds2 - Total number of bonds (including bonds to hydrogens)

nRotBt - Number of rotatable bonds, including terminal bonds

SssCH$_2$ - Sum of atom-type E-State: -CH$_2$-

VABC - Van der Waals volume

REFERENCES

[1] M. North, P. Styring, Perspectives and visions on CO_2 capture and utilisation, Faraday Discuss. 183 (2015) 489–502. doi:10.1039/C5FD90077H.

[2] R.M. Cuéllar-Franca, A. Azapagic, Carbon capture, storage and utilisation technologies: A critical analysis and comparison of their life cycle environmental impacts, J. CO_2 Util. 9 (2015) 82–102. doi:10.1016/j.jcou.2014.12.001.

[3] M. Alves, B. Grignard, R. Mereau, C. Jerome, T. Tassaing, C. Detrembleur, Organocatalyzed coupling of carbon dioxide with epoxides for the synthesis of cyclic carbonates: catalyst design and mechanistic studies, Catal. Sci. Technol. 7 (2017) 2651–2684. doi:10.1039/C7CY00438A.

[4] H. Büttner, L. Longwitz, J. Steinbauer, C. Wulf, T. Werner, H. Buttner, L. Longwitz, J. Steinbauer, C. Wulf, T. Werner, H. Büttner, L. Longwitz, J. Steinbauer, C. Wulf, T. Werner, Recent Developments in the Synthesis of Cyclic Carbonates from Epoxides and CO_2, Top. Curr. Chem. 375 (2017) 50. doi:10.1007/s41061-017-0136-5.

[5] A. Sternberg, C.M. Jens, A. Bardow, Life cycle assessment of CO_2-based C1-chemicals, Green Chem. 19 (2017) 2244–2259. doi:10.1039/C6GC02852G.

[6] M. Poliakoff, W. Leitner, E.S. Streng, The Twelve Principles of CO_2 CHEMISTRY., Faraday Discuss. 183 (2015) 9–17. doi:10.1039/c5fd90078f.

[7] X. Cai, J.L. Zheng, J. Wärnå, T. Salmi, B. Taouk, S. Leveneur, Influence of gas-liquid mass transfer on kinetic modeling: Carbonation of epoxidized vegetable oils, Chem. Eng. J. 313 (2017) 1168–1183. doi:10.1016/j.cej.2016.11.012.

[8] M.O. Vieira, W.F. Monteiro, B.S. Neto, R. Ligabue, V. V. Chaban, S. Einloft, Surface Active Ionic Liquids as Catalyst for CO_2 Conversion to Propylene Carbonate, Catal. Letters. 148 (2018) 108–118. doi:10.1007/s10562-017-2212-4.

[9] A.S. Aquino, F.L. Bernard, J. V. Borges, L. Mafra, F.D. Vecchia, M.O. Vieira, R. Ligabue, M. Seferin, V. V. Chaban, E.J. Cabrita, S. Einloft, Rationalizing the role of the anion in CO_2 capture and conversion using imidazolium-based ionic liquid modified mesoporous silica, RSC Adv. 5 (2015) 64220–64227. doi:10.1039/C5RA07561K.

[10] M. Alves, B. Grignard, S. Gennen, C. Detrembleur, C. Jerome, T. Tassaing, Organocatalytic synthesis of bio-based cyclic carbonates from CO_2 and vegetable oils, RSC Adv. 5 (2015) 53629–53636. doi:10.1039/C5RA10190E.

[11] M. Cokoja, M.E. Wilhelm, M.H. Anthofer, W.A. Herrmann, F.E. Kühn, Synthesis of Cyclic Carbonates from Epoxides and Carbon Dioxide by Using Organocatalysts, ChemSusChem.

8 (2015) 2436–2454. doi:10.1002/cssc.201500161.

[12] W. Desens, T. Werner, Convergent Activation Concept for CO_2 Fixation in Carbonates, Adv. Synth. Catal. 358 (2016) 622–630. doi:10.1002/adsc.201500941.

[13] A.M. Appel, J.E. Bercaw, A.B. Bocarsly, H. Dobbek, D.L. DuBois, M. Dupuis, J.G. Ferry, E. Fujita, R. Hille, P.J.A. Kenis, C.A. Kerfeld, R.H. Morris, C.H.F. Peden, A.R. Portis, S.W. Ragsdale, T.B. Rauchfuss, J.N.H. Reek, L.C. Seefeldt, R.K. Thauer, G.L. Waldrop, Frontiers, Opportunities, and Challenges in Biochemical and Chemical Catalysis of CO_2 Fixation, Chem. Rev. 113 (2013) 6621–6658. doi:10.1021/cr300463y.

[14] V. Blay, J. Gullón-Soleto, M. Gálvez-Llompart, J. Gálvez, R. García-Domenech, Biodegradability Prediction of Fragrant Molecules by Molecular Topology, ACS Sustain. Chem. Eng. 4 (2016) 4224–4231. doi:10.1021/acssuschemeng.6b00717.

[15] M. Stec, T. Spietz, L. Więcław-Solny, A. Tatarczuk, A. Krótki, Predicting normal densities of amines using quantitative structure-property relationship (QSPR), SAR QSAR Environ. Res. 26 (2015) 893–904. doi:10.1080/1062936X.2015.1095239.

[16] A.R. Katritzky, V.S. Lobanov, QSPR: The Correlation and Quantitative Prediction of Chemical and Physical Properties from Structure, Chem. Soc. Rev. 24 (1995) 279–287. doi:10.1039/CS9952400279.

[17] B.F. Begam, J.S. Kumar, Computer Assisted QSAR/QSPR Approaches – A Review, Indian J. Sci. Technol. 9 (2016) 1–8. doi:10.17485/ijst/2016/v9i8/87901.

[18] K. Roy, P. Ambure, R.B. Aher, How important is to detect systematic error in predictions and understand statistical applicability domain of QSAR models?, Chemom. Intell. Lab. Syst. 162 (2017) 44–54. doi:10.1016/j.chemolab.2017.01.010.

[19] K. Roy, I. Mitra, S. Kar, P.K. Ojha, R.N. Das, H. Kabir, Comparative Studies on Some Metrics for External Validation of QSPR Models, J. Chem. Inf. Model. 52 (2012) 396–408.

[20] K. Roy, P. Ambure, S. Kar, P.K. Ojha, Is it possible to improve the quality of predictions from an “intelligent” use of multiple QSAR/QSPR/QSTR models?, J. Chemom. (2018) e2992. doi:10.1002/cem.2992.

[21] M. Karelson, V.S. Lobanov, A.R. Katritzky, Quantum-Chemical Descriptors in QSAR/QSPR Studies, Chem. Rev. 96 (1996) 1027–1044. doi:10.1021/cr950202r.

[22] E. Zeini Jahromi, J. Gailer, Probing bioinorganic chemistry processes in the bloodstream to gain new insights into the origin of human diseases, Dalt. Trans. 39 (2010) 329–336. doi:10.1039/B912941N.

[23] A.G. Maldonado, G. Rothenberg, Predictive modeling in homogeneous catalysis: a tutorial, Chem. Soc. Rev. 39 (2010) 1891. doi:10.1039/b921393g.

[24] G. Rothenberg, Data mining in catalysis: Separating knowledge from garbage, Catal.

Today. 137 (2008) 2–10. doi:10.1016/j.cattod.2008.02.014.

[25] S. Yao, T. Shoji, Y. Iwamoto, E. Kamei, Consideration of an activity of the metallocene catalyst by using molecular mechanics, molecular dynamics and QSAR, Comput. Theor. Polym. Sci. 9 (1999) 41–46. doi:10.1016/S1089-3156(98)00051-8.

[26] S. Martínez, V.L. Cruz, J. Ramos, J. Martínez-Salazar, Polymerization Activity Prediction of Zirconocene Single-Site Catalysts Using 3D Quantitative Structure–Activity Relationship Modeling, Organometallics. 31 (2012) 1673–1679. doi:10.1021/om2007776.

[27] V.L. Cruz, S. Martinez, J. Martinez-Salazar, D. Polo-Cerón, S. Gómez-Ruiz, M. Fajardo, S. Prashar, 3D-QSAR study of ansa-metallocene catalytic behavior in ethylene polymerization, Polymer (Guildf). 48 (2007) 4663–4674. doi:10.1016/j.polymer.2007.05.081.

[28] G. Fayet, P. Raybaud, H. Toulhoat, T. de Bruin, Iron bis(arylimino)pyridine precursors activated to catalyze ethylene oligomerization as studied by DFT and QSAR approaches, J. Mol. Struct. THEOCHEM. 903 (2009) 100–107. doi:10.1016/j.theochem.2008.10.048.

[29] P.G.R. Achary, S. Begum, A.P. Toropova, A.A. Toropov, A quasi-SMILES based QSPR Approach towards the prediction of adsorption energy of Ziegler − Natta catalysts for propylene polymerization, Mater. Discov. 5 (2016) 22–28. doi:10.1016/j.md.2016.12.003.

[30] M. Ratanasak, T. Rungrotmongkol, O. Saengsawang, S. Hannongbua, V. Parasuk, Towards the design of new electron donors for Ziegler–Natta catalyzed propylene polymerization using QSPR modeling, Polymer (Guildf). 56 (2015) 340–345. doi:10.1016/j.polymer.2014.11.022.

[31] S. Samanta, S. Selvakumar, J. Bahr, D.S. Wickramaratne, M. Sibi, B.J. Chisholm, Synthesis and Characterization of Polyurethane Networks Derived from Soybean-Oil-Based Cyclic Carbonates and Bioderivable Diamines, ACS Sustain. Chem. Eng. 4 (2016) 6551–6561. doi:10.1021/acssuschemeng.6b01409.

[32] G. Karmakar, P. Ghosh, B. Sharma, Chemically Modifying Vegetable Oils to Prepare Green Lubricants, Lubricants. 5 (2017) 44. doi:10.3390/lubricants5040044.

[33] S. Miao, P. Wang, Z. Su, S. Zhang, Vegetable-oil-based polymers as future polymeric biomaterials, Acta Biomater. 10 (2014) 1692–1704. doi:10.1016/j.actbio.2013.08.040.

[34] S.M. Danov, O.A. Kazantsev, A.L. Esipovich, A.S. Belousov, A.E. Rogozhin, E.A. Kanakov, Recent advances in the field of selective epoxidation of vegetable oils and their derivatives: a review and perspective, Catal. Sci. Technol. 7 (2017) 3659–3675. doi:10.1039/C7CY00988G.

[35] N. Von Der Assen, L.J. Müller, A. Steingrube, P. Voll, A. Bardow, Selecting CO_2 Sources for CO_2 Utilization by Environmental-Merit-Order Curves, Environ. Sci. Technol. 50 (2016) 1093–1101. doi:10.1021/acs.est.5b03474.

[36] B. Tamami, S. Sohn, G.L. Wilkes, Incorporation of carbon dioxide into soybean oil and subsequent preparation and studies of nonisocyanate polyurethane networks, J. Appl. Polym. Sci. 92 (2004) 883–891. doi:10.1002/app.20049.

[37] J.L. Zheng, P. Tolvanen, B. Taouk, K. Eränen, S. Leveneur, T. Salmi, Synthesis of carbonated vegetable oils: Investigation of microwave effect in a pressurized continuous-flow recycle batch reactor, Chem. Eng. Res. Des. 132 (2018) 9–18. doi:10.1016/j.cherd.2017.12.037.

[38] L. Peña Carrodeguas, À. Cristòfol, J.M. Fraile, J.A. Mayoral, V. Dorado, C.I. Herrerías, A.W. Kleij, Fatty acid based biocarbonates: Al-mediated stereoselective preparation of mono-, di- and tricarbonates under mild and solvent-less conditions, Green Chem. 19 (2017) 3535–3541. doi:10.1039/C7GC01206C.

[39] L. Longwitz, J. Steinbauer, A. Spannenberg, T. Werner, Calcium-Based Catalytic System for the Synthesis of Bio-Derived Cyclic Carbonates under Mild Conditions, ACS Catal. 8 (2018) 665–672. doi:10.1021/acscatal.7b03367.

[40] J. Wang, Y. Zhao, Q. Li, N. Yin, Y. Feng, M. Kang, X. Wang, Pt doped $H_3PW_{12}O_{40}/ZrO_2$ as a heterogeneous and recyclable catalyst for the synthesis of carbonated soybean oil, J. Appl. Polym. Sci. 124 (2012) 4298–4306. doi:10.1002/app.35418.

[41] B. Schäffner, M. Blug, D. Kruse, M. Polyakov, A. Köckritz, A. Martin, P. Rajagopalan, U. Bentrup, A. Brückner, S. Jung, D. Agar, B. Rüngeler, A. Pfennig, K. Müller, W. Arlt, B. Woldt, M. Graß, S. Buchholz, Synthesis and Application of Carbonated Fatty Acid Esters from Carbon Dioxide Including a Life Cycle Analysis, ChemSusChem. 7 (2014) 1133–1139. doi:10.1002/cssc.201301115.

[42] H. Büttner, C. Grimmer, J. Steinbauer, T. Werner, Iron-Based Binary Catalytic System for the Valorization of CO_2 into Biobased Cyclic Carbonates, ACS Sustain. Chem. Eng. 4 (2016) 4805–4814. doi:10.1021/acssuschemeng.6b01092.

[43] N. Tenhumberg, H. Büttner, B. Schäffner, D. Kruse, M. Blumenstein, T. Werner, Cooperative catalyst system for the synthesis of oleochemical cyclic carbonates from CO_2 and renewables, Green Chem. 18 (2016) 3775–3788. doi:10.1039/C6GC00671J.

[44] H. Büttner, J. Steinbauer, C. Wulf, M. Dindaroglu, H.-G. Schmalz, T. Werner, Organocatalyzed Synthesis of Oleochemical Carbonates from CO_2 and Renewables, ChemSusChem. 10 (2017) 1076–1079. doi:10.1002/cssc.201601163.

[45] A.R. Katritzky, M. Karelson, V.S. Lobanov, QSPR as a means of predicting and understanding chemical and physical properties in terms of structure, Pure Appl. Chem. 69 (1997) 245–248. doi:10.1351/pac199769020245.

[46] A. Golbraikh, A. Tropsha, Beware of Q^2!, J. Mol. Graph. Model. 20 (2002) 269–276. doi:10.1016/S1093-3263(01)00123-1.

[47] S. Kim, Getting the most out of PubChem for virtual screening, Expert Opin. Drug Discov.

11 (2016) 843–855. doi:10.1080/17460441.2016.1216967.

[48] C.W. Yap, PaDEL-descriptor: An open source software to calculate molecular descriptors and fingerprints, J. Comput. Chem. 32 (2011) 1466–1474. doi:10.1002/jcc.21707.

[49] R. Kiralj, M.M.C. Ferreira, Is your QSAR/QSPR descriptor real or trash?, J. Chemom. 24 (2010) 681–693. doi:10.1002/cem.1331.

[50] L. Xu, W.-J. Zhang, Comparison of different methods for variable selection, Anal. Chim. Acta. 446 (2001) 475–481. doi:10.1016/S0003-2670(01)01271-5.

[51] I. Mitra, P.P. Roy, S. Kar, P.K. Ojha, K. Roy, On further application of rm^2 as a metric for validation of QSAR models, J. Chemom. 24 (2010) 22–33. doi:10.1002/cem.1268.

[52] M. Gonzalez, C. Teran, L. Saiz-Urra, M. Teijeira, Variable Selection Methods in QSAR: An Overview, Curr. Top. Med. Chem. 8 (2008) 1606–1627. doi:10.2174/156802608786786552.

[53] J. Langanke, L. Greiner, W. Leitner, Substrate dependent synergetic and antagonistic interaction of ammonium halide and polyoxometalate catalysts in the synthesis of cyclic carbonates from oleochemical epoxides and CO_2, Green Chem. 15 (2013) 1173. doi:10.1039/c3gc36710j.

[54] H. Büttner, K. Lau, A. Spannenberg, T. Werner, Bifunctional One-Component Catalysts for the Addition of Carbon Dioxide to Epoxides, ChemCatChem. 7 (2015) 459–467. doi:10.1002/cctc.201402816.

[55] H. Büttner, J. Steinbauer, T. Werner, Synthesis of Cyclic Carbonates from Epoxides and Carbon Dioxide by Using Bifunctional One-Component Phosphorus-Based Organocatalysts, ChemSusChem. 8 (2015) 2655–2669. doi:10.1002/cssc.201500612.

[56] R. Todeschini, V. Consonni, Molecular Descriptors for Chemoinformatics, Wiley-VCH Verlag GmbH & Co. KGaA, Weinheim, Germany, 2009. doi:10.1002/9783527628766.

[57] Y.H. Zhao, M.H. Abraham, A.M. Zissimos, Fast Calculation of van der Waals Volume as a Sum of Atomic and Bond Contributions and Its Application to Drug Compounds, J. Org. Chem. 68 (2003) 7368–7373. doi:10.1021/jo034808o.

[58] R. Liu, H. Sun, S.-S. So, Development of Quantitative Structure−Property Relationship Models for Early ADME Evaluation in Drug Discovery. 2. Blood-Brain Barrier Penetration, J. Chem. Inf. Comput. Sci. 41 (2001) 1623–1632. doi:10.1021/ci010290i.

[59] K. Roy, G. Ghosh, QSTR with Extended Topochemical Atom Indices. 2. Fish Toxicity of Substituted Benzenes, J. Chem. Inf. Comput. Sci. 44 (2004) 559–567. doi:10.1021/ci0342066.

[60] A.K. Ghose, G.M. Crippen, Atomic physicochemical parameters for three-dimensional-structure-directed quantitative structure-activity relationships. 2. Modeling dispersive and

hydrophobic interactions, J. Chem. Inf. Model. 27 (1987) 21–35. doi:10.1021/ci00053a005.

[61] A.K. Ghose, G.M. Crippen, Atomic Physicochemical Parameters for Three-Dimensional Structure-Directed Quantitative Structure-Activity Relationships I. Partition Coefficients as a Measure of Hydrophobicity, J. Comput. Chem. 7 (1986) 565–577. doi:10.1002/jcc.540070419.

[62] P. Pratim Roy, S. Paul, I. Mitra, K. Roy, On Two Novel Parameters for Validation of Predictive QSAR Models, Molecules. 14 (2009) 1660–1701. doi:10.3390/molecules14051660.

[63] R. Todeschini, D. Ballabio, F. Grisoni, Beware of Unreliable Q^2! A Comparative Study of Regression Metrics for Predictivity Assessment of QSAR Models, J. Chem. Inf. Model. 56 (2016) 1905–1913. doi:10.1021/acs.jcim.6b00277.

[64] D.L.J. Alexander, A. Tropsha, D.A. Winkler, Beware of R^2: Simple, Unambiguous Assessment of the Prediction Accuracy of QSAR and QSPR Models, J. Chem. Inf. Model. 55 (2015) 1316–1322. doi:10.1021/acs.jcim.5b00206.

[65] P. Gramatica, A. Sangion, A Historical Excursus on the Statistical Validation Parameters for QSAR Models: A Clarification Concerning Metrics and Terminology, J. Chem. Inf. Model. 56 (2016) 1127–1131. doi:10.1021/acs.jcim.6b00088.

[66] A. Tropsha, P. Gramatica, V. Gombar, The Importance of Being Earnest: Validation is the Absolute Essential for Successful Application and Interpretation of QSPR Models, QSAR Comb. Sci. 22 (2003) 69–77. doi:10.1002/qsar.200390007.

[67] A. Tropsha, Best Practices for QSAR Model Development, Validation, and Exploitation, Mol. Inform. 29 (2010) 476–488. doi:10.1002/minf.201000061.

[68] K. Roy, I. Mitra, P.K. Ojha, S. Kar, R.N. Das, H. Kabir, Introduction of rm^2(rank) metric incorporating rank-order predictions as an additional tool for validation of QSAR/QSPR models, Chemom. Intell. Lab. Syst. 118 (2012) 200–210. doi:10.1016/j.chemolab.2012.06.004.

[69] K. Roy, I. Mitra, On the Use of the Metric rm^2 as an Effective Tool for Validation of QSAR Models in Computational Drug Design and Predictive Toxicology, Mini-Reviews Med. Chem. 12 (2012) 491–504. doi:10.2174/138955712800493861.

[70] K. Roy, I. Mitra, On Various Metrics Used for Validation of Predictive QSAR Models with Applications in Virtual Screening and Focused Library Design, Comb. Chem. High Throughput Screen. 14 (2011) 450–474. doi:10.2174/138620711795767893.

[71] T. Scior, A. Bender, G. Tresadern, J.L. Medina-Franco, K. Martínez-Mayorga, T. Langer, K. Cuanalo-Contreras, D.K. Agrafiotis, Recognizing Pitfalls in Virtual Screening: A Critical Review, J. Chem. Inf. Model. 52 (2012) 867–881. doi:10.1021/ci200528d.

[72] V. V. Goud, A. V. Patwardhan, S. Dinda, N.C. Pradhan, Epoxidation of karanja (Pongamia

glabra) oil catalysed by acidic ion exchange resin, Eur. J. Lipid Sci. Technol. 109 (2007) 575–584. doi:10.1002/ejlt.200600298.

[73] S. Dinda, A. V. Patwardhan, V. V. Goud, N.C. Pradhan, Epoxidation of cottonseed oil by aqueous hydrogen peroxide catalysed by liquid inorganic acids, Bioresour. Technol. 99 (2008) 3737–3744. doi:10.1016/j.biortech.2007.07.015.

[74] S. Wold, M. Sjöström, L. Eriksson, PLS-regression: a basic tool of chemometrics, Chemom. Intell. Lab. Syst. 58 (2001) 109–130. doi:10.1016/S0169-7439(01)00155-1.

[75] S. Das, P.K. Ojha, K. Roy, Development of a temperature dependent 2D-QSPR model for viscosity of diverse functional ionic liquids, J. Mol. Liq. 240 (2017) 454–467. doi:10.1016/j.molliq.2017.05.113.

[76] J.L. Zheng, F. Burel, T. Salmi, B. Taouk, S. Leveneur, Carbonation of Vegetable Oils: Influence of Mass Transfer on Reaction Kinetics, Ind. Eng. Chem. Res. 54 (2015) 10935–10944. doi:10.1021/acs.iecr.5b02006.

[77] H. Yang, J. Guo, Y. Wen, T. Ren, L. Wang, J. Zhang, Solvent effect on the fixation of CO_2 catalyzed by quaternary ammonium-based ionic liquids bearing different numbers of hydroxyl groups: A combined molecular dynamics simulation and ONIOM study, Mol. Catal. 441 (2017) 134–139. doi:10.1016/j.mcat.2017.08.009.

[78] M.M. Dharman, J.-I. Yu, J.-Y. Ahn, D.-W. Park, Selective production of cyclic carbonate over polycarbonate using a double metal cyanide–quaternary ammonium salt catalyst system, Green Chem. 11 (2009) 1754. doi:10.1039/b916875n.

[79] L. Han, S.-J. Choi, M.-S. Park, S.-M. Lee, Y.-J. Kim, M.-I. Kim, B. Liu, D.-W. Park, Carboxylic acid functionalized imidazolium-based ionic liquids: efficient catalysts for cycloaddition of CO_2 and epoxides, React. Kinet. Mech. Catal. 106 (2012) 25–35. doi:10.1007/s11144-011-0399-8.

[80] R. Wei, X. Zhang, B. Du, Z. Fan, G. Qi, Highly active and selective binary catalyst system for the coupling reaction of CO_2 and hydrous epoxides, J. Mol. Catal. A Chem. 379 (2013) 38–45. doi:10.1016/j.molcata.2013.07.014.

[81] S. Narang, D. Berek, S.N. Upadhyay, R. Mehta, Effect of electron density on the catalysts for copolymerization of propylene oxide and CO_2, J. Polym. Res. 23 (2016) 96. doi:10.1007/s10965-016-0994-5.

[82] L. Wang, T. Huang, C. Chen, J. Zhang, H. He, S. Zhang, Mechanism of hexaalkylguanidinium salt/zinc bromide binary catalysts for the fixation of CO_2 with epoxide: A DFT investigation, J. CO_2 Util. 14 (2016) 61–66. doi:10.1016/j.jcou.2016.02.006.

[83] H. Sun, D. Zhang, Density Functional Theory Study on the Cycloaddition of Carbon Dioxide with Propylene Oxide Catalyzed by Alkylmethylimidazolium Chlorine Ionic Liquids, J. Phys. Chem. A. 111 (2007) 8036–8043. doi:10.1021/jp073873p.

[84] C. Carvalho Rocha, T. Onfroy, J. Pilmé, A. Denicourt-Nowicki, A. Roucoux, F. Launay, Experimental and theoretical evidences of the influence of hydrogen bonding on the catalytic activity of a series of 2-hydroxy substituted quaternary ammonium salts in the styrene oxide/CO_2 coupling reaction, J. Catal. 333 (2016) 29–39. doi:10.1016/j.jcat.2015.10.014.

[85] L. Wang, X. Jin, Y. Li, P. Li, J. Zhang, H. He, S. Zhang, Insight into the activity of efficient acid–base bifunctional catalysts for the coupling reaction of CO_2, Mol. Phys. 113 (2015) 3524–3530. doi:10.1080/00268976.2015.1037804.

[86] M.H. Anthofer, M.E. Wilhelm, M. Cokoja, M. Drees, W.A. Herrmann, F.E. Kühn, Hydroxy-Functionalized Imidazolium Bromides as Catalysts for the Cycloaddition of CO_2 and Epoxides to Cyclic Carbonates, ChemCatChem. 7 (2015) 94–98. doi:10.1002/cctc.201402754.

[87] A. Ion, V. Parvulescu, P. Jacobs, D. de Vos, Sc and Zn-catalyzed synthesis of cyclic carbonates from CO_2 and epoxides, Appl. Catal. A Gen. 363 (2009) 40–44. doi:10.1016/j.apcata.2009.04.036.

[88] Z. Bu, Z. Wang, L. Yang, S. Cao, Synthesis of propylene carbonate from carbon dioxide using trans-dichlorotetrapyridineru- thenium(II) as catalyst, Appl. Organomet. Chem. 24 (2010) 813–816. doi:10.1002/aoc.1708.

[89] J. Tharun, M.M. Dharman, Y. Hwang, R. Roshan, M.S. Park, D.-W. Park, Tuning double metal cyanide catalysts with complexing agents for the selective production of cyclic carbonates over polycarbonates, Appl. Catal. A Gen. 419–420 (2012) 178–184. doi:10.1016/j.apcata.2012.01.024.

[90] R. Wei, X. Zhang, B. Du, Z. Fan, G. Qi, Synthesis of bis(cyclic carbonate) and propylene carbonate via a one-pot coupling reaction of CO_2, bisepoxide and propylene oxide, RSC Adv. 3 (2013) 17307. doi:10.1039/c3ra42570c.

[91] Z. Guo, Q. Lin, X. Wang, C. Yu, J. Zhao, Y. Shao, T. Peng, Rapid synthesis of nanoscale double metal cyanide catalysts by ball milling for the cycloaddition of CO_2 and propylene oxide, Mater. Lett. 124 (2014) 184–187. doi:10.1016/j.matlet.2014.03.076.

[92] B. Liu, Y.-Y. Zhang, X.-H. Zhang, B. Du, Z.-Q. Fan, Fixation of carbon dioxide concurrently or in tandem with free radical polymerization for highly transparent polyacrylates with specific UV absorption, Polym. Chem. 7 (2016) 3731–3739. doi:10.1039/C6PY00525J.

[93] S. Narang, R. Mehta, S.N. Upadhyay, Solvent-free cycloaddition of CO_2 and propylene oxide to cyclic carbonates using different ligand metal complexes, Inorg. Nano-Metal Chem. 47 (2017) 909–916. doi:10.1080/15533174.2016.1228673.

[94] V. Caló, A. Nacci, A. Monopoli, A. Fanizzi, Cyclic Carbonate Formation from Carbon Dioxide and Oxiranes in Tetrabutylammonium Halides as Solvents and Catalysts, Org. Lett. 4 (2002) 2561–2563. doi:10.1021/ol026189w.

[95] M. Alves, R. Mereau, B. Grignard, C. Detrembleur, C. Jerome, T. Tassaing, A comprehensive density functional theory study of the key role of fluorination and dual hydrogen bonding in the activation of the epoxide/CO_2 coupling by fluorinated alcohols, RSC Adv. 6 (2016) 36327–36335. doi:10.1039/C6RA03427F.

[96] J.-Q. Wang, J. Sun, W. Cheng, K. Dong, X.-P. Zhang, S.-J. Zhang, Experimental and theoretical studies on hydrogen bond-promoted fixation of carbon dioxide and epoxides in cyclic carbonates, Phys. Chem. Chem. Phys. 14 (2012) 11021. doi:10.1039/c2cp41698k.

[97] W. Xia, S.M. Budge, M.D. Lumsden, ^{1}H-NMR Characterization of Epoxides Derived from Polyunsaturated Fatty Acids, J. Am. Oil Chem. Soc. 93 (2016) 467–478. doi:10.1007/s11746-016-2800-2.

[98] H.A.J. Aerts, P.A. Jacobs, Epoxide yield determination of oils and fatty acid methyl esters using ^{1}H NMR, J. Am. Oil Chem. Soc. 81 (2004) 841–846. doi:10.1007/s11746-004-0989-1.

[99] P.C. Mazo, L.A. Rios, Improved synthesis of carbonated vegetable oils using microwaves, Chem. Eng. J. 210 (2012) 333–338. doi:10.1016/j.cej.2012.08.099.

Supporting Information

A Perspective of QSPR Modeling to Screen/Design Catalysts for Oleochemical Carbonates Synthesis

Victor H. J. M. dos Santos [†,‡], Darlan Pontin [†], Raoní S. Rambo [†], Marcus Seferin [*†,‡]

† Escola de Ciências – PUCRS – Pontifícia Universidade Católica do Rio Grande do Sul, Av. Ipiranga, 6681 – Prédio 12, 90619-900, Porto Alegre, Brasil.

‡ Escola Politécnica, Programa de Pós-Graduação em Engenharia e Tecnologia de Materiais – PUCRS – Pontifícia Universidade Católica do Rio Grande do Sul, Av. Ipiranga, 6681 – Prédio 32, 90619-900, Porto Alegre, Brasil.

Authors' email:

Victor Hugo Jacks Mendes dos Santos - victor.santos@pucrs.br or victor.hugo@acad.pucrs.br

Darlan Pontin - darlan.pontin@acad.pucrs.br

Raoní Scheibler Rambo – raoni.rambo@pucrs.br or raoni.rambo@gmail.com

Marcus Seferin - seferin@pucrs.br (corresponding author) [*]

Table of Contents:

General Information

All reagents were of analytical grade and obtained from commercial suppliers and used without further purification. Three vegetable oil (rice bran oil, canola oil and soybean) were obtained from local suppliers. The hydrogen peroxide (35% purity) were obtained from Synth. The glacial acetic acid (>99%), the sulfuric acid (>95%) and the n-butanol (99% purity) were obtained from Fluka. The cetyltrimethylammonium bromide or hexadecyltrimethylammonium bromide (CTAB, 98% purity) were obtained from Sigma-Aldrich. The high purity carbon dioxide (CO_2, 99.995%) were obtained from Air Liquide.

All the infrared spectra are acquired using the Spectrum One spectrometer (PerkinElmer) with HATR accessory. The spectral ranges from 4000 to 650 cm^{-1} wavenumbers, resolution of 4 cm^{-1}, 16 scans per spectrum.

All NMR spectra were recorded on a Bruker Avance 400 running at 400 MHz for ^{1}H and at 101 MHz for ^{13}C. Chemical shifts (δ) are reported in parts per million (ppm) relative to TMS signal (0 ppm) for ^{1}H NMR and using deuterated chloroform ($CDCl_3$) as solvent. The following abbreviations are used to indicate the multiplicity in NMR spectra: s – singlet; bs – broad singlet; d – doublet; t – triplet; q – quartet; m – multiplet; dd – double doublet.

Rice Bran Oil: ^{1}H NMR (400 MHz, $CDCl_3$) δ: 5.39–5.32 (m, 7H), 4.30 (dd, *J*=11.9, 4.3 Hz, 2H), 4.14 (dd, *J*=11.9, 6.0 Hz, 2H), 2.77 (t, *J*=6.4 Hz, 2H), 2.31 (td, *J*=7.5, 2.5 Hz, 6H), 2.07–1.98 (m, 10H), 1.64–1.59 (m, 7H), 1.37–1.26 (m, 58H), 0.91–0.86 (m, 9H).

Canola Oil: ^{1}H NMR (400 MHz, $CDCl_3$) δ: 5.40–5.25 (m, 8H), 4.30 (dd, *J*=11.9, 4.3 Hz, 2H), 4.14 (dd, *J*=11.9, 6.0 Hz, 2H), 2.80–2.75 (m, 2H), 2.31 (td, *J*=7.5, 2.5 Hz, 6H), 2.07–1.99 (m, 11H), 1.64–1.59 (m, 6H), 1.37–1.26 (m, 58H), 0.99–0.80 (m, 9H).

Soybean Oil: ^{1}H NMR (400 MHz, $CDCl_3$) δ: 5.39–5.26 (m, 9H), 4.30 (dd, *J*=11.9, 4.3 Hz, 2H), 4.14 (dd, *J*=11.9, 6.0 Hz, 2H), 2.79–2.75 (m, 4H), 2.31 (td, *J*=7.5, 2.6 Hz, 6H), 2.07–2.00 (m, 9H), 1.63–1.59 (m, 6H), 1.37–1.26 (m, 31H), 0.97–0.86 (m, 8H).

Epoxidized rice bran oil: ^{1}H NMR (400 MHz, $CDCl_3$) δ: 5.36–5.19 (m, 1H), 4.30 (dd, *J*=11.9, 4.2 Hz, 2H), 4.14 (dd, *J*=11.9, 5.9 Hz, 2H), 3.15–3.05 (m, 2H), 3.00–2.88 (m, 4H), 2.32 (t, *J*=7.6 Hz, 6H), 1.75–1.26 (m, 77H), 0.93–0.86 (m, 10H).

Epoxidized canola oil: ^{1}H NMR (300 MHz, $CDCl_3$) δ: 5.26 (t, *J*=5.1 Hz, 1H), 4.30 (dd, *J*=11.9, 4.2 Hz, 2H), 4.14 (dd, *J*=11.9, 5.9 Hz, 2H), 3.19–3.06 (m, 2H), 2.99–2.88 (m, 5H), 2.32 (t, *J*=7.6 Hz, 7H), 1.75–1.25 (m, 78H), 1.09–0.86 (m, 10H).

Epoxidized soybean oil: ^{1}H NMR (400 MHz, $CDCl_3$) δ: 5.27 (bs, 1H), 4.30 (dd, *J*=11.9, 4.3 Hz, 2H), 4.15 (dd, *J*=12.0, 5.9 Hz, 2H), 3.14–3.07 (m, 3H), 3.00–2.90 (m, 4H), 2.32 (td, *J*=7.5, 2.3 Hz, 6H), 1.78–1.26 (m, 70H), 0.92–0.86 (m, 9H).

Carbonated rice bran oil: ^{1}H NMR (400 MHz, $CDCl_3$) δ: 5.26 (p, *J*=5.1 Hz, 1H), 4.94–4.49 (m, 2H), 4.33–4.23 (m, 2H), 4.17–4.08 (m, 3H), 3.39–3.30 (m, 1H), 2.41–2.29 (m, 7H), 1.63–1.25 (m, 76H), 0.91–0.86 (m, 11H).

Carbonated canola oil: ^{1}H NMR (400 MHz, $CDCl_3$) δ: 5.26 (t, *J*=5.2 Hz, 1H), 4.99–4.46 (m, 3H), 4.34–4.20 (m, 3H), 4.15 (dd, *J*=12.1, 6.1 Hz, 3H), 4.07 (td, *J*=6.7, 1.5 Hz, 1H), 2.41–2.26 (m, 11H), 1.80–1.19 (m, 114H), 0.98–0.81 (m, 17H).

Carbonated soybean oil: ^{1}H NMR (300 MHz, $CDCl_3$) δ: 5.26 (t, *J*=5.2 Hz, 1H), 4.94–4.49 (m, 5H), 4.30 (dd, *J*=12.1, 4.6 Hz, 3H), 4.71–4.06 (m, 4H), 2.41–2.29 (m, 9H), 1.92–1.27 (m, 87H), 0.97–0.86 (m, 11H).

General Prodecure for Epoxidation

The vegetable oils in situ epoxidation reactions was conducted using glacial acetic acid, hydrogen peroxide 35% and sulfuric acid. The reaction was performed at 75 °C, for 6 hours, with mechanical stirring and using the reactants molar ratio of 2:1 (H_2O_2:ethylenic unsaturation), 0.5:1 (CH_3COOH:ethylenic unsaturation) and 2% sulfuric acid (wt% of the aqueous fraction) [1,2]. After the reaction, the product was dissolved in ethyl ether and washed with water until neutral pH, followed by the solvent removal under vacuum.

General Prodecure for Cyclic Carbonate Synthesis

The carbonation reaction of the epoxidized triglycerides was conducted using cetyltrimethylammonium bromide (CTAB) catalyst, high purity carbon dioxide and n-butanol as solvent. The reaction was performed in a 50 cm^3 stainless steel autoclave at 120°C, for 48 hours, without stirring, 5 MPa (*p*, CO_2), 2 g of epoxidized oil, 4 mL of butanol and 5 mol% of CTAB. After the reaction, the butanol is removed under vacuum, which causes the catalyst to precipitate after some time. After the butanol removal, the product was dissolved in ethyl acetate and washed two times with water and once with brine. The oleochemical carbonate product are dried with anhydrous sodium sulfate and the solvent removed under vacuum.

QSPR Modeling: Data Set 02

The data set 02 was applied to evaluate the transferability of the QSPR model and are built based on the same descriptors selected for Data Set 01.The Data Set 02 (Table S1) are retrieved from the Büttner and coworkers papers [3], and comprises 09 catalyst with structure registered in public database. The application domain of this set comprises the synthesis of cyclic carbonate derived from epoxidized methyl oleate and CO_2 under the reaction conditions: T = 100 °C, P = 5 MPa, t = 16 h and catalyst load = 2 mol%.

Table S1. Data set 02: transferability evaluation of the QSPR model.

Catalyst	PubChem CID	CAS	Conversion (%)
(2-Hydroxyethyl)triphenylphosphonium bromide	2733550	7237-34-5	9%
(2-Hydroxyethyl)triphenylphosphonium chloride	520034	23250-03-5	5%
(2-Hydroxyethyl)triphenylphosphonium iodide	89439517	4336-77-0	14%
Tributyl(2-hydroxyethyl) chloride	[a]CT1084236377	54580-84-6	10%
Tributyl(2-hydroxyethyl) iodide	[a]CT1081904619	54580-85-7	24%
Tributyl(2-hydroxyethyl) bromide	[a]CT1081904620	54580-43-7	22%
Tetrabutylphosphonium bromide	76564	3115-68-2	38%
Tetrabutylphosphonium chloride	75311	2304-30-5	35%
Tetrabutylphosphonium iodide	201022	3115-66-0	38%

Retrieved from the Büttner and coworkers paper,[3] [a] – Available at Mol-Instincts: www.molinstincts.com

Descriptor Calculation

The molecular descriptors transcribes the chemical, physical and biological features of the chemical structure in mathematical terms which are posteriorly treated by statistical tools [4,5]. The catalysts molecular structures were mostly obtained from the PubChem database and the molecular representation stored in SDF files (Structured Data Format) [6]. In the present work, the 2D molecular descriptors of the optimized structures are generated using the PaDEL-Descriptor (http://www.yapcwsoft.com/dd/padeldescriptor) software, resulting in an initial data sets of 1444 descriptors [7]. The 2D molecular descriptors of the data set 02 ate presented in the Table.S2.

Table S2. Molecular descriptors for the QSPR modeling of the data set 02

CAS	nCl^-	nBr^-	nI^-	ALogP	apol	ATS2e	bpol	C2SP3	[a]ETA	GATS6i	[b]LI	MATS4m	nAtom	[c]LAC	nBonds2	nRotBt	$SssCH_2$	VABC
7237-34-5	0	1	0	2.44	52.97	533.88	29.3	0	0.132	1.076	11.1	-0.148	42	2	44	6	1.134	290.91
23250-03-5	1	0	0	2.44	52.97	533.88	29.3	0	0.132	1.076	11.1	-0.148	42	2	44	6	1.134	290.91
4336-77-0	0	0	1	2.44	52.97	533.88	29.3	0	0.132	1.076	11.1	-0.148	42	2	44	6	1.134	290.91
54580-84-6	1	0	0	-2.53	50.41	646.78	42.5	6	0.000	1.100	10.1	-0.019	48	4	47	15	14.725	280.64
54580-85-7	0	0	1	-2.53	50.41	646.78	42.5	6	0.000	1.100	10.1	-0.019	48	4	47	15	14.725	280.64
54580-43-7	0	1	0	-2.53	50.41	646.78	42.5	6	0.000	1.100	10.1	-0.019	48	4	47	15	14.725	280.64
3115-68-2	0	1	0	-2.80	55.79	716.70	46.8	8	0.000	1.172	13.2	-0.011	53	4	52	16	18.783	306.44
2304-30-5	1	0	0	-2.80	55.79	716.70	46.8	8	0.000	1.172	13.2	-0.011	53	4	52	16	18.783	306.44
3115-66-0	0	0	1	-2.80	55.79	716.70	46.8	8	0.000	1.172	13.2	-0.011	53	4	52	16	18.783	306.44

[a] ETA – ETA_Shape_Y, [b] LI – LipoaffinityIndex, [c] LAC – nAtomLAC

QSPR Development

For the QSPR modelling of the present work, the molecular descriptors are applied as predictor variables (X) while the epoxide conversion to carbonates are applied as response variable (Y). After the exhaustive variable selection step, the 18 molecular descriptors are applied to perform the multivariate regression with the data autoscaled and mean centered [8]. The PLS was performed using the SIMPLS algorithm, while the SVM was developed using the Linear Kernel Function. The internal validations of the models are performed by mean of LOO and LMO cross-validation. Furthermore, to evaluate the model sensitivity to the sample removal from the training set, the LMO was performed by keeping out 25% and 33% of the data at each cycle of model training. The results of the QSPR model are presented in the Table S3.

Table S3. QSPR model for the synthesis of oleochemical carbonate: Data set 02

Data set 2	LOO		[a]LMO		[b]LMO	
	PLS	**SVM**	**PLS**	**SVM**	**PLS**	**SVM**
R^2_{Cal}	0.9550	0.9608	0.9699	0.9455	0.9550	0.9454
Q^2	0.8721	0.8847	0.9014	0.9151	0.8678	0.8754
RMSEC	2.6	2.54	2.13	2.94	2.60	2.95
RMSECV	4.38	4.18	3.85	3.62	4.52	4.41
F/SV	3	7	3	9	2	9

[a] – 25% of the sample kept out in the Leave-Many-Out cross-validation,[b] - 33% of the sample kept out in the Leave-Many-Out cross-validation.

In a first assessment, the model presents considerable good outputs, with high calibration R^2 (>0.94) and good cross validation coefficient of determination (Q^2 >0.6) satisfying the minimum criteria for obtaining a reliable QSPR model. Also, acceptable values of Root-mean-square error of cross-validation (RMSECV) are obtained, with values around 10% of mean squared error. In the Figure S1, it is possible to observe the regression data profile, while the Table S4 presents the estimated conversion values for each of PLS and SVM models.

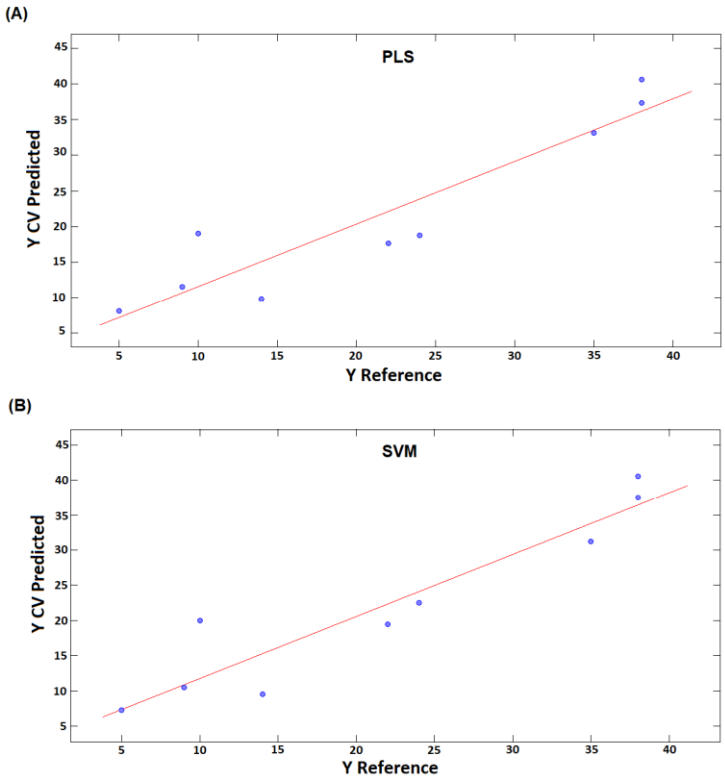

Figure S1. Predicted versus reference plot for the estimation of epoxide conversion to cyclic carbonate: Data set 02.

Table S4. Predicted values of the conversion of epoxide to cyclic carbonate: Data set 02

Catalyst	[a]Ref (%)	PLS (%)			SVM (%)		
		LOO	[b]LMO	[c]LMO	LOO	[b]LMO	[c]LMO
(2-Hydroxyethyl)triphenylphosphonium bromide	9.0	11.6	13.5	8.1	10.5	10.1	12.0
(2-Hydroxyethyl)triphenylphosphonium chloride	5.0	8.1	5.0	5.9	7.3	6.0	6.2
(2-Hydroxyethyl)triphenylphosphonium iodide	14.0	9.8	11.7	9.0	9.5	10.4	11.6
Tributyl(2-hydroxyethyl) chloride	10.0	19.0	17.1	20.5	20.0	18.0	21.0
Tributyl(2-hydroxyethyl) iodide	24.0	18.8	20.0	19.1	22.5	25.9	22.2
Tributyl(2-hydroxyethyl) bromide	22.0	17.6	17.1	19.0	19.5	19.0	21.4
Tetrabutylphosphonium bromide	38.0	37.4	39.2	35.3	37.5	36.6	36.0
Tetrabutylphosphonium chloride	35.0	33.2	32.0	32.6	31.2	32.0	30.2
Tetrabutylphosphonium iodide	38.0	40.6	40.5	38.7	40.5	41.9	40.6

[a] Ref – [3], [b] – 25% of the sample kept out in the Leave-Many-Out cross-validation,[c] - 33% of the sample kept out in the Leave-Many-Out cross-validation.

The model validation is a crucial step on the QSPR development and over the years several criteria / threshold values have been presented as minimum requirements, but not always sufficient, to ensure the robustness and transferability of QSAR/QSPR models [9–13]. The present work applies the Golbraikh and Tropsha's criteria [5,13,14], in addition to the Roy and coworkers r^2_m metrics [15,9,16,17].

Considering the small size of the data set, the stability of the model was evaluated based on both leave one out (Q^2-LOO) and leave-many-out (Q^2-LMO) internal validation and the model predictivity was evaluated by using the $r^2_{m\,(LOO)}$ and $r^2_{m\,(LMO)}$ parameters by replacing the R^2 (test set) with the cross validation Q^2 and the respective values obtained for the QSPR validation are presented in the Table S5 [15,9,12,17].

Table S5. Validation of the PLS and SVM model performed based on the Data Set 02

Data set 2	PLS			SVM			Reference threshold value
	LOO	[a]LMO	[b]LMO	LOO	[a]LMO	[b]LMO	
R^2	0.96	0.97	0.96	0.96	0.95	0.95	>0.6
Q^2	0.87	0.90	0.87	0.88	0.92	0.88	>0.5
$\frac{(Q^2 - Q^2_o)}{Q^2}$	0.00	0.00	0.00	0.00	0.00	0.00	<0.1
$\frac{(Q^2 - Q'^2_o)}{Q^2}$	0.02	0.01	0.01	0.02	0.01	0.04	<0.1
k	0.00	0.00	0.00	0.00	0.00	0.00	<0.3
k′	0.01	0.01	0.01	0.02	0.01	0.04	<0.3
$\lvert Q^2 - Q^2_o \rvert$	0.99	0.99	1.03	0.99	0.98	0.99	$0.85 \leq k \leq 1.15$
$\lvert Q^2 - Q'^2_o \rvert$	0.97	0.98	0.94	0.98	1.00	0.98	$0.85 \leq k \leq 1.15$
Q^2_m	0.87	0.89	0.83	0.87	0.91	0.82	>0.5
Q'^2_m	0.77	0.83	0.80	0.77	0.84	0.71	>0.5
$\lvert Q^2_m - Q'^2_m \rvert$	0.10	0.06	0.04	0.10	0.07	0.11	<0.2
$\frac{\lvert Q^2_m - Q'^2_m \rvert}{2}$	0.82	0.86	0.82	0.82	0.87	0.76	>0.5
Validation	V	V	V	V	V	V	All criteria met

V – Validated, [a] – 25% of the sample kept out in the Leave-Many-Out cross-validation,[b] - 33% of the sample kept out in the Leave-Many-Out cross-validation.

From the Table S5, we found that all the developed QSPR models are validated. After the validation phase, it follows for the interpretation of the data obtained by calibration models. The interpretation of the principals relationship between the molecular descriptors (X) and the estimated conversion response (Y) is performed through the PLS Regression Coefficient, presented in the Figure S2 [18,19].

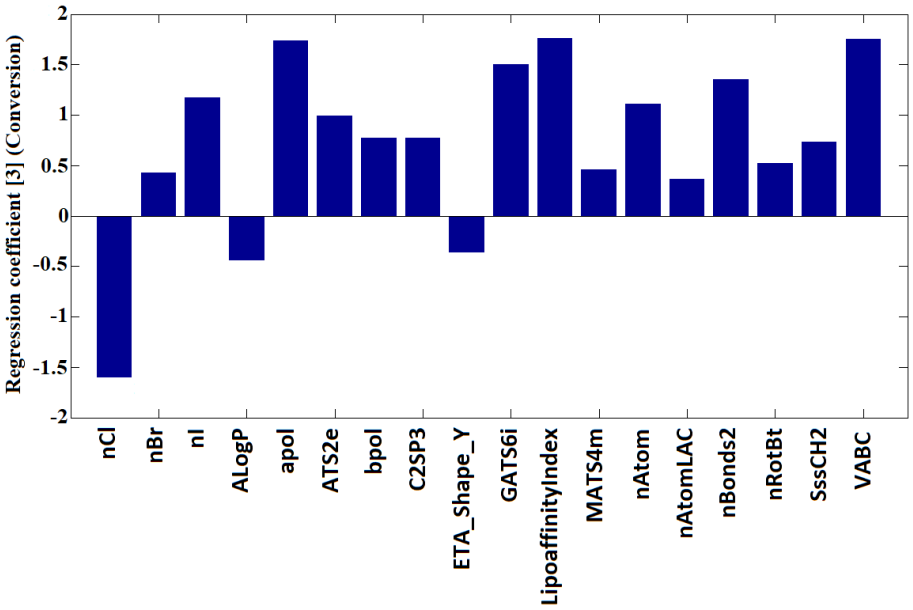

Figure S2. PLS regression coefficient for the estimation of epoxide conversion to cyclic carbonate: data set 02.

From the regression coefficient results it is possible the observe the halide influence on the catalyst effectiveness for this data set, with the order of anion activity to produce oleochemical carbonates being identified as $I^- > Br^- > Cl^-$. For the application domain of the QSPR based on the data set 02, the halide effectiveness follows the leaving group character of the chemical species [20]. The reaction performed without the presence of supercritical CO_2 and the high polarizability index regression coefficient (apol and bpol) also could play an important role on this order.

The autocorrelation descriptors (ATS2e, GATS6i and MATS4m) presents a positive regression coefficient and are related with a property distribution along the molecular structure. Due to the complexity of these indices, no clear interpretation is possible.

Another important feature of the catalyst is the size of the organic structure and the molecule polarizability. This behavior is translated by the model in function of the molecular descriptors apol, bpol, C2SP3, nAtom, nAtomLAC, nBonds2, $SssCH_2$ and VABC, all presenting the positive regression coefficient with respect to the conversion. This characteristic has already been described in the literature, which relate the increase in the bulkiness of the catalyst to the weakening of the electrostatic interactions between cation and anion resulting in the increase of the nucleophilic character of the halide [21–25].

Unlike the results obtained for the data set 01, the nAtomLAC do not presents a significant regression coefficient, however, the data set 02 does not allow to obtain this information since, among the catalysts in the set, there are no significant changes in the carbon aliphatic chain size. On the other hand, from this data set it is possible to observe the importance of the molecular volume (VABC) for the catalyst efficiency.

The catalyst solubility play an important role in the reaction in homogeneous phase, however the catalysts solubility in epoxidized derivatives is limitedly addressed in the literature [26]. From the QSPR regression coefficient, we found that the lipophilicity descriptors (ALogP and Lipoaffinity index) are important to justify the catalyst efficiency, in which the effectiveness of the catalyst increases with their lipophilicity.

Since application domain of this model comprises the synthesis of cyclic carbonate derived from epoxidized triglycerides, the lipophilicity character is being related with the catalyst solubility in the medium. The solvent effects of the oily matrix over the bulky organic cation, which results in charge stabilization and in the increase of the nucleophilicity of halide anion [24,27]. Observed the regression coefficients, the Variable Influence on Projection (VIP scores) was analyzed to rank the relative importance of the molecular descriptors for the model [18,19].

From the Figure S3, it is possible to easily identify the relative importance of all the molecular descriptors applied for the regression. From the VIP plot, in addition to the regression coefficient, it’s possible to conclude that: the size of the carbon chain, the lipophilicity/solubility of the catalyst and the distribution of the properties along the molecular structure define the

effectiveness of the catalyst to produce oleochemical carbonates. For this data set, the halide species presents a secondary importance compared to the others molecular features.

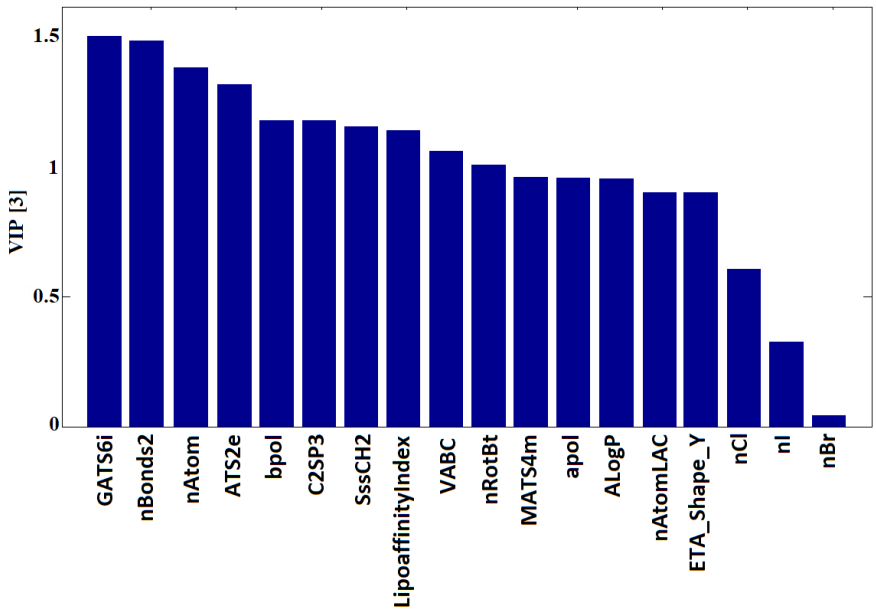

Figure S3. Variable influence plot of the PLS model: data set 02

This data set was applied to evaluate the transferability of the QSPR model and are built based on the same descriptors selected for Data Set 01. The data interpretation of both QSPR models (Data set 01 and 02) lead to almost the same features and the variable influence in the organocatalyst are found to be highly supported by the literature. The differences found can be attributed to the differences in the QSPR application domains and to the difference in the catalyst set profile applied in each modelling. Thus, based on the results, there is a positive perspective of applying the QSPR Modeling to Screen/Design Active Organocatalysts for the Synthesis of Oleochemical Carbonates.

Descriptor nomemclature

nCl$^-$ - Number of chlorine atoms

nBr$^-$ - Number of bromine atoms

nI$^-$ - Number of iodine atoms

ALogP - Ghose-Crippen-Viswanadhan octanol-water partition coefficient

apol - Sum of the atomic polarizabilities (including implicit hydrogens)

ATS2e - Broto-Moreau autocorrelation - lag 2 / weighted by Sanderson electronegativities

bpol - Sum of the absolute value of the difference between atomic polarizabilities of all bonded atoms in the molecule (including implicit hydrogens)

C2SP3 - Singly bound carbon bound to two other carbons

ETA Shape Y – Extended topochemical atom shape index Y

GATS6i - Geary autocorrelation - lag 6 / weighted by first ionization potential

Lipoaffinity Index - Atom type electrotopological state lipoaffinity index

MATS4m - Moran autocorrelation - lag 4 / weighted by mass

nAtom - Number of atoms

nAtomLAC - Number of atoms in the longest aliphatic chain

nBonds2 - Total number of bonds (including bonds to hydrogens)

nRotBt - Number of rotatable bonds, including terminal bonds

SssCH$_2$ - Sum of atom-type E-State: -CH2-

VABC - Van der Waals volume

Supporting Tables

T**able S6.** Potential catalyst set compiled based on virtual screening method

Compound	Catalyst	PubChem CID	CAS
1	Tetramethylphosphonium bromide	357594	4519-28-2
2	Tetramethylphosphonium iodide	120511	993-11-3
3	Tetraethylphosphonium bromide	9859378	(4317-07-1)
4	Tetrapropylphosphonium bromide	11011483	63462-98-6
5	Diethyl(dihexyl)phosphonium bromide	87778605	125239-35-2
6	Heptyl(tripropyl)phosphonium bromide	87777292	-
7	Methyl(tripentyl)phosphonium bromide	87777644	-
8	Tetrakis(2-methylpropyl)phosphonium bromide	19867405	-
9	Tributyl(pentyl)phosphonium bromide	20446536	2017557-26-3
10	Methyl(triphenyl)phosphonium bromide	74505	1779-49-3
11	Tributyl(hexyl)phosphonium bromide	22712793	105890-71-9
12	Trihexyl(methyl)phosphonium bromide	87777842	1258887-14-7
13	Ethyl(trihexyl)phosphonium bromide	19826698	120224-02-4
14	Hexyl(tripentyl)phosphonium bromide	87776814	1431978-73-2
15	Dibutyl(diheptyl)phosphonium bromide	87778487	-
16	Tributyl(hexadecyl)phosphonium bromide	84716	14937-45-2
17	Tetraoctylphosphonium bromide	3015167	23906-97-0
18	Tetramethylammonium bromide	66137	64-20-0
19	Tetramethylammonium iodide	6381	75-58-1
20	Trimethylphenylammonium bromide	27663	16056-11-4
21	Triethylmethylammonium bromide	3083778	2700-16-5
22	Benzyltrimethylammonium bromide	21449	5350-41-4
23	Tetraethylammonium bromide	6285	71-91-0
24	Pentyltrimethylammonium bromide	9021	150-98-1
25	Cyclohexyl(trimethyl)ammonium bromide	12653942	3237-34-1

Table S6. (Continued)

26	Hexyl(trimethyl)ammonium bromide	10059492	2650-53-5
27	Benzyl(triethyl)ammonium bromide	165294	5197-95-5
28	Trimethyl(octyl)ammonium bromide	74964	2083-68-3
29	Tetrapropylammonium bromide	74745	1941-30-6
30	Triethylhexylammonium bromide	10825627	13028-71-2
31	Trimethyl(nonyl)ammonium bromide	74750	(1943-11-9)
32	Decyl(trimethyl)ammonium bromide	16388	2082-84-0
33	Tributyl(methyl)ammonium bromide	10062191	37026-88-3
34	Decyl-ethyl-dimethylammonium bromide	85809143	39995-56-7
35	Dibutyl(dipropyl)ammonium bromide	87778023	-
36	Tributyl(ethyl)ammonium bromide	19043781	37026-89-4
37	Triethyloctylammonium bromide	21951230	13028-73-4
38	Trimethyl-undecyl-ammonium bromide	44345296	(2650-58-0)
39	Dodecyltrimethylammonium bromide	14249	1119-94-4
40	Triethyl(nonyl)ammonium bromide	22301429	13028-74-5
41	Dibutyl-bis(2-methylpropyl) ammonium bromide	57477251	1627505-91-2
42	Diethyl(dihexyl)ammonium bromide	85992863	75174-76-4
43	Methyl(tripentyl)ammonium bromide	71463862	108178-12-7
44	Tetraisobutylammonium bromide	13726125	401569-73-1
45	Tributyl(2-methylpropyl)ammonium bromide	19858533	74900-80-4
46	Trimethyl(tridecyl)ammonium bromide	11484093	21424-21-5
47	Diheptyl(dimethyl)ammonium bromide	23018948	187731-22-2
48	Tributyl(3-methylbutyl)ammonium bromide	18185861	43017-77-2
49	Trimethyl(tetradecyl)ammonium bromide	14250	8044-71-1
50	Tris(2-methylpropyl)-pentylammonium bromide	19035239	172871-68-0
51	Dodecyl(triethyl)ammonium bromide	28939	18186-71-5
52	Ethyl-dihexyl-(2-methylpropyl)ammonium bromide	87480233	-
53	Trimethyl(pentadecyl)ammonium bromide	14611710	21424-22-6
54	Benzyl(tributyl)ammonium bromide	2724282	25316-59-0
55	Butyl-tris(3-methylbutyl)ammonium bromide	71404253	7322-37-4

Table S6. (Continued)

56	Tributyl(heptyl)ammonium bromide	15461354	85169-31-9
57	Trihexyl(methyl)ammonium bromide	11783457	2390-64-9
58	Ethyl(trihexyl)ammonium bromide	71398586	61175-73-3
59	Ethyl-hexadecyl-dimethylammonium bromide	31280	124-03-8
60	Heptadecyl(trimethyl)ammonium bromide	10045219	21424-24-8
61	Tetrapentylammonium bromide	70086	866-97-7
62	Hexadecyl-(2-hydroxyethyl)-dimethylammonium bromide	10960220	20317-32-2
63	Hexyl(tripentyl)ammonium bromide	87777464	1843246-52-5
64	Octadecyltrimethylammonium bromide	70708	1120-02-1
65	Trihexyl(propyl)ammonium bromide	87478716	-
66	Didecyl(dimethyl)ammonium bromide	16957	2390-68-3
67	Heptyl(tripentyl)ammonium bromide	87778582	-
68	Eicosyltrimethylammonium bromide	23767	7342-61-2
69	Tributyl(undecyl)ammonium bromide	20572340	75294-53-0
70	Tetrahexylammonium bromide	78026	4328-13-6
71	Triheptyl(propyl)ammonium bromide	87777356	187731-24-4
72	Cetyltrimethylammonium bromide	5974	57-09-0
73	Methyl(trioctyl)ammonium bromide	11503288	35675-80-0
74	Docosyl(trimethyl)ammonium bromide	10216960	21396-56-5
75	Didodecyl(dimethyl)ammonium bromide	18669	3282-73-3
76	Diheptyl(dihexyl)ammonium bromide	87777513	-
77	Trioctyl(propyl)ammonium bromide	90449	24298-17-7
78	Tributyl(hexadecyl)ammonium bromide	11420451	6439-67-4
79	Tetraheptylammonium bromide	78073	4368-51-8
80	Hexacosyl(trimethyl)ammonium bromide	23196158	-
81	Tetrakis(decyl)ammonium bromide	3014876	14937-42-9
82	1,3-dimethylimidazolium bromide	71404763	71027-57-1
83	1,3-dimethylimidazolium iodide	20334	4333-62-4
84	1-Ethyl-3-methylimidazolium bromide	2734235	65039-08-9
85	1-Butyl-3-Vinylimidazolium bromide	87560886	34311-90-5

Table S6. (Continued)

86	1-Hexyl-3-methylimidazolium bromide	2734237	85100-78-3
87	1-Octyl-2H-imidazolium bromide	87125623	125750-22-3
88	1-Ethyl-3-hexylimidazolium bromide	87942414	547719-00-6
89	1-Heptyl-2,3-dimethylimidazolium bromide	89858560	1513876-75-9
90	1-Ethenyl-3-octylimidazolium bromide	86657882	349148-77-2
91	1-Ethyl-3-octylimidazolium bromide	88794580	61546-02-9
92	1-Methyl-3-nonylimidazolium bromide	10017026	343851-34-3
93	1-Butyl-3-methylimidazolium bromide	2734236	85100-77-2
94	1-Decyl-3-methylimidazolium bromide	22078297	188589-32-4
95	1-Propyl-3-(2,4,6-trimethylphenyl)imidazolium bromide	86653215	1176198-41-6
96	1-Decyl-3-ethenylimidazolium bromide	86657884	349148-78-3
97	1-Decyl-3-ethylimidazolium bromide	87942577	581101-93-1
98	1-Methyl-3-undecylimidazolium bromide	87777766	1426325-53-2
99	1-Butyl-3-(2,4,6-trimethylphenyl)imidazolium bromide	86653217	1165815-77-9
100	1-Hexyl-3-(4-methylphenyl)imidazolium bromide	87306883	1176199-92-0
101	1-Dodecyl-3-methylimidazolium bromide	16749605	61546-00-7
102	1-Pentyl-3-(2,4,6-trimethylphenyl)imidazolium bromide	86653220	1176198-43-8
103	1-Dodecyl-3-ethenylimidazolium bromide	23196178	163733-82-2
104	1-Butyl-3-decylimidazolium bromide	90220482	919611-98-6
105	1-Dodecyl-3-ethylimidazolium bromide	88794546	61546-03-0
106	1-Hexyl-3-octylimidazolium bromide	89654411	1373818-67-7
107	1-Hexyl-3-(2,4,6-trimethylphenyl)imidazolium bromide	86653222	1176198-44-9
108	1-Dodecyl-3-propylimidazolium bromide	88795075	61546-06-3
109	1-Methyl-3-tetradecylimidazolium bromide	77520435	471907-87-6
110	1-Heptyl-3-(2,4,6-trimethylphenyl)imidazolium bromide	86653224	1176198-45-0
111	1-Methyl-3-pentadecylimidazolium bromide	45045358	349148-74-9
112	1-Octyl-3-(2,4,6-trimethylphenyl)imidazolium bromide	86653226	1176198-47-2
113	1-Hexadecyl-3-methylimidazolium bromide	2846928	132361-22-9
114	1,3-Di(nonyl)imidazolium bromide	11395506	370085-31-7
115	1-(2,4,6-trimethylphenyl)-3-undecylimidazolium bromide	86653228	1176198-48-3

Table S6. (Continued)

116	1-Butyl-3-hexadecylimidazolium bromide	90220325	937716-18-2
117	1-(4-Ethylphenyl)-3-tetradecylimidazolium bromide	90374052	1421755-47-6
118	1-Docosyl-3-methylimidazolium bromide	86647477	943834-80-8
119	1-Methylpyridinium bromide	12248289	2350-76-7
120	1-Methylpyridinium iodide	13596	930-73-4
121	1,1-Dimethylpyrrolidinium bromide	15935266	23827-15-8
122	1,1-Dimethylpyrrolidinium iodide	200181	872-44-6

Table S7. Molecular descriptors for the QSPR modeling of the data set 01

CAS	nCl⁻	nBr⁻	nI⁻	ALogP	apol	ATS2e	bpol	C2SP3	[a]ETA	GATS6i	[b]LI	MATS4m	nAtom	[c]LAC	nBonds2	nRotBt	$SssCH_2$	VABC
56511-17-2	0	0	1	-2.408	30.28	441.51	24.5	4	0.000	1.083	6.8	-0.018	30	4	30	5	9.960	164.18
874-81-7	0	0	1	-1.957	26.28	309.53	17.3	2	0.082	1.072	5.8	-0.063	24	4	24	4	3.688	145.37
61545-99-1	0	1	0	-2.994	38.66	509.50	29.1	6	0.118	0.922	8.3	-0.024	37	8	37	9	9.427	210.89
64697-40-1	1	0	0	-2.994	38.66	509.50	29.1	6	0.118	0.922	8.3	-0.024	37	8	37	9	9.427	210.89
188589-28-8	0	0	1	-3.362	39.99	554.89	31.3	6	0.118	0.934	8.3	0.006	39	8	39	9	12.009	224.43
1643-19-2	0	1	0	-3.496	53.26	738.24	42.0	8	0.000	1.226	12.1	0.004	53	4	52	16	16.770	297.61
1112-67-0	1	0	0	-3.496	53.26	738.24	42.0	8	0.000	1.226	12.1	0.004	53	4	52	16	16.770	297.61
311-28-4	0	0	1	-3.496	53.26	738.24	42.0	8	0.000	1.226	12.1	0.004	53	4	52	16	16.770	297.61
3115-68-2	0	1	0	-2.796	55.79	716.70	46.8	8	0.000	1.172	13.2	-0.011	53	4	52	16	18.783	306.44
2304-30-5	1	0	0	-2.796	55.79	716.70	46.8	8	0.000	1.172	13.2	-0.011	53	4	52	16	18.783	306.44
3115-66-0	0	0	1	-2.796	55.79	716.70	46.8	8	0.000	1.172	13.2	-0.011	53	4	52	16	18.783	306.44
1829-92-1	0	0	1	1.058	23.46	280.35	19.8	0	0.217	0.000	5.3	-0.197	22	2	21	6	4.738	132.16

[a] ETA – ETA_Shape_Y, [b] LI – LipoaffinityIndex, [c] LAC – nAtomLAC

Table S8. Predicted values of the conversion of epoxide to cyclic carbonate: Data set 01

Catalyst	Reference (%)[a]	PLS			SVM		
		LOO (%)	[b]LMO (%)	[b]LMO (%)	LOO (%)	[c]LMO (%)	[c]LMO (%)
1-Butyl-1-methylpyrrolidinium iodide	19.0	15.7	16.5	15.2	15.2	16.1	15.2
1-Butylpyridinium iodide	12.0	15.6	16.2	15.7	15.8	17.5	15.7
1-Methyl-3-octylimidazolium bromide	30.0	29.9	29.7	29.4	29.0	30.0	29.0
1-Methyl-3-octylimidazolium chloride	20.0	17.9	17.9	18.3	21.0	18.1	20.3
1-Methyl-3-octylimidazolium iodide	25.0	27.1	24.6	26.3	26.1	28.0	23.4
Tetrabutylammonium bromide	30.0	29.6	30.1	29.4	29.2	28.2	29.8
Tetrabutylammonium chloride	17.0	20.6	21.9	21.2	21.0	22.2	21.0
Tetrabutylammonium iodide	26.0	22.7	23.0	22.3	22.2	21.5	22.3
Tetrabutylphosphonium bromide	28.0	28.8	29.0	28.7	29.0	27.4	29.0
Tetrabutylphosphonium chloride	19.0	16.8	17.2	17.4	18.0	15.3	18.0
Tetrabutylphosphonium iodide	21.0	23.8	23.2	23.9	22.5	24.4	24.0
Triethylsulfonium iodide	0.0	2.8	1.3	4.7	1.9	2.0	5.5

[a] Ref - [28], [b] – 16.7% of the sample kept out in the Leave-Many-Out cross-validation,[c] – 25% of the sample kept out in the Leave-Many-Out cross-validation.

Table S9. Molecular descriptors of the potential catalyst set

Catalyst	nCl^-	nBr^-	nI^-	ALogP	apol	ATS2e	bpol	C2SP3	[a]ETA	GATS6i	[b]LI	MATS4m	nAtom	[c]LAC	nBonds2	nRotBt	$SssCH_2$	VABC
1	0	1	0	1.66	18.67	204.09	20.60	0	0.00	0.000	4.19	0.304	17	0	16	4	0.000	98.89
2	0	0	1	1.66	18.67	204.09	20.60	0	0.00	0.000	4.19	0.304	17	0	16	4	0.000	98.89
3	0	1	0	1.44	31.05	374.87	29.34	0	0.00	0.000	7.20	-0.234	29	2	28	8	6.313	168.07
4	0	1	0	-1.64	43.42	545.78	38.09	4	0.00	0.785	10.19	-0.176	41	3	40	12	12.588	237.25
5	0	1	0	-1.83	55.79	716.70	46.84	8	0.00	0.919	13.11	-0.085	53	6	52	16	18.541	306.44
6	0	1	0	-2.80	55.79	716.70	46.84	8	0.00	0.886	13.13	-0.112	53	7	52	16	18.672	306.44
7	0	1	0	-2.55	55.79	716.74	46.84	9	0.00	1.047	13.11	-0.005	53	5	52	16	18.420	306.44
8	0	1	0	2.63	55.79	716.80	46.84	0	0.22	0.764	13.18	-0.037	53	3	52	16	6.555	306.44
9	0	1	0	-3.08	58.89	759.43	49.02	9	0.00	1.148	13.89	-0.010	56	5	55	17	20.316	323.73
10	0	1	0	0.41	49.07	475.65	27.16	0	0.14	1.028	11.96	-0.204	38	0	40	4	0.000	264.83
11	0	1	0	-3.37	61.98	802.16	51.21	10	0.00	1.136	14.63	-0.010	59	6	58	18	21.835	341.03
12	0	1	0	-3.41	65.08	844.93	53.39	12	0.00	1.018	15.31	-0.004	62	6	61	19	22.962	358.33
13	0	1	0	-3.46	68.17	887.62	55.58	12	0.00	1.013	16.07	-0.040	65	6	64	20	24.754	375.62
14	0	1	0	-4.24	71.26	930.35	57.77	13	0.00	1.077	16.84	-0.007	68	6	67	21	26.451	392.92
15	0	1	0	-4.52	74.36	973.08	59.95	14	0.00	1.098	17.56	-0.007	71	7	70	22	27.925	410.21
16	0	1	0	-6.25	92.92	1229.46	73.07	20	0.00	1.099	21.89	-0.005	89	16	88	28	36.874	513.99
17	0	1	0	-7.40	105.29	1400.38	81.82	24	0.00	1.044	24.88	-0.004	101	8	1	32	43.185	583.17
18	0	1	0	-1.03	16.14	225.21	15.76	0	0.00	0.000	3.67	0.414	17	0	16	4	0.000	90.06
19	0	0	1	-1.03	16.14	225.21	15.76	0	0.00	0.000	3.67	0.414	17	0	16	4	0.000	90.06
20	0	1	0	-1.14	26.28	314.18	17.94	0	0.10	0.757	6.20	0.016	24	0	24	4	0.000	145.37
21	0	1	0	-0.28	25.42	353.61	22.32	0	0.00	0.000	5.71	-0.329	26	2	25	7	3.771	141.94
22	0	1	0	0.08	29.37	358.00	20.13	0	0.09	0.970	6.82	0.328	27	0	27	5	1.098	162.67
23	0	1	0	-0.03	28.52	396.40	24.50	0	0.00	0.000	6.40	-0.386	29	2	28	8	5.125	159.24
24	0	1	0	-1.94	28.52	396.20	24.50	3	0.00	0.781	6.49	0.131	29	5	28	8	5.406	159.24
25	0	1	0	-2.63	30.28	441.46	24.50	6	0.10	0.637	6.91	-0.028	30	0	30	4	7.282	164.18
26	0	1	0	-2.23	31.61	438.93	26.69	4	0.00	0.934	7.21	0.120	32	6	31	9	6.862	176.54
27	0	1	0	-0.37	38.65	486.40	26.69	0	0.07	0.907	8.82	-0.174	36	0	36	8	4.843	214.55
28	0	1	0	-2.80	37.80	524.39	31.06	6	0.00	0.948	8.65	0.104	38	8	37	11	9.802	211.13
29	0	1	0	-2.34	40.89	567.32	33.25	4	0.00	0.834	9.24	-0.019	41	3	40	12	10.871	228.42

Table S9. (Continued)

30	0	1	0	-1.47	40.89	567.32	33.25	4	0.00	0.715	9.26	-0.207	41	6	40	12	10.919	228.42
31	0	1	0	-3.09	40.89	567.12	33.25	7	0.00	0.953	9.37	0.097	41	9	40	12	11.280	228.42
32	0	1	0	-3.38	43.98	609.85	35.44	8	0.00	0.957	10.09	0.091	44	10	43	13	12.763	245.72
33	0	1	0	-2.88	43.98	609.98	35.44	6	0.00	1.200	9.99	0.001	44	4	43	13	12.353	245.72
34	0	1	0	-3.13	47.08	652.64	37.62	8	0.00	0.961	10.77	-0.034	47	10	46	14	14.076	263.02
35	0	1	0	-2.92	47.08	652.78	37.62	6	0.00	1.050	10.67	-0.006	47	4	46	14	13.811	263.02
36	0	1	0	-2.63	47.08	652.78	37.62	6	0.00	1.166	10.68	-0.057	47	4	46	14	13.811	263.02
37	0	1	0	-2.05	47.08	652.78	37.62	6	0.00	0.755	10.70	-0.182	47	8	46	14	13.876	263.02
38	0	1	0	-3.67	47.08	652.57	37.62	9	0.00	0.961	10.81	0.086	47	11	46	14	14.249	263.02
39	0	1	0	-3.95	50.17	695.30	39.81	10	0.00	0.963	11.53	0.082	50	12	49	15	15.736	280.31
40	0	1	0	-2.34	50.17	695.51	39.81	7	0.00	0.771	11.43	-0.172	50	9	49	15	15.360	280.31
41	0	1	0	-1.30	53.26	738.29	42.00	4	0.12	1.018	12.11	0.132	53	4	52	16	10.993	297.61
42	0	1	0	-2.92	53.26	738.24	42.00	8	0.00	0.923	12.13	-0.107	53	6	52	16	16.779	297.61
43	0	1	0	-3.74	53.26	738.17	42.00	9	0.00	0.894	12.14	0.001	53	5	52	16	16.767	297.61
44	0	1	0	0.89	53.26	738.34	42.00	0	0.24	0.799	12.13	0.238	53	3	52	16	5.367	297.61
45	0	1	0	-2.40	53.26	738.26	42.00	6	0.06	1.124	12.11	0.072	53	4	52	16	13.863	297.61
46	0	1	0	-4.24	53.26	738.03	42.00	11	0.00	0.966	12.26	0.077	53	13	52	16	17.226	297.61
47	0	1	0	-3.99	53.26	738.10	42.00	10	0.00	0.975	12.19	0.025	53	7	52	16	16.885	297.61
48	0	1	0	-2.69	56.36	780.99	44.18	7	0.06	1.303	12.82	0.032	56	4	55	17	15.340	314.90
49	0	1	0	-4.53	56.36	780.76	44.18	12	0.00	0.968	12.98	0.074	56	14	55	17	18.716	314.90
50	0	1	0	-0.49	56.36	781.04	44.18	3	0.17	0.856	12.84	0.179	56	5	55	17	9.616	314.90
51	0	1	0	-3.20	59.45	823.70	46.37	10	0.00	0.808	13.59	-0.147	59	12	58	18	19.825	332.20
52	0	1	0	-2.68	59.45	823.72	46.37	8	0.05	0.983	13.56	0.017	59	6	58	18	16.826	332.20
53	0	1	0	-4.82	59.45	823.49	46.37	13	0.00	0.970	13.70	0.070	59	15	58	18	20.208	332.20
54	0	1	0	-2.97	57.21	742.77	39.81	6	0.05	1.149	13.03	0.038	54	4	54	14	13.303	318.33
55	0	1	0	-1.07	62.55	866.50	48.55	5	0.15	1.437	14.26	0.073	62	4	61	19	12.507	349.50
56	0	1	0	-4.36	62.55	866.43	48.55	11	0.00	1.161	14.27	0.003	62	7	61	19	21.230	349.50
57	0	1	0	-4.61	62.55	866.36	48.55	12	0.00	1.008	14.30	0.001	62	6	61	19	21.211	349.50
58	0	1	0	-4.36	65.64	909.16	50.74	12	0.00	1.007	15.00	-0.043	65	6	64	20	22.705	366.79
59	0	1	0	-4.86	65.64	909.02	50.74	14	0.00	0.973	15.11	-0.024	65	16	64	20	23.017	366.79

Table S9. (Continued)

60	0	1	0	-5.39	65.64	908.95	50.74	15	0.00	0.973	15.15	0.064	65	17	64	20	23.195	366.79
61	0	1	0	-4.65	65.64	909.16	50.74	12	0.00	0.940	14.98	0.003	65	5	64	20	22.723	366.79
62	0	1	0	-5.65	66.44	924.56	50.74	14	0.00	0.941	13.66	0.037	66	16	65	21	22.303	375.58
63	0	1	0	-4.94	68.73	951.89	52.93	13	0.00	0.968	15.71	0.002	68	6	67	21	24.214	384.09
64	0	1	0	-5.68	68.73	951.68	52.93	16	0.00	0.974	15.87	0.062	68	18	67	21	24.689	384.09
65	0	1	0	-4.94	68.73	951.89	52.93	13	0.00	1.006	15.71	-0.002	68	6	67	21	24.207	384.09
66	0	1	0	-5.72	71.83	994.48	55.11	16	0.00	0.981	16.52	0.019	71	10	70	22	25.796	401.38
67	0	1	0	-5.22	71.83	994.62	55.11	14	0.00	0.969	16.43	0.002	71	7	70	22	25.707	401.38
68	0	1	0	-6.26	74.92	1037.14	57.30	18	0.00	0.976	17.31	0.057	74	20	73	23	27.679	418.68
69	0	1	0	-5.51	74.92	1037.35	57.30	15	0.00	1.138	17.16	0.002	74	11	73	23	27.196	418.68
70	0	1	0	-5.80	78.01	1080.08	59.49	16	0.00	1.040	17.87	0.002	77	6	76	24	28.698	435.98
71	0	1	0	-5.80	78.01	1080.08	59.49	16	0.00	1.005	17.87	-0.002	77	7	76	24	28.683	435.98
72	0	1	0	-5.11	62.55	866.22	48.55	14	0.00	0.971	14.42	0.067	62	16	61	19	21.701	349.50
73	0	1	0	-6.34	81.11	1122.74	61.67	18	0.00	1.005	18.63	0.000	80	8	79	25	30.140	453.27
74	0	1	0	-6.83	81.11	1122.60	61.67	20	0.00	0.978	18.76	0.053	80	22	79	25	30.671	453.27
75	0	1	0	-6.87	84.20	1165.40	63.86	20	0.00	0.983	19.41	0.017	83	12	82	26	31.760	470.57
76	0	1	0	-6.38	84.20	1165.54	63.86	18	0.00	1.038	19.31	0.002	83	7	82	26	31.690	470.57
77	0	1	0	-6.66	87.29	1208.27	66.05	19	0.00	1.004	20.04	-0.002	86	8	85	27	33.166	487.86
78	0	1	0	-6.95	90.39	1251.00	68.23	20	0.00	1.117	20.77	0.001	89	16	88	28	34.670	505.16
79	0	1	0	-6.95	90.39	1250.99	68.23	20	0.00	1.035	20.76	0.001	89	7	88	28	34.685	505.16
80	0	1	0	-7.99	93.48	1293.52	70.42	24	0.00	0.981	21.65	0.046	92	26	91	29	36.659	522.46
81	0	1	0	-10.41	127.51	1763.75	94.47	32	0.00	1.026	29.42	0.001	125	10	124	40	52.672	712.71
82	0	1	0	-1.79	18.33	254.95	15.33	0	0.24	0.000	3.54	0.012	18	0	18	2	1.111	103.36
83	0	0	1	-1.79	18.33	254.95	15.33	0	0.24	0.000	3.54	0.012	18	0	18	2	1.111	103.36
84	0	1	0	-0.98	20.09	253.12	15.99	0	0.21	0.735	4.14	-0.208	19	0	19	3	1.056	107.11
85	0	1	0	-1.76	28.04	338.71	20.36	2	0.15	1.107	6.18	-0.055	26	4	26	5	3.593	156.37
86	0	1	0	-2.42	32.47	424.04	24.73	4	0.14	0.913	6.90	-0.030	31	6	31	7	6.522	176.30
87	0	1	0	-1.65	34.90	449.42	25.16	6	0.06	0.917	5.46	0.009	33	8	33	8	9.305	201.86
88	0	1	0	-2.17	35.56	466.84	26.92	4	0.13	0.966	7.52	-0.072	34	6	34	8	7.609	193.59
89	0	1	0	-2.65	38.66	509.26	29.10	5	0.19	0.922	8.22	-0.241	37	7	37	9	7.972	210.89

Table S9. (Continued)

90	0	1	0	-2.91	40.42	509.63	29.10	6	0.11	0.943	9.00	-0.026	38	8	38	9	9.275	225.55
91	0	1	0	-2.74	41.75	552.29	31.29	6	0.11	0.963	8.94	-0.057	40	8	40	10	10.516	228.19
92	0	1	0	-3.28	41.75	552.23	31.29	7	0.11	0.926	9.04	-0.022	40	9	40	10	10.893	228.19
93	0	1	0	-4.00	26.28	338.58	20.36	2	0.17	1.064	5.49	-0.040	25	4	25	5	3.688	141.71
94	0	1	0	-3.57	44.84	594.96	33.48	8	0.10	0.930	9.75	-0.021	43	10	43	11	12.365	245.48
95	0	1	0	0.27	42.60	511.88	26.92	1	0.34	0.492	9.18	-0.002	38	3	39	7	2.248	231.61
96	0	1	0	-3.49	46.60	595.08	33.48	8	0.10	0.946	10.43	-0.020	44	10	44	11	12.196	260.14
97	0	1	0	-3.32	47.94	637.75	35.66	8	0.10	0.964	10.37	-0.047	46	10	46	12	13.456	262.78
98	0	1	0	-3.86	47.94	637.68	35.66	9	0.10	0.934	10.47	-0.019	46	11	46	12	13.841	262.78
99	0	1	0	-0.02	45.70	554.61	29.10	2	0.32	0.618	9.86	0.013	41	4	42	8	3.578	248.91
100	0	1	0	-1.88	45.70	555.36	29.10	4	0.20	0.906	9.98	-0.008	41	6	42	8	6.378	248.91
101	0	1	0	-4.15	51.03	680.41	37.85	10	0.09	0.937	11.19	-0.018	49	12	49	13	15.321	280.07
102	0	1	0	-0.31	48.79	597.34	31.29	3	0.30	0.555	10.56	0.018	44	5	45	9	4.958	266.20
103	0	1	0	-4.06	52.79	680.54	37.85	10	0.09	0.949	11.86	-0.017	50	12	50	13	15.140	294.73
104	0	1	0	-4.18	54.12	723.21	40.04	10	0.09	1.045	11.73	0.002	52	10	52	14	16.128	297.37
105	0	1	0	-3.90	54.12	723.21	40.04	10	0.09	0.965	11.81	-0.040	52	12	52	14	16.413	297.37
106	0	1	0	-4.18	54.12	723.21	40.04	10	0.09	0.994	11.71	0.002	52	8	52	14	16.039	297.37
107	0	1	0	-0.59	51.88	640.07	33.48	4	0.29	0.622	11.26	0.022	47	6	48	10	6.369	283.50
108	0	1	0	-4.47	57.22	765.94	42.22	11	0.08	0.934	12.48	-0.003	55	12	55	15	17.710	314.67
109	0	1	0	-4.72	57.22	765.87	42.22	12	0.08	0.942	12.63	-0.016	55	14	55	15	18.288	314.67
110	0	1	0	-0.88	54.98	682.80	35.66	5	0.27	0.643	11.97	0.025	50	7	51	11	7.798	300.80
111	0	1	0	-5.01	60.31	808.60	44.41	13	0.08	0.945	13.35	-0.015	58	15	58	16	19.775	331.96
112	0	1	0	-1.17	58.07	725.53	37.85	6	0.26	0.661	12.68	0.027	53	8	54	12	9.242	318.09
113	0	1	0	-5.30	63.40	851.33	46.60	14	0.07	0.947	14.07	-0.014	61	16	61	17	21.263	349.26
114	0	1	0	-5.34	66.50	894.13	48.78	14	0.07	0.991	14.56	0.003	64	9	64	18	21.896	366.55
115	0	1	0	-2.03	67.35	853.72	44.41	9	0.23	0.706	14.82	0.030	62	11	63	15	13.623	369.98
116	0	1	0	-5.91	72.69	979.59	53.15	16	0.07	1.025	16.04	0.003	70	16	70	20	25.033	401.15
117	0	1	0	-4.52	73.54	939.93	48.78	13	0.14	0.939	16.34	-0.018	68	14	69	17	19.171	404.57
118	0	1	0	-7.03	81.97	1107.71	59.71	20	0.06	0.958	18.40	-0.011	79	22	79	23	30.213	453.03
119	0	1	0	-1.34	16.99	181.28	10.73	0	0.12	0.000	3.85	-0.121	15	0	15	1	0.000	93.48

Table S9. (Continued)

120	0	0	1	-1.34	16.99	181.28	10.73	0	0.12	0.000	3.85	-0.121	15	0	15	1	0.000	93.48
121	0	1	0	-1.79	21.00	313.25	17.94	2	0.00	0.000	4.71	0.050	21	0	21	2	5.653	112.29
122	0	0	1	-1.79	21.00	313.25	17.94	2	0.00	0.000	4.71	0.050	21	0	21	2	5.653	112.29

[a] ETA – ETA_Shape_Y, [b] LI – LipoaffinityIndex, [c] LAC – nAtomLAC

Table S10. Predicted activity for the potential catalyst set based on the PLS and SVM methods.

Compound	Catalyst	[a]PLS (%)	[a]SVM (%)
1	Tetramethylphosphonium bromide	17.2	17.2
2	Tetramethylphosphonium iodide	10.9	10.1
3	Tetraethylphosphonium bromide	5.5	5.5
4	Tetrapropylphosphonium bromide	17.3	16.5
5	Diethyl(dihexyl)phosphonium bromide	26.7	25.9
6	Heptyl(tripropyl)phosphonium bromide	28.3	27.6
7	Methyl(tripentyl)phosphonium bromide	29.6	28.3
8	Tetrakis(2-methylpropyl)phosphonium bromide	14.6	14.3
9	Tributyl(pentyl)phosphonium bromide	30.8	29.4
10	Methyl(triphenyl)phosphonium bromide	8.9	8.0
11	Tributyl(hexyl)phosphonium bromide	33.0	31.8
12	Trihexyl(methyl)phosphonium bromide	33.9	33.1
13	Ethyl(trihexyl)phosphonium bromide	33.3	32.7
14	Hexyl(tripentyl)phosphonium bromide	36.1	35.4
15	Dibutyl(diheptyl)phosphonium bromide	38.4	37.8
16	Tributyl(hexadecyl)phosphonium bromide	55.3	55.2
17	Tetraoctylphosphonium bromide	47.6	47.4
18	Tetramethylammonium bromide	24.0	24.0
19	Tetramethylammonium iodide	17.7	16.6
20	Trimethylphenylammonium bromide	8.9	8.9
21	Triethylmethylammonium bromide	4.7	5.1
22	Benzyltrimethylammonium bromide	23.5	20.1
23	Tetraethylammonium bromide	3.0	3.8
24	Pentyltrimethylammonium bromide	27.2	24.7
25	Cyclohexyl(trimethyl)ammonium bromide	12.4	13.1
26	Hexyl(trimethyl)ammonium bromide	23.3	22.6
27	Benzyl(triethyl)ammonium bromide	10.4	9.5
28	Trimethyl(octyl)ammonium bromide	33.6	31.2
29	Tetrapropylammonium bromide	22.9	21.5
30	Triethylhexylammonium bromide	19.4	18.8
31	Trimethyl(nonyl)ammonium bromide	35.6	33.4
32	Decyl(trimethyl)ammonium bromide	37.7	35.6
33	Tributyl(methyl)ammonium bromide	27.4	25.6
34	Decyl-ethyl-dimethylammonium bromide	34.0	32.6
35	Dibutyl(dipropyl)ammonium bromide	27.1	25.7
36	Tributyl(ethyl)ammonium bromide	25.6	24.2
37	Triethyloctylammonium bromide	24.7	24.2
38	Trimethyl-undecyl-ammonium bromide	39.7	37.8
39	Dodecyltrimethylammonium bromide	41.8	40.0
40	Triethyl(nonyl)ammonium bromide	27.3	26.8
41	Dibutyl-bis(2-methylpropyl)ammonium bromide	28.4	26.9

Table S10. (Continued)

42	Diethyl(dihexyl)ammonium bromide	27.6	26.9
43	Methyl(tripentyl)ammonium bromide	30.9	30.0
44	Tetraisobutylammonium bromide	24.9	23.6
45	Tributyl(2-methylpropyl)ammonium bromide	29.3	27.9
46	Trimethyl(tridecyl)ammonium bromide	44.0	42.2
47	Diheptyl(dimethyl)ammonium bromide	34.9	33.6
48	Tributyl(3-methylbutyl)ammonium bromide	29.7	28.3
49	Trimethyl(tetradecyl)ammonium bromide	46.1	44.5
50	Tris(2-methylpropyl)-pentylammonium bromide	29.2	27.9
51	Dodecyl(triethyl)ammonium bromide	34.8	34.5
52	Ethyl-dihexyl-(2-methylpropyl)ammonium bromide	31.5	30.6
53	Trimethyl(pentadecyl)ammonium bromide	48.2	46.7
54	Benzyl(tributyl)ammonium bromide	29.4	28.0
55	Butyl-tris(3-methylbutyl)ammonium bromide	28.7	27.4
56	Tributyl(heptyl)ammonium bromide	36.5	35.5
57	Trihexyl(methyl)ammonium bromide	35.6	34.9
58	Ethyl(trihexyl)ammonium bromide	34.3	33.9
59	Ethyl-hexadecyl-dimethylammonium bromide	47.7	46.8
60	Heptadecyl(trimethyl)ammonium bromide	52.5	51.2
61	Tetrapentylammonium bromide	34.7	34.2
62	Hexadecyl-(2-hydroxyethyl)-dimethylammonium bromide	50.5	49.6
63	Hexyl(tripentyl)ammonium bromide	37.0	36.6
64	Octadecyltrimethylammonium bromide	54.7	53.5
65	Trihexyl(propyl)ammonium bromide	37.0	36.6
66	Didecyl(dimethyl)ammonium bromide	44.6	44.1
67	Heptyl(tripentyl)ammonium bromide	39.2	38.9
68	Eicosyltrimethylammonium bromide	59.0	58.1
69	Tributyl(undecyl)ammonium bromide	45.4	44.8
70	Tetrahexylammonium bromide	40.4	40.4
71	Triheptyl(propyl)ammonium bromide	41.4	41.3
72	Cetyltrimethylammonium Bromide	50.4	49.0
73	Methyl(trioctyl)ammonium bromide	44.3	44.5
74	Docosyl(trimethyl)ammonium bromide	63.3	62.6
75	Didodecyl(dimethyl)ammonium bromide	51.1	51.2
76	Diheptyl(dihexyl)ammonium bromide	43.7	43.9
77	Trioctyl(propyl)ammonium bromide	45.7	46.1
78	Tributyl(hexadecyl)ammonium bromide	56.4	56.4
79	Tetraheptylammonium bromide	45.8	46.4
80	Hexacosyl(trimethyl)ammonium bromide	72.0	71.8
81	Tetrakis(decyl)ammonium bromide	62.1	64.4
82	1,3-dimethylimidazolium bromide	13.2	13.2
83	1,3-dimethylimidazolium iodide	6.9	8.2

Table S10. (Continued)

84	1-Ethyl-3-methylimidazolium bromide	7.7	6.9
85	1-Butyl-3-Vinylimidazolium bromide	20.4	18.4
86	1-Hexyl-3-methylimidazolium bromide	25.1	23.5
87	1-Octyl-2H-imidazolium bromide	28.7	26.8
88	1-Ethyl-3-hexylimidazolium bromide	24.0	22.6
89	1-Heptyl-2,3-dimethylimidazolium bromide	21.3	21.0
90	1-Ethenyl-3-octylimidazolium bromide	29.8	28.2
91	1-Ethyl-3-octylimidazolium bromide	28.9	27.6
92	1-Methyl-3-nonylimidazolium bromide	32.1	30.6
93	1-Butyl-3-methylimidazolium bromide	23.7	21.7
94	1-Decyl-3-methylimidazolium bromide	34.4	33.0
95	1-Propyl-3-(2,4,6-trimethylphenyl)imidazolium bromide	16.9	16.5
96	1-Decyl-3-ethenylimidazolium bromide	34.4	33.0
97	1-Decyl-3-ethylimidazolium bromide	33.7	32.5
98	1-Methyl-3-undecylimidazolium bromide	36.7	35.4
99	1-Butyl-3-(2,4,6-trimethylphenyl)imidazolium bromide	19.9	19.4
100	1-Hexyl-3-(4-methylphenyl)imidazolium bromide	25.9	24.7
101	1-Dodecyl-3-methylimidazolium bromide	39.0	37.7
102	1-Pentyl-3-(2,4,6-trimethylphenyl)imidazolium bromide	22.2	21.7
103	1-Dodecyl-3-ethenylimidazolium bromide	39.0	37.8
104	1-Butyl-3-decylimidazolium bromide	37.9	36.7
105	1-Dodecyl-3-ethylimidazolium bromide	38.4	37.3
106	1-Hexyl-3-octylimidazolium bromide	35.5	34.4
107	1-Hexyl-3-(2,4,6-trimethylphenyl)imidazolium bromide	24.7	24.2
108	1-Dodecyl-3-propylimidazolium bromide	40.9	39.8
109	1-Methyl-3-tetradecylimidazolium bromide	43.5	42.4
110	1-Heptyl-3-(2,4,6-trimethylphenyl)imidazolium bromide	27.1	26.6
111	1-Methyl-3-pentadecylimidazolium bromide	45.8	44.8
112	1-Octyl-3-(2,4,6-trimethylphenyl)imidazolium bromide	29.5	29.0
113	1-Hexadecyl-3-methylimidazolium bromide	48.0	47.1
114	1,3-Di(nonyl)imidazolium bromide	41.0	40.4
115	1-(2,4,6-trimethylphenyl)-3-undecylimidazolium bromide	36.4	36.1
116	1-Butyl-3-hexadecylimidazolium bromide	51.3	50.6
117	1-(4-Ethylphenyl)-3-tetradecylimidazolium bromide	44.8	44.4
118	1-Docosyl-3-methylimidazolium bromide	61.6	61.2
119	1-Methylpyridinium bromide	8.6	8.6
120	1-Methylpyridinium iodide	2.3	3.6
121	1,1-Dimethylpyrrolidinium bromide	16.0	16.0
122	1,1-Dimethylpyrrolidinium iodide	9.7	10.2

[a] – Conversion estimated by PLS and SVM models performed with 16.7% of the sample kept out in the Leave-Many-Out cross-validation

Table S11. Predicted activity of the best organocatalyst targets based on the PLS and SVM models

Catalyst	[a]PLS (%)	Catalyst	[a]SVM (%)
Hexacosyl(trimethyl)ammonium bromide	72.0	Hexacosyl(trimethyl)ammonium bromide	71.8
Docosyl(trimethyl)ammonium bromide	63.3	Tetrakis(decyl)ammonium bromide	64.4
1-Docosyl-3-methylimidazolium bromide	62.1	Docosyl(trimethyl)ammonium bromide	62.6
Tetrakis(decyl)ammonium bromide	61.6	1-Docosyl-3-methylimidazolium bromide	61.2
Eicosyltrimethylammonium bromide	59.0	Eicosyltrimethylammonium bromide	58.1
Tributyl(hexadecyl)ammonium bromide	56.4	Tributyl(hexadecyl)ammonium bromide	56.4
Octadecyltrimethylammonium bromide	55.3	Tributyl(hexadecyl)phosphonium bromide	55.2
Tributyl(hexadecyl)phosphonium bromide	54.7	Octadecyltrimethylammonium bromide	53.5
Heptadecyl(trimethyl)ammonium bromide	52.5	Didodecyl(dimethyl)ammonium bromide	51.2
Didodecyl(dimethyl)ammonium bromide	51.2	Heptadecyl(trimethyl)ammonium bromide	51.2
Hexadecyl-(2-hydroxyethyl)-dimethylammonium bromide	50.6	1-Butyl-3-hexadecylimidazolium bromide	50.6
1-Butyl-3-hexadecylimidazolium bromide	50.5	Hexadecyl-(2-hydroxyethyl)-dimethylammonium bromide	49.6
Cetyltrimethylammonium Bromide	50.4	Cetyltrimethylammonium Bromide	49.0
Trimethyl(pentadecyl)ammonium bromide	48.2	Tetraoctylphosphonium bromide	47.4
Tetraoctylphosphonium bromide	48.0	1-Hexadecyl-3-methylimidazolium bromide	47.1
1-Hexadecyl-3-methylimidazolium bromide	47.7	Ethyl-hexadecyl-dimethylammonium bromide	46.8
Ethyl-hexadecyl-dimethylammonium bromide	47.6	Trimethyl(pentadecyl)ammonium bromide	46.7
Trioctyl(propyl)ammonium bromide	46.1	Tetraheptylammonium bromide	46.4
1-Methyl-3-pentadecylimidazolium bromide	45.8	Trioctyl(propyl)ammonium bromide	46.1
Tetraheptylammonium bromide	45.8	1-Methyl-3-pentadecylimidazolium bromide	44.8

[a] – Conversion estimated by PLS and SVM models performed with 16.7% of the sample kept out in the Leave-Many-Out cross-validation

Table S12. Molecular descriptors for the exploratory analysis of the data set 03

CAS	nCl^-	nBr^-	nI^-	ALogP	apol	ATS2e	bpol	C2SP3	[a]ETA	GATS6i	[b]LI	MATS4m	nAtom	[c]LAC	nBonds2	nRotBt	$SssCH_2$	VABC
7237-34-5	0	1	0	2.4	53.0	533.9	29.3	0	0.132	1.076	11.1	-0.148	42	2	44	6	1.13	290.9
23250-03-5	1	0	0	2.4	53.0	533.9	29.3	0	0.132	1.076	11.1	-0.148	42	2	44	6	1.13	290.9
4336-77-0	0	0	1	2.4	53.0	533.9	29.3	0	0.132	1.076	11.1	-0.148	42	2	44	6	1.13	290.9
20650-57-1	0	0	1	2.7	49.9	488.6	27.2	0	0.185	1.046	10.8	-0.225	39	0	41	5	0.00	273.6
85100-77-2	0	1	0	-4.0	26.3	338.6	20.4	2	0.167	1.064	5.5	-0.040	25	4	25	5	3.69	141.7
32353-64-3	0	0	1	-2.2	29.4	351.9	19.5	2	0.167	1.226	6.5	-0.085	27	4	27	5	3.69	162.7
471907-87-6	0	1	0	-5.3	58.6	810.5	43.7	12	0.082	0.952	12.7	-0.002	57	14	57	15	19.69	328.2
60254-13-9	0	0	1	2.6	49.9	489.8	27.2	0	0.277	0.986	10.2	-0.112	39	0	41	5	1.03	273.6
5350-41-4	0	1	0	0.1	29.4	358.0	20.1	0	0.093	0.970	6.8	0.328	27	0	27	5	1.10	162.7
79917-90-1	1	0	0	-4.0	26.3	338.6	20.4	2	0.167	1.064	5.5	-0.040	25	4	25	5	3.69	141.7
2065-66-9	0	0	1	3.3	49.1	475.7	27.2	0	0.143	1.028	12.0	-0.204	38	0	40	4	0.00	264.8
4368-51-8	0	1	0	-7.0	90.4	1251.0	68.2	20	0.000	1.035	20.8	0.001	89	7	88	28	34.68	505.2
54580-84-6	1	0	0	-2.5	50.4	646.8	42.5	6	0.000	1.100	10.1	-0.019	48	4	47	15	14.72	280.6
54580-85-7	0	0	1	-2.5	50.4	646.8	42.5	6	0.000	1.100	10.1	-0.019	48	4	47	15	14.72	280.6
54580-43-7	0	1	0	-2.5	50.4	646.8	42.5	6	0.000	1.100	10.1	-0.019	48	4	47	15	14.72	280.6
23906-97-0	0	1	0	-7.4	105.3	1400.4	81.8	24	0.000	1.044	24.9	-0.004	101	8	1	32	43.18	583.2
57-09-0	0	1	0	-5.1	62.5	866.2	48.6	14	0.000	0.971	14.4	0.067	62	16	61	19	21.70	349.5
56511-17-2	0	0	1	-2.4	30.3	441.5	24.5	4	0.000	1.083	6.8	-0.018	30	4	30	5	9.96	164.2
874-81-7	0	0	1	-2.0	26.3	309.5	17.3	2	0.082	1.072	5.8	-0.063	24	4	24	4	3.69	145.4
61545-99-1	0	1	0	-3.0	38.7	509.5	29.1	6	0.118	0.922	8.3	-0.024	37	8	37	9	9.43	210.9
64697-40-1	1	0	0	-3.0	38.7	509.5	29.1	6	0.118	0.922	8.3	-0.024	37	8	37	9	9.43	210.9
188589-28-8	0	0	1	-3.4	40.0	554.9	31.3	6	0.118	0.934	8.3	0.006	39	8	39	9	12.01	224.4
1643-19-2	0	1	0	-3.5	53.3	738.2	42.0	8	0.000	1.226	12.1	0.004	53	4	52	16	16.77	297.6
1112-67-0	1	0	0	-3.5	53.3	738.2	42.0	8	0.000	1.226	12.1	0.004	53	4	52	16	16.77	297.6
311-28-4	0	0	1	-3.5	53.3	738.2	42.0	8	0.000	1.226	12.1	0.004	53	4	52	16	16.77	297.6
3115-68-2	0	1	0	-2.8	55.8	716.7	46.8	8	0.000	1.172	13.2	-0.011	53	4	52	16	18.78	306.4
2304-30-5	1	0	0	-2.8	55.8	716.7	46.8	8	0.000	1.172	13.2	-0.011	53	4	52	16	18.78	306.4
3115-66-0	0	0	1	-2.8	55.8	716.7	46.8	8	0.000	1.172	13.2	-0.011	53	4	52	16	18.78	306.4
1829-92-1	0	0	1	1.1	23.5	280.4	19.8	0	0.217	0.000	5.3	-0.197	22	2	21	6	4.74	132.2

[a] ETA – ETA_Shape_Y, [b] LI – LipoaffinityIndex, [c] LAC – nAtomLAC

Supporting Figures

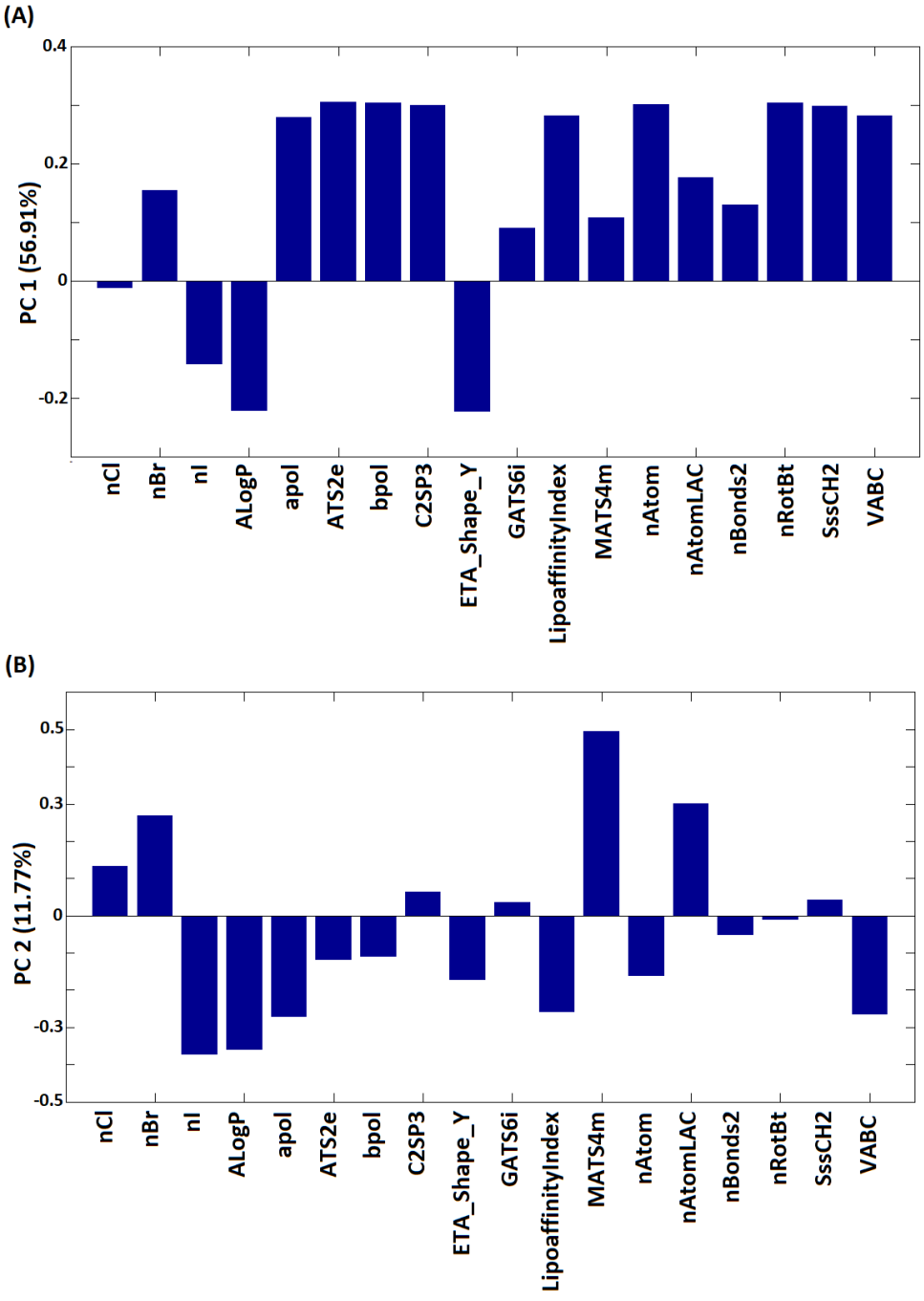

Figure S4. PCA loading of the exploratory analysis of the organocatalyst

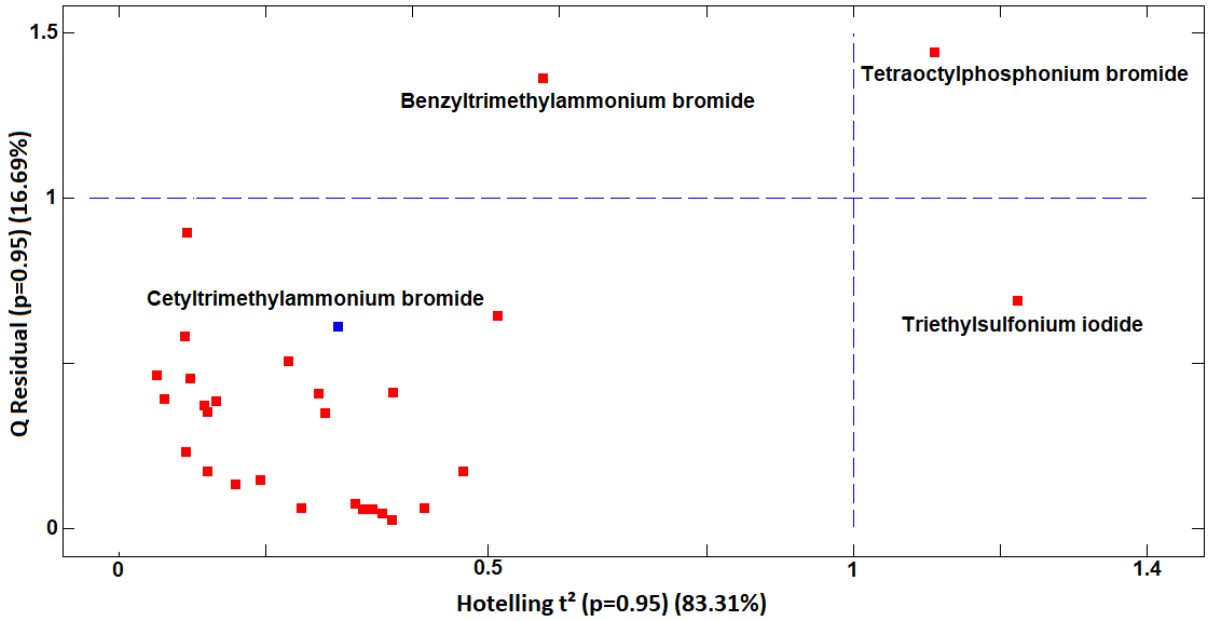

Figure S5. PCA residuals of the exploratory analysis of the organocatalyst

FTIR Spectra for oils (Figure S6-S8)

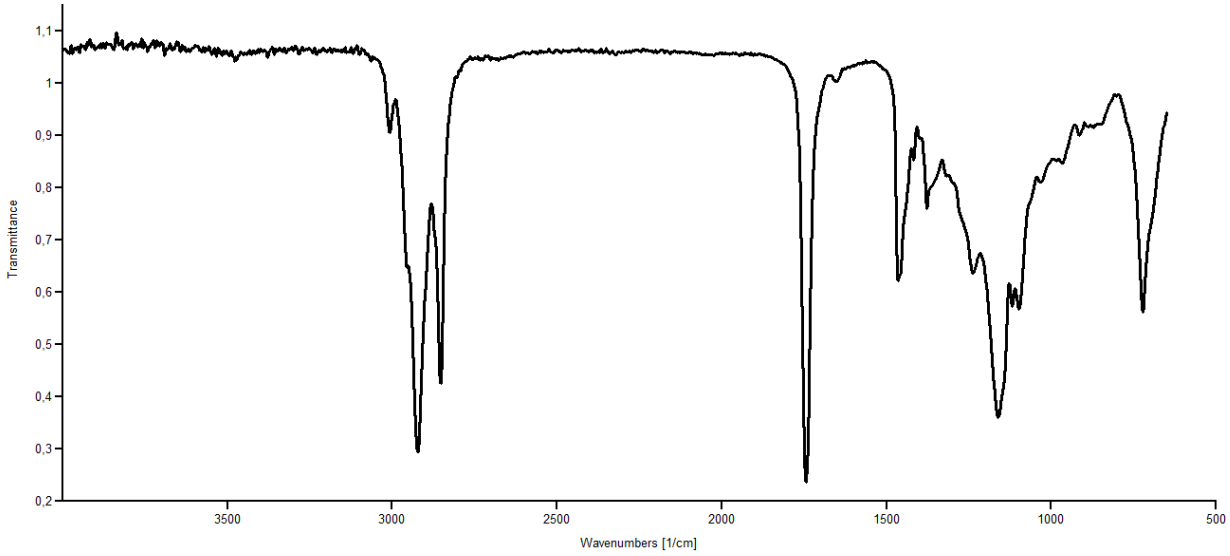

Figure S6. FTIR spectra of rice bran oil

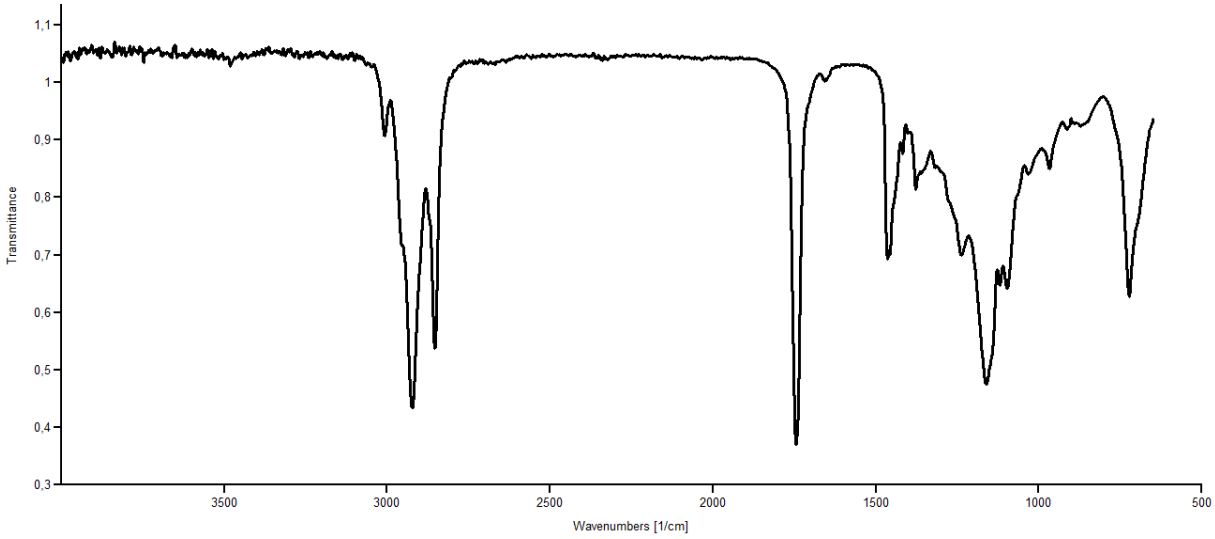

Figure S7. FTIR spectra of canola oil

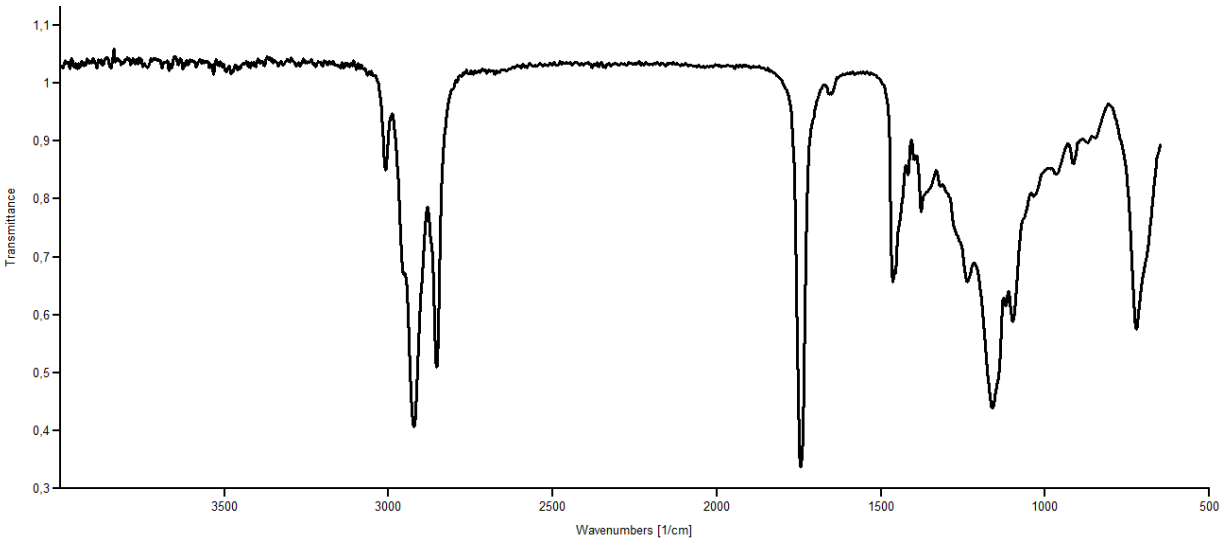

Figure S8. FTIR spectra of soybean oil

FTIR Spectra for epoxides (Figure S9-S11)

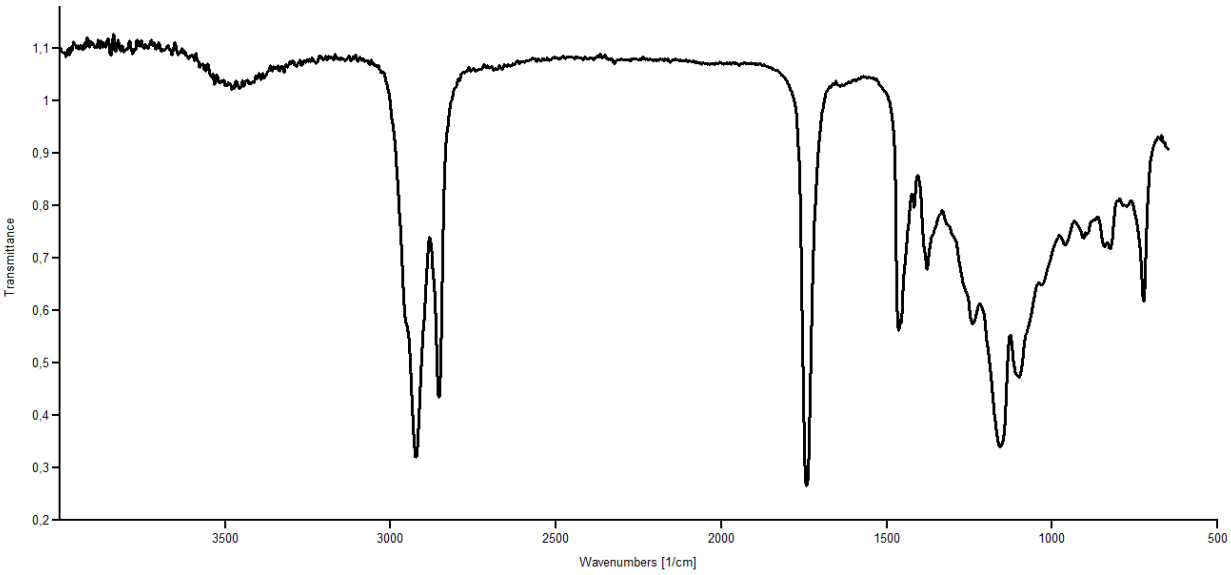

Figure S9. FTIR spectra of epoxidized rice bran oil

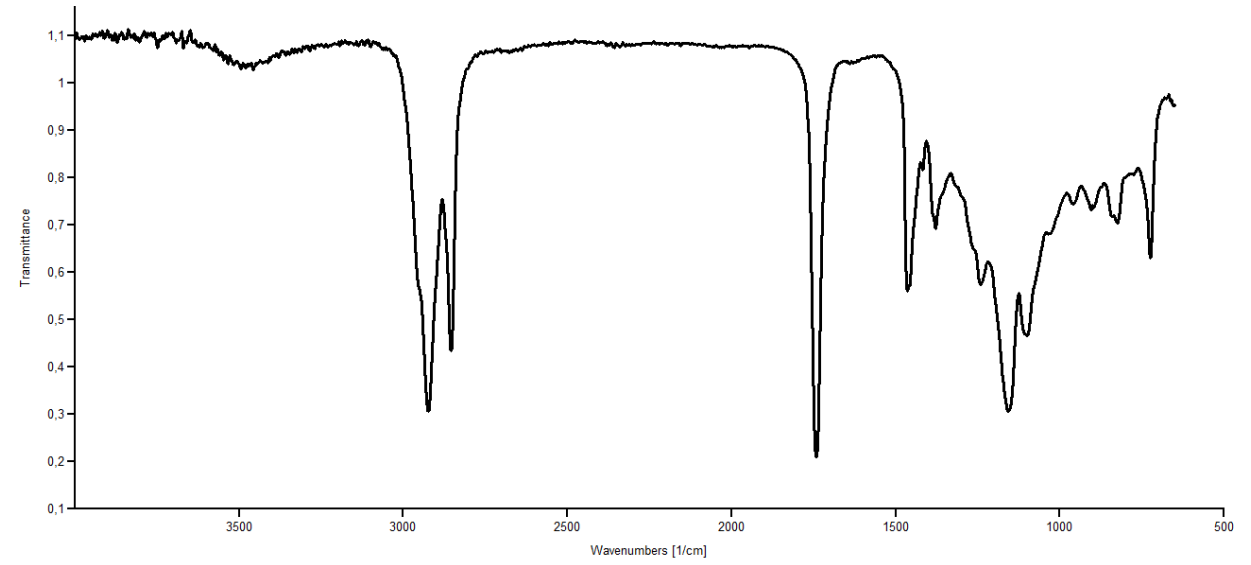

Figure S10. FTIR spectra of epoxidized canola oil

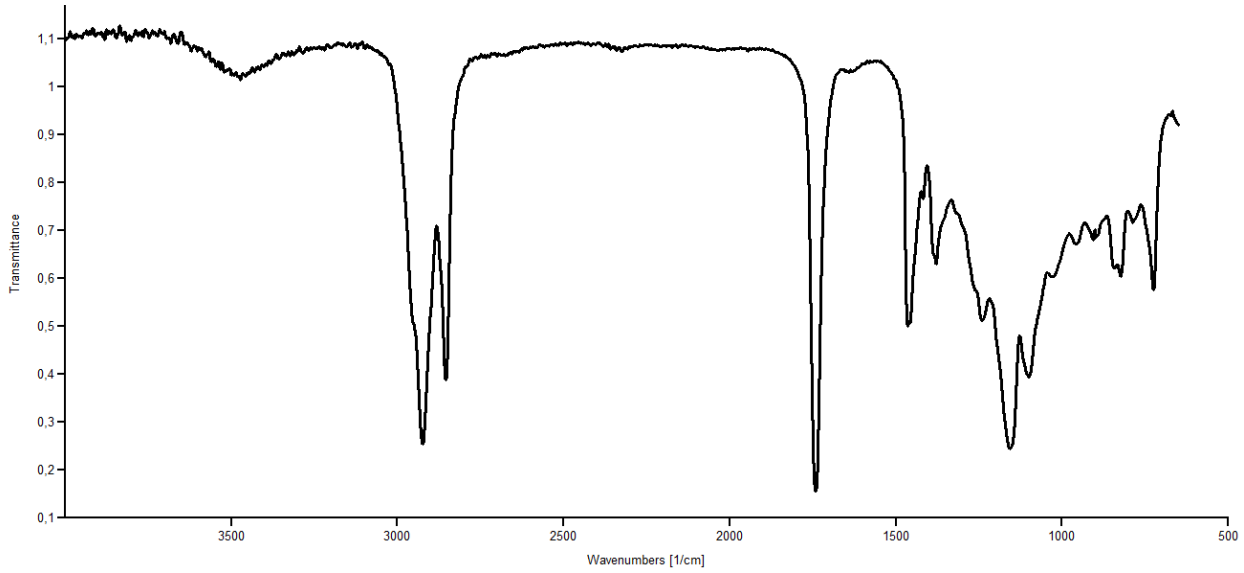

Figure S11. FTIR spectra of epoxidized soybean oil

FTIR Spectra for Cyclic Carbonates (Figure S12-S14)

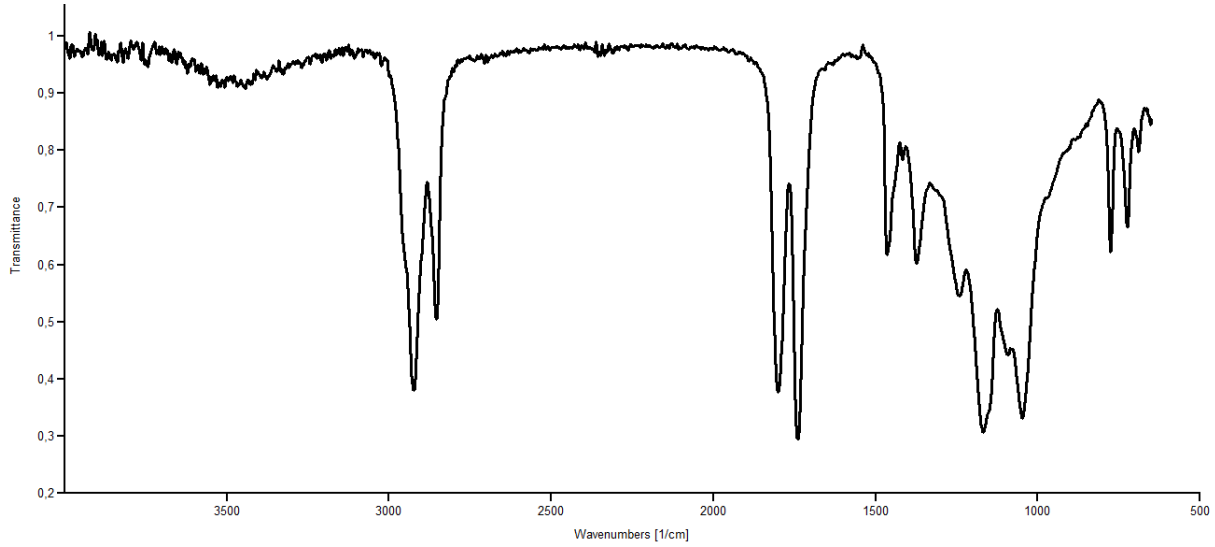

Figure S12. FTIR spectra of carbonated rice bran oil

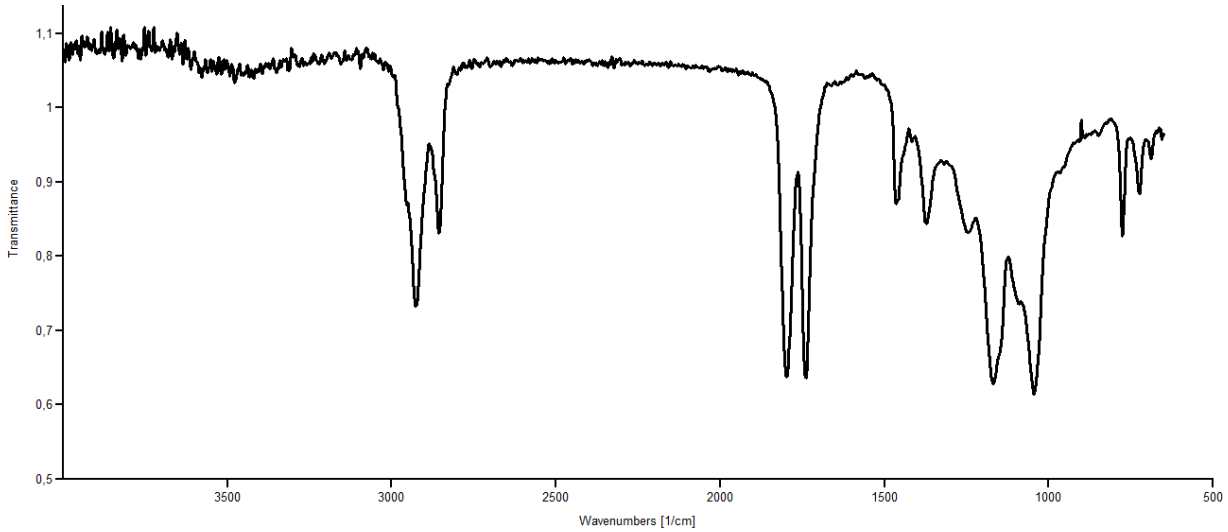

Figure S13. FTIR spectra of carbonated canola oil

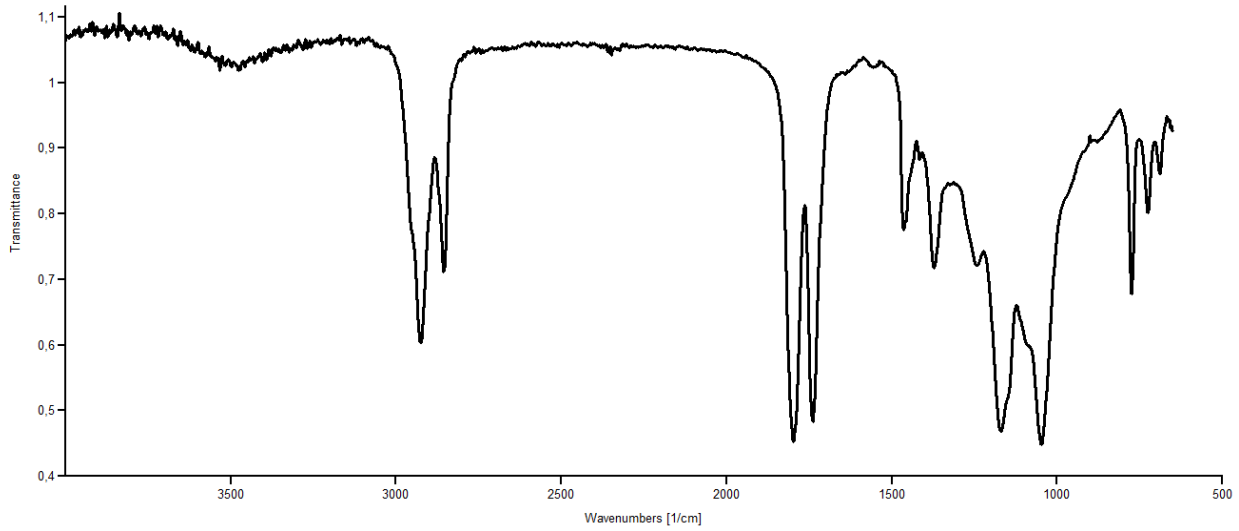

Figure S14. FTIR spectra of carbonated soybean oil

NMR Spectra for oils (Figure S15-S17)

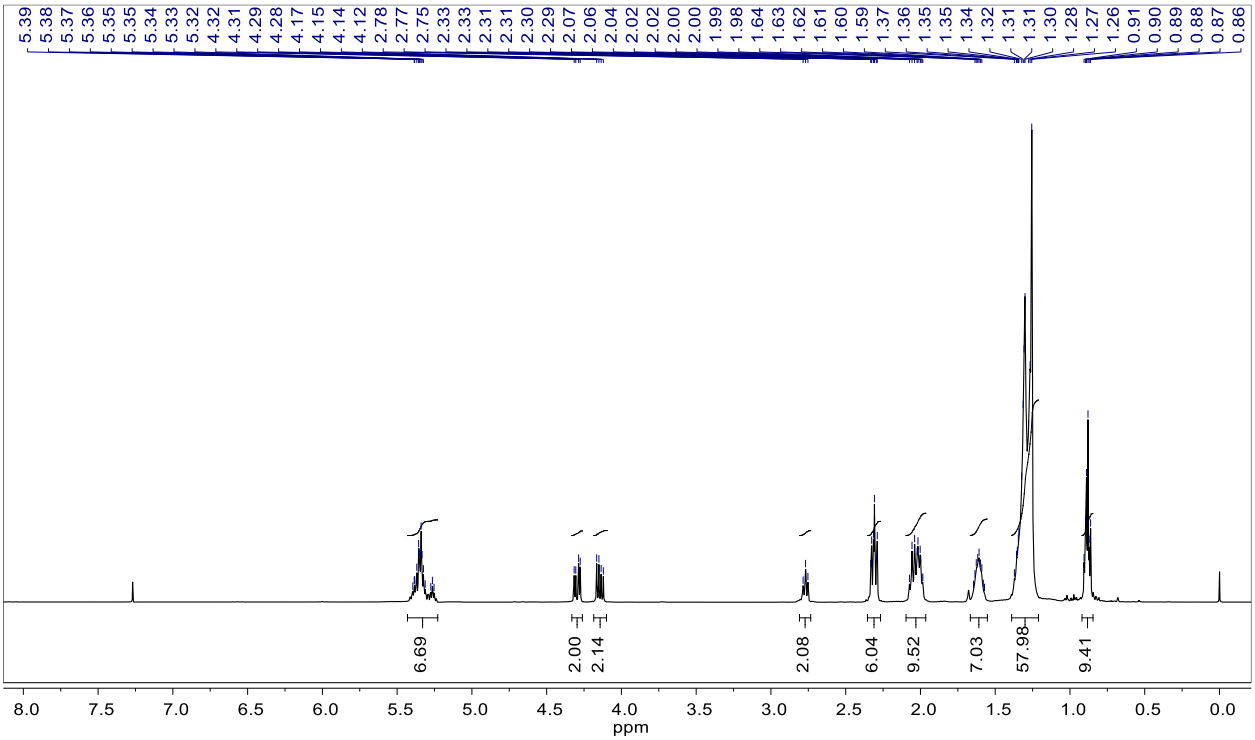

Figure S15. ^{1}H NMR spectra of rice bran oil

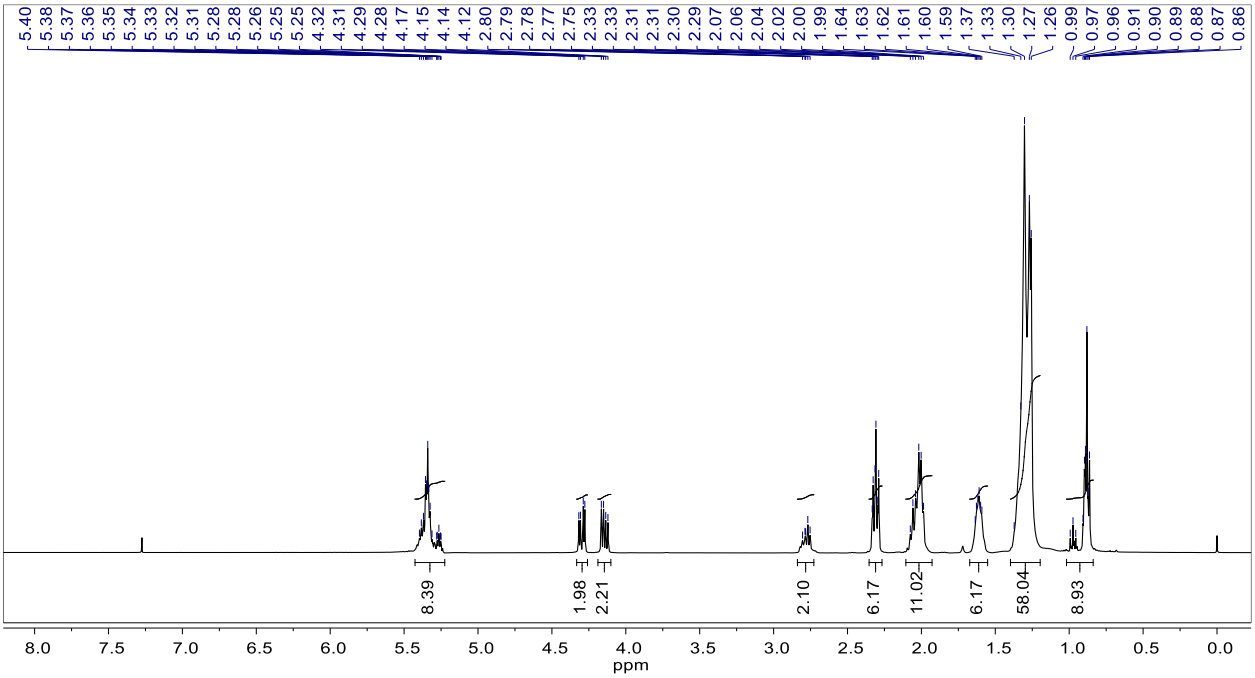

Figure S16. ^{1}H NMR spectra of canola oil

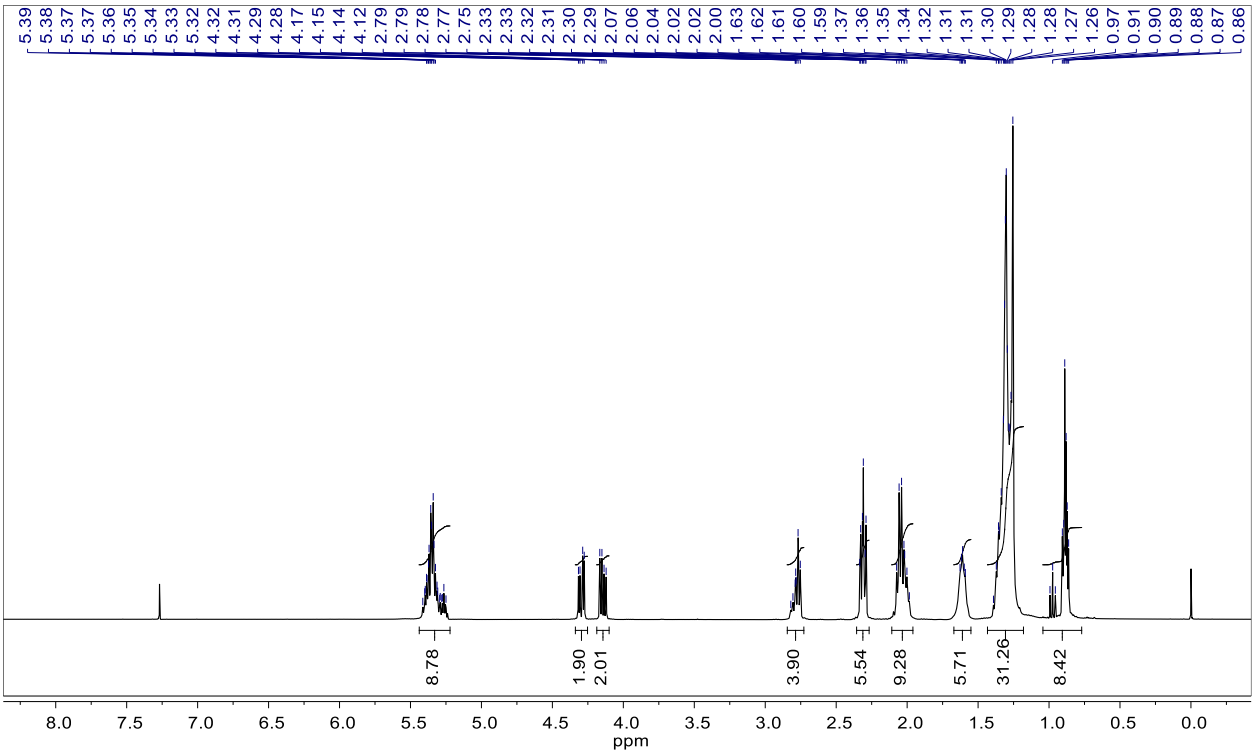

Figure S17. ^{1}H NMR spectra of soybean oil

NMR Spectra for epoxides (Figure S18-S20)

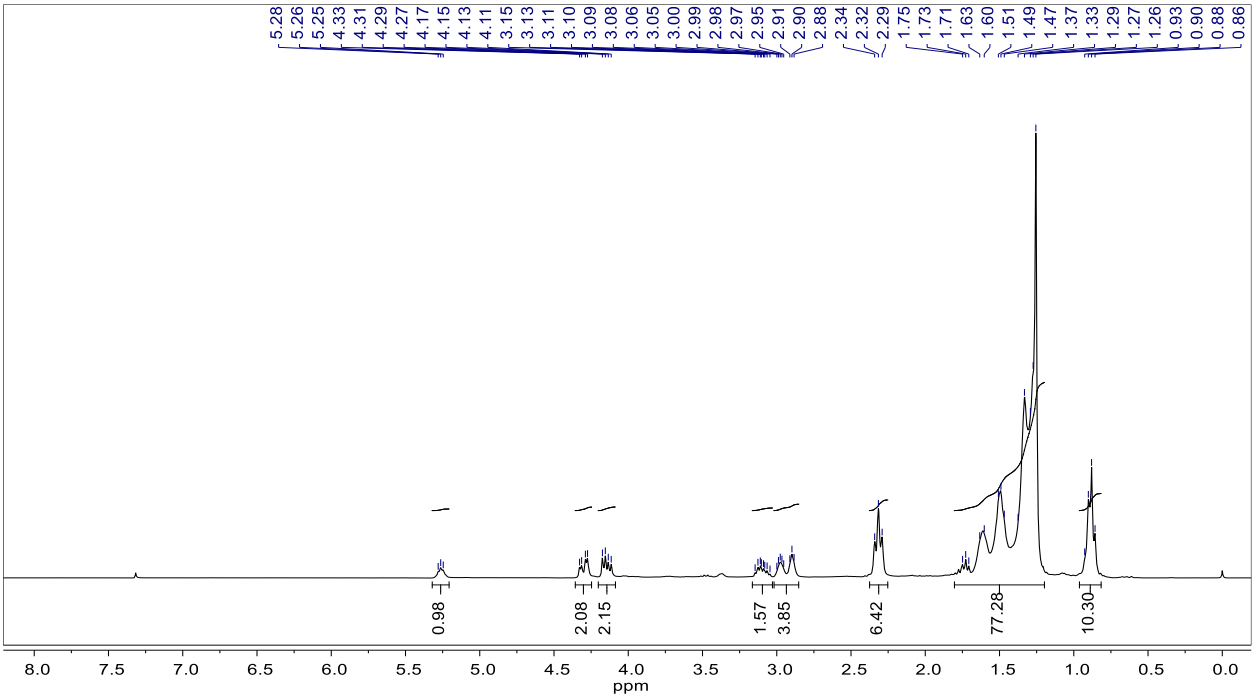

Figure S18. ^{1}H NMR spectra of epoxidized rice bran oil

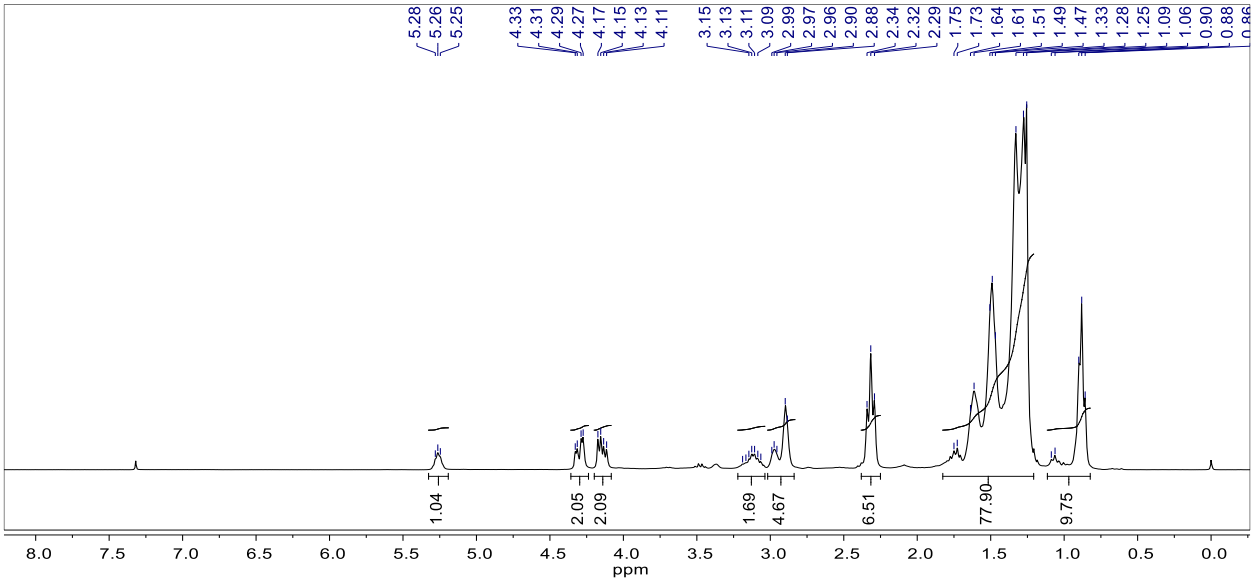

Figure S19. ^{1}H NMR spectra of epoxidized canola oil

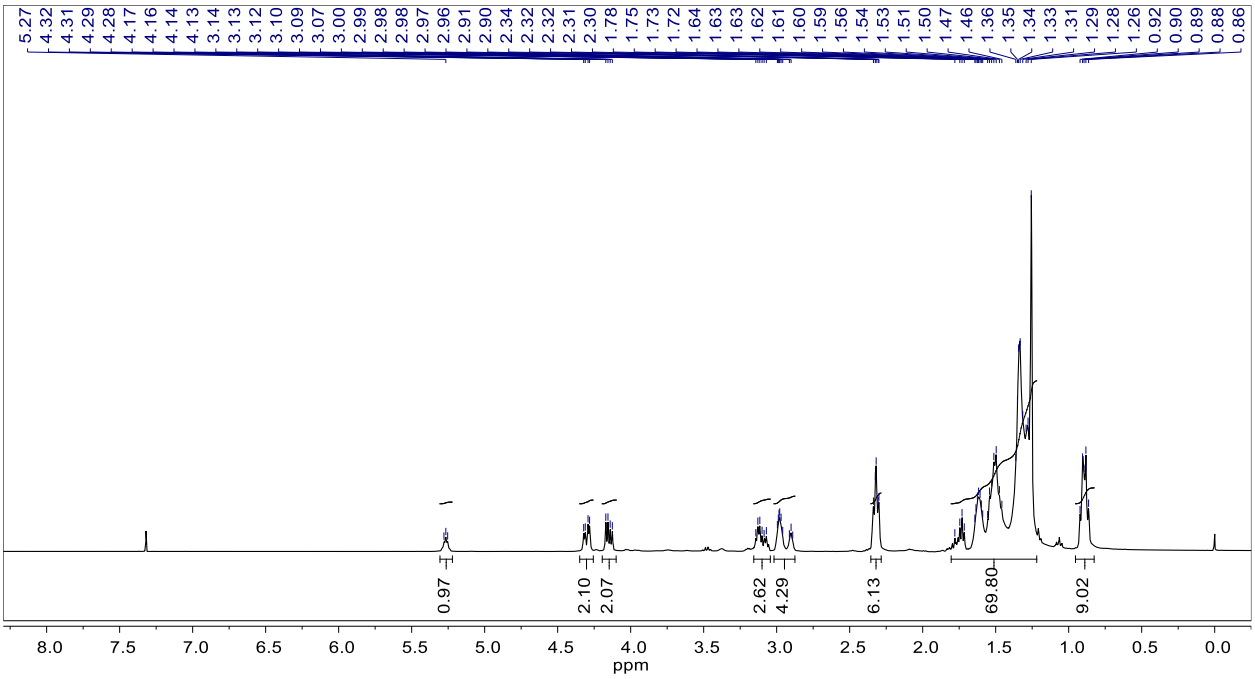

Figure S20. ^{1}H NMR spectra of epoxidized soybean oil

NMR Spectra for Cyclic Carbonates (Figure S21-S23)

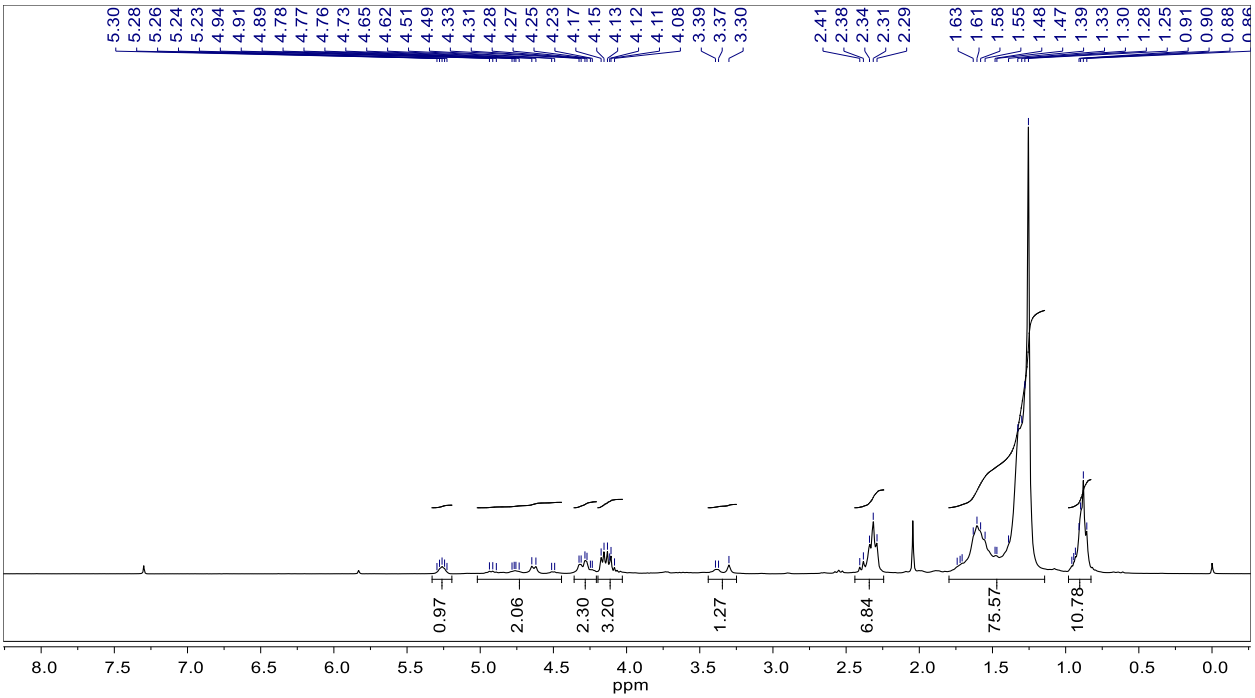

Figure S21. ^{1}H NMR spectra of carbonated rice bran oil

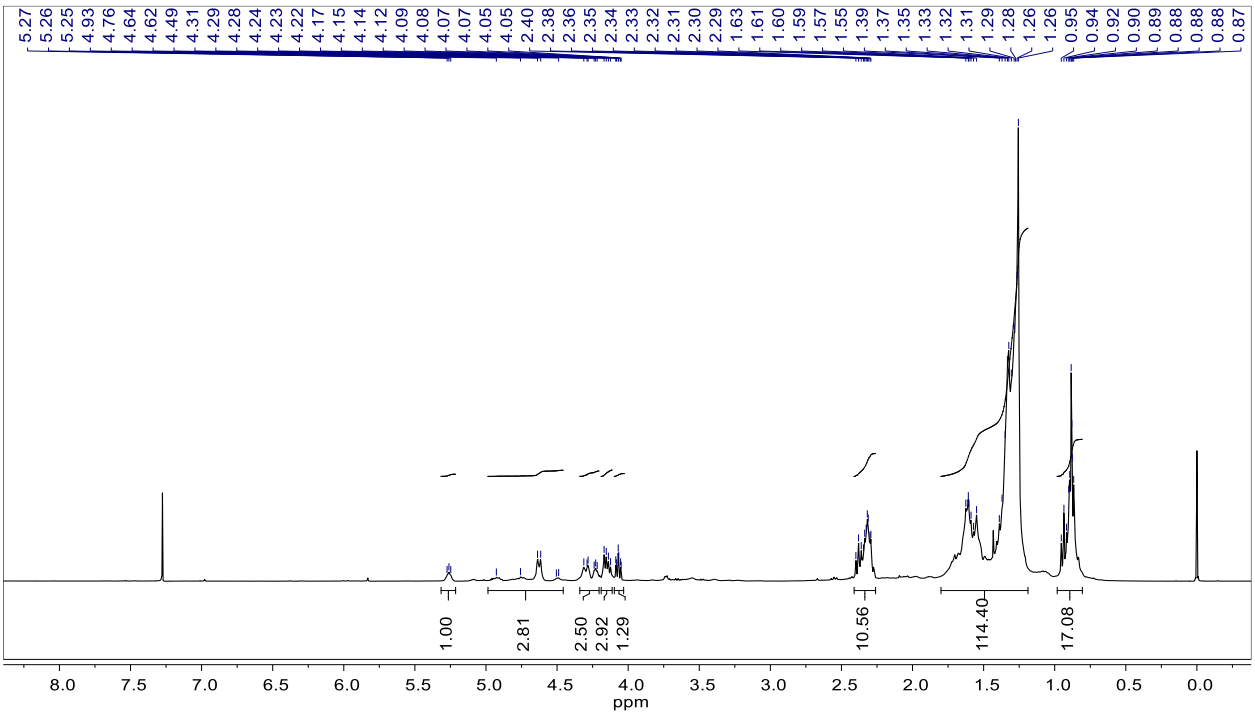

Figure S22. ^{1}H NMR spectra of carbonated canola oil

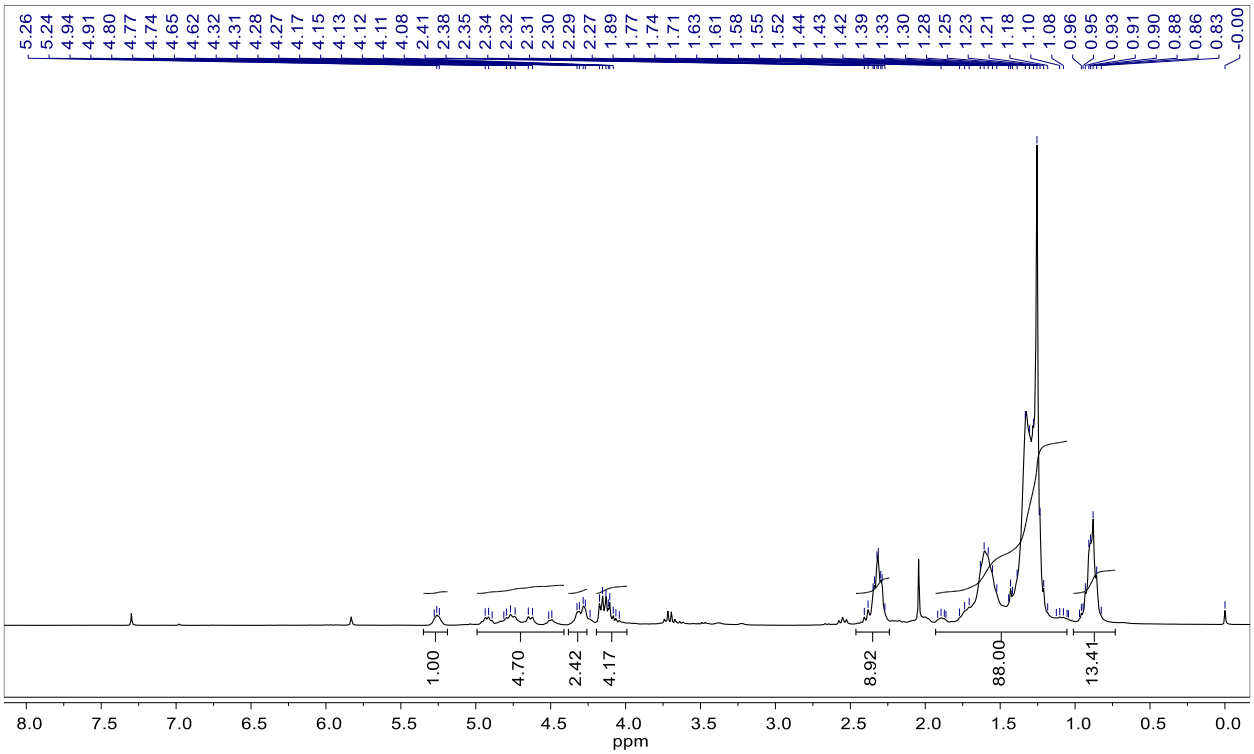

Figure S23. ^{1}H NMR spectra of carbonated soybean oil

REFERENCES

[1] V. V. Goud, A. V. Patwardhan, S. Dinda, N.C. Pradhan, Epoxidation of karanja (Pongamia glabra) oil catalysed by acidic ion exchange resin, Eur. J. Lipid Sci. Technol. 109 (2007) 575–584. doi:10.1002/ejlt.200600298.

[2] S. Dinda, A. V. Patwardhan, V. V. Goud, N.C. Pradhan, Epoxidation of cottonseed oil by aqueous hydrogen peroxide catalysed by liquid inorganic acids, Bioresour. Technol. 99 (2008) 3737–3744. doi:10.1016/j.biortech.2007.07.015.

[3] H. Büttner, J. Steinbauer, C. Wulf, M. Dindaroglu, H.-G. Schmalz, T. Werner, Organocatalyzed Synthesis of Oleochemical Carbonates from CO_2 and Renewables, ChemSusChem. 10 (2017) 1076–1079. doi:10.1002/cssc.201601163.

[4] A.R. Katritzky, M. Karelson, V.S. Lobanov, QSPR as a means of predicting and understanding chemical and physical properties in terms of structure, Pure Appl. Chem. 69 (1997) 245–248. doi:10.1351/pac199769020245.

[5] A. Golbraikh, A. Tropsha, Beware of Q^2!, J. Mol. Graph. Model. 20 (2002) 269–276. doi:10.1016/S1093-3263(01)00123-1.

[6] S. Kim, Getting the most out of PubChem for virtual screening, Expert Opin. Drug Discov. 11 (2016) 843–855. doi:10.1080/17460441.2016.1216967.

[7] C.W. Yap, PaDEL-descriptor: An open source software to calculate molecular descriptors and fingerprints, J. Comput. Chem. 32 (2011) 1466–1474. doi:10.1002/jcc.21707.

[8] G. Rothenberg, Data mining in catalysis: Separating knowledge from garbage, Catal. Today. 137 (2008) 2–10. doi:10.1016/j.cattod.2008.02.014.

[9] P. Pratim Roy, S. Paul, I. Mitra, K. Roy, On Two Novel Parameters for Validation of Predictive QSAR Models, Molecules. 14 (2009) 1660–1701. doi:10.3390/molecules14051660.

[10] R. Todeschini, D. Ballabio, F. Grisoni, Beware of Unreliable Q^2! A Comparative Study of Regression Metrics for Predictivity Assessment of QSAR Models, J. Chem. Inf. Model. 56 (2016) 1905–1913. doi:10.1021/acs.jcim.6b00277.

[11] D.L.J. Alexander, A. Tropsha, D.A. Winkler, Beware of R^2: Simple, Unambiguous Assessment of the Prediction Accuracy of QSAR and QSPR Models, J. Chem. Inf. Model. 55 (2015) 1316–1322. doi:10.1021/acs.jcim.5b00206.

[12] P. Gramatica, A. Sangion, A Historical Excursus on the Statistical Validation Parameters for QSAR Models: A Clarification Concerning Metrics and Terminology, J. Chem. Inf. Model. 56 (2016) 1127–1131. doi:10.1021/acs.jcim.6b00088.

[13] A. Tropsha, P. Gramatica, V. Gombar, The Importance of Being Earnest: Validation is the Absolute Essential for Successful Application and Interpretation of QSPR Models, QSAR Comb. Sci. 22 (2003) 69–77. doi:10.1002/qsar.200390007.

[14] A. Tropsha, Best Practices for QSAR Model Development, Validation, and Exploitation, Mol. Inform. 29 (2010) 476–488. doi:10.1002/minf.201000061.

[15] I. Mitra, P.P. Roy, S. Kar, P.K. Ojha, K. Roy, On further application of rm^2 as a metric for validation of QSAR models, J. Chemom. 24 (2010) 22–33. doi:10.1002/cem.1268.

[16] K. Roy, I. Mitra, P.K. Ojha, S. Kar, R.N. Das, H. Kabir, Introduction of rm^2(rank) metric incorporating rank-order predictions as an additional tool for validation of QSAR/QSPR models, Chemom. Intell. Lab. Syst. 118 (2012) 200–210. doi:10.1016/j.chemolab.2012.06.004.

[17] K. Roy, I. Mitra, On the Use of the Metric rm^2 as an Effective Tool for Validation of QSAR Models in Computational Drug Design and Predictive Toxicology, Mini-Reviews Med. Chem. 12 (2012) 491–504. doi:10.2174/138955712800493861.

[18] S. Wold, M. Sjöström, L. Eriksson, PLS-regression: a basic tool of chemometrics, Chemom. Intell. Lab. Syst. 58 (2001) 109–130. doi:10.1016/S0169-7439(01)00155-1.

[19] S. Das, P.K. Ojha, K. Roy, Development of a temperature dependent 2D-QSPR model for viscosity of diverse functional ionic liquids, J. Mol. Liq. 240 (2017) 454–467. doi:10.1016/j.molliq.2017.05.113.

[20] J. Langanke, L. Greiner, W. Leitner, Substrate dependent synergetic and antagonistic interaction of ammonium halide and polyoxometalate catalysts in the synthesis of cyclic carbonates from oleochemical epoxides and CO_2, Green Chem. 15 (2013) 1173. doi:10.1039/c3gc36710j.

[21] M.M. Dharman, J.-I. Yu, J.-Y. Ahn, D.-W. Park, Selective production of cyclic carbonate over polycarbonate using a double metal cyanide–quaternary ammonium salt catalyst system, Green Chem. 11 (2009) 1754. doi:10.1039/b916875n.

[22] L. Han, S.-J. Choi, M.-S. Park, S.-M. Lee, Y.-J. Kim, M.-I. Kim, B. Liu, D.-W. Park, Carboxylic acid functionalized imidazolium-based ionic liquids: efficient catalysts for cycloaddition of CO_2 and epoxides, React. Kinet. Mech. Catal. 106 (2012) 25–35. doi:10.1007/s11144-011-0399-8.

[23] R. Wei, X. Zhang, B. Du, Z. Fan, G. Qi, Highly active and selective binary catalyst system for the coupling reaction of CO_2 and hydrous epoxides, J. Mol. Catal. A Chem. 379 (2013) 38–45. doi:10.1016/j.molcata.2013.07.014.

[24] S. Narang, D. Berek, S.N. Upadhyay, R. Mehta, Effect of electron density on the catalysts for copolymerization of propylene oxide and CO_2, J. Polym. Res. 23 (2016) 96. doi:10.1007/s10965-016-0994-5.

[25] L. Wang, T. Huang, C. Chen, J. Zhang, H. He, S. Zhang, Mechanism of hexaalkylguanidinium salt/zinc bromide binary catalysts for the fixation of CO_2 with epoxide: A DFT investigation, J. CO_2 Util. 14 (2016) 61–66. doi:10.1016/j.jcou.2016.02.006.

[26] M. Alves, B. Grignard, R. Mereau, C. Jerome, T. Tassaing, C. Detrembleur, Organocatalyzed coupling of carbon dioxide with epoxides for the synthesis of cyclic carbonates: catalyst design and mechanistic studies, Catal. Sci. Technol. 7 (2017) 2651–2684. doi:10.1039/C7CY00438A.

[27] H. Sun, D. Zhang, Density Functional Theory Study on the Cycloaddition of Carbon Dioxide with Propylene Oxide Catalyzed by Alkylmethylimidazolium Chlorine Ionic Liquids, J. Phys. Chem. A. 111 (2007) 8036–8043. doi:10.1021/jp073873p.

[28] M. Alves, B. Grignard, S. Gennen, C. Detrembleur, C. Jerome, T. Tassaing, Organocatalytic synthesis of bio-based cyclic carbonates from CO_2 and vegetable oils, RSC Adv. 5 (2015) 53629–53636. doi:10.1039/C5RA10190E.

5. CONCLUSÕES

Os carbonatos oleoquímicos representam uma classe de compostos químicas de grande potencial de aplicação em um contexto de química de baixo carbono. Até o momento, apenas um pequeno número de organocatalisadores foram aplicados para produção de carbonatos oleoquímicos, enquanto a descrição do novo sistema de catalisadores ainda é limitada. Portanto, a triagem/desenho de catalisadores para promover a cicloadição de CO_2 em derivados epoxidados é um desafio que deve ser abordado pela comunidade acadêmica.

Este trabalho apresenta uma perspectiva preliminar do potencial da modelagem QSPR para auxiliar na escolha/desenho de novos organocatalisadores ativos para produção de carbonatos oleoquímicos. O modelo QSPR foi desenvolvido aplicando os descritores moleculares (2D) e validado com base em critérios reconhecidos pela comunidade acadêmica. A partir dos nossos resultados, conclui-se que é possível estabelecer uma relação estrutura-propriedade entre as características dos organocatalisadores e suas atividades respectivas para produção de carbonatos oleoquímicos a partir de epóxidos e CO_2.

A partir da triagem virtual, um total de 122 catalisadores potenciais tem sua atividade prevista, os melhores alvos moleculares são listados e o brometo de cetiltrimetilamônio (CTAB) foi selecionado para aplicação sintética. As principais características moleculares (estrutura orgânica, arranjo molecular, tamanho da cadeia de carbono e tipo de substituinte) foram identificadas e descritas através da mineração de dados, enquanto a PCA provou ser um método adequado para realizar uma análise exploratória rápida do conjunto de moléculas.

Além disso, é apresentado o primeiro relato da aplicação do brometo de cetiltrimetilamônio (CTAB) como um catalisador para a produção de carbonato oleoquímico, com mais de 98% de conversão de epóxido em carbonato cíclico para todos os óleos vegetais. Quando comparado com os resultados obtidos pelo

catalisador convencional TBAB, observa-se que conversões superiores foram obtidas pelo CTAB em um tempo equivalente, porém a uma temperatura menor.

Desta forma, a ferramenta QSPR pode ser aplicada para reduzir os custos e o tempo envolvido no processo de desenvolvimento de catalisadores para a síntese de carbonatos cíclicos a partir do CO_2.

6. PROPOSTAS PARA TRABALHOS FUTUROS

Ao longo do desenvolvimento deste trabalho, foram observadas oportunidades para dar continuidade ao trabalho, bem como, ampliar o escopo da presente dissertação para tópicos relacionados. Abaixo estão listados algumas das propostas para trabalhos futuros.

a) Escrita de um artigo de revisão sobre a produção de carbonatos oleoquímicos.

b) Redigir um artigo com foco nos procedimentos sintéticos do novo sistema descrito, estendendo a aplicação do CTAB como um catalisador para a produção de carbonatos oleoquímicos derivados de ésteres monoalquílicos e avaliando a estereosseletividade do catalisador.

c) Realizar um estudo de otimização dos parâmetros reacionais (pressão, temperatura, solvente, agitação, etc.) do sistema reacional com base em CTAB por meio de estratégias de *design* de experimentos como o planejamento fatorial e/ou análise de experimentos de superfície de resposta.

d) Aplicar os carbonatos oleoquímicos para produção de poliuretanos sem isocianato.

e) Aumentar o número e a diversidade de catalisadores incluídos no modelo QSPR para aumentar sua robustez.

f) Estudar o sistema de catálise por CTAB por meio de outras ferramentas de Quimioinformática como: Dinâmica Molecular (Molecular Dynamics) e Teoria do Funcional da Densidade (*Density Functional Theory*).

g) Aplicar a modelagem QSPR para a seleção de catalisadores ativos para a produção de carbonatos cíclicos derivados de outros materiais epoxidados.

7. REFERÊNCIAS BIBLIOGRÁFICAS

ACHARY, P. G. R. et al. A quasi-SMILES based QSPR Approach towards the prediction of adsorption energy of Ziegler−Natta catalysts for propylene polymerization. **Materials Discovery**, v. 5, p. 22–28, ago. 2016.

ADHVARYU, A.; ERHAN, S. Z. Epoxidized soybean oil as a potential source of high-temperature lubricants. **Industrial Crops and Products**, v. 15, n. 3, p. 247–254, 2002.

AIT AISSA, K. et al. Thermal Stability of Epoxidized and Carbonated Vegetable Oils. **Organic Process Research and Development**, v. 20, n. 5, p. 948–953, 2016.

ALVES, M. et al. Organocatalytic synthesis of bio-based cyclic carbonates from CO_2 and vegetable oils. **RSC Advances**, v. 5, n. 66, p. 53629–53636, 2015.

ALVES, M. et al. Organocatalyzed coupling of carbon dioxide with epoxides for the synthesis of cyclic carbonates: catalyst design and mechanistic studies. **Catalysis Science & Technology**, v. 7, n. 13, p. 2651–2684, 2017.

ANASTAS, P.; EGHBALI, N. Green Chemistry: Principles and Practice. **Chem. Soc. Rev.**, v. 39, n. 1, p. 301–312, 2010.

ANUAR, S. T. et al. Monitoring the Epoxidation of Canola Oil by Non-aqueous Reversed Phase Liquid Chromatography/Mass Spectrometry for Process Optimization and Control. **Journal of the American Oil Chemists Society**, v. 89, n. 11, p. 1951–1960, 2012.

APPEL, A. M. et al. Frontiers, Opportunities, and Challenges in Biochemical and Chemical Catalysis of CO_2 Fixation. **Chemical Reviews**, v. 113, n. 8, p. 6621–6658, 14 ago. 2013.

BÄHR, M.; MÜLHAUPT, R. Linseed and soybean oil-based polyurethanes prepared via the non-isocyanate route and catalytic carbon dioxide conversion. **Green**

Chemistry, v. 14, n. 2, p. 483, 2012.

BALABIN, R. M.; LOMAKINA, E. I.; SAFIEVA, R. Z. Neural network (ANN) approach to biodiesel analysis: Analysis of biodiesel density, kinematic viscosity, methanol and water contents using near infrared (NIR) spectroscopy. **Fuel**, v. 90, n. 5, p. 2007–2015, 2011.

BARTHUS, R. C.; POPPI, R. J. Multivariate Quality Control Applied To Detect the Soybean Oil Oxidation Using Fourier Transform Infrared Spectroscopy. **Spectroscopy Letters**, v. 35, n. 5, p. 729–739, 2002.

BARTHUS, R.; POPPI, R.; ANDRADE, J. Determination of total unsaturation in vegetable oil by Fourier Transform Raman Spectroscopy and Multivariate calibration. **Vibrational Spectroscopy**, v. 26, p. 99–105, 2001.

BEGAM, B. F.; KUMAR, J. S. Computer Assisted QSAR/QSPR Approaches – A Review. **Indian Journal of Science and Technology**, v. 9, n. 8, p. 1–8, 4 mar. 2016.

BENANIBA, M. T.; BELHANECHE-BENSEMRA, N.; GELBARD, G. Kinetics of tungsten-catalyzed sunflower oil epoxidation studied by ^{1}H NMR. **European Journal of Lipid Science and Technology**, v. 109, n. 12, p. 1186–1193, dez. 2007.

BLAY, V. et al. Biodegradability Prediction of Fragrant Molecules by Molecular Topology. **ACS Sustainable Chemistry & Engineering**, v. 4, n. 8, p. 4224–4231, 6 ago. 2016.

BOBBINK, F. D.; DYSON, P. J. Synthesis of carbonates and related compounds incorporating CO_2 using ionic liquid-type catalysts: State-of-the-art and beyond. **Journal of Catalysis**, v. 343, p. 52–61, 2016.

BORUGADDA, V. B.; GOUD, V. V. Epoxidation of castor oil fatty acid methyl esters (COFAME) as a lubricant base stock using heterogeneous ion-exchange resin (IR-120) as a catalyst. **Energy Procedia**, v. 54, n. 361, p. 75–84, 2014.

BORUGADDA, V. B.; GOUD, V. V. In-Situ Epoxidation of Castor Oil Using Heterogeneous Acidic Ion-Exchange Resin Catalyst (IR-120) for Bio-Lubricant Application. **Tribology Online**, v. 10, n. 5, p. 354–359, 2015.

BOYDE, S. Green Lubricants. Environmental Benefits and Impacts of Lubrication. **Green Chemistry**, v. 4, n. 4, p. 293–307, 2002.

BÜTTNER, H. et al. Bifunctional One-Component Catalysts for the Addition of Carbon Dioxide to Epoxides. **ChemCatChem**, v. 7, n. 3, p. 459–467, fev. 2015.

BÜTTNER, H. et al. Iron-Based Binary Catalytic System for the Valorization of CO_2 into Biobased Cyclic Carbonates. **ACS Sustainable Chemistry & Engineering**, v. 4, n. 9, p. 4805–4814, 6 set. 2016.

BÜTTNER, H. et al. Organocatalyzed Synthesis of Oleochemical Carbonates from CO_2 and Renewables. **ChemSusChem**, v. 10, n. 6, p. 1076–1079, 22 mar. 2017a.

BÜTTNER, H. et al. Recent Developments in the Synthesis of Cyclic Carbonates from Epoxides and CO_2. **Topics in Current Chemistry**, v. 375, n. 3, p. 50, 24 jun. 2017b.

BÜTTNER, H.; STEINBAUER, J.; WERNER, T. Synthesis of Cyclic Carbonates from Epoxides and Carbon Dioxide by Using Bifunctional One-Component Phosphorus-Based Organocatalysts. **ChemSusChem**, v. 8, n. 16, p. 2655–2669, 24 ago. 2015.

CAI, C. et al. Studies on the kinetics of in situ epoxidation of vegetable oils. **European Journal of Lipid Science and Technology**, v. 110, n. 4, p. 341–346, 2008.

CAI, X. et al. Influence of gas-liquid mass transfer on kinetic modeling: Carbonation of epoxidized vegetable oils. **Chemical Engineering Journal**, v. 313, p. 1168–1183, abr. 2017.

CALÓ, V. et al. Cyclic Carbonate Formation from Carbon Dioxide and Oxiranes in Tetrabutylammonium Halides as Solvents and Catalysts. **Organic Letters**, v. 4, n. 15, p. 2561–2563, jul. 2002.

CAMPANELLA, A. et al. Lubricants from chemically modified vegetable oils. **Bioresource Technology**, v. 101, n. 1, p. 245–254, 2010.

CAMPANELLA, A.; BALTANÁS, M. A. Degradation of the oxirane ring of epoxidized vegetable oils in liquid–liquid heterogeneous reaction systems. **Chemical Engineering Journal**, v. 118, n. 3, p. 141–152, maio 2006.

CAMPANELLA, A.; FONTANINI, C.; BALTANÁS, M. A. High yield epoxidation of fatty acid methyl esters with performic acid generated in situ. **Chemical Engineering Journal**, v. 144, n. 3, p. 466–475, 2008.

CHUA, S.-C. C.; XU, X.; GUO, Z. Emerging sustainable technology for epoxidation directed toward plant oil-based plasticizers. **Process Biochemistry**, v. 47, n. 10, p. 1439–1451, out. 2012.

COMERFORD, J. W. et al. Sustainable metal-based catalysts for the synthesis of cyclic carbonates containing five-membered rings. **Green Chem.**, v. 17, p. 1966–1987, 2015.

CRUZ, V. L. et al. 3D-QSAR study of ansa-metallocene catalytic behavior in ethylene polymerization. **Polymer**, v. 48, n. 16, p. 4663–4674, 2007.

DE LIRA, L. F. B. et al. Infrared spectroscopy and multivariate calibration to monitor stability quality parameters of biodiesel. **Microchemical Journal**, v. 96, n. 1, p. 126–131, 2010.

DE QUADROS, J. V.; GIUDICI, R. Epoxidation of soybean oil at maximum heat removal and single addition of all reactants. **Chemical Engineering and Processing: Process Intensification**, v. 100, p. 87–93, 2016.

DEVIERNO KREUDER, A. et al. A Method for Assessing Greener Alternatives between Chemical Products Following the 12 Principles of Green Chemistry. **ACS Sustainable Chemistry & Engineering**, v. 5, n. 4, p. 2927–2935, 3 abr. 2017.

DINDA, S. et al. Epoxidation of cottonseed oil by aqueous hydrogen peroxide catalysed by liquid inorganic acids. **Bioresource Technology**, v. 99, n. 9, p. 3737–3744, jun. 2008.

DOLEY, S.; DOLUI, S. K. Solvent and catalyst-free synthesis of sunflower oil based polyurethane through non-isocyanate route and its coatings properties. **European Polymer Journal**, v. 102, p. 161–168, maio 2018.

DOLL, K. M. et al. Synthesis of carbonated fatty methyl esters using supercritical carbon dioxide. **J Agric Food Chem**, v. 53, n. 24, p. 9608–9614, 2005.

DOLL, K. M. CHAPTER 2. Chemical Synthesis of Carbonates, Esters, and Acetals from Soybean Oil. In: **Rsc Green Chemistry**. [s.l: s.n.]. v. 2015p. 28–40.

DOLL, K. M. et al. Synthesis and Characterization of Estolide Esters Containing Epoxy and Cyclic Carbonate Groups. **JAOCS, Journal of the American Oil Chemists' Society**, v. 93, n. 8, p. 1149–1155, 2016.

DOLL, K. M. et al. Derivatization of castor oil based estolide esters: Preparation of epoxides and cyclic carbonates. **Industrial Crops and Products**, v. 104, n. January, p. 269–277, out. 2017.

DOLL, K. M.; ERHAN, S. Z. The improved synthesis of carbonated soybean oil using supercritical carbon dioxide at a reduced reaction time. **Green Chemistry**, v. 7, n. 12, p. 849, 2005.

DUAN, M. et al. Rapid determination of flash point and cold filter plugging point for biodiesel blending with diesel by use of FTNIR. **ICMREE2011 - Proceedings 2011 International Conference on Materials for Renewable Energy and Environment**, v. 1, p. 298–302, 2011.

DUBOIS, V. et al. Fatty acid profiles of 80 vegetable oils with regard to their nutritional potential. **European Journal of Lipid Science and Technology**, v. 109, n. 7, p. 710–732, 17 jul. 2007.

DUDEK, A. Z.; ARODZ, T.; GÁLVEZ, J. Computational methods in developing quantitative structure-activity relationships (QSAR): A review. **Combinatorial chemistry & high throughput screening**, v. 9, n. 3, p. 213-228, 2006.

ERHAN, S. Z. et al. Lubricant Base Stock Potential of Chemically Modified Vegetable Oils. p. 8919–8925, 2008.

FARHADIAN, A. et al. A Facile and Green Route for Conversion of Bifunctional Epoxide and Vegetable Oils to Cyclic Carbonate: A Green Route to CO_2 Fixation. **ChemistrySelect**, v. 2, n. 4, p. 1431–1435, 1 fev. 2017.

FAYET, G. et al. Iron bis(arylimino)pyridine precursors activated to catalyze ethylene oligomerization as studied by DFT and QSAR approaches. **Journal of Molecular Structure: THEOCHEM**, v. 903, n. 1–3, p. 100–107, jun. 2009.

FERRÃO, M. F. et al. Simultaneous determination of quality parameters of biodiesel/diesel blends using HATR-FTIR spectra and PLS, iPLS or siPLS regressions. **Fuel**, v. 90, n. 2, p. 701–706, 2011.

FIGOVSKY, O. et al. Modification of epoxy adhesives by hydroxyurethane components on the basis of renewable raw materials. **Polymer Science Series D**, v. 6, n. 4, p. 271–274, 2013.

GAŁUSZKA, A.; MIGASZEWSKI, Z.; NAMIEŚNIK, J. The 12 principles of green

analytical chemistry and the SIGNIFICANCE mnemonic of green analytical practices. **TrAC Trends in Analytical Chemistry**, v. 50, p. 78–84, out. 2013.

GAMAGE, P. K.; O'BRIEN, M.; KARUNANAYAKE, L. Epoxidation of some vegetable oils and their hydrolysed products with peroxyformic acid - optimised to industrial scale. **Journal of the National Science Foundation of Sri Lanka**, v. 37, n. 4, p. 229–240, 31 dez. 2009.

GERBASE, A. E. et al. Epoxidation of soybean oil by the methyltrioxorhenium-CH_2Cl_2/H_2O_2 catalytic biphasic system. **Journal of the American Oil Chemists' Society**, v. 79, n. 2, p. 179–181, fev. 2002.

GOLBRAIKH, A.; TROPSHA, A. Beware of Q^2! **Journal of Molecular Graphics and Modelling**, v. 20, n. 4, p. 269–276, jan. 2002.

GOUD, V. V. et al. Epoxidation of karanja (Pongamia glabra) oil catalysed by acidic ion exchange resin. **European Journal of Lipid Science and Technology**, v. 109, n. 6, p. 575–584, jun. 2007.

GOUD, V. V. et al. Epoxidation of Jatropha (Jatropha curcas) oil by peroxyacids. **Asia-Pacific Journal of Chemical Engineering**, v. 5, n. 2, p. 346–354, mar. 2010.

GOUD, V. V.; PATWARDHAN, A. V.; PRADHAN, N. C. Studies on the epoxidation of mahua oil (Madhumica indica) by hydrogen peroxide. **Bioresource Technology**, v. 97, n. 12, p. 1365–1371, 2006.

GOUD, V. V.; PRADHAN, N. C.; PATWARDHAN, A. V. Epoxidation of karanja (Pongamia glabra) oil by H_2O_2. **Journal of the American Oil Chemists' Society**, v. 83, n. 7, p. 635–640, jul. 2006.

GRIGNARD, B. et al. CO_2-blown microcellular non-isocyanate polyurethane (NIPU) foams: from bio- and CO_2-sourced monomers to potentially thermal insulating materials. **Green Chem.**, v. 18, n. 7, p. 2206–2215, 2016.

GUZMÁN, A. F.; ECHEVERRI, D. A.; RIOS, L. A. Carbonation of epoxidized castor oil: a new bio-based building block for the chemical industry. **Journal of Chemical Technology & Biotechnology**, v. 92, n. 5, p. 1104–1110, maio 2017.

HAMBALI, R. A. et al. Synthesis and Characterization of Non-Isocyanate Polyurethane from Epoxidized Linoleic Acid – A Preliminary Study. **Advanced Materials Research**, v. 812, n. March, p. 73–79, 2013.

HANIFFA, M. A. C. M. et al. Synthesis, characterization and the solvent effects on interfacial phenomena of jatropha curcas oil based non-isocyanate polyurethane. **Polymers**, v. 9, n. 5, p. 162, 1 maio 2017.

HARO, J. C. DE et al. Modelling the epoxidation reaction of grape seed oil by peracetic acid. **Journal of Cleaner Production**, v. 138, p. 70–76, dez. 2016.

HECHINGER, M.; LEONHARD, K.; MARQUARDT, W. What is Wrong with Quantitative Structure–Property Relations Models Based on Three-Dimensional Descriptors? **Journal of Chemical Information and Modeling**, v. 52, n. 8, p. 1984–1993, 27 ago. 2012.

HOLSER, R. A. Carbonation of epoxy methyl soyate at atmospheric pressure. **Journal of Oleo Science**, v. 56, n. 12, p. 629–632, 2007.

HUANG, Y. B. et al. Influence of alkenyl structures on the epoxidation of unsaturated fatty acid methyl esters and vegetable oils. **RSC Adv.**, v. 5, n. 91, p. 74783–74789, 2015.

HWANG, H. S.; ERHAN, S. Z. Modification of epoxidized soybean oil for lubricant formulations with improved oxidative stability and low pour point. **Journal of the American Oil Chemists' Society**, v. 78, n. 12, p. 1179–1184, 2001.

ISSARIYAKUL, T.; DALAI, A. K. Biodiesel from vegetable oils. **Renewable and Sustainable Energy Reviews**, v. 31, p. 446–471, mar. 2014.

JALILIAN, M.; YEGANEH, H.; HAGHIGHI, M. N. Synthesis and properties of polyurethane networks derived from new soybean oil-based polyol and a bulky blocked polyisocyanate. **Polymer International**, v. 57, n. 12, p. 1385–1394, dez. 2008.

JALILIAN, M.; YEGANEH, H.; HAGHIGHI, M. N. Preparation and characterization of polyurethane electrical insulating coatings derived from novel soybean oil-based polyol. **Polymers for Advanced Technologies**, v. 21, n. 2, p. 118–127, 2010.

JALILIAN, S.; YEGANEH, H. Preparation and properties of biodegradable polyurethane networks from carbonated soybean oil. **Polymer Bulletin**, v. 72, n. 6, p. 1379–1392, 2015.

JAVIDNIA, K. et al. Discrimination of edible oils and fats by combination of multivariate pattern recognition and FT-IR spectroscopy: A comparative study between

different modeling methods. **Spectrochimica Acta - Part A: Molecular and Biomolecular Spectroscopy**, v. 104, p. 175–181, mar. 2013.

JAVNI, I.; HONG, D. P.; PETROVIĆ, Z. S. Soy-based polyurethanes by nonisocyanate route. **Journal of Applied Polymer Science**, v. 108, n. 6, p. 3867–3875, 15 jun. 2008.

JAVNI, I.; HONG, D. P.; PETROVIC̈, Z. S. Polyurethanes from soybean oil, aromatic, and cycloaliphatic diamines by nonisocyanate route. **Journal of Applied Polymer Science**, v. 128, n. 1, p. 566–571, 2013.

KARELSON, M.; LOBANOV, V. S.; KATRITZKY, A. R. Quantum-Chemical Descriptors in QSAR/QSPR Studies. **Chemical Reviews**, v. 96, n. 3, p. 1027–1044, jan. 1996.

KATHALEWAR, M. S. et al. Non-isocyanate polyurethanes: from chemistry to applications. **RSC Advances**, v. 3, n. 13, p. 4110, 2013.

KATRITZKY, A. R.; KARELSON, M.; LOBANOV, V. S. QSPR as a means of predicting and understanding chemical and physical properties in terms of structure. **Pure and Applied Chemistry**, v. 69, n. 2, p. 245–248, 28 fev. 1997.

KATRITZKY, A. R.; LOBANOV, V. S. QSPR: The Correlation and Quantitative Prediction of Chemical and Physical Properties from Structure. **Chemical Society Reviews**, v. 24, p. 279–287, 1995.

KENAR, J. A.; TEVIS, I. D. Convenient preparation of fatty ester cyclic carbonates. **European Journal of Lipid Science and Technology**, v. 107, n. 2, p. 135–137, 2005.

KHOT, S. N. et al. Development and application of triglyceride-based polymers and composites. **Journal of Applied Polymer Science**, v. 82, n. 3, p. 703–723, 17 out. 2001.

KÖCKRITZ, A.; MARTIN, A. Oxidation of unsaturated fatty acid derivatives and vegetable oils. **European Journal of Lipid Science and Technology**, v. 110, n. 9, p. 812–824, 2008.

KRALISCH, D. et al. Transfer of the epoxidation of soybean oil from batch to flow chemistry guided by cost and environmental issues. **ChemSusChem**, v. 5, n. 2, p. 300–311, 2012.

KUMAR, R. et al. 1 H Nuclear Magnetic Resonance (NMR) Determination of the Iodine Value in Biodiesel Produced from Algal and Vegetable Oils. Energy & Fuels, v. 26, n. 11, p. 7005–7008, 15 nov. 2012.

LANGANKE, J.; GREINER, L.; LEITNER, W. Substrate dependent synergetic and antagonistic interaction of ammonium halide and polyoxometalate catalysts in the synthesis of cyclic carbonates from oleochemical epoxides and CO_2. **Green Chemistry**, v. 15, n. 5, p. 1173, 2013.

LATHI, P. S.; MATTIASSON, B. Green approach for the preparation of biodegradable lubricant base stock from epoxidized vegetable oil. **Applied Catalysis B: Environmental**, v. 69, n. 3–4, p. 207–212, 2007.

LEE, A.; DENG, Y. Green polyurethane from lignin and soybean oil through non-isocyanate reactions. **European Polymer Journal**, v. 63, p. 67–73, 2015.

LEVINA, M. A. et al. Green chemistry of polyurethanes: Synthesis, structure, and functionality of triglycerides of soybean oil with epoxy and cyclocarbonate groups—renewable raw materials for new urethanes. **Polymer Science Series B**, v. 57, n. 6, p. 584–592, 2015.

LI, X. et al. A combination of chemometrics methods and GC–MS for the classification of edible vegetable oils. **Chemometrics and Intelligent Laboratory Systems**, v. 155, p. 145–150, jul. 2016.

LI, Z. et al. Catalytic synthesis of carbonated soybean oil. **Catalysis Letters**, v. 123, n. 3–4, p. 246–251, 2008.

LIU, S.; WANG, X. Polymers from carbon dioxide: Polycarbonates, polyurethanes. **Current Opinion in Green and Sustainable Chemistry**, v. 3, p. 61–66, fev. 2017.

LONGWITZ, L. et al. Calcium-Based Catalytic System for the Synthesis of Bio-Derived Cyclic Carbonates under Mild Conditions. **ACS Catalysis**, v. 8, n. 1, p. 665–672, 5 jan. 2018.

LOULERGUE, P. et al. Polyurethanes prepared from cyclocarbonated broccoli seed oil (PUcc): New biobased organic matrices for incorporation of phosphorescent metal nanocluster. **Journal of Applied Polymer Science**, v. 134, n. 45, p. 45339, 5 dez. 2017.

MAHENDRAN, A. R. et al. Bio-Based Non-Isocyanate Urethane Derived from Plant Oil. **Journal of Polymers and the Environment**, v. 20, n. 4, p. 926–931, 2012.

MAHENDRAN, A. R. et al. Synthesis, characterization, and properties of isocyanate-free urethane coatings from renewable resources. **Journal of Coatings Technology Research**, v. 11, n. 3, p. 329–339, 2014.

MALDONADO, A. G.; ROTHENBERG, G. Predictive modeling in homogeneous catalysis: a tutorial. **Chemical Society Reviews**, v. 39, n. 6, p. 1891, 2010.

MALIK, M.; KAUR, R. Synthesis of NIPU by the carbonation of canola oil using highly efficient 5,10,15-tris(pentafluorophenyl)corrolato-manganese(III) complex as novel catalyst. **Polymers for Advanced Technologies**, n. May, p. 1–8, 2017.

MANN, N. et al. Synthesis of carbonated vernonia oil. **JAOCS, Journal of the American Oil Chemists' Society**, v. 85, n. 8, p. 791–796, 2008.

MARTÍNEZ, S. et al. Polymerization Activity Prediction of Zirconocene Single-Site Catalysts Using 3D Quantitative Structure–Activity Relationship Modeling. **Organometallics**, v. 31, n. 5, p. 1673–1679, 12 mar. 2012.

MAZO, P. C.; RIOS, L. A. Improved synthesis of carbonated vegetable oils using microwaves. **Chemical Engineering Journal**, v. 210, p. 333–338, nov. 2012.

MAZO, P.; RIOS, L. Carbonation of epoxidized soybean oil improved by the addition of water. **JAOCS, Journal of the American Oil Chemists' Society**, v. 90, n. 5, p. 725–730, 2013.

MCNUTT, J.; HE, Q. (SOPHIA). Development of biolubricants from vegetable oils via chemical modification. **Journal of Industrial and Engineering Chemistry**, v. 36, p. 1–12, abr. 2016.

MEIER, M. A R.; METZGER, J. O.; SCHUBERT, U. S. Plant oil renewable resources as green alternatives in polymer science. **Chemical Society Reviews**, v. 36, n. 11, p. 1788, 2007.

MEYER, P. P. et al. Epoxidation of soybean oil and Jatropha oil. **Thammasat Int J Sci Technol**, v. 13, p. 1–5, 2008.

MIAO, S. et al. Vegetable-oil-based polymers as future polymeric biomaterials. **Acta Biomaterialia**, v. 10, n. 4, p. 1692–1704, abr. 2014.

MILOSLAVSKIY, D. et al. Cyclic carbonates based on vegetable oils. **International Letters of Chemistry, Physics and Astronomy**, v. 8, n. 27, p. 20–29, 2014.

MIRGHANI, M. E. S. et al. Rapid Method for the Determination of Moisture Content in Biodiesel Using FTIR Spectroscopy. **Journal of the American Oil Chemists' Society**, v. 88, n. 12, p. 1897–1904, 2011.

MONONO, E. M.; HAAGENSON, D. M.; WIESENBORN, D. P. Characterizing the epoxidation process conditions of canola oil for reactor scale-up. **Industrial Crops and Products**, v. 67, p. 364–372, 2015.

MUNGROO, R. et al. Epoxidation of canola oil with hydrogen peroxide catalyzed by acidic ion exchange resin. **JAOCS, Journal of the American Oil Chemists' Society**, v. 85, n. 9, p. 887–896, 2008.

MUTURI, P.; WANG, D.; DIRLIKOV, S. Epoxidized vegetable oils as reactive diluents I. Comparison of vernonia, epoxidized soybean and epoxidized linseed oils. **Progress in Organic Coatings**, v. 25, n. 1, p. 85–94, 1994.

NADUPPARAMBIL, M. S.; STOFFER, J. O. Synthesis of Carbonate Functional Monomer and Polymers from Epoxidized Soybean Oil. **Polymer Preprints**, v. 47, n. 1, p. 329–330, 2006.

NANTASENAMAT, C. et al. A Practical Overview of Quantitative Structure-Activity Relationship. **EXCLI Journal**, v. 8, p. 74–88, 2009.

NARRA, N. et al. Lewis-acid catalyzed synthesis and characterization of novel castor fatty acid-based cyclic carbonates. **RSC Adv.**, v. 6, n. 31, p. 25703–25712, 2016.

NIHUL, P. G.; MHASKE, S. T.; SHERTUKDE, V. V. Epoxidized rice bran oil (ERBO) as a plasticizer for poly(vinyl chloride) (PVC). **Iranian Polymer Journal (English Edition)**, v. 23, n. 8, p. 599–608, 2014.

NORTH, M.; PASQUALE, R.; YOUNG, C. Synthesis of cyclic carbonates from epoxides and CO_2. **Green Chemistry**, v. 12, n. 9, p. 1514, 2010.

OMONOV, T. S.; KHARRAZ, E.; CURTIS, J. M. The epoxidation of canola oil and its derivatives. **RSC Adv.**, v. 6, n. 95, p. 92874–92886, 2016.

PALUVAI, N. R.; MOHANTY, S.; NAYAK, S. K. Synthesis and Characterization of Acrylated Epoxidized Castor Oil Nanocomposites. **International Journal of Polymer Analysis and Characterization**, v. 20, n. 4, p. 298–306, 2015.

PAN, X.; SENGUPTA, P.; WEBSTER, D. C. High biobased content epoxy-anhydride thermosets from epoxidized sucrose esters of fatty acids. **Biomacromolecules**, v. 12, n. 6, p. 2416–2428, 2011.

PANCHAL, T. M. et al. A methodological review on bio-lubricants from vegetable oil based resources. **Renewable and Sustainable Energy Reviews**, v. 70, n. August 2016, p. 65–70, abr. 2017.

PARZUCHOWSKI, P. G. et al. Epoxy resin modified with soybean oil containing cyclic carbonate groups. **Journal of Applied Polymer Science**, v. 102, n. 3, p. 2904–2914, 2006.

PEÑA CARRODEGUAS, L. et al. Fatty acid based biocarbonates: Al-mediated stereoselective preparation of mono-, di- and tricarbonates under mild and solvent-less conditions. **Green Chemistry**, v. 19, n. 15, p. 3535–3541, 2017.

PENG, Y. H.; LIN, H. DI. Preparation of Environment-Friendly Epoxidized Corn Oil as a Plasticizer. **Advanced Materials Research**, v. 852, p. 256–261, jan. 2014.

POLIAKOFF, M.; LEITNER, W.; STRENG, E. S. The Twelve Principles of CO_2 CHEMISTRY. **Faraday discussions**, v. 183, p. 9–17, 2015.

POUSSARD, L. et al. Non-Isocyanate Polyurethanes from Carbonated Soybean Oil Using Monomeric or Oligomeric Diamines to Achieve Thermosets or Thermoplastics. **Macromolecules**, v. 49, n. 6, p. 2162–2171, 22 mar. 2016.

RANGARAJAN, B. et al. Kinetic parameters of a two-phase model for in situ epoxidation of soybean oil. **Journal of the American Oil Chemists' Society**, v. 72, n. 10, p. 1161–1169, out. 1995.

RATANASAK, M. et al. Towards the design of new electron donors for Ziegler–Natta catalyzed propylene polymerization using QSPR modeling. **Polymer**, v. 56, p. 340–345, jan. 2015.

RILEY, S. J.; VERKADE, J. G.; ANGELICI, R. J. Chemical characterization and physical properties of solvents derived from epoxidized methyl soyate. **JAOCS, Journal of the American Oil Chemists' Society**, v. 92, n. 4, p. 589–601, 2015.

RONDA, J. C. et al. Vegetable oils as platform chemicals for polymer synthesis. **European Journal of Lipid Science and Technology**, v. 113, n. 1, p. 46–58, jan. 2011.

ROTHENBERG, G. Data mining in catalysis: Separating knowledge from garbage. **Catalysis Today**, v. 137, p. 2–10, 2008.

ROY, K. et al. Comparative Studies on Some Metrics for External Validation of QSPR Models. **Journal of Chemical Information and Modeling**, v. 52, p. 396–408, 2012.

ROY, K. et al. Is it possible to improve the quality of predictions from an “intelligent” use of multiple QSAR/QSPR/QSTR models? **Journal of Chemometrics**, p. e2992, 30 jan. 2018.

ROY, K.; AMBURE, P.; AHER, R. B. How important is to detect systematic error in predictions and understand statistical applicability domain of QSAR models? **Chemometrics and Intelligent Laboratory Systems**, v. 162, p. 44–54, mar. 2017.

RUIZ, L. et al. Upgrading castor oil: From heptanal to non-isocyanate poly(amide-hydroxyurethane)s. **Polymer (United Kingdom)**, v. 124, p. 226–234, 2017.

RÜSCH GEN. KLAAS, M.; WARWEL, S. Complete and partial epoxidation of plant oils by lipase-catalyzed perhydrolysis. **Industrial Crops and Products**, v. 9, n. 2, p. 125–132, jan. 1999.

SAMANTA, S. et al. Synthesis and Characterization of Polyurethane Networks Derived from Soybean-Oil-Based Cyclic Carbonates and Bioderivable Diamines. **ACS Sustainable Chemistry & Engineering**, v. 4, n. 12, p. 6551–6561, 5 dez. 2016.

SANTACESARIA, E. et al. A biphasic model describing soybean oil epoxidation with H_2O_2 in a fed-batch reactor. **Chemical Engineering Journal**, v. 173, n. 1, p. 198–209, set. 2011.

SAPTAL, V. B.; BHANAGE, B. M. Current Opinion in Green and Sustainable Chemistry Current advances in heterogeneous catalysts for the synthesis of cyclic carbonates from carbon dioxide. **Current Opinion in Green and Sustainable Chemistry**, v. 3, p. 1–10, fev. 2017.

SARPAL, A. S. et al. Direct Method for the Determination of the Iodine Value of

Biodiesel by Quantitative Nuclear Magnetic Resonance (q^{1}H-NMR) Spectroscopy. **Energy & Fuels**, p. acs.energyfuels.5b01462, 2015.

SCALA, J.; WOOL, R. P. Effect of FA composition on epoxidation kinetics of TAG. **Journal of the American Oil Chemists' Society**, v. 79, n. 4, p. 373–378, 2002.

SCHÄFFNER, B. et al. Synthesis and Application of Carbonated Fatty Acid Esters from Carbon Dioxide Including a Life Cycle Analysis. **ChemSusChem**, v. 7, n. 4, p. 1133–1139, abr. 2014.

SENIHA GÜNER, F.; YAĞCI, Y.; TUNCER ERCIYES, A. Polymers from triglyceride oils. **Progress in Polymer Science**, v. 31, n. 7, p. 633–670, jul. 2006.

SHARMA, R. V.; DALAI, A. K. Synthesis of bio-lubricant from epoxy canola oil using sulfated Ti-SBA-15 catalyst. **Applied Catalysis B: Environmental**, v. 142–143, p. 604–614, 2013.

STEC, M. et al. Predicting normal densities of amines using quantitative structure-property relationship (QSPR). **SAR and QSAR in Environmental Research**, v. 26, n. 11, p. 893–904, 2 nov. 2015.

STEINBAUER, J. et al. Immobilized bifunctional phosphonium salts as recyclable organocatalysts in the cycloaddition of CO_2 and epoxides. **Green Chemistry**, v. 19, n. 18, p. 4435–4445, 2017.

STERNBERG, A.; JENS, C. M.; BARDOW, A. Life cycle assessment of CO_2 -based C1-chemicals. **Green Chemistry**, v. 19, n. 9, p. 2244–2259, 2017.

SUN, J. et al. Water as an efficient medium for the synthesis of cyclic carbonate. **Tetrahedron Letters**, v. 50, n. 4, p. 423–426, 2009.

SWERN, D. Reactions of the oxirane group. **Journal of the American Oil Chemists Society**, v. 47, n. 11, p. 424–429, nov. 1970.

TAMAMI, B.; SOHN, S.; WILKES, G. L. Incorporation of carbon dioxide into soybean oil and subsequent preparation and studies of nonisocyanate polyurethane networks. **Journal of Applied Polymer Science**, v. 92, n. 2, p. 883–891, 15 abr. 2004.

TAN, S. G.; CHOW, W. S. Biobased Epoxidized Vegetable Oils and Its Greener Epoxy Blends: A Review. **Polymer-Plastics Technology and Engineering**, v. 49, n. 15, p. 1581–1590, 22 nov. 2010.

TENHUMBERG, N. et al. Cooperative catalyst system for the synthesis of oleochemical cyclic carbonates from CO_2 and renewables. **Green Chemistry**, v. 18, n. 13, p. 3775–3788, 2016.

TERFLOTH, L. Calculation of Structure Descriptors. In: **Chemoinformatics**. Weinheim, FRG: Wiley-VCH Verlag GmbH & Co. KGaA, 2003. p. 401–437.

TÜRÜNÇ, O. et al. Nonisocyanate based polyurethane/silica nanocomposites and their coating performance. **Journal of Sol-Gel Science and Technology**, v. 47, n. 3, p. 290–299, 2008.

VLČEK, T.; PETROVIĆ, Z. S. Optimization of the chemoenzymatic epoxidation of soybean oil. **Journal of the American Oil Chemists' Society**, v. 83, n. 3, p. 247–252, mar. 2006.

WANG, J. et al. Pt doped $H_3PW_{12}O_{40}/ZrO_2$ as a heterogeneous and recyclable catalyst for the synthesis of carbonated soybean oil. **Journal of Applied Polymer Science**, v. 124, n. 5, p. 4298–4306, 5 jun. 2012.

WERNER, T.; TENHUMBERG, N.; BÜTTNER, H. Hydroxyl-Functionalized Imidazoles : Highly Active Additives for the Potassium Iodide-Catalyzed Synthesis of 1,3-Dioxolan-2-one Derivatives from Epoxides and Carbon Dioxide. **ChemCatChem**, v. 6, p. 3493–3500, 2014.

WU, X. et al. The study of epoxidized rapeseed oil used as a potential biodegradable lubricant. **Journal of the American Oil Chemists Society**, v. 77, n. 5, p. 561–563, 2000.

XIA, W.; BUDGE, S. M.; LUMSDEN, M. D. ^{1}H-NMR Characterization of Epoxides Derived from Polyunsaturated Fatty Acids. **Journal of the American Oil Chemists' Society**, v. 93, n. 4, p. 467–478, 12 abr. 2016.

XU, WEN-JIE et al. Microalgae oil-based polyurethane prepared from microalgae oil and CO_2 via the non-isocyanate route. **Xiandai Huagong/Modern Chemical Industry**, v. 33, n. 9, p. 61–65, 2013.

XU, W. et al. Optimization of Epoxidized Methyl Acetoricinoleate Synthesis by Response Surface Methodology. **Chemical Engineering & Technology**, v. 40, n. 3, p. 571–580, 2017.

YANG, Z.; GAO, X.; LIU, Z. Synthesis of chemicals using CO_2 as a building

block under mild conditions. **Current Opinion in Green and Sustainable Chemistry**, v. 1, p. 13–17, ago. 2016.

YAO, S. et al. Consideration of an activity of the metallocene catalyst by using molecular mechanics, molecular dynamics and QSAR. **Computational and Theoretical Polymer Science**, v. 9, n. 1, p. 41–46, mar. 1999.

YAP, C. W. PaDEL-descriptor: An open source software to calculate molecular descriptors and fingerprints. **Journal of Computational Chemistry**, v. 32, n. 7, p. 1466–1474, maio 2011.

ZEINI JAHROMI, E.; GAILER, J. Probing bioinorganic chemistry processes in the bloodstream to gain new insights into the origin of human diseases. **Dalton Trans.**, v. 39, n. 2, p. 329–336, 2010.

ZHANG, L. et al. Synthesis of carbonated cotton seed oil and its application as lubricating base oil. **JAOCS, Journal of the American Oil Chemists' Society**, v. 91, n. 1, p. 143–150, 8 jan. 2014a.

ZHANG, L. et al. Classification and Adulteration Detection of Vegetable Oils Based on Fatty Acid Profiles. **Journal of Agricultural and Food Chemistry**, v. 62, n. 34, p. 8745–8751, 27 ago. 2014b.

ZHENG, J. L. et al. Carbonation of Vegetable Oils: Influence of Mass Transfer on Reaction Kinetics. **Industrial & Engineering Chemistry Research**, v. 54, n. 43, p. 10935–10944, 4 nov. 2015.

ZHENG, J. L. et al. Synthesis of carbonated vegetable oils: Investigation of microwave effect in a pressurized continuous-flow recycle batch reactor. **Chemical Engineering Research and Design**, v. 132, n. April, p. 9–18, abr. 2018.

ANEXO A

Elsevier Editorial System(tm) for Journal of Catalysis

Manuscript Draft

Manuscript Number:

Title: A Perspective of QSPR Modeling to Screen/Design Organocatalysts for Oleochemical Carbonates Synthesis

Article Type: Research paper

Keywords: Vegetable oil; Oleochemical carbonate; QSPR; Quantitative Structure-Property Relationship; Cyclic carbonate; Carbon dioxide; Multivariate Analysis; Organocatalyst; Metal-free catalys; , Green chemistry.

Corresponding Author: Dr. Marcus seferin, Ph.D.

Corresponding Author's Institution: Pontificial Catholyc University of Rio Grande do Sul

First Author: Victor Hugo J Mendes dos Santos

Order of Authors: Victor Hugo J Mendes dos Santos; Darlan Pontin; Raoni S Rambo ; Marcus seferin, Ph.D.

ANEXO B

Tabela B1. Catalisadores aplicados para produção de óleos carbonatados.

Catalisador	Conversão (%)	Referência
[a]LiBr	100,0%	(NADUPPARAMBIL; STOFFER, 2006)
Brometo de tetrabutilamônio (TBAB)	100,0%	(BÄHR; MÜLHAUPT, 2012; DOLL; ERHAN, 2005; ZHANG et al., 2014a)
Complexo de 5,10,15-tris(pentafluorofenil)corrolato-manganês(III)	95,0%	(MALIK; KAUR, 2017)
$H_3PW_{12}O_{40}$	94,5%	(WANG et al., 2012)
$H_3PMo_{12}O_{40}$	91,6%	(WANG et al., 2012)
$H_4SiW_{12}O_{40}$	90,3%	(WANG et al., 2012)
Brometo de difenil-propil-2-hidroxifenil-fosfônio	88,0%	(BÜTTNER et al., 2017a)
$SnCl_4.5H_2O$	64,4%	(LI et al., 2008)
Brometo de 1-Butil-3,4,6,7,8,9-hexahidro-2H-pirimido [1,2-a]pirimidin-1-o	36,0%	(ALVES et al., 2015)
Brometo de 1-metil-3-octilimidazólio	30,0%	(ALVES et al., 2015)
Brometo de 1-Butil-2,3,4,5,7,8,9,10-octahidropirido[1,2-a][1,3]diazepin-1-o	28,0%	(ALVES et al., 2015)
Brometo de tetrabutilfosfônio	28,0%	(ALVES et al., 2015)
Iodeto de tetrabutilamônio (TBAI)	26,0%	(ALVES et al., 2015)
Iodeto de 1-metil-3-octilimidazólio	25,0%	(ALVES et al., 2015)
Iodeto de tetrabutilfosfônio	21,0%	(ALVES et al., 2015)
Cloreto de 1-metil-3-octilimidazólio	20,0%	(ALVES et al., 2015)
Iodeto de 1-butil-1-metilpirrolidino	19,0%	(ALVES et al., 2015)
Cloreto de tetrabutilfosfônio	19,0%	(ALVES et al., 2015)
Cloreto de tetrabutilamônio (TBACl)	17,0%	(ALVES et al., 2015)
Iodeto de 1-butilpiridínio	12,0%	(ALVES et al., 2015)
KBr	6,0%	(DOLL; ERHAN, 2005)
Amberlite IR 400(Cl)	0,0%	(TAMAMI; SOHN; WILKES, 2004)
Brometo de trimetil-benzil-amônio	0,0%	(TAMAMI; SOHN; WILKES, 2004)
LiBr	0,0%	(DOLL; ERHAN, 2005; TAMAMI; SOHN; WILKES, 2004)
Sem Catalisador	0,0%	(DOLL; ERHAN, 2005)
NaI	0,0%	(TAMAMI; SOHN; WILKES, 2004)
Hidróxido de tetrabutilamônio (TBAOH)	0,0%	(DOLL; ERHAN, 2005)
Iodeto de trietilsulfônio	0,0%	(ALVES et al., 2015)

[a] Solvente N-metil pirrolidona

ANEXO C

Tabela C1. Co-catalisadores aplicados para produção de óleos carbonatados.

Catalisador	Co-Cat	Conversão	Referência
$[Oct_4P]Br$	$FeCl_3$	100,0%	(BÜTTNER et al., 2016)
CaI_2	Diciclohexano-18-crown-6 / Ph_3P	100,0%	(LONGWITZ et al., 2018)
SiO_2 (sílica)	Iodeto de 4-pirrolidina piridina	100,0%	(BÄHR; MÜLHAUPT, 2012)
TBAB	$CaCl_2$	100,0%	(JALILIAN; YEGANEH, 2015)
TBAB	MoO_3	100,0%	(TENHUMBERG et al., 2016)
TBAB	$SnCl_4.5H_2O$	98,6%	(LI et al., 2008)
KI	18-crown-6	98,3%	(PARZUCHOWSKI et al., 2006)
TBAB	perfluoro-terc-butanol	98,0%	(ALVES et al., 2015)
TBAB	H_2O	95,0%	(MAZO; RIOS, 2013)
$H_3PW_{12}O_{40}$	ZrO_2	94,3%	(WANG et al., 2012)
$H_3PW_{12}O_{40}$	ZrO_2.Pt (dopado)	93,0%	(WANG et al., 2012)
$H_3PW_{12}O_{40}$	ZrO_2	86,1%	(WANG et al., 2012)
$H_3PW_{12}O_{40}$	SiO_2	81,3%	(WANG et al., 2012)
$H_3PW_{12}O_{40}$	V_2O_5	64,3%	(WANG et al., 2012)
TBAB	Catecol	63,0%	(ALVES et al., 2015)
TBAB	4- trifluorometilfenol	58,0%	(ALVES et al., 2015)
TBAB	1,1,1,3,3,3-Hexafluoro-2-metil-2-propanol	58,0%	(ALVES et al., 2015)
TBAB	2,2'-(1,3-Fenileno)bis(1,1,1,3,3,3-hexafluoro-2-propanol)	58,0%	(ALVES et al., 2015)
TBAB	4-terc-butilcatecol	57,0%	(ALVES et al., 2015)
TBAB	Pirogalol	56,0%	(ALVES et al., 2015)
TBAB	3-Metoxicatecol	55,0%	(ALVES et al., 2015)
TBAB	2-(p-toluil)hexafluoroisopropanol	55,0%	(ALVES et al., 2015)
TBAB	4- nitrofenol	47,0%	(ALVES et al., 2015)
$H_3PW_{12}O_{40}$	Al_2O_3	45,3%	(WANG et al., 2012)
TBAB	Pentafluorofenol	45,0%	(ALVES et al., 2015)
TBAB	3-Trifluorometil-4-nitrofenol	42,0%	(ALVES et al., 2015)
TBAB	1,1,1-Trifluoro-2-metil-2-propanol	42,0%	(ALVES et al., 2015)
$H_3PW_{12}O_{40}$	Nb_2O_5	41,6%	(WANG et al., 2012)
TBAB	THA-Cr-Si-POM	41,0%	(LANGANKE; GREINER; LEITNER, 2013)
TBAB	3,4,5-Trifluorofenol	41,0%	(ALVES et al., 2015)
$H_3PW_{12}O_{40}$	MgO	40,7%	(WANG et al., 2012)
TBAB	2,3,5,6-Tetrafluoro-4-(trifluorometil)fenol	38,0%	(ALVES et al., 2015)
TBAB	fenol	32,0%	(ALVES et al., 2015)
TBAB	4-metoxifenol	31,0%	(ALVES et al., 2015)
$H_3PW_{12}O_{40}$	In_2O_3	26,7%	(WANG et al., 2012)

ANEXO D

Tabela D1. Catalisadores aplicados para produção de ésteres monoalquílicos carbonatados

Catalisador	Conversão	Seletividade	Referência
Brometo de difenil-propil-2-hidroxifenil-fosfônio	100,0%	99,0%	(BÜTTNER et al., 2017a)
Iodeto de difenil-propil-2-hidroxifenil-fosfônio	100,0%	76,0%	(BÜTTNER et al., 2017a)
Complexo de Al(III) aminotrifenolato (R= Cl ; Ligante−Tetrahidrofurano)	100,0%	99,0%	(PEÑA CARRODEGUAS et al., 2017)
Cloreto de bis(trifenilfosfina)imínio	100,0%	95,0%	(PEÑA CARRODEGUAS et al., 2017)
TBAB	100,0%	100,0%	(PEÑA CARRODEGUAS et al., 2017)
Brometo de tetraheptilamônio	99,0%	100,0%	(LANGANKE; GREINER; LEITNER, 2013)
Brometo de difenil-propil-(2-hidroxi-3-metilfenil)-fosfônio	99,0%	53,0%	(BÜTTNER et al., 2017a)
Brometo de tetradecil(tri-n-hexil)fosfônio	97,0%	97,0%	(LANGANKE; GREINER; LEITNER, 2013)
Brometo de 1-metil-3-tetradecilimidazólio	97,0%	96,0%	(SCHÄFFNER et al., 2014)
Brometo de difenil-octadecil-2-hidroxietil-fosfônio	96,0%	91,0%	(BÜTTNER et al., 2017a)
THA-Cr-Si-POM	95,0%	98,0%	(LANGANKE; GREINER; LEITNER, 2013)
Iodeto de difenil-metil-2-hidroxietil-fosfônio	92,0%	66,0%	(BÜTTNER et al., 2017a)
TBACl	80,0%	100,0%	(LANGANKE; GREINER; LEITNER, 2013)
TBAI	80,0%	92,0%	(LANGANKE; GREINER; LEITNER, 2013)
$((C_7H_{13})_4N)_5$-[α-$SiW_{11}O_{39}Fe$].$(C_7H_8)_2$	73,0%	97,0%	(SCHÄFFNER et al., 2014)
$((C_4H_9)_4N)_6$-[α-$SiW_{11}O_{39}Co$].$(C_7H_8)_1$	69,0%	100,0%	(SCHÄFFNER et al., 2014)
Iodeto 1-Butil-4-Metilpiridinio	65,0%	100,0%	(BÜTTNER et al., 2017a)
Brometo de tributil-2-hidroxietil-fosfônio	65,0%	-	(BÜTTNER et al., 2017a)
Fluoreto de tetrabutilamônio (TBAF)	62,0%	0,0%	(LANGANKE; GREINER; LEITNER, 2013)
$[Bu_4P]Br$	51,0%	100,0%	(BÜTTNER et al., 2016)
Brometo de 1-Butil-3-metilimidazólio	50,0%	100,0%	(SCHÄFFNER et al., 2014)
$[Bu_4P]Cl$	39,0%	99,0%	(TENHUMBERG et al., 2016)
$((C_4H_9)_4N)_6$-[α-$SiW_{11}O_{39}Ni$].$(C_7H_8)_2$	38,0%	100,0%	(SCHÄFFNER et al., 2014)
Iodeto de difenil-metil-3-hidroxifenil-fosfônio	37,0%	74,0%	(BÜTTNER et al., 2017a)

Tabela D1. (Continuação)

$[Bu_4P]I$	35,0%	72,0%	(TENHUMBERG et al., 2016) (BÜTTNER et al., 2017a)
$((C_4H_9)_4N)_6$-[α-$SiW_{11}O_{39}Cu$]	33,0%	100,0%	(SCHÄFFNER et al., 2014)
$((C_4H_9)_4N)_6$-[α-$SiW_{11}O_{39}Mn$]	33,0%	100,0%	(SCHÄFFNER et al., 2014)
$((C_7H_{13})_4N)_5$-[α-$SiW_{11}O_{39}Cr$].$(C_7H_8)_2$	30,0%	95,0%	(SCHÄFFNER et al., 2014)
Cloreto de 1-Butil-3-metilimidazólio	26,0%	100,0%	(SCHÄFFNER et al., 2014)
Cloreto de difenil-propil-2-hidroxifenil-fosfônio	26,0%	97,0%	(BÜTTNER et al., 2017a)
Iodeto de tributil-2-hidroxietil-fosfônio	24,0%	98,0%	(BÜTTNER et al., 2017a)
Iodeto de difenil-metil-2-metoxifenil-fosfônio	22,0%	97,0%	(BÜTTNER et al., 2017a)
Brometo de tributil-2-hidroxietil-fosfônio	22,0%	97,0%	(BÜTTNER et al., 2017a)
Iodeto de difenil-metil-4-hidroxifenil-fosfônio	18,0%	64,0%	(BÜTTNER et al., 2017a)
Iodeto de trifenil-2-hidroxietil-fosfônio	14,0%	80,0%	(BÜTTNER et al., 2017a)
SiO_2 (Aerosil 200)	12,0%	100,0%	(SCHÄFFNER et al., 2014)
Iodeto de difenil-metil-2-carboxifenil-fosfônio	11,0%	84,0%	(BÜTTNER et al., 2017a)
Cloreto de tributil-2-hidroxietil-fosfônio	10,0%	100,0%	(BÜTTNER et al., 2017a)
Brometo de trifenil-2-hidroxietil-fosfônio	9,0%	99,0%	(BÜTTNER et al., 2017a)
Iodeto de metil-trifenil-fosfônio	9,0%	91,0%	(BÜTTNER et al., 2017a)
Brometo de difenil-propil-2-hidroxi-3,5-di-terc-pentilfenil-fosfônio	9,0%	100,0%	(BÜTTNER et al., 2017a)
$AlCl_3$	6,4%	-	(HOLSER, 2007)
Cloreto de trifenil-2-hidroxietil-fosfônio	5,0%	0,0%	(BÜTTNER et al., 2017a)
Brometo de difenil-propil-2-hidroxi-3-terc-pentilfenil-fosfônio	4,0%	0,0%	(BÜTTNER et al., 2017a)
$FeCl_3$	4,0%	0,0%	(BÜTTNER et al., 2016)
NH_4Br	4,0%	75,0%	(LANGANKE; GREINER; LEITNER, 2013)
KI	2,0%	100,0%	(SCHÄFFNER et al., 2014)
MoO_3	1,0%	0,0%	(TENHUMBERG et al., 2016)
$((C_7H_{13})_4N)_5$-[α-$SiW_{11}O_{39}Fe$].$(C_7H_8)_2$	0,0%	0,0%	(SCHÄFFNER et al., 2014)
Al-Salen	0,0%	0,0%	(SCHÄFFNER et al., 2014)
LiBr	0,0%	-	(HOLSER, 2007)
Sem Catalisador	0,0%	0,0%	(BÜTTNER et al., 2016)
SmOCl	0,0%	0,0%	(SCHÄFFNER et al., 2014)

ANEXO E

Tabela E1. Co-catalisadores aplicados para produção de ésteres monoalquílicos carbonatados

Catalisador	Co-Cat	Conversão	Referência
$[Bu_4P]Br$	$FeBr_3$	100,0%	(BÜTTNER et al., 2016)
$[Bu_4P]Br$	$FeBr_2$	100,0%	(BÜTTNER et al., 2016)
$[Bu_4P]Br$	$Fe(OTf)_3$	100,0%	(BÜTTNER et al., 2016)
$[Bu_4P]Br$	$FeCl_3$	100,0%	(BÜTTNER et al., 2016)
$[Oct_4P]Br$	$FeCl_3$	100,0%	(BÜTTNER et al., 2016)
Complexo de Al(III) aminotrifenolato (R= Cl ; Ligante−Tetraidrofurano)	TBACl	100,0%	(PEÑA CARRODEGUAS et al., 2017)
Complexo de Al(III) aminotrifenolato (R= Cl ; Ligante−Tetraidrofurano)	Cloreto de bis(trifenilfosfina)imínio	100,0%	(PEÑA CARRODEGUAS et al., 2017)
Complexo de Al(III) aminotrifenolato (R= H ; Sem Ligante)	TBAB	100,0%	(PEÑA CARRODEGUAS et al., 2017)
Complexo de Al(III) aminotrifenolato (R= Me ; Ligante−Tetraidrofurano)	TBAB	100,0%	(PEÑA CARRODEGUAS et al., 2017)
Complexo de Al(III) aminotrifenolato (R= Me ; Ligante−Tetraidrofurano)	Cloreto de bis(trifenilfosfina)imínio	100,0%	(PEÑA CARRODEGUAS et al., 2017)
CaI_2	Diciclohexano-18-crown-6	100,0%	(LONGWITZ et al., 2018)
$[Bu_4P]Br$	MoO_3	99,0%	(TENHUMBERG et al., 2016)
$[Bu_4P]Br$	$CeBr_3.7H_2O$	99,0%	(BÜTTNER et al., 2016)
CaI_2	Diciclohexano-18-crown-6 / DBU (diazabicicloundeceno)	98,0%	(LONGWITZ et al., 2018)
CaI_2	Diciclohexano-18-crown-6 / Ph_3P	98,0%	(LONGWITZ et al., 2018)
TBAB	$FeCl_3$	98,0%	(BÜTTNER et al., 2016)
TBAB	THA-Cr-Si-POM	98,0%	(LANGANKE; GREINER; LEITNER, 2013)
TBAI	$FeCl_3$	98,0%	(BÜTTNER et al., 2016)
$[Bu_4P]Br$	H_2MoO_4	96,0%	(TENHUMBERG et al., 2016)
$[Bu_4P]I$	$FeCl_3$	96,0%	(BÜTTNER et al., 2016)

Tabela E1. (Continuação)

CaI_2	Diciclohexano-18-crown-6 / DABCO (diazabiciclooctano)	95,0%	(LONGWITZ et al., 2018)
$[Bu_4P]Br$	$MoO_2(acac)_2$	94,0%	(TENHUMBERG et al., 2016)
Complexo de Al(III) aminotrifenolato (R= Cl ; Ligante−Tetraidrofurano)	TBAB	94,0%	(PEÑA CARRODEGUAS et al., 2017)
NaI	15-crown-5	94,0%	(SCHÄFFNER et al., 2014)
$[Bu_4P]Br$	$Mo(CO)_6$	93,0%	(TENHUMBERG et al., 2016)
Complexo de Al(III) aminotrifenolato (R= tBu ; Ligante−Tetraidrofurano)	Cloreto de bis(trifenilfosfina)imínio	92,0%	(PEÑA CARRODEGUAS et al., 2017)
KI	18-crown-6	90,0%	(SCHÄFFNER et al., 2014)
CaI_2	Diciclohexano-18-crown-6 / TBD (triazabiciclodeceno)	89,0%	(LONGWITZ et al., 2018)
CsI	Polietilenoglicol 200	89,0%	(SCHÄFFNER et al., 2014)
TBACl	$FeCl_3$	88,0%	(BÜTTNER et al., 2016)
$ZnBr_2$	C_5H_5N	88,0%	(SCHÄFFNER et al., 2014)
$[Bu_4P]Br$	$AlCl_3$	87,0%	(BÜTTNER et al., 2016)
KI	Polietilenoglicol 400	84,0%	(SCHÄFFNER et al., 2014)
KI	Polietilenoglicol 600	84,0%	(SCHÄFFNER et al., 2014)
$[Bu_4P]Br$	$Na_2MoO_4 \cdot 2H_2O$	83,0%	(TENHUMBERG et al., 2016)
KI	[2.2.2] cripitante (4,7,13,16,21,24-Hexaoxa-1,10-diaza-biciclo[8.8.8]hexacosano)	83,0%	(SCHÄFFNER et al., 2014)
CaI_2	Diciclohexano-18-crown-6 / DMAP (Dimetil-amino-piridina)	81,0%	(LONGWITZ et al., 2018)
$[Bu_4P]Br$	MoO_2	80,0%	(TENHUMBERG et al., 2016)
$[Bu_4P]Br$	H_2WO_4	80,0%	(BÜTTNER et al., 2016)
TBAB	Al-Salen	80,0%	(SCHÄFFNER et al., 2014)
KI	Polietilenoglicol 200	79,0%	(SCHÄFFNER et al., 2014)
$[Bu_4P]Br$	$Fe(acac)_3$	78,0%	(BÜTTNER et al., 2016)

Tabela E1. (Continuação)

$[Bu_4P]Br$	FeF_3	77,0%	(BÜTTNER et al., 2016)
$[Bu_4P]Br$	$CeCl_3.7H_2O$	73,0%	(BÜTTNER et al., 2016)
KI	dietilenoglicol	73,0%	(SCHÄFFNER et al., 2014)
$[Bu_4P]Cl$	$FeCl_3$	72,0%	(BÜTTNER et al., 2016)
$[Bu_4P]Br$	$CaCl_2$	71,0%	(BÜTTNER et al., 2016)
$[Bu_4P]Br$	$CeSO_4.4H_2O$	70,0%	(BÜTTNER et al., 2016)
TBAB	$CaCl_2$	70,0%	(SCHÄFFNER et al., 2014)
CaI_2	Diciclohexano-18-crown-6/ NHC (1,3-bis(2,6-diisopropilfenil)-1,3-dihidro-2H-imidazol-2-ilideno)	68,0%	(LONGWITZ et al., 2018)
$[Bu_4P]Br$	$Al(OiPr)_3$	66,0%	(BÜTTNER et al., 2016)
TBAB	$SnCl_4.(H_2O)_5$	64,0%	(SCHÄFFNER et al., 2014)
KI	Polietilenoglicol 1000	62,0%	(SCHÄFFNER et al., 2014)
CaI_2	18-Crown-6	61,0%	(LONGWITZ et al., 2018)
CaI_2	Benzo-18-crown-6	60,0%	(LONGWITZ et al., 2018)
Complexo de Al(III) aminotrifenolato (R= Me ; Ligante−Tetraidrofurano)	TBACl	59,0%	(PEÑA CARRODEGUAS et al., 2017)
$[Bu_4P]Br$	$Fe(OAc)_2$	58,0%	(BÜTTNER et al., 2016)
$[Bu_4P]Br$	$Fe(estearato)_3$	57,0%	(BÜTTNER et al., 2016)
KBr	18-crown-6	55,0%	(SCHÄFFNER et al., 2014)
$[Bu_4P]Br$	$FeCl_3 \cdot 6H_2O$	47,0%	(BÜTTNER et al., 2016)
LiI	Polietilenoglicol 200	43,0%	(SCHÄFFNER et al., 2014)
$[Bu_4P]Br$	$Fe(citrato)_3 \cdot (aq.)$	37,0%	(BÜTTNER et al., 2016)
CaI_2	1-Aza-18-crown-6	36,0%	(LONGWITZ et al., 2018)
$[Bu_4P]Br$	$FeSO_4 \cdot 7H_2O$	27,0%	(BÜTTNER et al., 2016)
2-difenil-fosfônio-fenol	suportado em silica gel funcionalizada com 4-bromopropil	26,0%	(STEINBAUER et al., 2017)
CaI_2	DMF	23,0%	(LONGWITZ et al., 2018)

Tabela E1. (Continuação)

KI	Podandg (Tris[2-(2-metoxi-etoxi)etil]-amina)	23,0%	(SCHÄFFNER et al., 2014)
KI	Lecitina de soja	22,0%	(SCHÄFFNER et al., 2014)
CaI_2	Ph_3P	19,0%	(LONGWITZ et al., 2018)
CaI_2	Dibenzo-18-crown-6	18,0%	(LONGWITZ et al., 2018)
LiI	12-crown-4	18,0%	(SCHÄFFNER et al., 2014)
KI	Monoetilenoglicol	17,0%	(SCHÄFFNER et al., 2014)
KI	Polietilenoglicol 100000	17,0%	(SCHÄFFNER et al., 2014)
TBAB	SiO_2	15,0%	(SCHÄFFNER et al., 2014)
CaI_2	Diciclohexano-18-crown-6/TBABr	10,0%	(LONGWITZ et al., 2018)
CsI	18-crown-6	10,0%	(SCHÄFFNER et al., 2014)
CaI_2	2-Hidroximetil-18-crown-6	0,0%	(LONGWITZ et al., 2018)
NH_4Br	Al-Salen	0,0%	(SCHÄFFNER et al., 2014)

APÊNDICE A

No Apendice A, são apresentados os procedimentos experimentais aplicados para a síntese de óleos carbonatados utilizando o brometo de tetrabutilamônio (TBAB) como catalisador, bem como são descritos os métodos de caracterização e de cálculo aplicados no presente trabalho.

Óleos Vegetais

Os óleos vegetais que foram investigados no presente trabalho são: Arroz, Canola, Oliva, Palma e Soja.

Reação de Epoxidação

As reações de epoxidação *in situ* dos óleos foram conduzidas utilizando-se ácido acético glacial, peróxido de hidrogênio 30 %, temperatura de 75ºC com as proporções de 2/1 (mol/mol) de H_2O_2/C=C, 0,5/1 (mol/mol) CH_3COOH/C=C, 2% ácido sulfúrico (fração aquosa) e tempo reacional de 4-8 horas. O valor de C=C por triglicerídeo será obtido a partir da Tabela 3.1, cromatografia gasosa e índice de iodo (DINDA et al., 2008; GOUD et al., 2007).

Reação de Carbonatação

As reações de carbonatação foram conduzidas utilizando-se os óleos epoxidados, catalisador (Brometo de tetrabutilamônio), com uma proporção de 5% molar em relação ao grupo oxirano, tempo reacional de 48h, sem agitação e pressão de CO_2 de 50 bar (LI et al., 2008; ZHANG et al., 2014a; ZHENG et al., 2015).

Caracterização

A fim de caracterizar os produtos obtidos, as análises descritas a seguir são propostas de maneira a realizar o controle de qualidade dos produtos e processos realizados.

Espectroscopia no Infravermelho

Os espectros de Infravermelho por transformada de Fourier (HATR –FTIR) dos óleos vegetais, óleos epoxidados e óleos carbonatados, serão obtidos utilizando um espectrômetro da PerkinElmer modelo Spectrum One com um cristal de ZnSe utilizando a faixa espectral de 4000 cm^{-1} a 650 cm^{-1} e com resolução de 4 cm^{-1}.

Espectrocopia por ^{1}H-NMR

Todos os espectros de ^{1}H-NMR foram registrados em um Bruker Avance 400 operando a 400 MHz para ^{1}H. Os desvios químicos (δ) são apresentados em partes por milhão (ppm) em relação ao sinal de TMS (0 ppm) e usando clorofórmio deuterado ($CDCl_3$) como solvente. As seguintes abreviaturas são usadas para indicar a multiplicidade em espectros de ^{1}H-NMR: s - singlet; bs - singuleto largo; d - doublet; t - tripleto; q - quarteto; m - multipleto; dd - dupleto duplo.

Parâmetros estimados por ^{1}H-NMR

No presente trabalho os parâmetros: I) número de insaturações dos óleos vegetais, II) número de grupos epóxi nos óleos epoxidados e III) conversão de grupo epóxi na reação de carbonatação foram estimados com base nos espectros de ^{1}H-NMR. Na Figura A1 é representado a estrutura dos óleos vegetais e sinais característicos aplicados para os cálculos.

Para os dados de ^{1}H-NMR, os cálculos foram realizados da seguinte forma. Um fator de normalização (NF) foi calculado a partir dos sinais dos quatro prótons metil da porção glicerol (B), usando a Equação A1 (MAZO; RIOS, 2012, 2013).

$$\text{Fator de Normalização (NF)} = \frac{B}{4} \qquad (A1)$$

Ligações Duplas. A seguir, o número de insaturações dos óleos vegetais é estimado com base na área integrada dos sinais respectivos aos hidrogênios olefínicos (C). O número total de ligações duplas é estimado a partir dos sinais de

hidrogênios olefínicos (C) normalizados contra os quatro prótons metil da porção glicerol (B) (Equação A2) (KUMAR et al., 2012).

$$\text{Ligações duplas (C = C)} = \frac{C}{2NF} \qquad (A2)$$

Grupos epóxi. Após a etapa de epoxidação, os sinais respectivos aos hidrogênios olefínicos (C) são consumidos, enquanto os sinais atribuídos aos prótons do grupamento oxirano (D) são formados entre 2.9 ppm 3.1 ppm. O número de grupos oxiranos é estimado com base na área integrada dos sinais respectivos aos hidrogênios do grupo epóxi (D). O número total de grupos oxiranos é estimado a partir dos sinais dos hidrogênios do grupo epóxi (D) normalizados contra os quatro prótons metil da porção glicerol (B) (Equação A3) (MAZO; RIOS, 2012, 2013).

$$\text{Grupos Oxiranos } (E_p) = \frac{D}{2NF} \qquad (A3)$$

Conversão. O cálculo de conversão é realizado com base no consumo de grupos epóxi ao longo da reação de carbonatação e é estimado por meio da Equação A4) (MAZO; RIOS, 2012, 2013).

$$\text{Conversão } (\eta\%) = \left[\frac{E_{p\ inicial} - E_{p\ final}}{E_{p\ inicial}}\right] x100 \qquad (A4)$$

Uma vez que existe a possibilidade de ocorrer a sobreposição dos sinais dos hidrogênios do carbonato (E) e dos sinais dos quatro prótons metil da porção glicerol (B), os cálculos de rendimento e de seletividade são estimados utilizando as Equações A5 e A6 e são aplicados quando não existem indícios de sobreposições de sinais no espectro de ^{1}H-NMR (MAZO; RIOS, 2012, 2013). Considerando que no presente trabalho foi constatado a sobreposição de sinais, os parâmetros rendimento e seletividade não foram estimados.

Rendimento. O cálculo de rendimento é estimado a partir dos sinais dos hidrogênios do grupo carbonato (E) gerados (4.19 - 4.24 ppm e 4.45 - 5.12 ppm)

durante a reação de carbonatação em relação ao número de grupos oxiranos iniciais. O cálculo de rendimento é realizado por meio da Equação A5 (MAZO; RIOS, 2012, 2013).

$$\text{Rendimento (Y\%)} = \left[\frac{\frac{E}{2}}{NF\ x\ E_{p\ inicial}}\right] x100 \qquad (A5)$$

Seletividade. O cálculo de seletividade é estimado a partir da razão entre o rendimento e a conversão e é realizado por meio da Equação A6 (MAZO; RIOS, 2012, 2013).

$$\text{Grupos Oxiranos } (S\%) = \left[\frac{\text{Y}(\%)}{\eta(\%)}\right] x100 \qquad (A6)$$

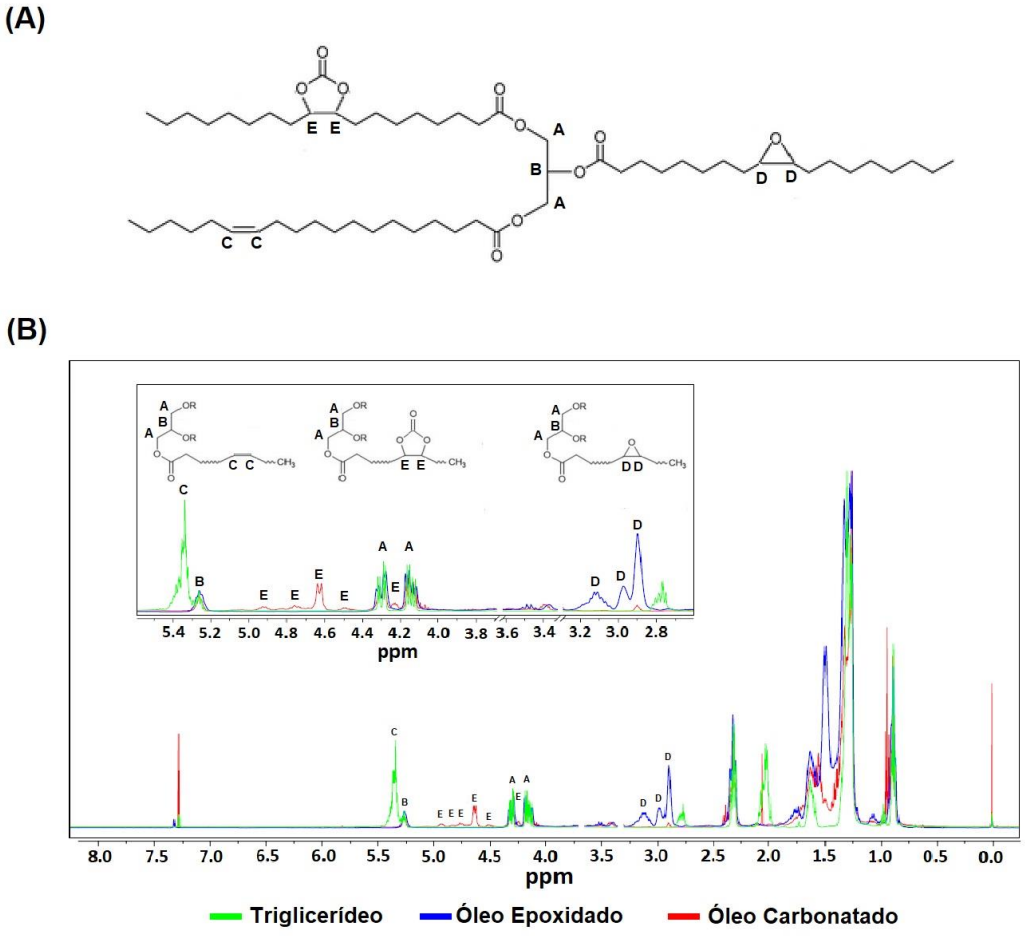

Figura A1. Estrutura e sinais característicos dos derivados oleoquímicos

APÊNDICE B

No Apêndice B, é brevemente discutido os resultados obtidos na síntese de óleos carbonatados utilizando o brometo de tetrabutilamônio (TBAB) como catalisador.

Reação de Carbonatação com TBAB

As reações de carbonatação dos óleos de soja, palma, canola, oliva e arroz, utilizando o TBAB, foram aplicadas nas condições descritas no Apêndice A. Devido a elevada viscosidade do meio, as reações foram conduzidas sem agitação devido à ineficiência da agitação magnética em promover a homogeneização dos reagentes. A caracterização dos produtos obtidos a partir da reação com TBAB foi conduzida por FTIR e os resultados são apresentados nas Figuras B1 - B5.

O infravermelho é realizado para identificar a presença do carbonato cíclico no produto. O desaparecimento da banda de oxirano entre 842 cm^{-1} e 823 cm^{-1} indica o consumo de epóxido, enquanto a formação de uma nova banda intensa de carbonila (C=O) em 1795 cm^{-1} indica a formação do carbonato cíclico de 5 membros. Adicionalmente, observa-se a presença de hidroxila (H-O), devido ao estiramento na região entre 3600 cm^{-1} e 3200 cm^{-1}, indicando que os grupamentos epóxi foram parcialmente hidrolisados ainda durante a etapa de epoxidação com a formação de álcoois secundários.

Conforme observado nas Figuras B1 - B5, todos os óleos vegetais epoxidados foram carbonatados parcialmente. A presença de grupos epóxidos residuais são identificados devido ao pequeno estiramento entre 842 cm^{-1} e 823 cm^{-1} e indicam que, nas condições em que foram conduzidas as reações, não é possível obter conversões completas de grupos epóxidos em carbonatos.

Em condições reacionais semelhantes (tempo, temperatura, pressão e catalisador) a literatura reporta conversões acima de 90% de epóxido em carbonatos (LI et al., 2008), porém a agitação é apontada como um fator determinante para a obtenção de conversões elevadas. Considerando que a elevada viscosidade do óleo epoxidado/carbonatado apresenta uma elevada barreira para a transferência de massas entre a fase gasosa (CO_2) e líquida (óleo + catalisador) (ZHENG et al., 2015, 2018), a baixa conversão justifica-se pela ausência de agitação durante as reações.

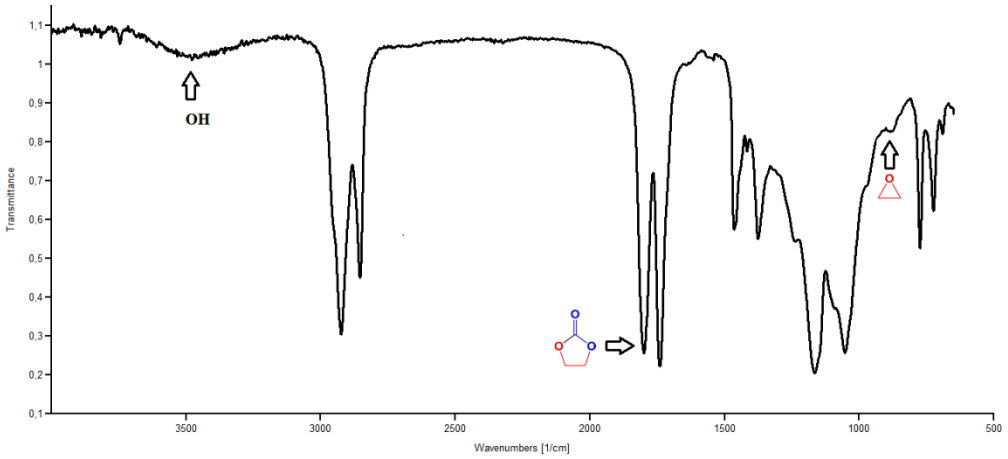

Figura B1. FTIR do carbonato de óleo de arroz catalisado pelo TBAB.

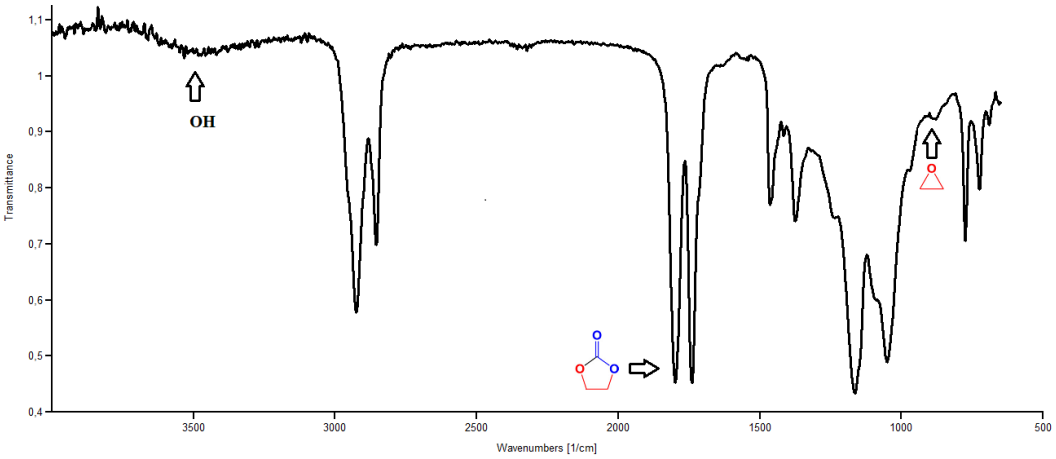

Figura B2. FTIR do carbonato de óleo de canola catalisado pelo TBAB.

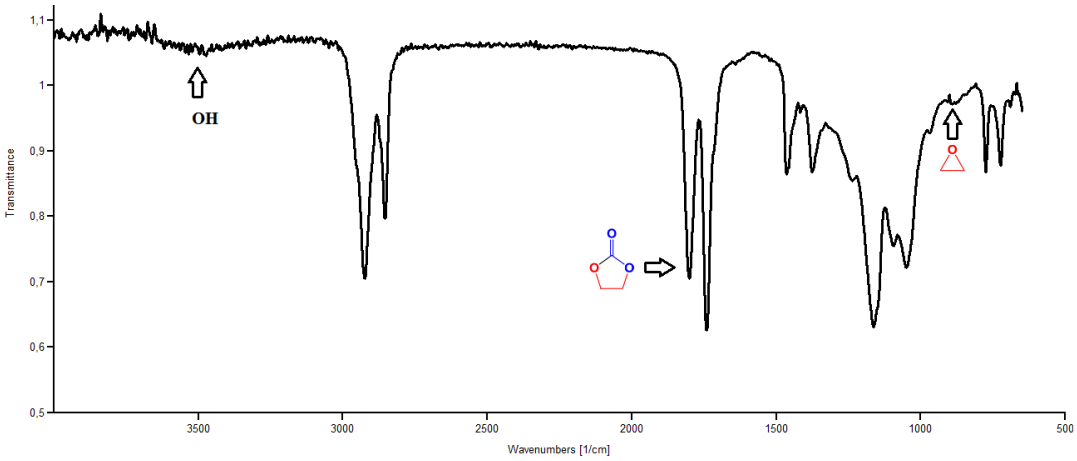

Figura B3. FTIR do carbonato de óleo de oliva catalisado pelo TBAB.

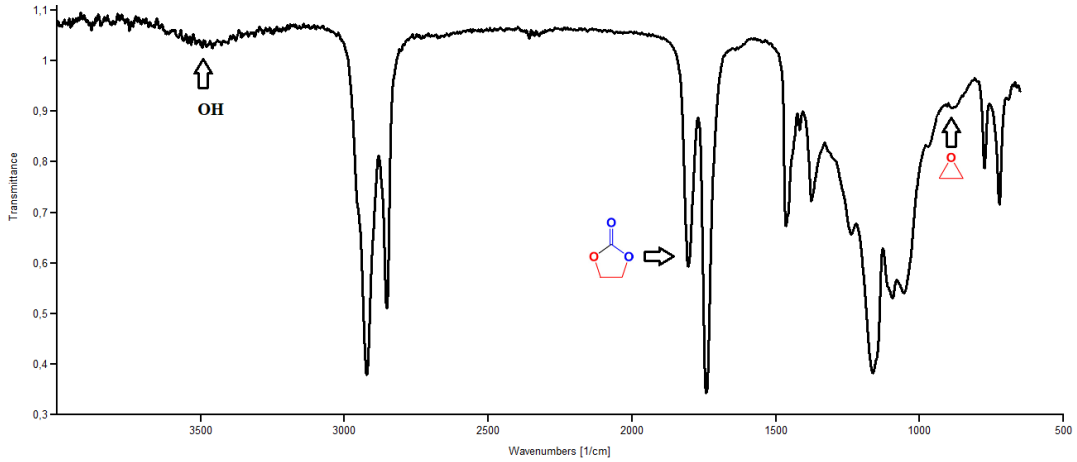

Figura B4. FTIR do carbonato de óleo de palma catalisado pelo TBAB.

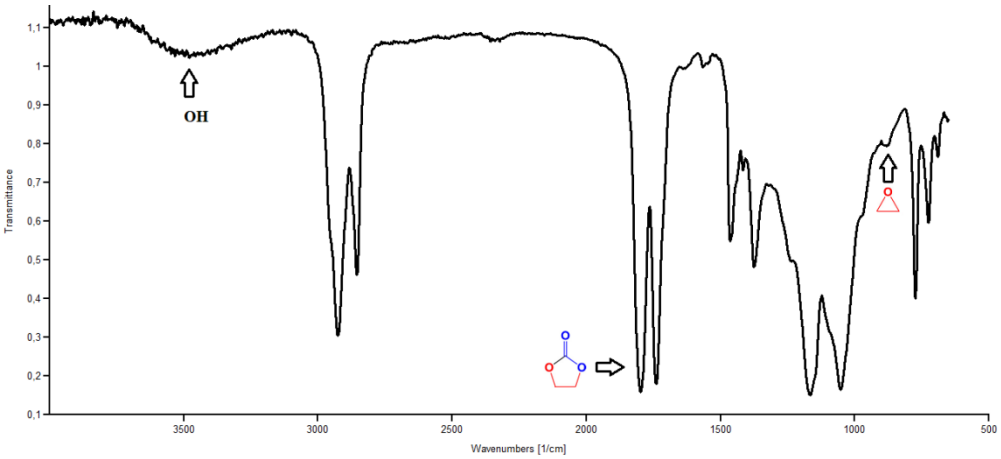

Figura B5. FTIR do carbonato de óleo de soja catalisado pelo TBAB.

Pontifícia Universidade Católica do Rio Grande do Sul
Pró-Reitoria de Graduação
Av. Ipiranga, 6681 - Prédio 1 - 3º. andar
Porto Alegre - RS - Brasil
Fone: (51) 3320-3500 - Fax: (51) 3339-1564
E-mail: prograd@pucrs.br
Site: www.pucrs.br